Mathematical Modeling to Evaluate Disease Control Policy

Mathematical Modeling to Evaluate Disease Control Policy

A dissertation presented

by

Nicolas Alan Menzies

to

The Committee on Higher Degrees in Health Policy

in partial fulfillment of the requirements

for the degree of

Doctor of Philosophy

in the subject of

Health Policy

Harvard University

Cambridge, Massachusetts

March 2014

Dissertation advisor: Professor Joshua Salomon Nicolas Alan Menzies

Mathematical Modeling to Evaluate Disease Control Policy

Abstract

In this dissertation I assessed three distinct policy questions: the implications of introducing a new tuberculosis diagnostic in southern Africa, the potential value of research related to HIV treatment policy in South Africa, and the causal effect of state cigarette taxes imposed between 1996 and 2013 on health outcomes in the United States.

In Chapter 1 I investigated use of a new TB diagnostic, Xpert MTB/RIF, to replace sputum smear-based diagnostic algorithms in southern Africa. Analyses were undertaken using a dynamic mathematical model, taking account of TB transmission and natural history, HIV epidemiology, TB drug resistance, and disease control interventions. Results suggest Xpert may substantially reduce TB morbidity and mortality, and modestly reduce transmission, while significantly increasing demands on healthcare resources. Xpert adoption was estimated to cost $711 to $1,083 per DALY averted, representing good value for money according to conventional benchmarks.

In Chapter 2 I estimated the value of new research on various targets relevant to HIV treatment policy in South Africa. I implemented the analysis with a mathematical model of HIV epidemiology, simulating HIV transmission, disease progression, and receipt of treatment. I used Value of Information (VOI) methods to identify priority research areas, based on the welfare gains possible by obtaining better information prior to decision-making. High priority research targets included issues of cost and implementation, relative infectiousness during late HIV, the reduction in

infectiousness following treatment initiation, and the therapeutic benefits of early treatment initiation.

In Chapter 3 I estimated how changes in state cigarette taxes over the period 1996-2013 affected smoking behavior and health outcomes in the United States. The causal effect of tax changes were estimated in the context of a demographic model directly linking smoking behavior with subsequent mortality risks, using data from the Behavioral Risk Factor Surveillance System. Results suggest national cigarette consumption by 2013 was 4.0% lower (3.3, 4.6) compared to a counterfactual with no new state cigarette taxes after 1996, averting 27 thousand (22, 34) deaths and producing 119 thousand (92, 151) extra life-years lived. The health impact of these taxes was projected to be far greater in future years.

Table of Contents

List of Tables

List of Figures

Acknowledgements

Firstly, I would like to thank Joshua Salomon, my dissertation chair. Josh somehow managed to be mentor and comrade at the same time, and I am deeply grateful for both. I would like to thank the other members of my committee – Milt Weinstein, for taking my sometimes loosely developed arguments and helping to add structure and sense, and Tom McGuire, for providing a willing ear and deep thought for any number of proposals trying to build an analysis that bridged disciplines.

I would also like to thank others who helped me develop or implement the analyses in this dissertation – Megan Murray, Barry Bloom, Leonid Chindelevitch, Dan Hogan, and many others. In particular I would like to thank Ted Cohen, who helped teach me both the fine detail and broad picture of TB epidemiological modelling, and who is generally a great guy.

I would like to thank the funding bodies that allowed me to devote my time to this work: the National Libraries of Medicine, the MGH Program in Cancer Outcomes Research Training, the Jeremy Knowles Graduate Fellowship, UNITAID, the HIV Modelling Consortium and the TB Modelling and Analysis Consortium. In addition to financial support, I would like to acknowledge the feedback and collegiality I received from the MGH Institute of Technology Assessment as well as the TB and HIV modeling consortia. The ability to share my work with interested experts helped to make it stronger.

I would like to thank the fellow students who provided companionship on a long journey – Mike Botta, Rebecca Cadigan, Laura Garabedian, Keren Ladin, Jessica Perkins, Tisa Sherry, Zirui Song, Sae Takeda, Melissa Valentine, and Beth Wikler within my cohort, and Dorothy Romanus, Sorapop Kiatpongsan, Paula Chu, Craig White, Arielle Bensimon, Mark Shrime, Emily Burger, and Lina Song within Decision Sciences. I would also like to thank my peer mentoring group—Ankur Pandya, Natalie Carvalho, Brendan Saloner, Tara Lavelle and Davene Wright—for providing a lesson in how

to get it done and letting me know that something actually happens after graduation. I would like to thank the Health Policy program office, Joan, Debbie, and Ayres, for being ever helpful and supportive, and Joe Newhouse and the rest of the Health Policy PhD program for providing an intellectually vigorous environment. I would like to thank Sue Goldie, Jim Hammitt, Stephen Resch, Jane Kim, Jennifer Yeh, Eve Wittenberg, Uwe Siebert, Myriam Hunink, and Natasha Stout, for counsel and encouragement at various points over the past years, and the CHDS community—including Christine Bell, Jeannie Millar, Steven Sweet and others—for providing a roof over my head and a happy place to work.

I would also like to thank colleagues and mentors in Atlanta—Deborah MacFarland, John Blandford, and others—who helped me realize a PhD might be a good idea in the first place.

I would like to thank my family – Will, Di, Oli, and Sarah, as well as Jack and Rumi. To my wife Michele, you make the sun come up in the morning and give food its flavor. I cannot thank you enough for your love and companionship, but over the years I will try.

Finally, I would like to dedicate this dissertation to my children Simon and Hazel. You certainly did not make this any easier, but I feel like I won the lottery with both of you. Don't prove me wrong.

Chapter 1. Dissertation Overview

In order to make good public policy, decision-makers must understand the consequences of competing policy options. In evaluating these options, it is rare to have all the information that might be desired – the available information about an intervention might be derived from a setting very different to that anticipated for the new policy, and understanding long-term outcomes may require piecing together information about many intermediate steps. Each of the three chapters in this dissertation takes a formal approach to combining available data to estimate policy outcomes. Addressing very different policy questions, each chapter develops a mathematical model describing how quantities about which we have some understanding—such as historical time trends in disease epidemiology, or the individual-level effects of an intervention under defined conditions—combine to generate population-level outcomes. This approach brings with it both weaknesses and strengths. From the outset, all of these mathematical models are known to be wrong, in the sense that they involve simplification of complex disease processes, and ignore various sources of heterogeneity in how individuals will be affected by a given policy. The challenge for policy analysis using these models is to produce reasonable estimates about quantities of interest, despite the simplifications. Of course, any attempt to predict future events requires assumptions, even if these are not plainly stated. A strength of the approach adopted for these analyses comes from the opportunity to examine and test modeling assumptions. By modeling the various processes that generate long-term outcomes, mechanistic models allow many different intermediate outcomes to be estimated. Even though we may not have empirical data on long-term outcomes to validate policy predictions, we often have data on these intermediate outcomes, which can be used to both calibrate model inputs and identify modeling assumptions that are inconsistent with reality, providing the opportunity for iterative model refinement.

1.1. Chapter 2: Population health impact and cost-effectiveness of tuberculosis diagnosis with Xpert MTB/RIF, a dynamic simulation and economic evaluation

In Chapter 1 I investigate the consequences of introducing new technology for diagnosis of tuberculosis (TB) in southern African countries. TB remains a leading cause of mortality and morbidity in southern Africa [1]. Although significant advances have been made, continued progress in TB control is threatened by the inadequacy of existing diagnosis. Diagnostic algorithms generally rely on sputum smear microscopy, which has limited sensitivity, especially among HIV-infected patients [2–4]. Recently, the Xpert MTB/RIF automated DNA test has been shown to provide rapid and sensitive detection of TB and rifampicin (RIF) resistance [5,6], and can be implemented by relatively unskilled healthcare workers [5,7]. In December 2010, the WHO recommended that Xpert be used for TB diagnosis where MDR-TB (multidrug resistant-TB) or HIV infection are suspected [8], and many countries have begun to adopt this technology [9].

In this study I estimated the potential health and economic consequences of introducing Xpert in southern African countries, which are characterized by a high prevalence of HIV infection and growing TB drug resistance. I compared two alternative strategies for diagnosing TB, the first based on the earlier diagnostic algorithms relying on sputum smear microscopy, and the second based on implementing Xpert in accordance with new WHO recommendations. Comparisons between these two strategies were made using a dynamic mathematical model of TB, which took account of key features of TB transmission dynamics and natural history, interactions with HIV infection, TB drug resistance patterns, and trends in TB and HIV control interventions. A Bayesian approach was used to calibrate model parameters to reported data on TB prevalence, incidence, and the distribution of drug resistance in each country [10]. Model simulations were undertaken for five southern African countries: Botswana, Lesotho, Namibia, South Africa, and Swaziland. The analysis assessed changes in epidemiological outcomes and health system costs over 10-year and 20-year time horizons, as

well as the incremental cost-effectiveness ratio (ICER) of the Xpert strategy compared to the current algorithm.

The results of this analysis indicated that the introduction of Xpert has the potential to substantially reduce TB morbidity and mortality in southern Africa, with TB prevalence estimated to be 28% lower (95% posterior interval: 14, 40) and TB mortality 21% lower (10, 32) 10 years after Xpert introduction, as compared to outcomes estimated for the continued use of earlier diagnostics. For individuals with smear-negative TB, the benefits of Xpert implementation would be immediate, leading to the diagnosis and early treatment of many individuals who would be missed by the conventional diagnostic algorithm. Over a longer time frame, the introduction of Xpert would reduce transmission, but these secondary effects are smaller than might have been anticipated, and TB incidence after 10 years was estimated to be 6% lower (2, 13) under the Xpert scenario as compared to the status quo. As a consequence, the analysis suggests that TB incidence would remain substantial after three decades of Xpert use, in the absence of other modifications to the TB control strategy.

Results also suggested that Xpert adoption would significantly increase demands on healthcare resources. While the direct costs of the Xpert technology itself are not small, a major financial impact of Xpert introduction would come from increased resource requirements in HIV treatment programs, with prompt TB treatment extending survival among TB/HIV-coinfected individuals. At 10 years after Xpert introduction, HIV treatment costs are estimated to comprise 58% (95% CI: 40–72) of the total incremental costs associated with the Xpert strategy. Treatment of MDR-TB represents another major cost, as the number of cases of MDR-TB identified increases two- to three-fold with Xpert introduction. Compared to continued use of earlier diagnostics, the introduction of Xpert was estimated to have an ICER that ranged from $711 to $1,083 per DALY averted, depending on the time horizon and assumptions about the Xpert test cost. These ratios

were generally robust to changes in analytic assumptions, though did rise substantially in scenarios that assumed much higher availability of TB culture (a more sensitive diagnostic test than sputum smear, but with long turn-around times) under the status quo.

While the ICERs estimated in this study are higher than those estimated by an earlier analysis [11], they still suggest that the introduction of Xpert represents good value for money according to typical international benchmarks. However, these results also raise important questions of affordability, due to the additional demand for various treatment services. It is likely that existing resources will be called upon to support the introduction of Xpert and the cascade of complementary services this will trigger, and our findings underscore the concern raised by other commentators regarding the possible pitfalls of introducing Xpert into health systems that are already facing capacity constraints [12,13].

1.2. Chapter 2: Value of new research to inform HIV control policy in South Africa

In Chapter 2 I report analyses to estimate the relative value of various targets for new research related to HIV control in developing countries. Despite unprecedented funding levels, many highly-affected countries are not yet able to provide antiretroviral therapy (ART) to all who might benefit [14]. While the therapeutic benefits of ART are well established [15], there is increasing evidence that ART may also reduce HIV transmission [16]. As a consequence, policy makers are considering expanded ART eligibility criteria [17]. Expanded eligibility will come at the expense of other care unless further funding is available [18], and must compete with efforts to increase enrollment among groups already eligible according to current guidelines. Recent modeled analyses suggest uncertainty about the optimal approach to expanding ART programs according to cost-effectiveness criteria [19], and this uncertainty hinders the development of long-term HIV control strategy [20]. Uncertainty about optimal ART policy is partially due to weaknesses in the evidence base used to understand the consequences of HIV treatment policy. A number of specific issues are particularly

uncertain, including the magnitude of incidence reductions associated with ART as implemented in routine programs [21], the therapeutic benefits of initiating ART at high CD4 cell count [22], the relative importance of early HIV infection to epidemic dynamics [23], and the cost and implementation challenges associated with expanding different programmatic components [21,24].

This study attempts to inform decisions about new HIV research to inform ART policy, using value of information (VOI) methods to identify high-priority research targets [25–27]. To implement this analysis I developed a mathematical model to represent an HIV epidemic in the South African adult population, simulating transmission of HIV infection through durable sexual partnerships and casual sexual contacts, the progression of HIV disease for HIV-infected individuals, and initiation and receipt of antiretroviral therapy. I used this model to project the costs and health outcomes resulting from various policy options that might be adopted by the South African national HIV control program, and used Monte Carlo methods to quantify how uncertainty in epidemiology, programmatic performance and cost translated into uncertainty in modeled outcomes. These results were then used to estimate VOI for individual parameters or groups of parameters. Finally, I compared VOI estimates for different parameters to draw conclusions about high-priority research targets for informing ART policy.

This analysis suggested that scaling-up ART would substantially reduce the burden of HIV in South Africa. Over the next 20 years the most aggressive scale-up policy was estimated to reduce cumulative incidence by 58% (44, 68) and reduce HIV mortality by 34% (29, 38), as compared to continuation of current policy. The relative impacts of therapeutic vs. preventive effects of ART were sensitive to the time horizon, with the prevention effects contributing the majority of DALYs averted from ART expansion over an extended timeline. Expanded ART was also estimated to require large increases in health system costs, with higher HIV programs costs being only modestly offset by savings in routine health services. The cost-effectiveness findings suggested that

expanding ART access, either through raising CD4 cell count-based eligibility criteria or through more aggressive testing programs, would be cost-effective under a wide range of assumptions, and despite uncertainties about epidemiology and intervention effects. These findings are broadly consistent with other analyses investigating the long-term outcomes of ART expansion in South Africa [19,28–30]. The relative ordering of ART scale-up approaches was sensitive to the time horizon, with expansions in eligibility preferred to expansions in coverage in analyses that adopted an extended time horizon.

The cost-effectiveness results described above formed the basis of the value-of-information analysis. Issues found to have the highest potential value of information included (1) issues of cost and implementation, (2) relative infectiousness during late HIV and the reduction in infectiousness for individuals on ART, and (3) the therapeutic health benefits of ART for individuals with CD4 cell counts above current eligibility guidelines. These findings generally held up across truncated and extended time horizons. The prevention benefits of ART are the subject of an increasing volume of research [31,32], as are the therapeutic benefits of early ART initiation [33,34]. There has been less systematic investigation of issues of cost and implementation, though recent work has focused on HIV treatment costs [35–38]. One challenge for new research on costs and implementation issues is generalizability: while studies examining physiological processes may generalize broadly, the costs and quality of service provision are a consequence of complex social and institutional interactions, and outcomes might differ substantially across settings or as intervention approaches change. The most notable finding of the VOI results is the apparent unimportance of information about transmission during early HIV infection. Resolving uncertainty for this parameter (the relative risk of transmission during early HIV infection) accounts for approximately 1% of the value of information estimated for the most valuable research targets, and suggests that research funding might be better devoted to other subjects.

1.3. Chapter 3: Estimating the health impact of recent changes in state-level cigarette taxes

Chapter 3 describes an analysis of the effects of changes in state cigarette taxes over the period 1996-2013 on smoking behavior and health outcomes in the United States. Cigarette smoking is estimated to cause one out of every five deaths in the U.S. [39], and both state and federal governments have introduced cigarette excise taxes to limit cigarette consumption. Many states have raised these taxes in recent years, with the real value of the average state cigarette tax rising by over 200% since 1996 [40]. Studies of the effect of state cigarette taxes over earlier periods [41–45] have identified a relationship between taxes and smoking behavior that is weaker and less robust than would be expected from the broader literature on taxes and smoking [46].

For this study I developed a mechanistic model of smoking behavior and associated health outcomes in the 50 U.S. states and District of Columbia, and used this model to assess the impact of state cigarette taxes introduced over 17 years from 1996 to 2013. This analysis departs from previous analyses of the causal effects of cigarette taxes by allowing for separate effects on smoking initiation, smoking intensity, and quitting behavior, and by estimating these effects in the context of a demographic model that directly links smoking behavior and smoking history with mortality risks [47]. I estimated causal effects of cigarette taxes using the 1996-2012 rounds of the CDC's Behavioral Risk Factor Surveillance System survey, which describe current and past smoking behavior for a large population-based sample of the adult in the United States [48]. These analyses made use of inter-state variation in the timing and magnitude of new cigarette taxes to identify causal effects, using a measure of anti-smoking sentiment [42] to control for state-level factors that influence both smoking behavior and the introduction of new cigarette taxes.

The results of this analysis suggest that average national cigarette consumption by the beginning of 2013 was 4.4% lower among men (3.7, 5.3), and 3.6% lower among women (2.6, 4.2), compared to a counterfactual scenario in which no new state cigarette taxes were introduced after 1996, for a

4.0% reduction in overall consumption (3.3,4.6). These reductions differ widely by state depending on the timing and magnitude of tax increases. The behavioral effects of tax increases were projected to be larger if a longer time horizon is considered, with the average number of years spent smoking estimated to drop by 10 months (7, 12) for the 2013 birth cohort if exposed to 2013 versus 1996 tax levels, for a 6.1% (4.5, 7.8) reduction in overall consumption. These behavioral effects are still modest, with estimates of the price elasticity of demand implied by these results varying from -0.14 to -0.39 depending on sex and the time horizon over which effects were estimated. These elasticities are smaller than conventional estimates for cigarette taxes and cigarette consumption, but are in line with other studies based on variation in cigarette taxes across U.S. states [41–45].

As a consequence of the behavioral outcomes, these analyses suggest that 27 thousand (22, 34) deaths have been averted as a result of the state cigarette taxes introduced over the period 1996-2013, for an extra 119 thousand life-years lived (92, 151). These mortality reductions are relatively trivial compared to overall U.S. mortality. However, projections of future health outcomes under scenarios that compared 2013 and 1996 tax levels suggest that the health benefits of recent state tax increases will largely accrue in future decades, with over a million extra life-years lived in the decade 2020-2029. The results indicate a 2.0 month (1.4, 2.7) overall gain in life expectancy for the 2013 birth cohort due to state tax increases since 1996, with larger gains for men. While valuable, these effects are still modest compared to recent estimates of the overall effect of tobacco control in the U.S. [49], which find life expectancy gains 10-20 times larger than estimated by this analysis. This finding of minor gains in life expectancy is consistent with the modest behavioral effects estimated for the recent tax changes.

In sum, this analysis confirms the beneficial effect of recent state-level cigarette tax increases on smoking behavior, providing detailed evidence about the magnitude and distribution of these effects on both smoking behavior and smoking-related mortality.

In addition to addressing three substantive questions of policy interest, this dissertation also features a number of small methodological innovations. As part of the analyses for Chapter 2, new methods were developed for the application of VOI methods in the context of calibrated models. Common calibration approaches result in a parameter distribution that is approximated by a large sample of parameter sets, rather than a mathematical function. In this context, it is difficult to draw new samples from the conditional distribution of model parameters (i.e., the distribution of other parameters when one parameter is held fixed at a specific value). However, simulating from this conditional distribution is necessary with conventional methods for estimating VOI for a single parameter[1], as it this is used to calculate the expected net monetary benefit for a given strategy and parameter value ($E(NMB|i,\theta_z)$ where i represents a strategy and θ_z is the parameter of interest). To resolve this problem, I developed a method that does not require simulating from this posterior distribution, and instead uses the information from the existing parameter sets to approximate $E(NMB|i,\theta_z)$ with a flexible function. These methods are more demanding than conventional approaches, yet will be of increasing relevance as a greater number of analyses adopt numerical methods to calibrate complex disease models.

The analysis undertaken for the third paper is novel in its use of a mechanistic disease model as the vehicle for an econometric analysis, estimating the behavioral response to tax changes. This approach more closely integrates the task of causal inference about the effects of cigarette taxation with the task of estimating final health outcomes, and in so doing may provide a more nuanced understanding of the long-term consequences of cigarette tax policy.

[1] Or, equally, for subsets of parameters.

1.4. Citations

1 WHO. *Global tuberculosis control: WHO report 2011*. Geneva: World Health Organization; 2011.

2 Corbett EL, Watt CJ, Walker N, Maher D, Williams BG, Raviglione MC, *et al.* The growing burden of tuberculosis: global trends and interactions with the HIV epidemic. *Arch Intern Med* 2003; 163:1009–1021.

3 Elliott AM, Halwiindi B, Hayes RJ, Luo N, Tembo G, Machiels L, *et al.* The impact of human immunodeficiency virus on presentation and diagnosis of tuberculosis in a cohort study in Zambia. *J Trop Med Hyg* 1993; 96:1–11.

4 Getahun H, Harrington M, O'Brien R, Nunn P. Diagnosis of smear-negative pulmonary tuberculosis in people with HIV infection or AIDS in resource-constrained settings: informing urgent policy changes. *Lancet* 2007; 369:2042–2049.

5 Boehme CC, Nicol MP, Nabeta P, Michael JS, Gotuzzo E, Tahirli R, *et al.* Feasibility, diagnostic accuracy, and effectiveness of decentralised use of the Xpert MTB/RIF test for diagnosis of tuberculosis and multidrug resistance: a multicentre implementation study. *Lancet* 2011; 377:1495–1505.

6 Boehme CC, Nabeta P, Hillemann D, Nicol MP, Shenai S, Krapp F, *et al.* Rapid molecular detection of tuberculosis and rifampin resistance. *New Engl J Med* 2010; 363:1005–1015.

7 Rachow A, Zumla A, Heinrich N, Rojas-Ponce G, Mtafya B, Reither K, *et al.* Rapid and accurate detection of Mycobacterium tuberculosis in sputum samples by Cepheid Xpert MTB/RIF assay--a clinical validation study. *PLoS One* 2011; 6:e20458.

8 WHO. Rapid implementation of the Xpert MTB/RIF diagnostic test: technical and operational "how-to."Geneva: World Health Organization; 2011.

9 WHO. WHO monitoring of Xpert MTB/RIF roll-out, last accessed July 21, 2013. 2013.http://www.stoptb.org/wg/gli/assets/documents/map/1/atlas.html

10 Raftery AE, Bao L. Estimating and projecting trends in HIV/AIDS generalized epidemics using Incremental Mixture Importance Sampling. *Biometrics* 2010; 66:1162–73.

11 Vassall A, van Kampen S, Sohn H, Michael JS, John KR, den Boon S, *et al.* Rapid diagnosis of tuberculosis with the Xpert MTB/RIF assay in high burden countries: a cost-effectiveness analysis. *PLOS Med* 2011; 8:e1001120.

12 Trébucq A, Enarson DA, Chiang CY, Van Deun A, Harries AD, Boillot F, *et al.* Xpert® MTB/RIF for national tuberculosis programmes in low-income countries: when, where and how? *Int J Tuberc Lung Dis* 2011; 15:1567–72.

13 Kirwan DE, Cárdenas MK, Gilman RH. Rapid implementation of new TB diagnostic tests: is it too soon for a global roll-out of Xpert MTB/RIF? *Am J Trop Med Hyg* 2012; 87:197–201.

14 UNAIDS. *World AIDS Day Report 2012*. Geneva: UNAIDS; 2012.

15 Wandel S, Egger M, Rangsin R, Nelson KE, Costello C, Lewden C, *et al.* Duration from seroconversion to eligibility for antiretroviral therapy and from ART eligibility to death in adult HIV-infected patients from low and middle-income countries: collaborative analysis of prospective studies. *Sex Transm Infect* 2008; 84 Suppl 1:i31–i36.

16 Cohen MS, Chen YQ, McCauley M, Gamble T, Hosseinipour MC, Kumarasamy N, *et al.* Prevention of HIV-1 infection with early antiretroviral therapy. *New Engl J Med* 2011; 365:493–505.

17 Granich RM, Gilks CF, Dye C, De Cock KM, Williams BG. Universal voluntary HIV testing with immediate antiretroviral therapy as a strategy for elimination of HIV transmission: a mathematical model. *Lancet* 2009; 373:48–57.

18 Lancet Editors. HIV treatment as prevention--it works. *Lancet* 2011; 377:1719.

19 Eaton J, Menzies N, Stover J, Cambiano V, Chindelevitch L, Cori A, *et al.* Health benefits, costs, and cost-effectiveness of earlier eligibility for adult antiretroviral therapy and expanded treatment coverage: a combined analysis of 12 mathematical models. *Lancet Glob Heal* 2014; 2:e23–34.

20 De Cock KM, El-Sadr WM. When to start ART in Africa — an urgent research priority. *New Engl J Med* 2013; 368:886–9.

21 Cohen MS, Smith MK, Muessig KE, Hallett TB, Powers KA, Kashuba AD. Antiretroviral treatment of HIV-1 prevents transmission of HIV-1: where do we go from here? *Lancet* 2013; 382:1515–24.

22 Sabin C, Cooper D, Collins S, Schechter M. Rating evidence in treatment guidelines: a case example of when to initiate combination antiretroviral therapy (cART) in HIV positive asymptomatic persons. *AIDS* 2013; 27:1839–46.

23 Cohen MS, Dye C, Fraser C, Miller WC, Powers KA, Williams BG. HIV treatment as prevention: debate and commentary--will early infection compromise treatment-as-prevention strategies? *PLOS Med* 2012; 9:e1001232.

24 Walker DG, Over M, Bertozzi SM. Can cost studies improve the performance of donor-financed HIV treatment? *AIDS* 2011; 25:1795–6.

25 Groot Koerkamp B, Myriam Hunink MG, Stijnen T, Weinstein MC. Identifying key parameters in cost-effectiveness analysis using value of information: a comparison of methods. *Heal Econ* 2006; 15:383–392.

26 Claxton K, Neumann PJ, Araki S, Weinstein MC. Bayesian value-of-information analysis. An application to a policy model of Alzheimer's disease. *Int J Technol Assess Heal Care* 2001; 17:38–55.

27 Claxton K, Cohen JT, Neumann PJ. When is evidence sufficient? *Heal Aff* 2005; 24:93–101.

28 Hontelez JA, de Vlas SJ, Tanser F, Bakker R, Barnighausen T, Newell ML, *et al.* The impact of the new WHO antiretroviral treatment guidelines on HIV epidemic dynamics and cost in South Africa. *PLoS One* 2011; 6:e21919.

29 Granich R, Kahn JG, Bennett R, Holmes CB, Garg N, Serenata C, *et al.* Expanding ART for treatment and prevention of HIV in South Africa: estimated cost and cost-effectiveness 2011-2050. *PLoS One* 2012; 7:e30216.

30 Bärnighausen T, Bloom DE, Humair S. Economics of antiretroviral treatment vs. circumcision for HIV prevention. *P Natl Acad Sci USA* 2012; 109:21271–6.

31 HIV Prevention Trials Network. Antiretroviral Therapy Research (TasP and PrEP) (website, accessed October 20 2013). 2013.http://www.hptn.org/prevention_science/art.asp

32 Granich R, Gupta S, Suthar AB, Smyth C, Hoos D, Vitoria M, *et al.* Antiretroviral therapy in prevention of HIV and TB: update on current research efforts. *Curr HIV Res* 2011; 9:446–69.

33 French National Agency for Research on AIDS and Viral Hepatitis. Early antiretroviral treatment and/or early isoniazid prophylaxis against tuberculosis in HIV-infected adults (ANRS 12136 TEMPRANO) (website, accessed October 8 2013). 2013.http://clinicaltrials.gov/ct2/show/NCT00495651

34 U.S. National Institutes of Health. Strategic Timing of Antiretroviral Treatment (START) (website, accessed February 20 2013). 2013.http://clinicaltrials.gov/ct2/show/NCT00867048

35 Menzies NA, Berruti AA, Berzon R, Filler S, Ferris R, Ellerbrock T V, *et al.* The cost of providing comprehensive HIV treatment in PEPFAR-supported programs. *AIDS* 2011; 25:1753–60.

36 Menzies NA, Berruti AA, Blandford JM. The determinants of HIV treatment costs in resource limited settings. *PLoS One* 2012; 7:e48726.

37 Tager E. The cost of scaling-up antiretroviral treatment: a costing study in 161 representative facilities in Ethiopia, Malawi, Rwanda, and Zambia. In: *7th International AIDS Economics Network Pre-Conference Meeting, July 20-21*. Washington DC: ; 2012.

38 Marseille E, Giganti MJ, Mwango A, Chisembele-Taylor A, Mulenga L, Over M, *et al.* Taking ART to scale: determinants of the cost and cost-effectiveness of antiretroviral therapy in 45 clinical sites in Zambia. *PLoS One* 2012; 7:e51993.

39 Adhikari B, Kahende J, Malarcher A, Pechacek T, Tong V. Smoking-attributable mortality, years of potential life lost, and productivity losses--United States, 2000-2004. *MMWR* 2008; 57:1226–8.

40 Orzechowski and Walker. *The tax burden on tobacco, historical compilation volume 46, 2011*. Arlington, VA: Orzechowski and Walker; 2011.

41 DeCicca P, McLeod L. Cigarette taxes and older adult smoking: evidence from recent large tax increases. *J Heal Econ* 2008; 27:918–29.

42 DeCicca P, Kenkel D, Mathios A, Shin Y-J, Lim J-Y. Youth smoking, cigarette prices, and anti-smoking sentiment. *Heal Econ* 2008; 17:733–49.

43 DeCicca P, Kenkel D, Mathios A. Cigarette taxes and the transition from youth to adult smoking: smoking initiation, cessation, and participation. *J Heal Econ* 2008; 27:904–17.

44 Carpenter C, Cook PJ. Cigarette taxes and youth smoking: new evidence from national, state, and local Youth Risk Behavior Surveys. *J Heal Econ* 2008; 27:287–99.

45 Nonnemaker JM, Farrelly MC. Smoking initiation among youth: the role of cigarette excise taxes and prices by race/ethnicity and gender. *J Heal Econ* 2011; 30:560–7.

46 Gallet CA, List JA. Cigarette demand: a meta-analysis of elasticities. *Heal Econ* 2003; 12:821–35.

47 Thun MJ, Carter BD, Feskanich D, Freedman ND, Prentice R, Lopez AD, *et al.* 50-year trends in smoking-related mortality in the United States. *New Engl J Med* 2013; 368:351–64.

48 U.S. Centers for Disease Control and Prevention. *Behavioral Risk Factor Surveillance System survey data*. Atlanta GA: U.S. Department of Health and Human Services; 1984.

49 Holford TR, Meza R, Warner KE, Meernik C, Jeon J, Moolgavkar SH, *et al.* Tobacco control and the reduction in smoking-related premature deaths in the United States, 1964-2012. *JAMA* 2014; 311:164.

Chapter 2. Population health impact and cost-effectiveness of tuberculosis diagnosis with Xpert MTB/RIF, a dynamic simulation and economic evaluation

Abstract

Background: The Xpert MTB/RIF test enables rapid detection of tuberculosis and rifampicin resistance. The World Health Organization recommends Xpert for initial diagnosis in people suspected of having multidrug-resistant-TB or HIV-associated-TB, and many countries are moving quickly toward adopting Xpert. As roll-out proceeds, it is essential to understand the potential health impact and cost-effectiveness of diagnostic strategies based on Xpert.

Methods and Findings: We evaluated potential health and economic consequences of implementing Xpert in five southern African countries—Botswana, Lesotho, Namibia, South Africa and Swaziland—where drug resistance and TB-HIV coinfection are prevalent. Using a calibrated, dynamic mathematical model, we compared the status quo diagnostic algorithm, emphasizing sputum smear, against an algorithm incorporating Xpert for initial diagnosis, with results projected over 10- and 20-year time periods starting from 2012. Compared to status quo, implementation of Xpert would avert 132 [95% CI: 55-284] thousand TB cases and 182 [97-302] thousand TB deaths in southern Africa over 10 years following introduction, and reduce prevalence by 28% [14-40%] by 2022, with more modest reductions in incidence. Health system costs are projected to increase substantially with Xpert, by US$460 [294-699] million over 10 years. Antiretroviral therapy for HIV represents a substantial fraction of these additional costs, due to improved survival in TB/HIV-infected populations through better TB case-finding and treatment. Costs for treating MDR-TB are also expected to rise significantly with Xpert scale-up. Relative to status quo, Xpert has an estimated cost-effectiveness of US$959 [$633-$1,485] per DALY averted over 10 years. Across countries, cost-effectiveness ratios ranged from $792 [$482-$1,785] in Swaziland to $1,257 [$767-$2,276] in Botswana. Assessing outcomes over a 10 year period focuses on the near-term consequences of Xpert adoption, but the cost-effectiveness results are conservative, with cost-effectiveness ratios assessed over a 20-year time horizon approximately 20% lower than the 10-year values.

***Conclusions**:* Introduction of Xpert could substantially change TB morbidity and mortality through improved case-finding and treatment, with more limited impact on long-term transmission dynamics. Despite extant uncertainty about TB natural history and intervention impact in this setting, it is nonetheless clear that Xpert offers reasonable value for money based on conventional benchmarks for cost-effectiveness. However, the additional financial burden would be substantial, including significant increases in costs for treating HIV and MDR-TB. Given the fundamental influence of HIV on TB dynamics and intervention costs, care should be taken when interpreting the results of this analysis outside of high HIV prevalence settings.

2.1. Introduction

Tuberculosis (TB) remains a leading cause of global mortality and morbidity, with an estimated 9 million new TB cases and 1.5 million TB-related deaths in 2010 [1]. Although significant advances have been made in improving TB outcomes under the DOTS approach championed by the World Health Organization (WHO) and its partners in the Stop TB Partnership [2], continued progress is threatened by the inadequacy of existing diagnostic tools [3]. In most high-burden settings, TB diagnosis relies principally on sputum smear microscopy, which has limited sensitivity, especially among HIV-infected patients [4–6]. Traditional culture-based diagnosis and evaluation of drug sensitivity is relatively costly and slow [7,8], and many resource-limited settings lack the laboratory capacity to perform culture and sensitivity testing at high volume [9,10]. Lack of prompt diagnosis and appropriate treatment of TB increases the risks of transmission, drug resistance, and case fatality [11–13].

Recently, the Xpert MTB/RIF automated DNA test has been shown to provide rapid and sensitive detection of TB and rifampicin (RIF) resistance [14–17]. The Xpert test uses a cartridge-based system that integrates sample processing and real-time PCR, accommodates use by relatively unskilled healthcare workers, and provides results in <2 h [15,18]. In a large multicenter evaluation and subsequent implementation study, a single Xpert MTB/RIF test was found to identify >98% of patients with smear-positive TB and >70% of patients with smear-negative TB [14,15]. Sensitivity and specificity for RIF resistance were above 94% and 98%, respectively. More recent analyses have suggested that Xpert can greatly reduce the delay until treatment initiation for individuals with active TB [19].

In December 2010, WHO recommended that Xpert be used for initial diagnosis in patients suspected of having multidrug-resistant TB (MDR-TB) or HIV-associated TB disease [20]. By the end of May 2012, 66 of 145 countries eligible to purchase Xpert equipment at reduced prices had

already done so [21]. A volume-dependent price mechanism is being used for purchase of test cartridges [22], such that by August 2012 the ex-works price of Xpert cartridges had dropped to less than US$10 for eligible countries [23]. Whereas the global TB control community has moved quickly to embrace the new technology, several studies and commentaries have sounded important notes of caution concerning the cost of the technology, the demand it will place on existing infrastructure, and the challenge of addressing false positive indications of RIF resistance [24–30]. As implementation advances, evidence on the epidemiologic impact and cost-effectiveness of Xpert is urgently needed, particularly as the consequences of Xpert introduction may vary across epidemiologic settings and may depend on the specific diagnostic algorithms that are considered [31,32].

In this study we used a calibrated, dynamic mathematical model of TB to quantify the potential health and economic consequences of introducing Xpert in five southern African countries characterized by high prevalence of HIV infection and extant multidrug resistance. Comparing a diagnostic strategy based on Xpert to the status quo, we predicted changes in TB incidence, prevalence, mortality, and drug resistance; estimated health system costs; and assessed the incremental cost-effectiveness of Xpert adoption.

2.2. Methods

2.2.1. Overview

We evaluated the population health outcomes and health system costs associated with two alternative strategies for diagnosing TB, the first based on current diagnostic algorithms and the second based on implementing Xpert in accordance with current WHO recommendations. Comparisons between these two strategies were made using a calibrated mathematical model of

TB, reflecting key features of TB transmission dynamics and natural history, interactions with HIV infection, and patterns and trends in TB control interventions and treatment for HIV/AIDS. Model simulations were undertaken for five southern African countries: Botswana, Lesotho, Namibia, South Africa, and Swaziland. We assessed changes in epidemiological outcomes and health system costs over 10-y and 20-y time horizons, as well as the incremental cost-effectiveness ratio (ICER) of the Xpert strategy compared to the current algorithm.

2.2.2. Diagnostic strategies

A "status quo scenario" was created to represent the current diagnostic approach. Under this approach, all patients with suspected TB receive an initial sputum smear, and those diagnosed as smear-positive are directed to treatment. Sputum culture is indicated for patients with suspected TB who test smear-negative but who have a history of TB treatment or in whom there is a strong suspicion of TB. Drug sensitivity testing (DST) is indicated for treatment-experienced patients diagnosed with TB. Those who receive DST are initiated on a treatment regimen appropriate to their drug resistance profile, while those who do not receive DST are initiated on the standard first-line regimen. In the main analysis we assumed that the coverage of culture testing would be 20% (range 10%–30%) among smear-negative, treatment-naïve patients, and 80% (range 70%–90%) among smear-negative, treatment-experienced patients. We assumed further that 80% (range 70%–90%) of treatment-experienced patients diagnosed with TB would go on to receive DST. Given limited empirical data on country-specific coverage of culture and DST, these values were all varied across wide ranges in sensitivity analyses.

An "Xpert scenario" was constructed based on the diagnostic algorithms suggested for high HIV prevalence settings in the May 2011 WHO recommendations for Xpert implementation [33]. These recommendations suggest the use of Xpert as an initial diagnostic for all individuals of HIV-positive or unknown status. Given the high prevalence of HIV among patients with suspected TB in southern

Africa and the low number of individuals with a recent HIV test result [34], we modeled an algorithm in which Xpert was used as the initial diagnostic for all patients with suspected TB. According to this algorithm, such patients are first tested with a single Xpert assay, and no sputum smear is performed. Those testing TB-positive but negative for RIF resistance are initiated on a standard first-line regimen. Those testing positive for RIF resistance go on to receive DST. If the DST result indicates drug resistance, the individual is treated with a drug regimen tailored to the observed resistance profile. Under this scenario we assumed that scale-up to full coverage of Xpert within the national TB program would occur over the 3-y period starting in 2012. A diagram of the two alternative diagnostic algorithms is shown in Figure 2.1.

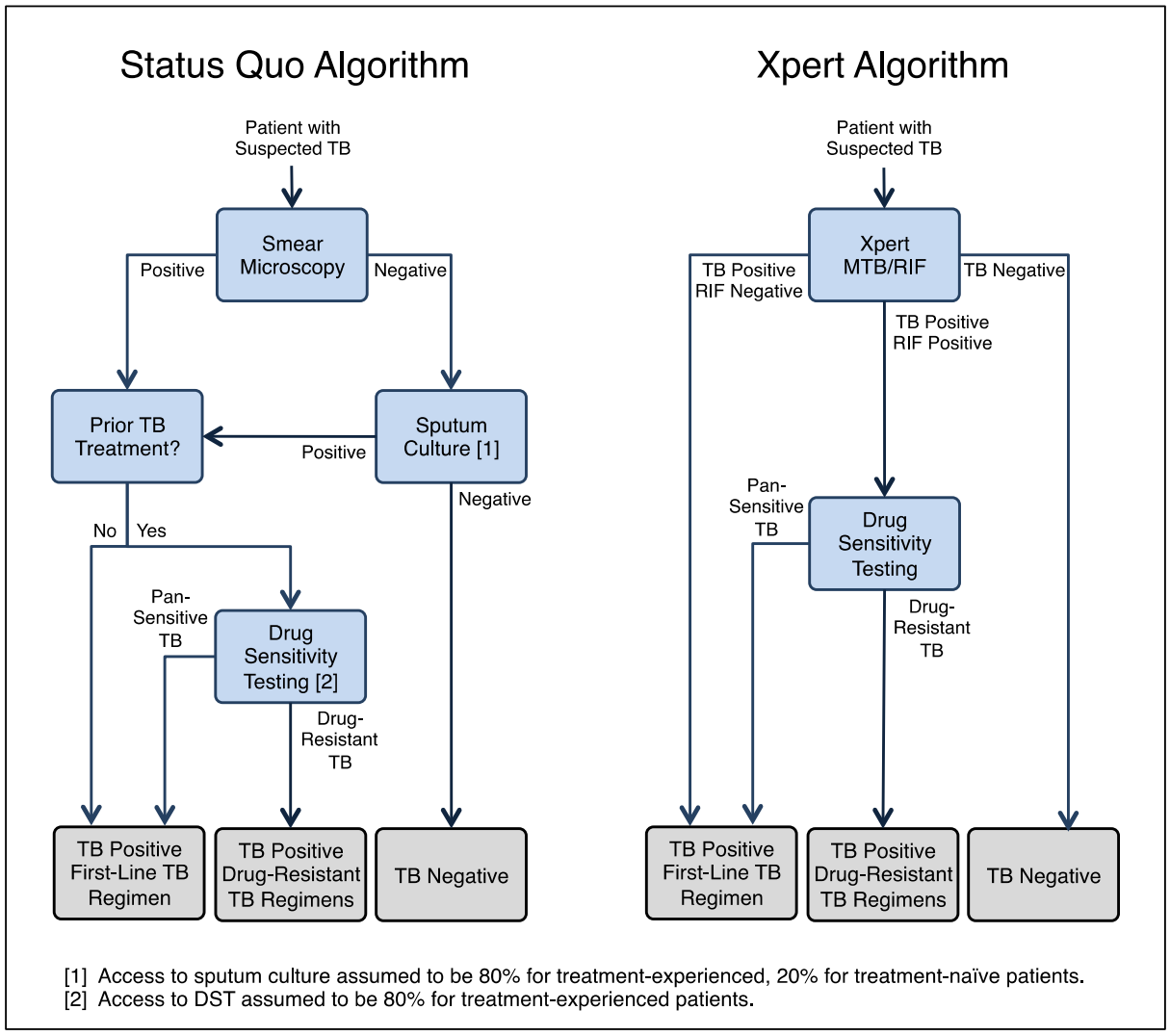

Figure 2.1. Status quo and Xpert diagnostic algorithms

2.2.3. Modeling approach

We developed a dynamic compartmental model of TB following the conventions of earlier models [35–41], with additional detail to accommodate evaluation of alternative diagnostic strategies. The model structure (Figure 2.2) is defined by a set of core TB states, and these states are further subdivided to account for (1) aspects of HIV infection, progression, and treatment relevant to TB

epidemiology; (2) multiple circulating TB strains, with different drug resistance profiles; and (3) tracking of TB treatment history.

2.2.3.1. Core TB states

The core TB model simulates the movements of individuals between states that capture important features of TB transmission, natural history, and treatment. Individuals enter the model in the susceptible state, where they face a risk of TB infection. The risk of infection is modeled as a time-dependent variable that reflects contact rates between infected and uninfected individuals, and transmission probabilities that allow for varying infectivity across different categories of active disease. Upon infection, individuals progress either directly to active disease or to latent infection. Individuals with latent infection may subsequently progress to active TB or be superinfected by a different TB strain. Active disease is categorized as smear-positive or smear-negative. Smear-negative cases may progress to smear-positive, and all individuals with active disease may spontaneously self-cure, which returns them to the latent/recovered state. An individual with active disease can be diagnosed as a TB case, according to the characteristics of the diagnostic algorithm, and initiated on treatment (as described in detail below). All individuals in the model are subject to a background mortality rate and to TB-related mortality specific to each active disease state.

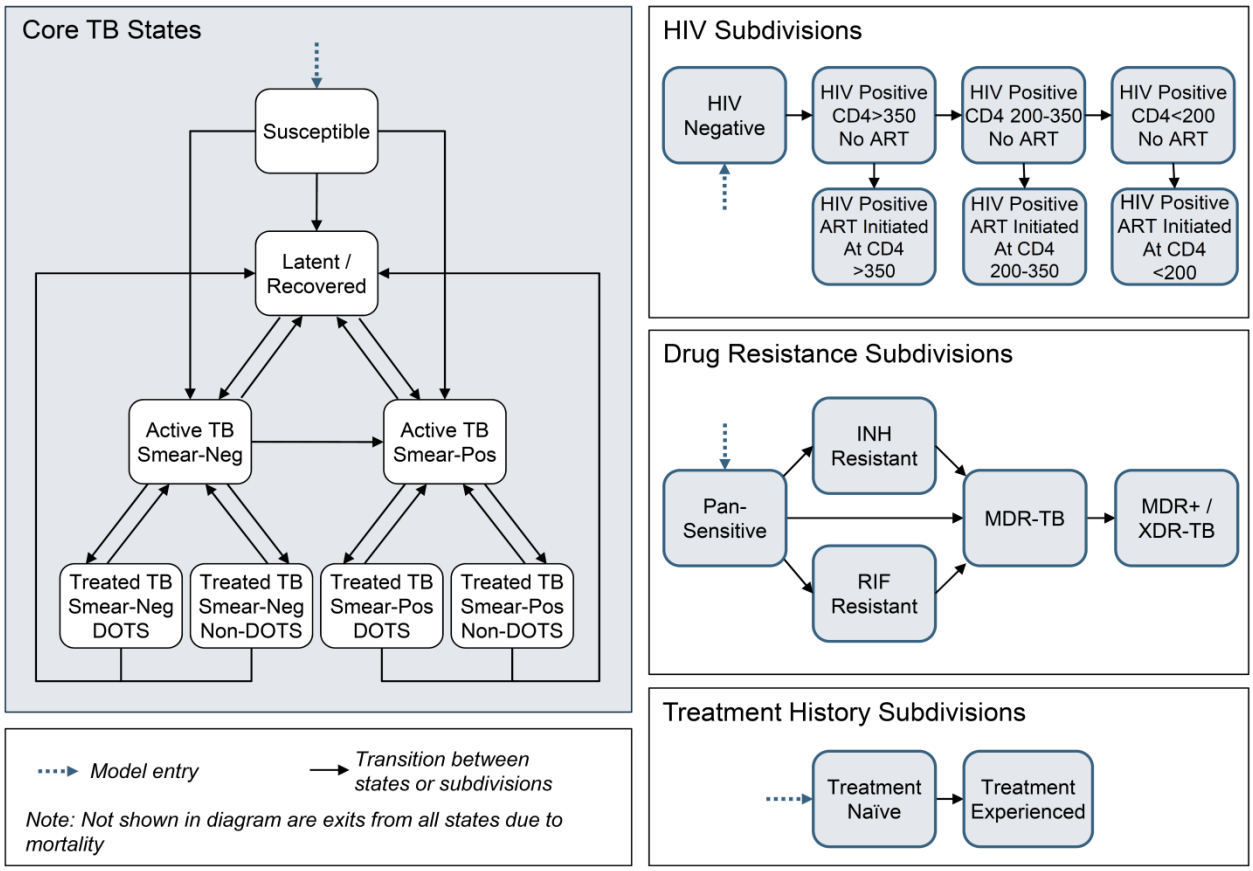

Figure 2.2. Model states, subdivisions, and transitions

2.2.3.2. HIV subdivisions

HIV coinfection can alter the natural history of TB, with HIV-infected individuals having a higher probability of primary progressive TB upon initial infection [42,43], a higher rate of breakdown from latent infection to active TB [44], a lower probability of smear-positivity amongst those with active disease [4–6], and higher mortality rates [4,45,46]. The HIV sub-model draws on model structure and key parameters from an array of published HIV models [47–50]. Seven HIV subdivisions were created, defined by CD4 cell count (>350 cells/μl, 200–350 cells/μl, and <200 cells/μl) and by whether or not an individual is receiving antiretroviral therapy (ART). HIV incidence is modeled as a transition from the HIV-negative category to the HIV-positive, CD4 count >350 cells/μl category, with time-varying incidence rates defined as exogenous model parameters.

HIV-positive individuals not on ART progress over time to subdivisions with lower CD4 counts. Untreated individuals transition onto ART at rates specific to their CD4 category. These rates are allowed to vary over time to capture changing eligibility criteria and coverage of testing and referral. HIV-related mortality occurs at rates specific to each subdivision.

2.2.3.3. Drug resistance subdivisions

Model states are further subdivided to account for differences in drug resistance among circulating TB strains, including (1) pan-sensitive TB, (2) isoniazid (INH) mono-resistant TB, (3) RIF mono-resistant TB, (4) TB resistant to both INH and RIF (MDR-TB), and (5) TB resistant to INH and RIF plus one or more second-line drugs (MDR+/XDR-TB). An individual in the susceptible state who is newly infected with TB transitions to the subdivision of the infecting strain. An individual with latent TB who is superinfected by a different strain transitions to the subdivision of the superinfecting strain. Individuals may also develop acquired drug resistance as a result of TB treatment, transitioning to subdivisions with broader resistance profiles.

2.2.3.4. Treatment history subdivisions

A final subdivision of model states distinguishes treatment-naïve from treatment-experienced individuals, as diagnostic algorithms may dictate different confirmatory tests depending on an individual's history of prior treatment. Individuals enter the model in the treatment-naïve subdivision, and all individuals exiting their first course of TB treatment (through default, failure, or cure) transition to the treatment-experienced subdivision.

The model is implemented as a series of difference equations with a monthly time step. A full description of model structure and equations is given in Section 2.6.

2.2.4. TB diagnosis and treatment

The model allows for TB diagnosis and treatment through the national TB DOTS program, or through non-DOTS providers functioning outside the national program. Uptake into treatment programs requires that individuals (1) present to a health facility and are identified as patients with suspected TB, (2) are diagnosed as active cases, and (3) are initiated on regimens determined by their background characteristics and information on drug sensitivity, if available. The model accounts for differences in test performance and information provided by each diagnostic algorithm, and for attrition between diagnosis and treatment, which varies depending on the delay to test results [51]. Individuals with false negative diagnoses for active TB will remain in the pool of undiagnosed active TB cases, with the possibility of presenting for diagnosis again. Individuals without active TB who attend with TB symptoms and are incorrectly diagnosed with active TB are assumed to undergo TB treatment, incurring costs but no positive or negative health effects. Algorithms for diagnosis and treatment in non-DOTS programs are assumed to be the same in both the status quo and Xpert scenarios, i.e., independent of the choice of diagnostic algorithm in the national DOTS program.

Individuals on TB treatment may successfully complete treatment, fail, default (become lost to follow-up), or die. Those who successfully complete treatment return to the latent/recovered state. A percentage of individuals failing therapy are identified as failures by the treatment program and reinitiate treatment, while all others return to active disease. Individuals who fail or default from treatment may acquire resistance to the drugs they have received. The model allows individuals with pan-sensitive TB to develop mono-INH-resistant TB, mono-RIF-resistant TB, or MDR-TB directly. Individuals with mono-INH- or mono-RIF-resistant TB can develop MDR-TB, and individuals with MDR-TB can develop MDR+/XDR-TB, with the rates of acquiring drug resistance dependent on a patient's TB drug regimen and current drug resistance profile (see Section 2.6).

2.2.5. Impact of diagnostic algorithms on TB epidemiology

Any change in diagnostic algorithm is assumed to impact TB epidemiology through two channels. The first major effect is via changes in the overall sensitivity and specificity of TB diagnosis. For the population with undiagnosed active TB, an improvement in diagnostic sensitivity results in improved case detection and reduced delay to treatment initiation and, consequently, increases survival and decreases the duration of infectiousness. The second major effect is via changes in the distribution of regimens received by newly diagnosed TB cases. Drug-resistant TB cases identified by an algorithm with better sensitivity for diagnosing resistance have a higher probability of being initiated on a more effective treatment regimen, which in turn improves cure rates, increases survival, and reduces the probability that a patient will return to an infectious state.

2.2.6. Estimation approach

We used a Bayesian estimation approach developed by Raftery and colleagues [52,53] and recently adopted by the Joint United Nations Programme on HIV/AIDS for HIV epidemic projections [54–56]. This approach provides a method for calibrating complex nonlinear models to reported data on disease burden, and for characterizing uncertainty in analysis results using Bayesian posterior intervals and similar metrics. These features are particularly important for our analysis, given the substantial uncertainty around many of the parameters describing TB epidemiology. We used this approach to calibrate the model to independent WHO estimates of TB incidence and prevalence in each of the five countries [57], and to data from drug resistance surveys available for all countries except Namibia [58]. The analysis was implemented using a sampling/importance resampling algorithm [52,55,59]. First, a large number of parameter sets were drawn from the joint prior distribution of the input parameters. For each of these parameter sets the model was run and a likelihood statistic calculated by comparing model outcomes to the corresponding calibration data. The likelihood for each parameter set was then used as the probability weight in a second-stage

resample of the parameter sets, which yielded draws representing the posterior parameter distribution, reflecting the information available on both model inputs and calibration data. The results of this simulation are similar to those produced by traditional Monte Carlo simulation and probabilistic sensitivity analyses, with the additional benefit of being constrained to be consistent with independent estimates on TB outcomes for each country. For each modeled outcome, uncertainty intervals were calculated by taking the 2.5th and 97.5th percentiles of the distribution for this outcome generated by the the resampled parameter sets, and the point estimate calculated by taking the arithmetic mean of this distribution (see Section 2.6 for further detail).

2.2.7. Model parameter values

We parameterized the model using historical demographic and epidemiologic data available for each country. Parameter values relating to population demographics were derived from United Nations Population Division estimates and projections. Parameter values relating to TB transmission dynamics were chosen to be consistent with data and assumptions used in earlier TB models [35–41]. Parameter values relating to TB program coverage and treatment outcomes were derived from published reporting data [57]. Key parameter values relating to TB diagnosis and treatment are summarized in Table 2.1. Estimates for HIV incidence and ART access between 1983 and 2010 were derived from unpublished data provided by the Joint United Nations Programme on HIV/AIDS. Future ART access was assumed to increase from current levels to the WHO universal access target of 80% coverage [60] over the course of 10 y. For Botswana, which was providing ART to an estimated 83% of those in need by 2009, coverage was maintained at current levels. ART eligibility was initially limited to individuals with CD4 count <200 cells/μl and then extended to include those with a CD4 count in the range 200–350 cells/μl from 2010 onward, consistent with the expansion of ART eligibility in WHO HIV treatment guidelines [61,62]. A full description of all parameters in the model is provided in Section 2.6.

Table 2.1. Selected model parameter values and ranges

Description	Base-Case Value	Range	Source
Sensitivity of sputum smear microscopy			
Smear-negative TB	0.0	—	
Smear-positive TB	1.0	—	Assumed[a]
Specificity of sputum smear microscopy	0.974	(0.965–0.982)	[82]
Sensitivity of sputum culture	1.0	—	Assumed[b]
Specificity of sputum culture	0.984	(0.978–0.989)	[83]
Sensitivity of Xpert for TB			
Smear-negative TB	0.725	(0.655–0.788)	
Smear-positive TB	0.982	(0.969–0.991)	[14]
Specificity of Xpert for TB	0.992	(0.982–0.997)	[14]
Sensitivity of Xpert for RIF resistance	0.976	(0.946–0.992)	[14]
Specificity of Xpert for RIF resistance	0.981	(0.966–0.990)	[14]
Probability of sputum culture following a negative sputum smear (status quo)			
Treatment-naïve patients	0.20	(0.11–0.31)	
Treatment-experienced patients	0.80	(0.69–0.89)	[84]
Probability of DST following a positive TB diagnosis (status quo algorithm)			
Treatment-naïve patients	0.00	—	
Treatment-experienced patients	0.80	(0.69–0.89)	[84]
Probability of loss to follow-up between presentation and treatment initiation			
With prompt diagnosis (smear, Xpert)	0.15	(0.09–0.24)	
With delayed diagnosis (culture, DST)	0.25	(0.14–0.39)	[51]
Background mortality rate (ages 15+ y)	Time-varying	—	WHO unpublished data
Excess mortality rate, active TB			
Smear-negative	0.21	(0.18–0.25)	
Smear-positive	0.30	(0.21–0.41)	[38]

Table 2.1. Selected model parameter values and ranges (continued)

Description	Base-Case Value	Range	Source
Excess mortality rate, HIV			
CD4 >350, no ART	0. 008	(0.005–0.012)	
CD4 200–350, no ART	0.030	(0.018–0.048)	
CD4 <200, no ART	0.230	(0.136–0.366)	
On ART initiated at CD4 >350	0.008	(0.005–0.012)	
On ART initiated at CD4 200–350	0.023	(0.014–0.037)	
On ART initiated at CD4 <200	0.050	(0.031–0.076)	[85–90]
Excess mortality rate, CD4<200, active TB	0.80	(0.472–1.272)	[45,46]
Per-test cost of Xpert	$20, $30, $40	Fixed[c]	[33,64,65]
Per-test cost of smear diagnosis			
Botswana	$6.13	(4.18–8.68)	
Lesotho	$3.31	(2.26–4.68)	
Namibia	$5.31	(3.63–7.51)	
South Africa	$5.94	(4.06–8.39)	
Swaziland	$4.24	(2.90–5.99)	[51,91–97]
Per-test cost of culture			
Botswana	$15.83	(13.07–18.99)	
Lesotho	$8.56	(7.07–10.27)	
Namibia	$13.72	(11.33–16.46)	
South Africa	$15.33	(12.66–18.39)	
Swaziland	$10.94	(9.04 -13.13)	[51,91,93,94,97]
Per-test cost of chest X-ray			
Botswana	$16.69	(11.35–23.70)	
Lesotho	$9.03	(6.14–12.81)	
Namibia	$14.46	(9.83–20.52)	
South Africa	$16.16	(10.99–22.94)	
Swaziland	$11.54	(7.85–16.38)	[91,96,98]

Table 2.1. Selected model parameter values and ranges (continued)

Description	Base-Case Value	Range	Source
Per-test cost of DST			
Botswana	$81.97	(61.44–107.17)	
Lesotho	$44.32	(33.22–57.94)	
Namibia	$71.02	(53.24–92.85)	
South Africa	$79.37	(59.50–103.77)	
Swaziland	$56.65	(42.47–74.07)	[7,99]
Cost of outpatient diagnostic visit			
Botswana	$10.32	(6.09–16.40)	
Lesotho	$2.94	(1.73–4.67)	
Namibia	$7.99	(4.71–12.70)	
South Africa	$10.30	(6.08–16.39)	
Swaziland	$6.21	(3.66–9.87)	[100]
Cost of outpatient treatment visit			
Botswana	$6.85	(4.04–10.89)	
Lesotho	$1.95	(1.15–3.10)	
Namibia	$5.31	(3.13–8.44)	
South Africa	$6.85	(4.04–10.89)	
Swaziland	$4.13	(2.44–6.57)	[100]
Cost of inpatient care, per day			
Botswana	$38.99	(23.00–61.99)	
Lesotho	$8.78	(5.18–13.96)	
Namibia	$28.76	(16.97–45.73)	
South Africa	$39.38	(23.23–62.61)	
Swaziland	$21.91	(12.93–34.84)	[100]
Monthly TB regimen cost			
First-line	$5.86	(3.46–9.32)	
Mono-INH resistant	$18.02	(10.63–28.65)	
Mono-RIF resistant	$33.91	(20.01–53.92)	
MDR-TB	$119.37	(70.43–189.79)	
MDR+/XDR-TB	$179.06	(105.64–284.70)	[63]

Table 2.1. Selected model parameter values and ranges (continued)

Description	Base-Case Value	Range	Source
Monthly cost of ART			
Botswana	$104.97	(84–80–128.48)	
Lesotho	$69.63	(57.22–83.92)	
Namibia	$94.68	(76.78–115.52)	
South Africa	$102.53	(82.90–125.40)	
Swaziland	$81.20	(66.25–98.52)	[63,101–105]
Disability weights			
Active TB	0.271	(0.151–0.422)	
HIV-positive, CD4 >350, no ART	0.135	(0.078–0.213)	
HIV-positive, CD4 200–350, no ART	0.320	(0.176–0.496)	
HIV-positive, CD4 <200, no ART	0.505	(0.252–0.757)	
HIV-positive, ART initiated at CD4 >350	0.135	(0.078–0.213)	
HIV-positive, ART initiated at CD4 200–350	0.151	(0.087–0.238)	
HIV-positive, ART initiated at CD4 <200	0.167	(0.096–0.262)	[66,67]

All costs are given in 2011 US dollars.

[a] As smear status is tracked in the model, the sensitivity of sputum smear for individuals classed as smear-negative and smear-positive is 0% and 100% (respectively) by construction.

[b] As sputum culture is the gold standard for TB detection, the sensitivity is assumed to be 100%.

[c] As the per-test cost of Xpert is of key interest to policy-makers (and potentially subject to price negotiation), the results of the analyses are presented for three separate values for the Xpert cost.

2.2.8. Measurement of resource use and costs

Costs were assessed from a health system perspective and expressed in 2011 US dollars. Costs reflected resources used to deliver TB diagnosis and treatment, as provided by both public and private providers, and resources used in providing ART to HIV-infected individuals. An ingredients approach to costing was used, by which the total cost to provide a particular diagnostic procedure

or a course of treatment was calculated by estimating the number of units of each specific type of resource input needed to deliver the service, multiplying each quantity by the corresponding unit cost of that resource input, and summing across all inputs.

Average costs for each type of service are shown in Table 2.1. Cost estimates extrapolated from the literature were adjusted for inflation, currency conversions, and price levels, where relevant. Treatment costs for TB and HIV included drugs, clinic visits, and monitoring tests, including regular smear examinations during TB treatment. Drug costs were derived from the WHO price reporting mechanism [63]. Costs for laboratory tests (excluding Xpert) were derived from the literature. Numbers of treatment monitoring visits and laboratory tests followed a previous global analysis [35]. For Xpert, estimates in WHO implementation guidelines [33] suggest an economic cost of US$25–US$35 per test in southern Africa (including consumables, equipment, personnel, transport, facilities, and managerial overheads). This range of estimates is consistent with the results from a cost analysis conducted for the South African national program, which found a cost range of US$25–US$33 [64], as well as an analysis of potential implementation strategies that reported costs of US$27 per patient with suspected TB for placement of equipment at central laboratories and US$39 for placement of equipment at point of care [65]. Costs of Xpert may continue to change as volume increases, through reductions in the prices of equipment and consumables [22,23], economies of scale, and accumulated implementation experience; we therefore conducted analyses using Xpert per-test costs of US$20, US$30, and US$40.

2.2.9. Outcomes

We estimated trends in population-level epidemiological outcomes including TB prevalence, incidence, mortality, and resistance to anti-TB drugs, prior to Xpert introduction in 2012, and over the subsequent 20-y period. Summary outcome measures computed based on population survivorship in the model included life-years and disability-adjusted life-years (DALYs), the latter

incorporating disability weights from the Global Burden of Disease study [66,67]. We evaluated the cost-effectiveness of introducing Xpert in terms of the ICER, expressed as the difference in total costs between the Xpert and status quo scenarios, divided by the difference in life-years or DALYs between the two scenarios. Cost-effectiveness ratios were computed over both 10-y and 20-y time horizons following Xpert introduction, in each case based only on the costs and health outcomes accrued during that period. Costs and health benefits were discounted at an annual rate of 3% [68,69]. Following standard benchmarks proposed in international work on cost-effectiveness, we compared the ICER to thresholds for cost-effectiveness defined in reference to the annual gross domestic product (GDP) per capita in each country. Interventions are considered to be highly cost-effective when they have ICERs that fall below the annual per-capita GDP, and are regarded as being potentially cost-effective if they have ICERs between one and three times annual per-capita GDP [70].

2.2.10. Sensitivity analysis

The sensitivity of the model to changes in individual parameters was investigated through traditional one-way sensitivity analyses as well as by computing partial rank correlation coefficients across the set of simulation results produced by the Bayesian uncertainty analysis [38,71,72]. For the one-way sensitivity analyses, we computed the change in the ICER (calculated over a 10-y time horizon) that would occur when we changed one parameter value by ±1 standard deviation from its posterior mean value while holding all other parameter values at their posterior means. We also conducted an array of additional sensitivity analyses that varied assumptions regarding the diagnostic algorithms being compared, the use of inpatient care as part of MDR-TB treatment, future ART coverage decisions, and trends in antiretroviral drug prices.

Finally, we conducted a probabilistic sensitivity analysis to assess the uncertainty around the optimal choice of diagnostic strategy resulting from the joint effects of uncertainty around all input

parameters simultaneously, and these results are presented as posterior intervals around key model outcomes and as cost-effectiveness acceptability curves.

2.3. Results

2.3.1. Epidemiological projections under the current diagnostic algorithm

Figure 2.3 shows estimates and projections for TB prevalence and incidence in the southern Africa region from 1990 through the end of 2032, under the assumption that the current (status quo) diagnostic algorithm is used over the whole period. The results for individual countries followed the general trend seen in the regional results, with historical declines in TB prevalence and incidence reversed over the period 1995–2010 as a consequence of concurrent HIV epidemics. The magnitude of the TB epidemic differed across individual countries, with Lesotho having the lowest prevalence and incidence and Swaziland the highest.

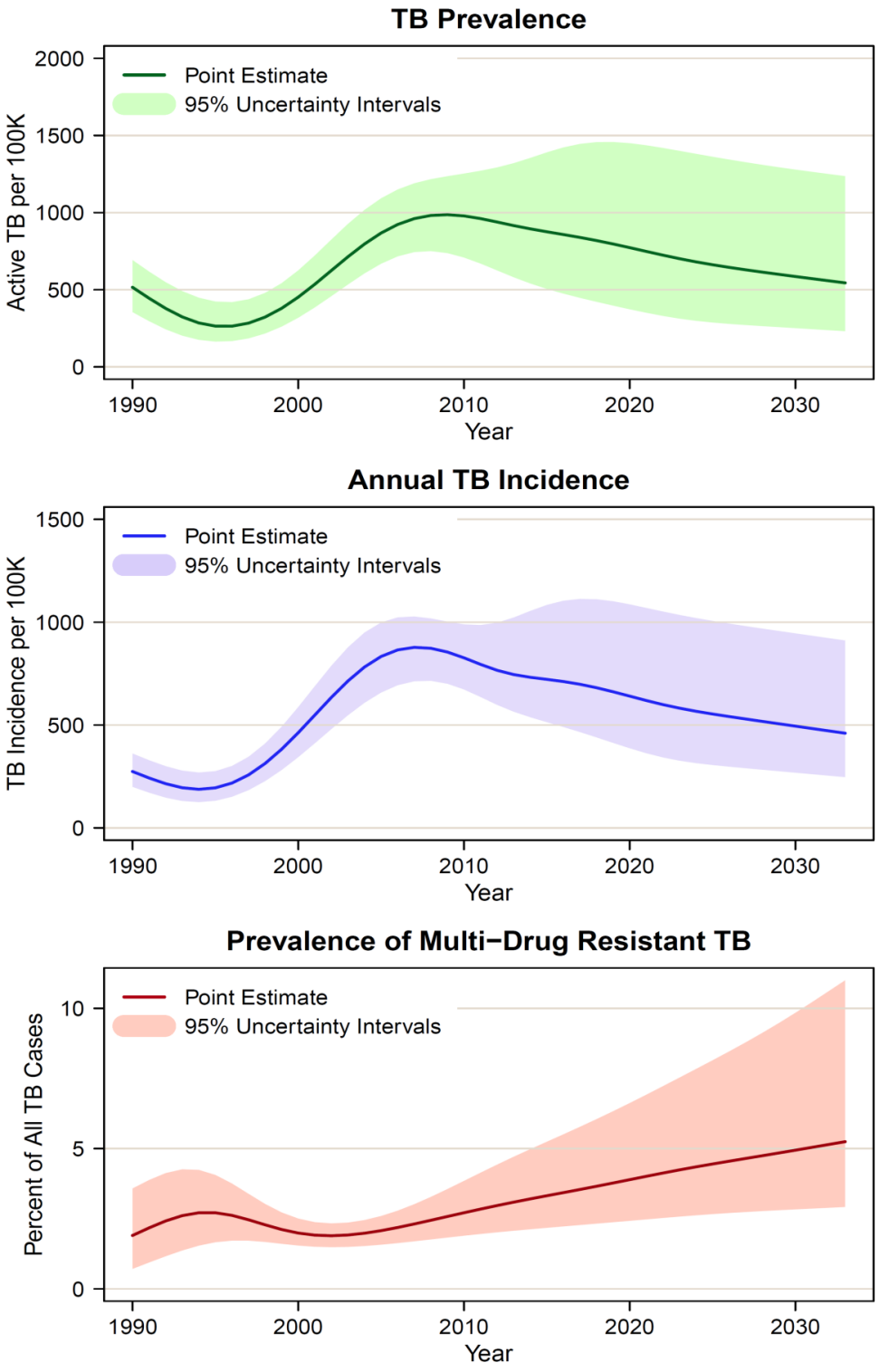

Figure 2.3. Estimated and projected TB prevalence, TB incidence, and multidrug-resistant TB prevalence in southern Africa under status quo diagnostic algorithm, 1990–2032

2.3.2. Performance of diagnostic algorithms

Based on our model simulations, the positive predictive value for Xpert diagnosis of active TB, at full coverage by 2014, would be 96.9% (95% CI: 93.4–98.7), compared to 88.4% (81.5–93.1) for the status quo algorithm. The negative predictive values for Xpert and the status quo would be 93.9% (88.8–97.2) and 79.3% (67.6–87.9), respectively. We estimate the positive predictive value for the diagnosis of RIF resistance by Xpert to be 67.3% (51.3–82.0) and the negative predictive value 99.9% (99.8–100.0). The relatively low positive predictive value indicates that Xpert is expected to produce a number of false positive diagnoses of RIF resistance, with relatively modest implications for treatment outcomes, as we assume that a subsequent DST is required before individuals receive an MDR-TB diagnosis. Under the Xpert algorithm, 5.8 (95% CI: 3.8–9.2) patients are tested for TB for each active case starting treatment, compared to 7.5 (4.9–12.1) under the status quo, a consequence of improved sensitivity in the Xpert algorithm. The average duration of infectiousness is 9.9 mo (95% CI: 6.7–14.0) under the Xpert algorithm compared to 12.8 mo (9.6–14.0) under the status quo. The benefit of the reduced duration of infectiousness is primarily accrued among individuals with smear-negative TB, for whom the duration of infectiousness is reduced from 19.3 mo (13.8–24.6) under the status quo to 12.1 mo (7.8–18.0) under the Xpert scenario. Results for those with smear-positive disease are comparable under both scenarios. Treatment effectiveness (the probability of cure for individuals starting treatment) rises only marginally under the Xpert scenario, with the probability of cure 2.7 (95% CI: 1.6–4.4) percentage points higher than in the status quo scenario. Table 2.2 presents estimates for the average cost per programmatic outcome for the status quo and Xpert strategies, summed over the first 10 y of Xpert implementation (2012–2022). These results show that adopting the Xpert algorithm increases the cost of achieving various diagnostic and treatment outcomes.

Table 2.2. Average programmatic outcomes and costs over 10 years following choice of strategy (2011 US dollars)*

	Status quo strategy	Xpert strategy
Programmatic measures for DOTS diagnosis		
Average annual DOTS diagnosis costs (US $, millions)	27 [15 –46]	37 [21 –61]
Average annual TB suspects (000s)	892 [519– 1,508]	829 [487 – 1,400]
Average annual true positive diagnoses (000s)	151 [100– 215]	175 [120 – 245]
Average diagnosis cost per suspect (US $)	31 [25 – 38]	45 [40 – 50]
Average diagnosis cost per true positive diagnosis (US $)	181 [117 – 287]	211 [136 – 334]
Programmatic measures for DOTS treatment		
Average annual DOTS treatment costs (US $, millions)	57 [30 – 102]	81 [42 – 137]
Average treatment volume (000s)	57 [38– 85]	69 [48– 100]
Average annual true positive treatment initiations (000s)	122 [81 – 175]	147 [103– 206]
Average annual cures (000s)	100 [66– 146]	121 [84– 172]
Average treatment cost per month (US $)	84 [59 – 135]	98 [67 – 147]
Average treatment cost per TB case initiated (US $)	469 [321 – 761]	556 [371 –861]
Average treatment cost per TB case cured (US $)	575 [396 – 914]	675 [461 – 1,008]

* Results are based on $30 Xpert per-test cost. Range in brackets represents the 95% posterior interval for each estimate.

2.3.3. Population health impact of introducing Xpert

Introduction of Xpert is projected to produce immediate and sustained changes in TB epidemiology (Figure 2.4). Within 10 y after the introduction of Xpert, prevalence would be lower by 186 (95% CI: 86–350) per 100,000 (28% [95% CI: 14–40]), incidence by 35 (13–79) per 100,000 (6% [2–13]), and annual TB mortality by 50 (23–89) per 100,000 (21% [10–32]), compared to status quo projections. The absolute number of MDR-TB cases after 10 y would be lower by 25% (6–44) in the Xpert scenario compared to the status quo scenario. The decline in MDR-TB cases parallels the

overall decline in TB prevalence in these projections. There is no significant change expected in MDR-TB as a percentage of all TB under the Xpert scenario (4.3% [−17.5 to 34.6] greater after 10 y). Figure 2.5 shows the incremental differences between Xpert and the status quo for these health outcomes, including uncertainty intervals around these differences.

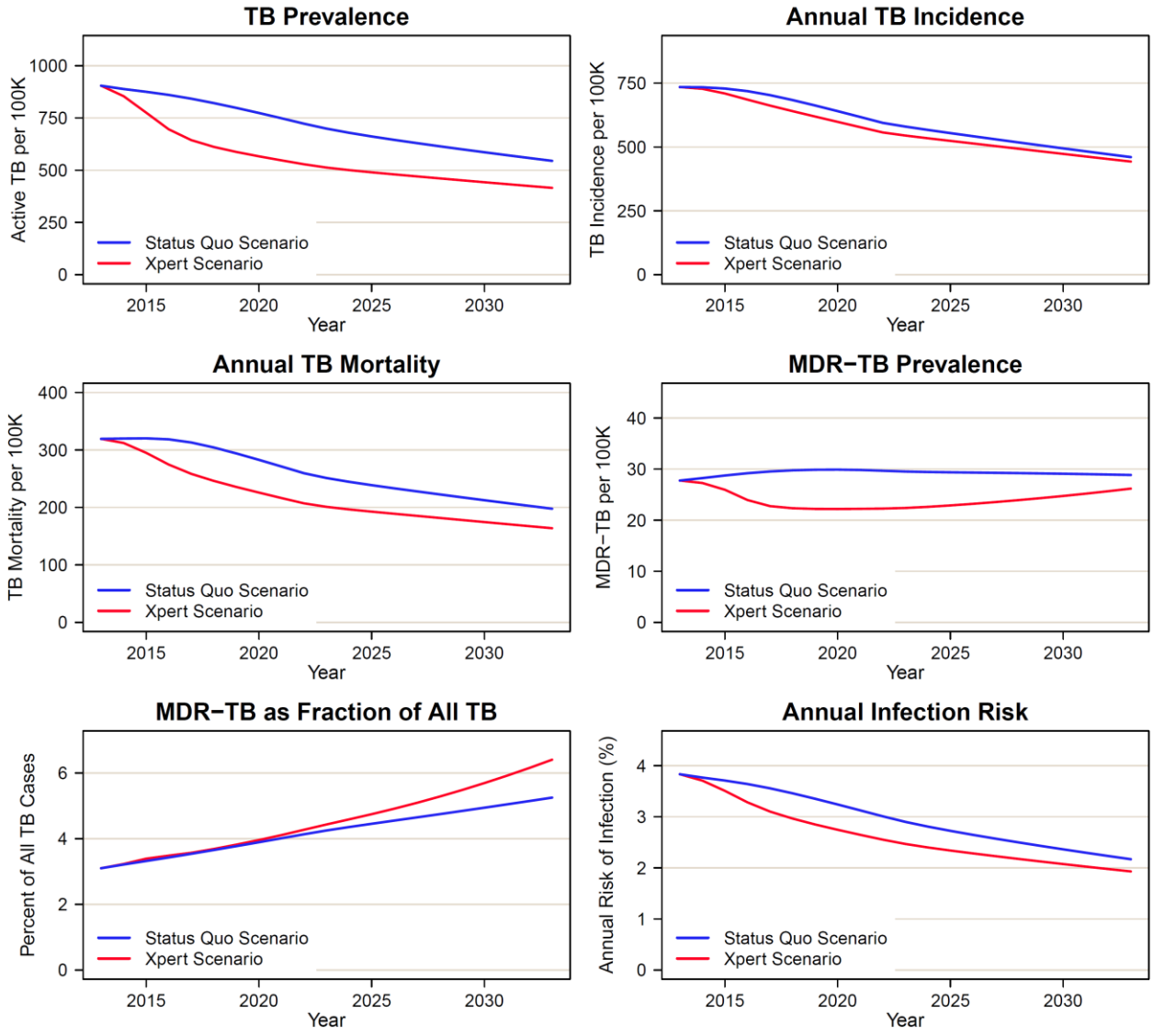

Figure 2.4. Epidemiologic outcomes in Xpert and status quo scenarios, 2012–2032

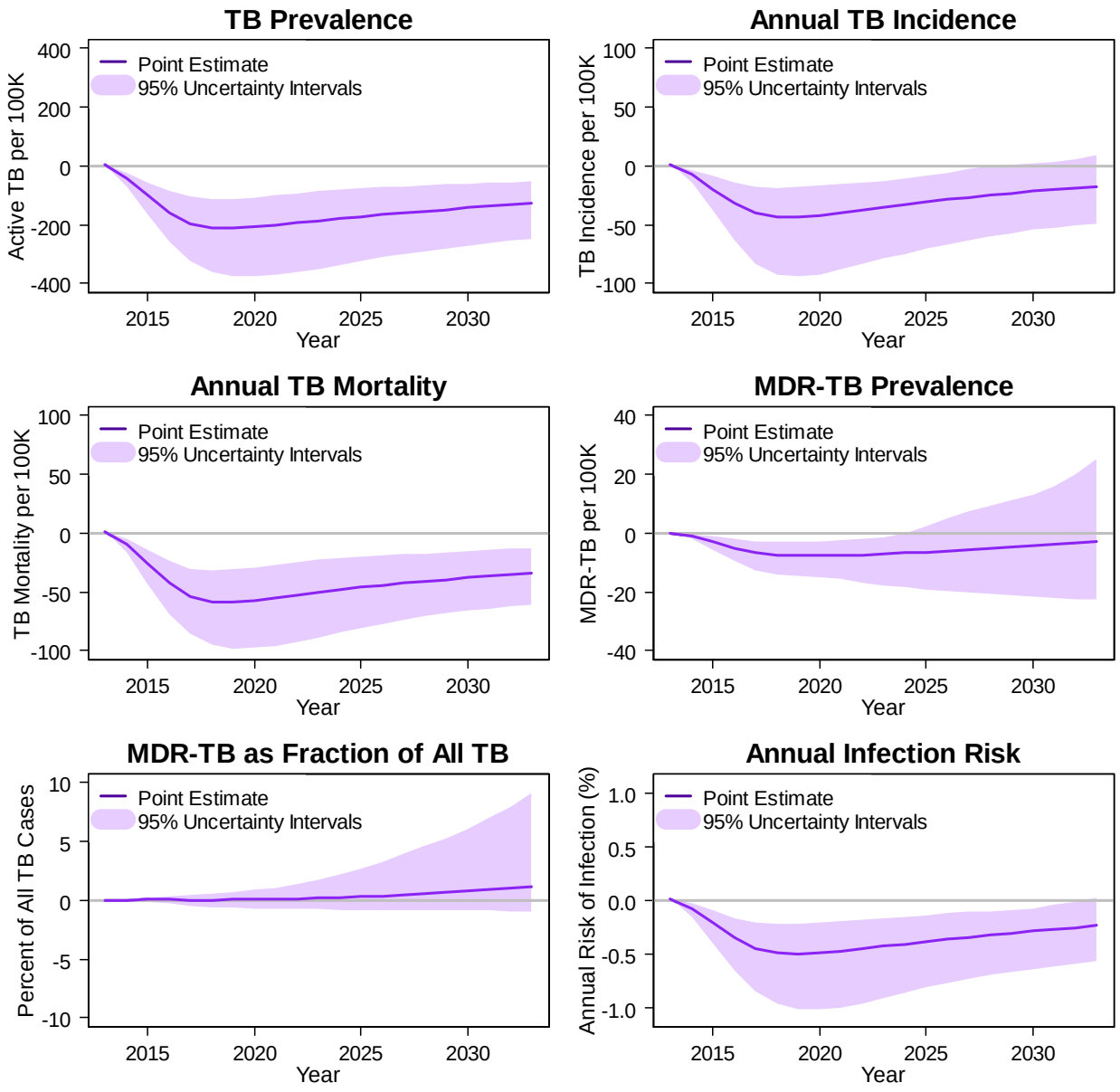

Figure 2.5. Incremental difference in epidemiologic outcomes between Xpert and status quo scenarios, 2012-2032

Summing the health effects of Xpert introduction over the first 10 y of implementation, this strategy is estimated to prevent 132,000 (95% CI: 55,000–284,000) of the estimated 2.6 million (1.7–4.3 million) new TB cases and 182,000 (97,000–302,000) of the estimated 1.2 million (0.6–2.0 million) TB deaths projected for southern Africa under the status quo.

2.3.4. Health system costs of introducing Xpert

Figure 2.6 shows the additional annual costs associated with the Xpert scenario compared to the status quo, subdivided by type of cost.

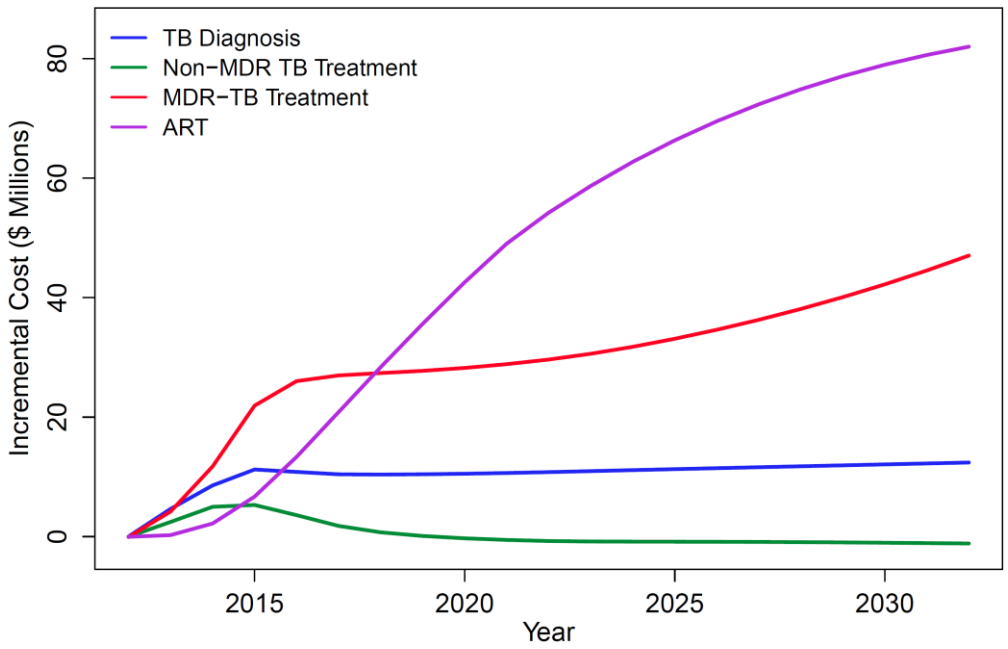

Figure 2.6. Incremental costs of Xpert strategy (based on US$30 Xpert per-test cost) compared to status quo strategy, by cost category, 2012–2032 (2011 US dollars)

TB program costs rise rapidly as Xpert scales up to full coverage over 2012–2015. While implementation of Xpert requires increased spending on TB diagnosis and treatment, the major financial impact of Xpert introduction in this region is on HIV treatment programs. This is because prompt TB treatment extends survival among TB/HIV-coinfected individuals, leading to increases in HIV treatment demand. The model predicts that at 10 y after Xpert introduction, HIV treatment costs will comprise 58% (95% CI: 40–72) of the total incremental costs associated with the Xpert strategy (assuming an Xpert per-test cost of US$30). Considering only the additional costs incurred by national DOTS programs, almost three-quarters (71% [47–87]) of these will be due to growth in

TB treatment costs, with almost all of this increase coming from a higher volume of MDR-TB treatment.

2.3.5. Cost-effectiveness of Xpert strategy versus the status quo

Table 2.3 shows ICERs for the Xpert strategy versus the status quo strategy under 10-y and 20-y analytic horizons and a range of Xpert costs. Assuming an Xpert cost of US$30 per test, the Xpert scenario is expected to avert approximately half a million DALYs during the first 10 y following introduction, at a cost of US$959 (95% CI: 633–1,485) per DALY averted.

Figure 2.7 presents the costs per DALY averted through implementation of Xpert in each of the five southern African countries. In almost all cases, the cost-effectiveness ratios fall below the standard benchmarks for cost-effectiveness suggested by WHO, whereby interventions with cost-effectiveness ratios less than three-times annual per-capita GDP are regarded as potentially cost-effective, and interventions with cost-effectiveness ratios less than annual per-capita GDP are deemed very cost-effective. Among these five countries, per-capita GDP in 2010 ranged from above US$7,000 in South Africa and Botswana down to US$982 in Lesotho [73].

Table 2.3. Cost-effectiveness results for Xpert compared to status quo in southern Africa*

Outcome	Xpert cost = US$20		Xpert cost = US$30		Xpert cost = US$40	
10-year analytic horizon (costs and benefits summed over 2012-2022)						
Incremental costs, health System (US $, millions)	401	[248 – 623]	460	[294 – 699]	520	[333 – 772]
Incremental costs, DOTS program only (US $, millions)	225	[119 – 378]	284	[166 – 448]	344	[209 – 522]
Incremental life-years Saved (000s)	421	[234 –679]	421	[234 –679]	421	[234 –679]
Incremental DALYs averted (000s)	480	[261 – 809]	480	[261 – 809]	480	[261 – 809]
Incremental cost per life-year saved*	952	[606 – 1,326]	1,093	[746 – 1,592]	1,234	[836 – 1,872]
Incremental cost per DALY averted*	836	[531 – 1,223]	959	[633 – 1,485]	1,083	[716 – 1,760]
20-year analytic horizon (costs and benefits summed over 2012-2032)						
Incremental costs, health System (US $, millions)	1,103	[594 – 1,979]	1,217	[691 – 2,093]	1,330	[784 – 2,205]
Incremental costs, DOTS program only (US $, millions)	481	[205 – 993]	594	[295 – 1,125]	707	[379 – 1,262]
Incremental life-years Saved (000s)	1,500	[800 – 2,570]	1,500	[800 – 2,570]	1,500	[800 – 2,570]
Incremental DALYs averted (000s)	1,550	[800 – 2,770]	1,550	[800 – 2,770]	1,550	[800 – 2,770]
Incremental cost per life-year saved*	734	[459 – 1,173]	810	[504 – 1,311]	885	[557 – 1,467]
Incremental cost per DALY averted*	711	[422 – 1,187]	784	[476 – 1,345]	857	[523 – 1,534]

* Incremental cost-effectiveness ratios calculated using health system costs (includes DOTS costs). Both costs and health outcomes discounted at 3%. Range in brackets represents the 95% posterior interval for each estimate.

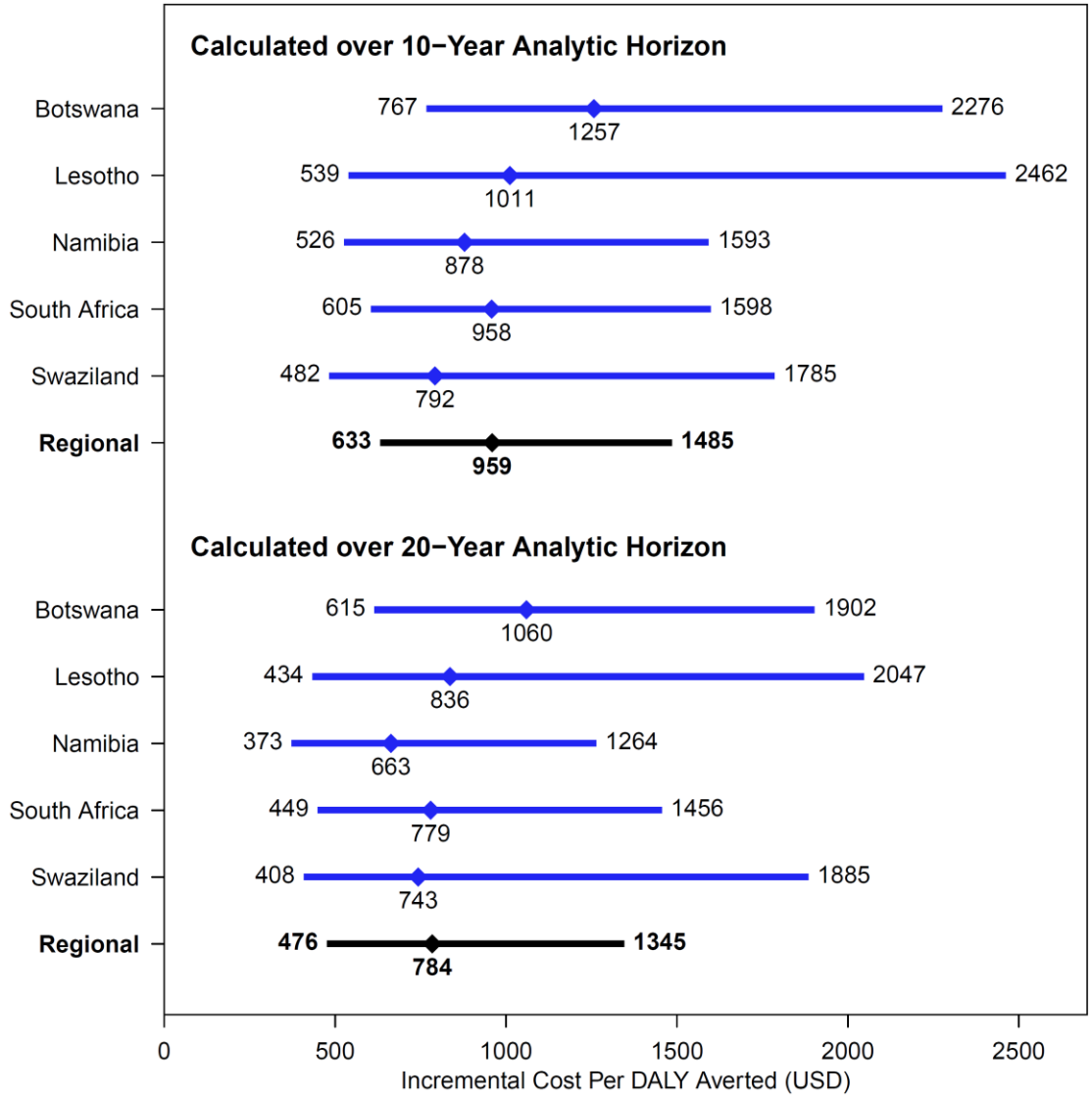

Figure 2.7. Cost-effectiveness of Xpert strategy compared to status quo strategy in five southern African countries (2011 US dollars)*

*For each ratio, the diamond indicates the point estimate (mean incremental costs divided by mean incremental DALYs averted), and the bar indicates the width of the 95% posterior interval. Results based on US$30 Xpert per-test cost.

2.3.6. Sensitivity analyses

We conducted one-way sensitivity analyses for all model inputs. Figure 2.8 shows the results for South Africa for the ten parameters producing the greatest variation in the cost-effectiveness ratio when varied by ±1 standard deviation from their posterior means. A complete listing of these one-way sensitivity analyses for each country is given in Tables 2.6-2.10.

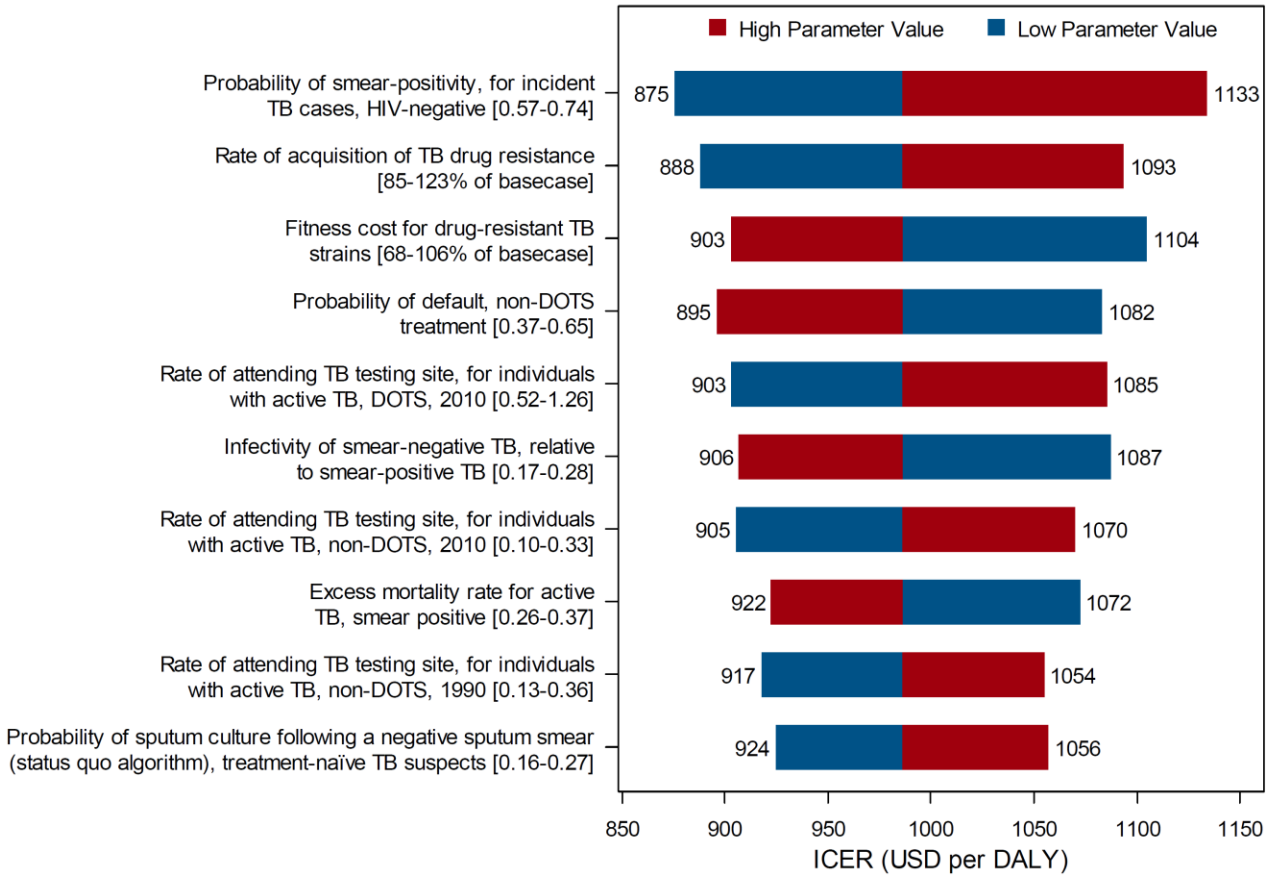

Figure 2.8. Results from univariate sensitivity analyses, showing 10 parameters with greatest influence on the cost-effectiveness of Xpert compared to status quo, South Africa*

* Sensitivity analyses on the incremental cost per DALY averted (2011 US dollars [US $]) over a 10-y analytic horizon, assuming a US$30 Xpert per-test cost. In each one-way analysis, one parameter was varied ±1 standard deviation from its posterior mean, with all other variables fixed at their posterior means.

While the overall uncertainty in model results—as expressed in the posterior intervals and in the cost-effectiveness acceptability curves described below—is not small, the uncertainty generated by any individual parameter is relatively small, and does not change the general conclusions of the study. Complete results, by country, for the one-way sensitivity analyses on all parameters are reported in Section 2.6. Partial rank correlation coefficients, which reflect a probabilistic approach to identifying influential parameters, were calculated for all model inputs based on the simulation results, and yielded conclusions that were largely consistent with those based on the one-way sensitivity analyses (results for South Africa presented in Figure 2.9).

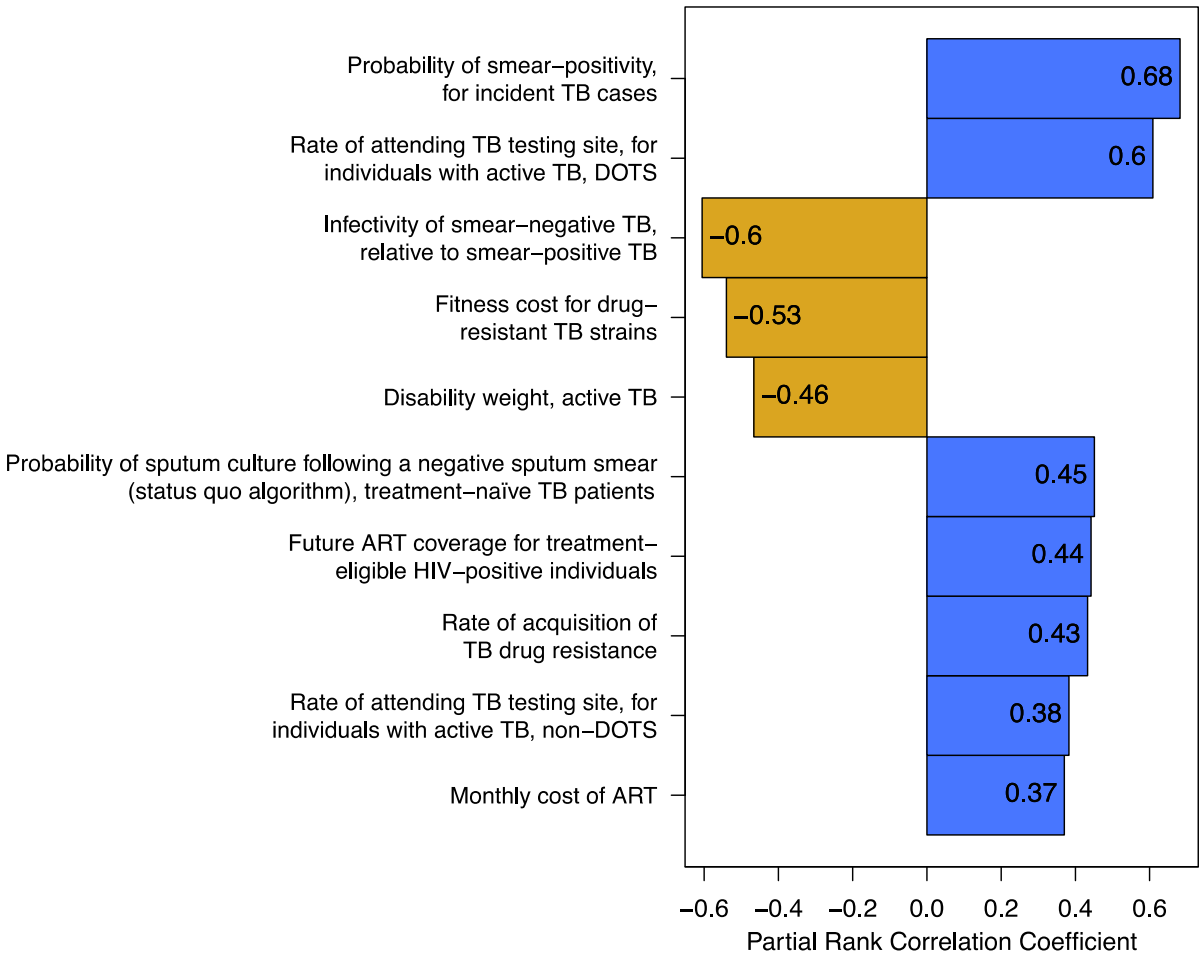

Figure 2.9. Partial rank correlation coefficients for 10 parameters with greatest influence on the cost-effectiveness of Xpert compared to status quo, South Africa, 10-year time horizon

The cost-effectiveness ratios presented in Table 2.3 and Figure 2.7 attempt to capture the major changes in health system resource use and health outcomes resulting from the adoption of the Xpert algorithm, including increases in TB treatment and HIV treatment volume. The increase in TB treatment volume is a direct consequence of better case-finding under the Xpert algorithm. The increase in ART volume is an indirect consequence of Xpert introduction, resulting from improved survival of TB/HIV-coinfected individuals who are currently receiving ART or who will go on to receive ART in the future. As shown in Figure 2.6, the increase in health system costs due to increased ART volume is substantial. In order to disentangle the direct effect of Xpert from this secondary effect through HIV survival, we constructed a scenario in which access to ART under a scaled-up Xpert approach was constrained to be the same as in the status quo scenario (as might be the case if the future HIV treatment budget were fixed and did not increase as a function of HIV treatment need). While artificial, this scenario allowed us to estimate the cost-effectiveness of Xpert adoption separate from the effects on HIV treatment. In this scenario, incremental costs and DALYs averted dropped by 35%–40% and 10%–15%, respectively, compared to the main analysis, and the cost per DALY averted (assuming a US$30 per-test cost for Xpert) dropped to US$656 (95% CI: 386–1,115) over a 10-y analytic horizon.

Further sensitivity analyses (described in Section 2.6) tested the robustness of the cost-effectiveness results to the use of clinical diagnosis as part of the status quo algorithm, to the removal of inpatient care from MDR-TB treatment, to the provision of empiric MDR-TB treatment while awaiting the results from DST for all patients diagnosed with RIF resistance by Xpert, and to a revised assumption about ART cost trends, in which ART prices drop 50% over 10 y. Each of these changes produced a change in the 10-y ICER of <20% and did not change the qualitative conclusions about Xpert cost-effectiveness. Detailed three-way sensitivity analyses were conducted to understand how current coverage of culture (among treatment-naïve and treatment-experienced patients) and DST affected the incremental costs, health benefits, and cost-effectiveness of Xpert in

each country. These analyses (Figures 2.13-2.17) show that if use of culture under the status quo algorithm is higher than the value used in the main analysis, this reduces the incremental costs and health benefits produced by adopting Xpert and results in a less favorable cost-effectiveness ratio. In some countries, very high values of culture use would result in the status quo strategy dominating the Xpert strategy, i.e., having lower costs and greater health benefits. The coverage levels that produce such a result (80% of all treatment- naïve and treatment-experienced TB patients diagnosed via culture), however, are unlikely to be in place at present, given current infrastructure and program constraints. Higher than expected DST access under the status quo would produce modest reductions in incremental costs and minimal changes in cost-effectiveness ratios.

We also considered an alternative Xpert algorithm that requires more aggressive investigation (via culture, chest X-ray, and antibiotic trial) of Xpert-determined TB-negative individuals with HIV-positive or unknown status, as described in recent South African Xpert guidelines [74]. The ICER for this aggressive Xpert algorithm, compared to the base-case Xpert algorithm evaluated in the main analysis, was US$2,128 (95% CI: 1,215–3,954) per DALY averted, suggesting that while this more aggressive algorithm may be cost-effective in some settings, limited programmatic resources might yield higher benefits by expanding access to a simplified Xpert algorithm.

Finally, we constructed cost-effectiveness acceptability curves to consider the likelihood that Xpert would be cost-effective under different thresholds for societal willingness to pay for additional years of healthy life (Figure 2.10). If society were willing to pay up to the average per-capita GDP (US$6,850 for the region) per averted DALY, our results suggest essentially no uncertainty in the conclusion that Xpert would be cost-effective. At a threshold of US$1,000 (representing <15% of per-capita GDP in the region), the probability that Xpert would be cost-effective was 85%, when we considered the benefits that would accumulate over 20 y, or 55%, over a 10-y horizon.

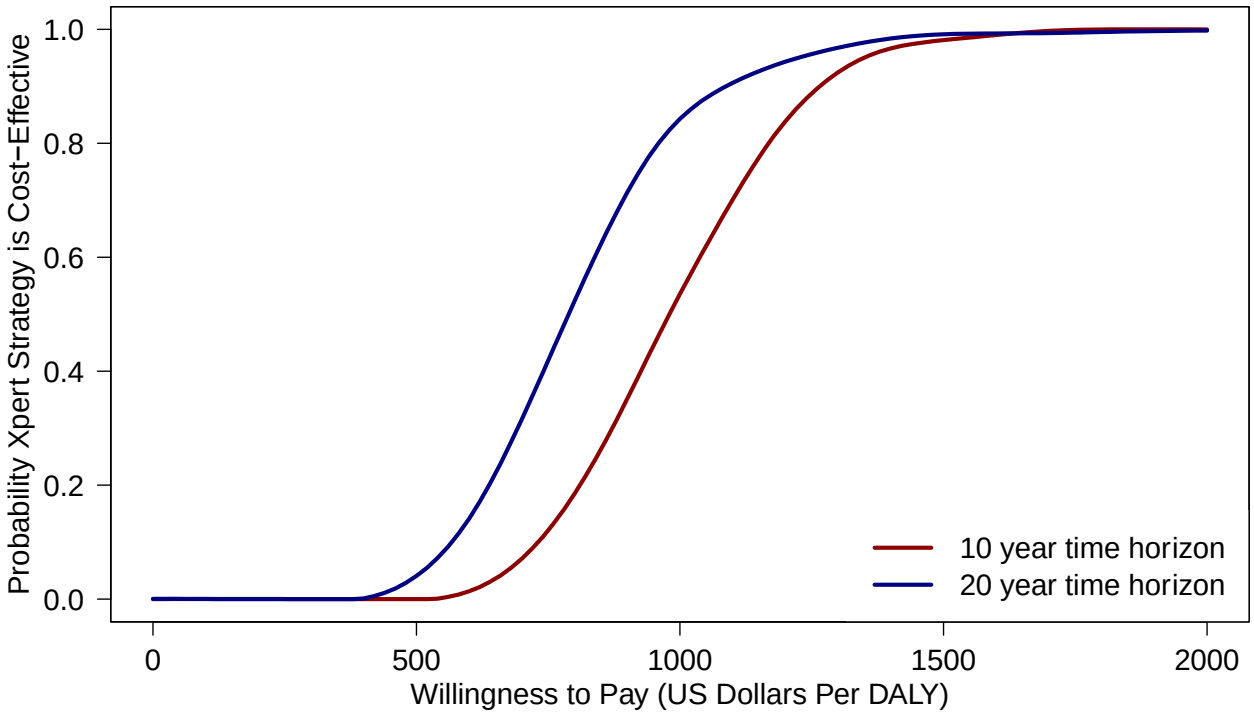

Figure 2.10. Cost-effectiveness acceptability curves showing probability that Xpert strategy is cost-effective as a function of willingness to pay for health benefits

2.4. Discussion

In this study, we used a dynamic, calibrated mathematical model of TB to evaluate the potential health and economic consequences associated with scaling up the new Xpert MTB/RIF test in settings with high TB burden, prevalent MDR-TB, and high concurrent prevalence of HIV. Our modeling approach enables quantification of the population-level health effects of alternative diagnostic strategies, projections of impact over the short term and longer time horizons, and assessment of the economic impact and cost-effectiveness of scaling up Xpert compared to continuation of the status quo diagnostic approach.

Our results indicate that the introduction of the Xpert MTB/RIF diagnostic has the potential to produce a substantial reduction in TB morbidity and mortality in southern Africa. For individuals with smear-negative TB, the benefits of Xpert implementation would be immediate, leading to the diagnosis and early treatment of many individuals who would be missed by the conventional diagnostic algorithm. Over a longer time frame, the introduction of Xpert would reduce transmission and reduce the reservoir of latent TB infection in the population, but these secondary effects are smaller than might have been anticipated. Even accounting for indirect transmission benefits, we project that TB incidence will remain substantial after three decades of Xpert use, in the absence of other modifications to the status quo TB control strategy. This is due to the large existing pool of latently infected individuals whose progression to active disease would be unmitigated by improved diagnostics, and to the fact that a substantial fraction of the additional cases diagnosed using Xpert will be smear-negative cases, who are less likely to transmit infection than smear-positive cases.

Along with the projected health benefits of scaling up Xpert will come significantly increased demands on healthcare resources. The large increase in funding required under the Xpert scenario raises the question of affordability. Although our cost-effectiveness results suggest that the introduction of Xpert represents good value for money according to typical international benchmarks, it does not automatically follow that TB program budgets will be able to absorb these changes. Whereas current debate about the costs of Xpert roll-out focuses largely on equipment and consumables connected directly to the assay, our results show that the indirect cost consequences associated with improved case-finding overshadow the direct costs of diagnosis. If current guidelines are followed, the adoption of Xpert places three key demands on a health system that are additional to the direct costs of diagnosis: providing first-line TB treatment to the large number of additional pan-sensitive TB cases that will be identified, providing additional HIV treatment to coinfected individuals who will live longer as a result of better TB care, and providing second-line

TB treatment to the limited number of individuals diagnosed with drug-resistant TB. While our analysis accounts for all three demands, we recognize that response to each of these demands could be evaluated as a separate policy question. Such analyses are beyond the scope of our present study, but it is nevertheless important to note how the economics of Xpert are dependent on the additional interventions triggered by Xpert introduction—which are sensitive to both epidemiologic context and policy decisions. It is likely that existing resources and infrastructure will be called upon to support the introduction of Xpert and the cascade of complementary services this will trigger, and our findings underscore the concern raised by other commentators regarding the possible pitfalls of introducing Xpert into health systems that are already facing capacity constraints [26,29].

An important observation in this study is that substantial increases in HIV treatment costs are expected following introduction of Xpert. This critical insight has a large influence on the cost-effectiveness of Xpert that would be missed in simpler models that do not capture the concurrent dynamics of TB and HIV, and is consistent with other analyses pointing to the importance of HIV and ART access for TB outcomes in this setting [27,75]. Sensitivity analyses show that if future HIV treatment access were limited by a hard budget constraint, this would actually result in a more attractive cost-effectiveness ratio for Xpert adoption (reducing the ICER to less than US$700 per DALY over a 10-y analytic horizon), with the subtraction of ART costs from the numerator of the ICER outweighing the reduction in health benefits in the denominator. Note that this finding provides no evidence about the appropriate level of ART access in the future, but does provide a clear illustration of the interlinked nature of TB and HIV policy in settings with dual epidemics. Although the absolute increase in HIV treatment spending would eventually be larger than the increase in TB program costs, the relative effects on total budgets for HIV and TB control are reversed; we estimate that introduction of Xpert would result in a 2% increase in HIV treatment costs after 10 y, but a 40% increase in the costs of TB control.

Providing treatment to additional cases diagnosed with MDR-TB represents another major component of the incremental costs of Xpert adoption. In our base-case analysis, we assumed that second-line TB treatment would be available for diagnosed MDR-TB cases, which resulted in an estimated 2- to 3-fold increase in the volume of MDR-TB treatment under an Xpert scale-up scenario. If second-line therapy were less available than we assumed, the cost-effectiveness of Xpert would actually improve in the short term (at the cost of faster growth in drug resistance), as the reduction in treatment costs would outweigh the reduction in survival among MDR-TB patients receiving ineffective first-line regimens. Recent empirical cost analyses suggest that MDR-TB care costs may be even higher than estimated in our analysis, with a South African study estimating per-patient costs of over US$17,000 during the inpatient phase of therapy alone, more than 40 times the cost of treating drug-sensitive TB [76]. While this might motivate the development of more efficient approaches to MDR-TB treatment, it also highlights the trade-offs involved in Xpert introduction.

Although the scenarios considered in this analysis assumed that DST would be used prior to the initiation of patients on second-line regimens, the availability of DST remains limited in some settings. Of note, the 67% positive predictive value of the Xpert test for RIF resistance in this setting suggests that a positive result on the Xpert RIF test would be insufficient evidence to initiate individuals on second-line regimens, and further screening would be necessary. Further, the benefits achieved through better detection and treatment of drug-resistant TB would be offset by increases in the number of cases developing resistance, resulting from Xpert's better case detection and the resulting increase in treatment volume. Consequently, the percentage of all TB cases with MDR-TB after 10 and 20 y is projected to be higher under the Xpert scenario, although this result is not statistically significant, and—given the overall reduction in TB prevalence produced by Xpert—the absolute number of MDR-TB cases would be lower than under the status quo.

A recent modeling study on Xpert introduction in three countries [77] reported an ICER of US$138 per DALY in South Africa for Xpert versus the status quo, which is around 5–8 times lower than the estimated ratios in our study. Because the prior study used a cohort model of patients with suspected TB, its results pertained only to the direct effects of diagnosis and treatment in a defined cohort, rather than reflecting the population-level health and economic consequences. The higher ratios in our study relate in part to our inclusion of HIV treatment costs, which are relevant to a health system or societal perspective. Exclusion of these costs from the prior analysis resulted in a more favorable assessment of Xpert, since the survival benefits of antiretroviral treatment were credited to Xpert when estimating DALYs averted, but at an implicit zero cost. An additional point of difference is that this prior study assumed no access to culture as part of the status quo algorithm, which also contributed to a lower cost-effectiveness ratio for Xpert when compared to the base-case assumptions about culture access used in our analysis. Another recent analysis looked at the use of Xpert for TB screening prior to ART initiation in South Africa. This analysis included ART costs in the cost-effectiveness ratio, and reported a cost-effectiveness ratio of US$5,100 per life-year saved for the Xpert algorithm compared to current diagnostics [78]. This analysis considered only the health benefits for the individual being screened, rather than counting the cases averted by reducing transmission, and focused on a population in which ART costs would dominate the cost-effectiveness ratio, and so it is understandable that the cost-effectiveness ratio was considerably higher than the cost per life-year saved estimated in our study.

Our analysis has several limitations. The application of any mathematical model of TB is inevitably limited by uncertainty regarding the true values of epidemiologic and programmatic parameters. Our approach aims to reduce this parameter uncertainty through calibration, and to provide a valid quantitative expression of what parameter uncertainty remains based on Bayesian statistical inference; however, the uncertainty associated with model structure is impossible to quantify without building and assessing the whole range of possible model structures that might be adopted.

For example, the results of this analysis would be different if the interdependency of TB and HIV epidemics were not considered, or if the indirect effect of Xpert on TB transmission were not captured. It will therefore be important to undertake continued empirical research evaluating the impact of Xpert as it is rolled out in practice, with the information generated by these evaluation efforts used to progressively refine the mathematical models used to estimate long-term intervention effects.

In the results reported here, we constrained estimates on costs and health outcomes to account only for those that would accrue during either the first 10 y or the first 20 y following introduction of Xpert. While the choice of a limited time horizon acknowledges our increasing uncertainty about the distant future and reflects the immediacy of policy decisions, it also makes our results somewhat conservative. This is particularly true for the 10-y results, which truncate the full streams of future benefits that will be enjoyed by those patients who avert TB mortality or infection during the 10-y analysis period. Likewise, we observe that cost-effectiveness ratios are more attractive over the 20-y horizon than the 10-y horizon, reflecting the compounding benefits of interrupting transmission dynamics through better diagnosis and treatment. Moreover, the restriction of our study to adult populations will underestimate the total burden of disease that might be averted, with Xpert adoption likely to reduce pediatric TB through reduced exposure to actively infected adults as well as the direct application of the test for pediatric diagnosis [79,80].

Finally, we note that the results of the present analysis emphasize the importance of interactions between TB and HIV epidemiology in settings where both are highly prevalent, but we caution against generalizing these results to regions where HIV rates are meaningfully different from those in southern Africa. Additional analyses are urgently needed to assess the consequences of introducing Xpert elsewhere, particularly regions of low HIV prevalence or with different TB drug resistance patterns. Similarly, this study focused on the relative benefits of the status quo algorithm

and the Xpert algorithm suggested by WHO for diagnosis of patients with suspected TB in settings with high HIV burden. While this is an important comparison to make, there is abundant scope for considering a wide array of alternatives, for example, considering different potential roles for sputum smear microscopy or chest X-ray within diagnostic algorithms designed around Xpert, or use of Xpert for different purposes, such as prior to provision of INH preventive therapy for individuals with HIV, or as part of active case-finding efforts [81]. Because the model developed for this analysis reflects detailed structure relating both to HIV and to patterns of resistance to major anti-TB drugs, it offers substantial flexibility to accommodate adaptation to other settings. In view of these features, and our statistical approach to calibrate this model to available epidemiologic data, we envision that the model can provide a durable platform for evaluating an array of different diagnostic strategies in diverse settings in the future.

2.5. Citations

1. World Health Organization (2011) *Global tuberculosis control: WHO report 2011*. Geneva: World Health Organization.

2. Obermeyer Z, Abbott-Klafter J, Murray CJ (2008) Has the DOTS strategy improved case finding or treatment success? An empirical assessment. *PLoS One* 3: e1721. doi:10.1371/journal.pone.0001721

3. Denkinger CM, Pai M (2011) Point-of-care tuberculosis diagnosis: are we there yet? *Lancet Infect Dis* 12: 169-170.

4. Corbett EL, Watt CJ, Walker N, Maher D, Williams BG, *et al*. (2003) The growing burden of tuberculosis: global trends and interactions with the HIV epidemic. *Arch Intern Med* 163: 1009-1021.

5. Elliott AM, Halwiindi B, Hayes RJ, Luo N, Tembo G, *et al*. (1993) The impact of human immunodeficiency virus on presentation and diagnosis of tuberculosis in a cohort study in Zambia*. J Trop Med Hyg* 96: 1-11.

6. Getahun H, Harrington M, O'Brien R, Nunn P (2007) Diagnosis of smear-negative pulmonary tuberculosis in people with HIV infection or AIDS in resource-constrained settings: informing urgent policy changes. *Lancet* 369: 2042-2049.

7. Acuna-Villaorduna C, Vassall A, Henostroza G, Seas C, Guerra H, *et al*. (2008) Cost-effectiveness analysis of introduction of rapid, alternative methods to identify multidrug-resistant tuberculosis in middle-income countries. *Clin Infect Dis* 47: 487-495.

8. Van Deun A, Martin A, Palomino JC (2010) Diagnosis of drug-resistant tuberculosis: reliability and rapidity of detection. *Int J Tuberc Lung Dis* 14: 131-140.

9. Parsons LM, Somoskovi A, Gutierrez C, Lee E, Paramasivan CN, *et al*. (2011) Laboratory diagnosis of tuberculosis in resource-poor countries: challenges and opportunities. *Clin Microbiol Rev* 24: 314-350.

10. Tuberculosis Division (2005) Tuberculosis bacteriology—priorities and indications in high prevalence countries: position of the technical staff of the Tuberculosis Division of the International Union Against Tuberculosis and Lung Disease. *Int J Tuberc Lung Dis* 9: 355-361.

11. Farmer P, Bayona J, Becerra M, Furin J, Henry C, *et al*. (1998) The dilemma of MDR-TB in the global era. *Int J Tuberc Lung Dis* 2: 869-876.

12. Meintjes G, Schoeman H, Morroni C, Wilson D, Maartens G (2008) Patient and provider delay in tuberculosis suspects from communities with a high HIV prevalence in South Africa: a cross-sectional study. *BMC Infect Dis* 8: 72.

13. Van Rie A, Enarson D (2006) XDR tuberculosis: an indicator of public-health negligence. *Lancet* 368: 1554-1556.

14. Boehme CC, Nabeta P, Hillemann D, Nicol MP, Shenai S, *et al*. (2010) Rapid molecular detection of tuberculosis and rifampin resistance. *N Engl J Med* 363: 1005-1015.

15. Boehme CC, Nicol MP, Nabeta P, Michael JS, Gotuzzo E, *et al*. (2011) Feasibility, diagnostic accuracy, and effectiveness of decentralised use of the Xpert MTB/RIF test for diagnosis of tuberculosis and multidrug resistance: a multicentre implementation study. *Lancet* 377: 1495-1505.

16. Helb D, Jones M, Story E, Boehme C, Wallace E, *et al*. (2010) Rapid detection of Mycobacterium tuberculosis and rifampin resistance by use of on-demand, near-patient technology. *J Clin Microbiol* 48: 229-237.

17. Theron G, Peter J, van Zyl-Smit R, Mishra H, Streicher E, *et al*. (2011) Evaluation of the Xpert MTB/RIF assay for the diagnosis of pulmonary tuberculosis in a high HIV prevalence setting. *Am J Respir Crit Care Med* 184: 132-140.

18. Rachow A, Zumla A, Heinrich N, Rojas-Ponce G, Mtafya B, *et al*. (2011) Rapid and accurate detection of Mycobacterium tuberculosis in sputum samples by Cepheid Xpert MTB/RIF assay—a clinical validation study. *PLoS One* 6: e20458. doi:10.1371/journal.pone.0020458

19. Selibas K, Hanrahan C, Deery C, Dansey H, Clouse K, *et al*. (2012) TB suspects with negative initial Xpert [abstract]. *3rd South African Tuberculosis Conference*; 12–15 June 2012; Durban, South Africa.

20. World Health Organization (2010) Roadmap for rolling out Xpert MTB/RIF for rapid diagnosis of TB and MDR-TB. Geneva: World Health Organization.

21. World Health Organization (2012) *WHO monitoring of Xpert MTB/RIF roll-out: orders of GeneXperts and Xpert MTB/RIF cartridges* [database]. Available: http://www.stoptb.org/wg/gli/assets/documents/map/1/atlas.html. Accessed 4 September 2012. Geneva: World Health Organization.

22. Mirzayev F (2012) Current dynamics in the Xpert MTB/RIF assay pricing mechanisms [abstract]. *Xpert MTB/RIF Early Implementers Meeting*; 18–19 April 2012; Annecy, France. Geneva: World Health Organization.

23. Cepheid Pharmaceuticals (2012 Aug 6) Cepheid announces first phase of Xpert MTB/RIF buy-down for high burden developing countries. Sunnyvale (California): Cepheid Pharmaceuticals.

24. Dowdy DW, Cattamanchi A, Steingart KR, Pai M (2011) Is scale-up worth it? Challenges in economic analysis of diagnostic tests for tuberculosis. *PLoS Med* 8: e1001063. doi:10.1371/journal.pmed.1001063

25. Evans CA (2011) GeneXpert—a game-changer for tuberculosis control? *PLoS Med* 8: e1001064. doi:10.1371/journal.pmed.1001064

26. Kirwan DE, Cardenas MK, Gilman RH (2012) Rapid implementation of new tb diagnostic tests: is it too soon for a global roll-out of Xpert MTB/RIF? *Am J Trop Med Hyg* 87: 197-201.

27. Lawn SD, Brooks SV, Kranzer K, Nicol MP, Whitelaw A, *et al*. (2011) Screening for HIV-associated tuberculosis and rifampicin resistance before antiretroviral therapy using the Xpert MTB/RIF assay: a prospective study. *PLoS Med* 8: e1001067. doi:10.1371/journal.pmed.1001067

28. Scott LE, McCarthy K, Gous N, Nduna M, Van Rie A, *et al*. (2011) Comparison of Xpert MTB/RIF with other nucleic acid technologies for diagnosing pulmonary tuberculosis in a high HIV prevalence setting: a prospective study. *PLoS Med* 8: e1001061. doi:10.1371/journal.pmed.1001061

29. Trebucq A, Enarson DA, Chiang CY, Van Deun A, Harries AD, *et al*. (2011) Xpert(R) MTB/RIF for national tuberculosis programmes in low-income countries: when, where and how? *Int J Tuberc Lung Dis* 15: 1567-1572.

30. Van Rie A, Mellet K, John MA, Scott L, Page-Shipp L, *et al*. (2012) False-positive rifampicin resistance on Xpert(R) MTB/RIF: case report and clinical implications. *Int J Tuberc Lung Dis* 16: 206-208.

31. Ramsay A, Steingart KR, Pai M (2010) Assessing the impact of new diagnostics on tuberculosis control. *Int J Tuberc Lung Dis* 14: 1506-1507.

32. Theron G, Pooran A, Peter J, van Zyl-Smit R, Kumar Mishra H, *et al*. (2012) Do adjunct tuberculosis tests, when combined with Xpert MTB/RIF, improve accuracy and the cost of diagnosis in a resource-poor setting? *Eur Respir J* 40: 161-168.

33. World Health Organization (2011) Rapid implementation of the Xpert MTB/RIF diagnostic test: technical and operational 'how-to'. Geneva: World Health Organization.

34. Peltzer K, Matseke G, Mzolo T, Majaja M (2009) Determinants of knowledge of HIV status in South Africa: results from a population-based HIV survey. *BMC Public Health* 9: 174.

35. Baltussen R, Floyd K, Dye C (2005) Cost effectiveness analysis of strategies for tuberculosis control in developing countries. *BMJ* 331: 1364.

36. Cohen T, Lipsitch M, Walensky RP, Murray M (2006) Beneficial and perverse effects of isoniazid preventive therapy for latent tuberculosis infection in HIV-tuberculosis coinfected populations. *Proc Natl Acad Sci U S A* 103: 7042-7047.

37. Dowdy DW, Chaisson RE (2009) The persistence of tuberculosis in the age of DOTS: reassessing the effect of case detection. *Bull World Health Organ* 87: 296-304.

38. Dye C, Garnett GP, Sleeman K, Williams BG (1998) Prospects for worldwide tuberculosis control under the WHO DOTS strategy. Directly observed short-course therapy. *Lancet* 352: 1886-1891.

39. Dye C, Williams BG (2000) Criteria for the control of drug-resistant tuberculosis. *Proc Natl Acad Sci U S A* 97: 8180-8185.

40. Murray CJ, Salomon JA (1998) Modeling the impact of global tuberculosis control strategies. *Proc Natl Acad Sci U S A* 95: 13881-13886.

41. Salomon JA, Lloyd-Smith JO, Getz WM, Resch S, Sanchez MS, *et al*. (2006) Prospects for advancing tuberculosis control efforts through novel therapies. *PLoS Med* 3: e273. doi:10.1371/journal.pmed.0030273

42. Daley CL, Small PM, Schecter GF, Schoolnik GK, McAdam RA, *et al*. (1992) An outbreak of tuberculosis with accelerated progression among persons infected with the human immunodeficiency virus. An analysis using restriction-fragment-length polymorphisms. *N Engl J Med* 326: 231-235.

43. Shafer RW, Singh SP, Larkin C, Small PM (1995) Exogenous reinfection with multidrug-resistant Mycobacterium tuberculosis in an immunocompetent patient. *Tuber Lung Dis* 76: 575-577.

44. Bucher HC, Griffith LE, Guyatt GH, Sudre P, Naef M, *et al*. (1999) Isoniazid prophylaxis for tuberculosis in HIV infection: a meta-analysis of randomized controlled trials. *AIDS* 13: 501-507.

45. Manosuthi W, Tantanathip P, Chimsuntorn S, Eampokarap B, Thongyen S, *et al*. (2010) Treatment outcomes of patients co-infected with HIV and tuberculosis who received a nevirapine-based antiretroviral regimen: a four-year prospective study. *Int J Infect Dis* 14: e1013-e1017.

46. van der Sande MA, Schim van der Loeff MF, Bennett RC, Dowling M, Aveika AA, *et al*. (2004) Incidence of tuberculosis and survival after its diagnosis in patients infected with HIV-1 and HIV-2. *AIDS* 18: 1933-1941.

47. Adam MA, Johnson LF (2009) Estimation of adult antiretroviral treatment coverage in South Africa. *S Afr Med J* 99: 661-667.

48. Granich RM, Gilks CF, Dye C, De Cock KM, Williams BG (2009) Universal voluntary HIV testing with immediate antiretroviral therapy as a strategy for elimination of HIV transmission: a mathematical model. *Lancet* 373: 48-57.

49. Stover J, Bollinger L, Avila C (2011) Estimating the impact and cost of the WHO 2010 recommendations for antiretroviral therapy. *AIDS Res Treat* 2011: 738271.

50. UNAIDS Reference Group on Estimates, Modelling and Projections (2011) *Technical meeting to review Spectrum 2011 and considering potential bias in DHS and ANC data*. Geneva: Joint United Nations Programme on HIV/AIDS.

51. Dowdy DW, O'Brien MA, Bishai D (2008) Cost-effectiveness of novel diagnostic tools for the diagnosis of tuberculosis. *Int J Tuberc Lung Dis* 12: 1021-1029.

52. Poole D, Raftery AE (2000) Inference for deterministic simulation models: the Bayesian melding approach. J Am Stat Assoc 95: 452.

53. Raftery AE, Givens GH, Zeh JE (1995) Inference from a deterministic population dynamics model for bowhead whales. *J Am Stat Assoc* 90: 402-430.

54. Alkema L, Raftery AE, Brown T (2008) Bayesian melding for estimating uncertainty in national HIV prevalence estimates. *Sex Transm Infect* 84: i11-i16.

55. Alkema L, Raftery AE, Clark SJ (2007) Probabilistic projections of HIV prevalence using Bayesian melding. *Ann Appl Stat* 1: 229-248.

56. Brown T, Bao L, Raftery AE, Salomon JA, Baggaley RF, *et al*. (2010) Modelling HIV epidemics in the antiretroviral era: the UNAIDS Estimation and Projection package 2009. *Sex Transm Infect* 86 (Suppl 2): ii3-ii10.

57. World Health Organization (2011) *Global TB Database*. Available: http://www.who.int/tb/country/data/download/en/index.html. Accessed 30 September 2011. Geneva: World Health Organization.

58. World Health Organization (2010) Multidrug and extensively drug-resistant TB (M/XDR-TB): 2010 global report on surveillance and response. Geneva: World Health Organization.

59. Rubin D (1988) Using the SIR algorithm to simulate posterior distributions. In: Bernardo JM, DeGroot MH, Lindley DV, Smith AFM, editors. *Bayesian Statistics* 3. Oxford: Oxford University Press. pp395–402.

60. Joint United Nations Programme on HIV/AIDS (2010) Towards universal access: scaling up priority HIV/AIDS interventions in the health sector. Progress report 2010. Geneva: Joint United Nations Programme on HIV/AIDS.

61. World Health Organization (2006) Antiretroviral therapy for HIV infection in adults and adolescents: recommendations for a public health approach—2006 revision. Geneva: World Health Organization.

62. World Health Organization (2010) Antiretroviral therapy for HIV infection in adults and adolescents: recommendations for a public health approach—2010 revision. Geneva: World Health Organization.

63. World Health Organization (2011) *Global price reporting mechanism for HIV, tuberculosis and malaria*. Available: http://www.who.int/hiv/amds/gprm/en/. Accessed 21 May 2011. Geneva: World Health Organization.

64. Meyer-Rath G, Schnippel K, Long L, MacLeod W, Sanne I, *et al*. (2012) The impact and cost of scaling up GeneXpert MTB/RIF in South Africa. *PLoS One* 7: e36966. doi:10.1371/journal.pone.0036966

65. Schnippel K, Meyer-Rath G, Long L, Macleod W, Sanne I, *et al*. (2012) Scaling up Xpert MTB/RIF technology: the costs of laboratory- vs. clinic-based roll-out in South Africa. *Trop Med Int Health* 17: 1142-1151.

66. Murray CJL, Lopez AD (1996) The global burden of disease: a comprehensive assessment of mortality and disability from diseases, injuries and risk factors in 1990 and projected to 2020. Cambridge (Massachusetts): Harvard University Press.

67. World Health Organization (2004) Global burden of disease 2004 update: disability weights for diseases and conditions. Geneva: World Health Organization.

68. Tan Torres T, Baltussen R, Adam T, Hutubessy R, Acharya A, *et al*. (2003) *Making choices in health: WHO guide to cost effectiveness analysis*. Geneva: World Health Organization.

69. Weinstein MC, Siegel JE, Gold MR, Kamlet MS, Russell LB (1996) Recommendations of the Panel on Cost-effectiveness in Health and Medicine. *JAMA* 276: 1253-1258.

70. Hutubessy R, Chisholm D, Edejer TT (2003) Generalized cost-effectiveness analysis for national-level priority-setting in the health sector. *Cost Eff Resour Alloc* 1: 8.

71. Iman RL, Helton JC, Campbell JE (1981) An approach to sensitivity analysis of computer models: part I—introduction, input variable selection and preliminary variable assessment. *J Qual Technol* 13: 174-183.

72. Iman RL, Helton JC, Campbell JE (1981) An approach to sensitivity analysis of computer models: part II—ranking of input variables, response surface validation, distribution effect, and technique synopsis variable assessment. *J Qual Technol* 13: 232-240.

73. World Bank (2011) *World development indicators 2011*. Washington (District of Columbia): World Bank.

74. National Health Laboratory Service (2012) *Xpert testing algorithm*. South Africa: National Health Laboratory Service.

75. Williams BG, Granich R, De Cock KM, Glaziou P, Sharma A, *et al*. (2010) Antiretroviral therapy for tuberculosis control in nine African countries. *Proc Natl Acad Sci U S A* 107: 19485-19489.

76. Schnippel K, Rosen S, Shearer K, Martinson N, Long L, *et al*. (2012) The cost of inpatient treatment for multi-drug resistant tuberculosis in South Africa [abstract]. *International AIDS Economics Network 7th AIDS & Economics Pre-Conference*; 22–27 July 2012; Washington, District of Columbia, US.

77. Vassall A, van Kampen S, Sohn H, Michael JS, John KR, *et al*. (2011) Rapid diagnosis of tuberculosis with the Xpert MTB/rif assay in high burden countries: a cost-effectiveness analysis. *PLoS Med* 8: e1001120. doi:10.1371/journal.pmed.1001120

78. Andrews JR, Lawn SD, Rusu C, Wood R, Noubary F, *et al*. (2012) The cost-effectiveness of routine tuberculosis screening with Xpert MTB/RIF prior to initiation of antiretroviral therapy: a model-based analysis. *AIDS* 26: 987-995.

79. Rachow A, Clowes P, Saathoff E, Mtafya B, Michael E, *et al*. (2012) Increased and expedited case detection by Xpert MTB/RIF assay in childhood tuberculosis: a prospective cohort study. *Clin Infect Dis* 54: 1388-1396.

80. Zar HJ, Workman L, Isaacs W, Munro J, Black F, *et al*. (2012) Rapid molecular diagnosis of pulmonary tuberculosis in children using nasopharyngeal specimens. *Clin Infect Dis* 55: 1088-1095.

81. Dye C, Williams BG (2008) Eliminating human tuberculosis in the twenty-first century. *J R Soc Interface* 5: 653-662.

82. Frieden T (2004) Toman's tuberculosis: case detection, treatment and monitoring: questions and answers, 2nd edition. Geneva: World Health Organization.

83. Levy H, Feldman C, Sacho H, van der Meulen H, Kallenbach J, *et al*. (1989) A reevaluation of sputum microscopy and culture in the diagnosis of pulmonary tuberculosis. *Chest* 95: 1193-1197.

84. Dowdy DW, Chaisson RE, Maartens G, Corbett EL, Dorman SE (2008) Impact of enhanced tuberculosis diagnosis in South Africa: a mathematical model of expanded culture and drug susceptibility testing. *Proc Natl Acad Sci U S A* 105: 11293-11298.

85. Anglaret X, Minga A, Gabillard D, Ouassa T, Messou E, *et al*. (2012) AIDS and non-AIDS morbidity and mortality across the spectrum of CD4 cell counts in HIV-infected adults before starting antiretroviral therapy in Cote d'Ivoire. *Clin Infect Dis* 54: 714-723.

86. Badri M, Lawn SD, Wood R (2006) Short-term risk of AIDS or death in people infected with HIV-1 before antiretroviral therapy in South Africa: a longitudinal study. *Lancet* 368: 1254-1259.

87. Egger M, May M, Chene G, Phillips AN, Ledergerber B, *et al*. (2002) Prognosis of HIV-1-infected patients starting highly active antiretroviral therapy: a collaborative analysis of prospective studies. *Lancet* 360: 119-129.

88. May M, Sterne JA, Sabin C, Costagliola D, Justice AC, *et al*. (2007) Prognosis of HIV-1-infected patients up to 5 years after initiation of HAART: collaborative analysis of prospective studies. *AIDS* 21: 1185-1197.

89. Phillips A, Pezzotti P, Cascade Collaboration (2004) Short-term risk of AIDS according to current CD4 cell count and viral load in antiretroviral drug-naive individuals and those treated in the monotherapy era. *AIDS* 18: 51-58.

90. When To Start Consortium, Sterne JA, May M, Costagliola D, de Wolf F, *et al*. (2009) Timing of initiation of antiretroviral therapy in AIDS-free HIV-1-infected patients: a collaborative analysis of 18 HIV cohort studies. *Lancet* 373: 1352-1363.

91. Albert H (2004) Economic analysis of the diagnosis of smear-negative pulmonary tuberculosis in South Africa: incorporation of a new rapid test, FASTPlaqueTB, into the diagnostic algorithm. *Int J Tuberc Lung Dis* 8: 240-247.

92. Floyd K, Skeva J, Nyirenda T, Gausi F, Salaniponi F (2003) Cost and cost-effectiveness of increased community and primary care facility involvement in tuberculosis care in Lilongwe District, Malawi. *Int J Tuberc Lung Dis* 7: S29-S37.

93. Hausler HP, Sinanovic E, Kumaranayake L, Naidoo P, Schoeman H, *et al*. (2006) Costs of measures to control tuberculosis/HIV in public primary care facilities in Cape Town, South Africa. *Bull World Health Organ* 84: 528-536.

94. Hudson CP, Wood R, Maartens G (2000) Diagnosing HIV-associated tuberculosis: reducing costs and diagnostic delay. *Int J Tuberc Lung Dis* 4: 240-245.

95. Nganda B, Wang'ombe J, Floyd K, Kangangi J (2003) Cost and cost-effectiveness of increased community and primary care facility involvement in tuberculosis care in Machakos District, Kenya. *Int J Tuberc Lung Dis* 7: S14-S20.

96. Samandari T, Bishai D, Luteijn M, Mosimaneotsile B, Motsamai O, *et al*. (2011) Costs and consequences of additional chest x-ray in a tuberculosis prevention program in Botswana. *Am J Respir Crit Care Med* 183: 1103-1111.

97. Suarez PG, Floyd K, Portocarrero J, Alarcon E, Rapiti E, *et al*. (2002) Feasibility and cost-effectiveness of standardised second-line drug treatment for chronic tuberculosis patients: a national cohort study in Peru. *Lancet* 359: 1980-1989.

98. van Cleeff MR, Kivihya-Ndugga LE, Meme H, Odhiambo JA, Klatser PR (2005) The role and performance of chest X-ray for the diagnosis of tuberculosis: a cost-effectiveness analysis in Nairobi, Kenya. *BMC Infect Dis* 5: 111.

99. Resch SC, Salomon JA, Murray M, Weinstein MC (2006) Cost-effectiveness of treating multidrug-resistant tuberculosis. *PLoS Med* 3: e241. doi:10.1371/journal.pmed.0030241

100. Adam T, Evans DB, Murray CJ (2003) Econometric estimation of country-specific hospital costs. *Cost Eff Resour Alloc* 1: 3.

101. Bikilla AD, Jerene D, Robberstad B, Lindtjorn B (2009) Cost estimates of HIV care and treatment with and without anti-retroviral therapy at Arba Minch Hospital in southern Ethiopia. *Cost Eff Resour Alloc* 7: 6.

102. Bratt JH, Torpey K, Kabaso M, Gondwe Y (2011) Costs of HIV/AIDS outpatient services delivered through Zambian public health facilities. *Trop Med Int Health* 16: 110-118.

103. Harling G, Wood R (2007) The evolving cost of HIV in South Africa: changes in health care cost with duration on antiretroviral therapy for public sector patients. *J Acquir Immune Defic Syndr* 45: 348-354.

104. Menzies NA, Berruti AA, Berzon R, Filler S, Ferris R, *et al*. (2011) The cost of providing comprehensive HIV treatment in PEPFAR-supported programs. *AIDS* 25: 1753-1760.

105. Rosen S, Long L, Sanne I (2008) The outcomes and outpatient costs of different models of antiretroviral treatment delivery in South Africa. *Trop Med Int Health* 13: 1005-1015.

2.6. Additional information

2.6.1. Model overview and structure

Analyses were conducted using a dynamic compartmental model of tuberculosis (TB) in adult populations. The model simulates transitions between health states deterministically, recalculating the population distribution across states in discrete monthly time steps. The model was constructed and run using **R** statistical computing software.

The model follows the conventions of earlier TB models [1-7], with additional detail to accommodate evaluation of alternative diagnostic strategies. The model structure is defined by a set of core TB states, and these states are further subdivided to account for: (1) aspects of HIV infection, progression and treatment relevant to TB epidemiology; (2) multiple circulating TB strains, with different drug resistance profiles; and (3) tracking of TB treatment history.

2.6.1.1. Core TB states

The core TB states capture important features of TB transmission, natural history, and treatment. Eight states are included. Individuals who have never been infected reside in the susceptible state. Those who are infected but do not have active disease are in the latent infection/recovered state. Active disease is categorized as smear-negative or smear-positive. Smear-negative or smear-positive active cases may be treated either through the national TB control program (DOTS), or through providers outside of the national program (non-DOTS).

2.6.1.2. HIV subdivisions

HIV co-infection can alter the rate of progression of TB disease, with HIV-infected individuals having a higher probability of primary progressive TB upon initial infection [8,9], a higher rate of breakdown from latent infection to active TB [10], a lower probability of smear-positivity amongst those with active disease [11-13] and higher mortality rates [11,14,15]. The HIV sub-model draws

on structure and assumptions from an array of published HIV models [16-19]. There are seven HIV subdivisions. Individuals may be HIV-negative, they may be in one of three categories reflecting untreated HIV infection with a specified CD4 cell count (>350 cells/μL, 200-350 cells/μL, and <200 cells/μL), or they may be receiving antiretroviral therapy (ART) in one of three categories distinguished by the CD4 count at treatment initiation.

2.6.1.3. Drug resistance subdivisions

Five subdivisions were created to account for differences in drug resistance among circulating TB strains, including: (1) pan-sensitive TB, (2) isoniazid (INH) mono-resistant TB, (3) rifampicin (RIF) mono-resistant TB, (4) resistance to both INH and RIF (MDR-TB), and (5) resistance to INH and RIF plus one or more second-line drugs (MDR+/XDR-TB).

2.6.1.4. Treatment history subdivisions

A final subdivision of model states distinguishes treatment-naïve from treatment-experienced individuals, as diagnostic algorithms may dictate different confirmatory tests depending on an individual's history of prior treatment.

2.6.1.5. Summary of model structure

At any point in time, all individuals in the model are categorized by the combination of their TB status and their status with respect to each of the three subdivisions. Thus, each of the 8 core states is 'exploded' into 70 unique sub-states (resulting from 7 HIV categories × 5 drug resistance categories × 2 treatment history categories), which yields a total of 8 × 70 = 560 unique compartments in the model. We note that some of these 560 compartments are null, in instances where the crossing of specific categories is meaningless; for example, susceptible individuals are defined by having never been infected, which means that they cannot be characterized in terms of a TB strain with a specific drug resistance profile.

2.6.2. Transitions between model states and subdivisions

The model transitions may be represented by a set of difference equations. Table 2.4 defines the general notation used in the formal description of the model that follows.

Table 2.4. Definition of core model states and transitions

Symbol	Description
Core model states	
X_1	Number of individuals in the susceptible state at time t
X_2	Number of individuals in the latent/recovered state at time t
X_3	Number of individuals in the smear-negative active TB state at time t
X_4	Number of individuals in the smear-positive active TB state at time t
X_5	Number of individuals in smear-negative DOTS treatment state, at time t
X_6	Number of individuals in smear-negative non-DOTS treatment state, at time t
X_7	Number of individuals in smear-positive DOTS treatment state, at time t
X_8	Number of individuals in smear-positive non-DOTS treatment state, at time t
Time-varying model transitions	
η_t	New entrants at time t
λ_t	Force of infection at time t
γ_{Dt}, γ_{Nt}	Rate of attending TB testing site, in DOTS (D) or non-DOTS (N) program, for individuals with active TB, at time t
y_{Dit}, y_{Nit}	Probability of positive diagnosis for individuals attending testing site in DOTS or non-DOTS program, for state $i \in \{3,4\}$, at time t
h_{Dit}, h_{Nit}	Probability of loss to follow-up between initial presentation and treatment initiation, for individuals attending testing site in DOTS or non-DOTS program, for state $i \in \{3,4\}$, at time t
δ_{it}	Default rate for treatment state $i \in \{5,6,7,8\}$, at time t
g_{it}	Probability of treatment success, for individuals completing treatment in state $i \in \{5,6,7,8\}$, at time t
μ_{it}	All-cause mortality rate for model state i at time t, calculated as the sum of background mortality at time t (μ_{bt}), and disease-specific excess mortality ($\mu_{TB}, \mu_{HIV}, \mu_{TB-HIV}$)
Time-invariant model transitions	
m	Partial immunity afforded by prior infection
p	Probability of fast breakdown to active TB, for new infections
f	Probability of smear positivity, for incident TB cases
τ	Rate of breakdown from latent / recovered to active TB
α	Rate of conversion from smear-negative to smear-positive active TB
σ	Rate of self-cure for active TB
κ_i	Rate of treatment completion for treatment state i
v	Probability that failed treatment cases are identified and returned to treatment

2.6.2.1. Transitions between core TB states

We begin with a set of model equations that describe changes in the population distribution across the eight core TB states between one time step and the next. In the following equations X_i indicates the number of residents in state i at time t, and $\dot{X}_i$ (with a dot above the X) indicates the number of residents in state i at time $t+1$.

$$\dot{X}_1 = X_1 + \eta_t - X_1\lambda_t - X_1\mu_{1t}$$

$$\dot{X}_2 = X_2 + X_1\lambda_t(1-p) - X_2(1-m)\lambda_t p + X_3\sigma + X_4\sigma + X_5\kappa_5 g_{5t} + X_6\kappa_6 g_{6t} + X_7\kappa_7 g_{7t} + X_8\kappa_8 g_{8t} - X_2\mu_{2t} - X_2\tau$$

$$\dot{X}_3 = X_3 + X_1\lambda_t p(1-f) + X_2\tau(1-f) + X_2(1-m)\lambda_t p(1-f) + X_5\kappa_5(1-g_{5t})(1-v) + X_6\kappa_6(1-g_{6t})(1-v) + X_5\delta_{5t} + X_6\delta_{6t} - X_3\mu_{3t} - X_3\sigma - X_3\alpha - X_3\gamma_{Dt}y_{D3t}(1-h_{D3t}) - X_3\gamma_{Nt}y_{N3t}(1-h_{N3t})$$

$$\dot{X}_4 = X_4 + X_1\lambda_t pf + X_2\tau f + X_2(1-m)\lambda_t pf + X_7\kappa_7(1-g_{7t})(1-v) + X_8\kappa_8(1-g_{8t})(1-v) + X_7\delta_{7t} + X_8\delta_{8t} - X_4\mu_{4t} - X_4\sigma + X_3\alpha - X_4\gamma_{Dt}y_{D4t}(1-h_{D4t}) - X_4\gamma_{Nt}y_{N4t}(1-h_{N4t})$$

$$\dot{X}_5 = X_5 + X_3\gamma_{Dt}y_{D3t}(1-h_{D3t}) - X_5\kappa_5\big(1-v(1-g_{5t})\big) - X_5\mu_{5t} - X_5\delta_{5t}$$

$$\dot{X}_6 = X_6 + X_3\gamma_{Nt}y_{N3t}(1-h_{N3t}) - X_6\kappa_6\big(1-v(1-g_{6t})\big) - X_6\mu_{6t} - X_6\delta_{6t}$$

$$\dot{X}_7 = X_7 + X_4\gamma_{Dt}y_{D4t}(1-h_{D4t}) - X_7\kappa_7\big(1-v(1-g_{7t})\big) - X_7\mu_{7t} - X_7\delta_{7t}$$

$$\dot{X}_8 = X_8 + X_4\gamma_{Nt}y_{N4t}(1-h_{N4t}) - X_8\kappa_8\big(1-v(1-g_{8t})\big) - X_8\mu_{8t} - X_8\delta_{8t}$$

The total population is given by

$$N = \sum_{i=1}^{8} X_i$$

Individuals enter the model in the susceptible state (X_1), where they face a time-varying risk of TB infection. Formally, the force of infection, λ_t, describes the hazard rate (at time t) by which a susceptible individual acquires TB. The population is assumed to mix randomly with density-independent contact rates, so transmission is modeled as frequency-dependent. The force of infection allows for varying infectivity across different categories of disease, and for temporal trends in contact rates, which yields the following formulation in the simple case of a single circulating TB strain:

$$\lambda_t = \sum_i \frac{X_i}{N} \beta_t q_i$$

where β_t is the transmission parameter for those with untreated, smear-positive, active disease at time t, and q_i is the infectivity of individuals in core state i relative to those with untreated, smear-positive active disease.

Upon infection, individuals progress either directly to active disease or to latent infection. Individuals with latent infection may subsequently progress to active TB, or they may be re-infected at a rate that is subject to the partial immunity conferred by an existing infection. Active disease is categorized as smear-positive or smear-negative. Smear-negative cases may progress to smear-positive, and all individuals with active disease may spontaneously self-cure, which returns them to the latent/recovered state. An individual with active disease can be diagnosed as a TB case, according to the characteristics of the diagnostic algorithm, and initiated on treatment. Treatment may be provided either through the national TB control program (DOTS), or through providers outside of the national program (non-DOTS). Treated individuals may complete treatment, default (returning to active disease) or die. Those who complete treatment are categorized as failures

(returning to active disease) or cures (returning to the latent/recovered state). In addition to these transitions, all individuals in the core model are subject to a background mortality rate that is updated in each time step based on demographic data for each country, and to TB-related mortality specific to each active disease state.

2.6.2.2. Transitions between HIV subdivisions

Rates of transition from one HIV subdivision to another are based on estimates of HIV incidence, disease progression and treatment initiation (see Section 2.6.3.4 and Table 2.5). These rates are assumed independent of core TB states and other subdivisions. HIV incidence is modeled as a transition from the HIV-negative category to the HIV-positive, CD4 count >350 cells/μL category, with time-varying incidence rates defined as exogenous model parameters. HIV-positive individuals not on ART may progress over time to lower CD4 counts. Untreated HIV-positive individuals transition onto ART at rates specific to CD4 count category, which are allowed to vary over time to capture changing eligibility criteria and coverage of testing and referral. HIV-related mortality occurs at rates specific to each subdivision. Certain parameters governing the natural history of TB vary with respect to HIV status, as indicated in Table 2.5.

2.6.2.3. Transitions between drug resistance subdivisions

Transitions between TB strain subdivisions occur through infection, superinfection and acquired resistance. First, we elaborate the specification for the force of infection to allow for multiple circulating strains distinguished by their drug resistance profiles. Individuals may be infected by any of the five types of strains. When calculating the force of infection for a particular strain (λ_s for strain s) we allow for differential fitness across strains, for example indicating lower transmissibility among drug resistant vs. drug sensitive strains. The total force of infection (λ) equals the sum across the five strain-specific forces of infection (λ_s). The general formulation for the force of infection is thus given by:

$$\lambda_t = \sum_s \sum_i \frac{X_{is}}{N} \beta_t q_i (1 - r_s)$$

where r_s is the relative reduction in fitness for strain *s* compared to the corresponding pan-sensitive strain. An individual in the susceptible state who is newly infected with TB transitions to the subdivision of the infecting strain. An individual with latent TB who is superinfected by a different strain transitions to the subdivision of the superinfecting strain. Following Lipsitch *et al*. [20], we allow for superinfection by the same strain in order to preserve model neutrality with respect to strain distribution.

Individuals may also develop acquired drug resistance during TB treatment, such that individuals with pan-sensitive TB can develop mono-INH resistance, mono-RIF resistance, or MDR-TB directly. Individuals with mono-INH or mono-RIF can develop MDR-TB, and individuals with MDR-TB can develop MDR+/XDR-TB. Cases of acquired resistance arise as individuals default from or fail treatment, with rates of acquiring resistance specified for each combination of current strain and specific treatment regimen (Table 2.5).

2.6.2.4. Transitions between treatment history subdivisions

Individuals enter the model in the treatment-naïve category. Treatment-naïve individuals move into the treatment-experienced category upon the first transition out of any of the TB treatment states (X_5, X_6, X_7 or X_8) in the core model.

2.6.3. Model parameterization

2.6.3.1. Initialization

The model was used to estimate TB prevalence and incidence starting in 1950 onwards, with this long historical projection allowing the simulation of a realistic TB epidemic as well as providing prevalence and incidence estimates for the recent past to compare to independent data in the

calibration procedure. First, we simulated a virgin epidemic, in which one infectious source case is introduced into a population of susceptibles. This epidemic was run to equilibrium, which was assumed to represent the starting conditions in 1950. The model was then run from 1950 through the end of 2011 to produce a historical time trend in TB epidemiology, with time-varying parameter values capturing changes in birth rates, background mortality rates, TB contact rates, access to TB and HIV treatment interventions, and treatment success and default rates.

Table 2.5 summarizes estimates and ranges for all model parameters. Following is a description of key data sources used to derive these values and ranges.

2.6.3.2. Demographics

Demographic inputs were estimated separately for each country. Historical estimates for mortality excluding HIV were obtained from the World Health Organization (unpublished data), and future background mortality was held constant at current values. Historical estimates and future projections for population growth were obtained from the United Nations Population Division [21].

2.6.3.3. TB epidemiology, diagnosis and treatment

Estimates for transition rates between TB-related health states were drawn from the literature and chosen to be consistent with prior TB modeling work [3-5,22-24]. ART delays the immunosuppression associated with HIV thereby reducing the effect of HIV on TB disease progression. We operationalized this as an ART effectiveness parameter (z); the values of TB natural history parameters for individuals on ART were calculated as weighted sums of parameter values for HIV-negative and untreated HIV-positives, with weights z and $(1 - z)$ respectively.

Individuals receiving TB treatment were assumed to have reduced infectiousness compared to untreated individuals, with the reduction in infectiousness approximated as 1 minus the failure probability for each regimen/strain pair. Diagnostic algorithms were based on current practice and

on WHO guidelines for Xpert implementation [25]. Values for the sensitivity and specificity for each diagnostic test were derived from the published literature [26-28]. As the model distinguishes between smear-negative and smear-positive TB the sensitivity of smear was defined as 0% and 100%, respectively, for these two groups. As sputum culture is considered the gold standard for diagnosis the sensitivity of this test was assumed to be 100%. Few data are available on the percentage of individuals testing negative on smear microscopy who subsequently have this diagnosis confirmed by sputum culture. Dowdy *et al*. [23] estimated this percentage as 5% and 37% for treatment-naïve and treatment-experienced individuals, respectively, based on 2004 South African data. It is likely that access to sputum coverage will have risen since then, and we assumed starting values for these parameters of 20% and 80% respectively. In addition, 80% of individuals who are diagnosed positive with a history of prior treatment were assumed to receive DST.

Parameters relating to treatment program coverage and performance were based on routine monitoring data aggregated by the WHO Stop TB Department [29]. Access to DOTS TB programs (parameterized as the rate at which those with active TB attend a health center providing TB diagnosis and treatment) was estimated from reported trends in the case detection rate (CDR). First, a simple time trend was fit to national CDR data using a logistic regression model (see Figure 2.11). As the CDR more closely approximates a probability rather than a rate, we transformed the predicted CDR ($\hat{CDR}$) to calculate the attendance rate (whereby rate = $1 - e^{-\hat{CDR}}$). For the pre-1990 period, the rate of attendance for DOTS diagnosis was assumed to increase from zero to the 1990 value over a 4-year period. For future years the attendance rate was held constant at the most recent value for which data were available. The imperfections of the CDR as a measure of the probability of detection are well understood [30], and this uncertainty was reflected in the analysis by assuming a wide prior distribution for the attendance rate, with a range spanning from zero to two times the point estimate. There is little information on non-DOTS diagnosis, but this was assumed to start earlier (1970) and to continue at a low level in the future (rate of 0.2 per year, also

varying within a range spanning zero to two times the point estimate). The volume of non-DOTS care was calibrated to produce observed drug resistance levels.

Rates of treatment default were based on reported program outcomes [29] for each country and calculated in a similar fashion to the attendance rate, by fitting a simple time trend to the national program data using a logistic regression model (Figure 2.11), and transforming the estimated probability of default to obtain the annualized default rate. TB-specific excess mortality rates were assumed to persist for the first two months of treatment before dropping to zero, and the treatment mortality rates produced by this assumption were consistent with reported program outcomes.

The probability of treatment success (probability of cure or completion among all individuals finishing a treatment regimen) will be determined by the appropriateness of the drug regimen as well as other characteristics of the treatment program—such as quality of adherence support—which might change over time. To capture the influence of these other program characteristics we assumed that the effectiveness of the first-line regimen in pan-sensitive TB was equivalent to the fraction of all individuals cured or completing treatment estimated from national program data. This was operationalized as a time trend fit to the observed data in a logistic regression model (Figure 2.11). The probabilities of treatment success for other strain-regimen combinations were assumed to be fixed proportions of this value, shown in Table 2.5.

It is assumed that diagnosis and treatment was more rudimentary in the early years of TB control programs. This assumption was operationalized in the model as a linear increase in the availability of culture, DST, and second-line regimens over the last 20 years, from an initial scenario in which there was no access to advanced tests or second line regimens.

Little information is available to estimate rates of acquired resistance by regimen and initial strain. We based our estimates on data reported in Lew *et al*. [31], adjusted for the prevalence of

resistance to other first-line drugs (streptomycin, ethambutol) not tracked in the model (values shown in Table 2.5).

2.6.3.4. HIV epidemiology and treatment

Estimates for HIV incidence and ART coverage were obtained from UNAIDS (unpublished data). For future years, HIV incidence was assumed to decline at an exponential rate estimated from the last 7 years of incidence data. Untreated HIV-positive individuals in the model transition onto ART at rates calculated to match national reporting data on ART program scale-up. ART coverage (the fraction of eligible individuals receiving ART) was assumed to increase from current levels to the WHO universal access target of 80% coverage [32] over the course of 10 years. For Botswana, which was providing ART to over 83% of those in need by 2009, coverage was maintained at current levels. Early HIV treatment guidelines suggested a CD4 count criterion of <200 cells/μL for initiating ART [33], while recent revisions to the guidelines have raised this CD4 count criterion to <350 cells/μL [34]. For this reason all ART initiations prior to 2010 were assumed to come from the CD4 count <200 cells/μL group, and for 2010 onwards the fraction of HIV initiations coming from the CD4 count 200–350 cells/μL group was assumed to rise such that by 2015 individuals in the CD4 count 200–350 and <200 cells/μL groups would have equal probability of initiation on ART. Estimates for HIV-specific mortality rates (with and without ART) were drawn from the literature [35-40].

2.6.3.5. Resource use and costs

Costs were assessed from a health system perspective and expressed in 2011 US dollars. Costs reflected resources used to deliver TB diagnosis and treatment, as provided by both public and private providers, and those used in providing ART to HIV-infected individuals. An ingredients approach to costing was used, by which the total cost to provide a particular diagnostic procedure

or a course of treatment was calculated as the number of units of each specific type of resource input needed to deliver the service, multiplied by the unit cost of each resource input.

Average costs for each type of service are shown in Table 2.5. Unit costs for service delivery (excluding Xpert) were calculated as the average of values reported in the literature, after adjustment for inflation and differences in price levels. These adjustments were undertaken by (i) inflating values to 2011 prices using the GDP deflator in the country in which the data were derived, then (ii) adjusting for price levels between countries using per-capita GDP as a price index and (iii) converting to US dollars based on market exchange rates. Treatment costs for TB and HIV included drugs, clinic visits and monitoring tests, as well as inpatient care for individuals receiving treatment for MDR-TB. Drug costs were derived from average prices reported to the WHO price reporting mechanism [41]. Quantities of treatment monitoring visits and laboratory tests (including monitoring smears and cultures) followed a previous global analysis [1]. The cost of clinic visits associated with TB diagnosis was based on the cost of a 10-minute outpatient clinic visit as reported for each country by the WHO-CHOICE project, and the cost of a clinic visit during TB treatment based on the cost of a short (<5 minute) outpatient clinic visit from the same source. Inpatient care for MDR-TB treatment was assumed to last for 4 months, with the cost per inpatient day estimated from the WHO-CHOICE data. For Xpert, limited data are available on the per-test cost of providing the test in routine programmatic settings, although information reported in WHO implementation guidance suggests an economic cost of US$25-35 in southern Africa (including consumables, equipment, personnel, transport, facilities and managerial overheads), and a recent costing study in South Africa suggested a per-test cost of US$26-US$36 in the national program [42]. As the per-test cost of Xpert is of interest to decision-makers and may be sensitive to negotiation, results were calculated and reported separately for three values for the Xpert per-test cost: US$20, US$30 and US$40.

2.6.3.6. Other parameters

Disability weights were derived from estimates published by the Global Burden of Disease study [43,44]. Published disability weights generally only cover individual conditions, and so to calculate disability weights for comorbid TB-HIV states we assumed a multiplicative functional form, whereby the combined weight was equal to one minus the product of one minus the disability weight for each of the individual conditions [45,46]. An annual discount rate of 3% was applied to all future costs and benefits included in the cost-effectiveness analysis. This value was varied between 0 and 10% in univariate sensitivity analyses.

Table 2.5. Base-case parameter values and ranges

Description	Base-case value	Range*	Source
Parameters related to η_t			
New entrants at time t	Time-varying	—	[21]
Parameters related to λ_t			
Transmission parameter for individuals with (pan-sensitive) smear-positive TB in 1950 (β_{1950})	11.0	[8.3-14.3]	Values chosen to produce plausible value on burn-in
Annual percentage decline in transmission parameter	0.7%	[0.2%-1.6%]	[4]
Infectivity of smear-negative TB, relative to smear-positive TB (q_i)	0.22	[0.12-0.37]	[3]
Fitness cost,drug-resistant TB strains (r_s):			
Mono-INH resistant	0.05	[0.03-0.08]	
Mono-RIF resistant	0.15	[0.08-0.23]	
MDR-TB	0.27	[0.15-0.42]	
MDR+ / XDR-TB	0.27	[0.15-0.42]	[5,22,47,48]
Parameters related to γ_{Dt} and γ_{Nt}			
Rate of attending TB testing site, for individuals with active TB	Time-varying	0-200% of base-case value	Trend estimated from country program data 1990-2011 [29]

Table 2.5. Base-case parameter values and ranges (continued)

Description	Base-case value	Range*	Source
Parameters related to η_t			
New entrants at time t	Time-varying	—	[21]
Parameters related to λ_t			
Transmission parameter for individuals with (pan-sensitive) smear-positive TB in 1950 (β_{1950})	11.0	[8.3-14.3]	Values chosen to produce plausible value on burn-in
Annual percentage decline in transmission parameter	0.7%	[0.2%-1.6%]	[4]
Infectivity of smear-negative TB, relative to smear-positive TB (q_i)	0.22	[0.12-0.37]	[3]
Fitness cost,drug-resistant TB strains (r_s):			
Mono-INH resistant	0.05	[0.03-0.08]	
Mono-RIF resistant	0.15	[0.08-0.23]	
MDR-TB	0.27	[0.15-0.42]	
MDR+ / XDR-TB	0.27	[0.15-0.42]	[5,22,47,48]
Parameters related to γ_{Dt} and γ_{Nt}			
Rate of attending TB testing site, for individuals with active TB	Time-varying	0-200% of base-case value	Trend estimated from country program data 1990-2011 [29]
Rate ratio of attending TB testing, for individuals without active TB compared to those with active TB	0.015	[0.009-0.023]	Calibrated to observed ratio of TB testing to TB notifications [29]
Parameters related to y_{Dit} and y_{Nit}			
Sensitivity of sputum smear microscopy:			
Smear-negative TB	0.0	—	
Smear-positive TB	1.0	—	Assumed
Specificity of sputum smear microscopy	0.974	[0.965-0.982]	[27]
Sensitivity of sputum culture	1.0	—	Assumed
Specificity of sputum culture	0.984	[0.978-0.989]	[28]
Sensitivity of Xpert for TB:			
Smear-negative TB	0.725	[0.655-0.788]	
Smear-positive TB	0.982	[0.969-0.991]	[26]
Specificity of Xpert for TB	0.992	[0.982-0.997]	[26]
Sensitivity of Xpert for RIF resistance	0.976	[0.946-0.992]	[26]

Table 2.5. Base-case parameter values and ranges (continued)

Description	Base-case value	Range*	Source
Specificity of Xpert for RIF resistance	0.981	[0.966-0.990]	[26]
Probability of sputum culture following a negative sputum smear (status quo):			
Treatment-naïve patients	0.20	[0.11-0.31]	
Treatment-experienced patients	0.80	[0.69-0.89]	[23]
Probability of DST following a positive TB diagnosis (status quo):			
Treatment-naïve patients	0.00	—	
Treatment-experienced patients	0.80	[0.69-0.89]	[23]
Sensitivity of clinical diagnosis	0.209	[0.12-0.33]	[49]
Specificity of clinical diagnosis	0.953	[0.92-0.97]	[49]
Parameters related to h_{Dit} and h_{Nit}			
Probability of loss to follow-up between presentation and treatment initiation:			
With prompt diagnosis (smear, Xpert)	0.15	[0.09 – 0.24]	
With delayed diagnosis (culture, DST)	0.25	[0.14 – 0.39]	[24]
Parameters related to δ_{it}			
Treatment default rate, DOTS	Time-varying	50-150% of point estimate	Trend estimated from country program data 1990-2011 [29]
Treatment default rate, non-DOTS	0.58	[0.27-0.85]	[27]
Parameters related to g_{it}			
Probability of treatment success, for individuals with pan-sensitive TB completing first-line regimen	Time-varying	50-150% of point estimate	Trend estimated from country program data 1990-2011 [29]
Risk ratio of treatment success, relative to pan-sensitive TB with first-line regimen:			
First-line regimen, partially-sens strain	0.83	[0.73-0.90]	
First-line regimen, non-sens strain	0.44	[0.23-0.67]	
Second-line regimen, sens strain	0.93	[0.89-0.96]	
Second-line regimen, non-sens strain	0.44	[0.23-0.67]	
Non-DOTS regimen, non-MDR strain	0.73	[0.58-0.85]	
Non-DOTS regimen, MDR strain	0.44	[0.23-0.67]	[50-54]

Table 2.5. Base-case parameter values and ranges (continued)

Description	Base-case value	Range*	Source
Parameters related to μ_{it}			
Background mortality rate, (ages 15+)	Time-varying	—	WHO unpublished data
Excess mortality rate, active TB (μ_{TB}):			
Smear-negative	0.21	[0.18 – 0.25]	
Smear-positive	0.30	[0.21 – 0.41]	[4]
Excess mortality rate, HIV (μ_{HIV}):			
CD4 >350 cells/μl, no ART	0. 008	[0.005-0.012]	
CD4 200–350 cells/μl, no ART	0.030	[0.018-0.048]	
CD4 <200 cells/μl, no ART	0.230	[0.136-0.366]	
On ART initiated at CD4 >350 cells/μl	0.008	[0.005-0.012]	
On ART initiated at CD4 200-350 cells/μl	0.023	[0.014-0.037]	
On ART initiated at CD4 <200 cells/μl	0.050	[0.031-0.076]	[35-40]
Excess mortality rate, CD4<200, active TB ($\mu_{TB\text{-}HIV}$)	0.80	[0.472-1.272]	[14,15]
Parameters related to m			
Partial immunity from prior infection:			
HIV-neg	0.65	[0.37-0.87]	
HIV-pos, CD4 >350 cells/μl, no ART	0.45	[0.23-0.68]	
HIV-pos, CD4 200–350 cells/μl, no ART	0.25	[0.14-0.39]	
HIV-pos, CD4 <200 cells/μl, no ART	0.25	[0.14-0.39]	[2,3,5,47]
Parameters related to p			
Probability of fast breakdown to active TB, for new infections:			
HIV-neg	0.115	[0.09-0.14]	
HIV-pos, CD4 >350 cells/μl, no ART	0.33	[0.18-0.51]	
HIV-pos, CD4 200–350 cells/μl, no ART	0.67	[0.49-0.82]	
HIV-pos, CD4 <200 cells/μl, no ART	0.94	[0.70-1.00]	[4,55]
Parameters related to f			
Probability of smear-positivity, for incident TB cases:			
HIV-neg	0.62	[0.42-0.80]	
HIV-pos, CD4 >350 cells/μl, no ART	0.45	[0.23-0.68]	
HIV-pos, CD4 200–350 cells/μl, no ART	0.35	[0.19-0.54]	
HIV-pos, CD4 <200 cells/μl, no ART	0.35	[0.19-0.54]	[3,11,55]

Table 2.5. Base-case parameter values and ranges (continued)

Description	Base-case value	Range*	Source
Parameters related to τ			
Rate of breakdown from latent/recovered to active TB (per 100,000):			
HIV-neg	0.001	[0.0003-0.0024]	
HIV-pos, CD4 >350 cells/μl, no ART	0.003	[0.001-0.006]	
HIV-pos, CD4 200–350 cells/μl, no ART	0.085	[0.060-0.130]	
HIV-pos, CD4 <200 cells/μl, no ART	0.170	[0.100-0.270]	[3,4,56]
Parameters related to α			
Rate of conversion from smear-negative to smear-positive active TB	0.015	[0.010-0.023]	[4]
Parameters related to σ			
Rate of self-cure for active TB:			
HIV-neg	0.2	[0.15-0.25]	
HIV-pos, CD4 >350 cells/μl, no ART	0.1	[0.06-0.16]	
HIV-pos, CD4 200–350 cells/μl, no ART	0.0	—	
HIV-pos, CD4 <200 cells/μl, no ART	0.0	—	[4,5,57]
Parameters related to κ_i			
Duration of TB treatment ($1/\kappa_i$):			
First-line	6 mo.	—	
Mono-INH resistant	9 mo.	—	
Mono-RIF resistant	18 mo.	—	
MDR-TB	21 mo.	—	
MDR+/XDR-TB	21 mo.	—	
Non-DOTS (averaged)	18 mo.	—	[58]
Parameters related to v			
Probability failed treatment cases are identified and returned to treatment	0.5	[0.25-0.75]	Assumed

Table 2.5. Base-case parameter values and ranges (continued)

Description	Base-case value	Range*	Source
Additional parameters related to TB strain subdivisions			
Rates of acquisition of TB drug resistance:			
Pan-sensitive → Mono-INH resistant, 1st-line regimen	0.020	[0.012-0.032]	
Pan-sensitive → Mono-RIF resistant, 1st -line regimen	0.003	[0.002-0.005]	
Pan-sensitive → MDR-TB, 1st -line regimen	0.010	[0.006-0.016]	
Mono-RIF or Mono-INH resistant → MDR-TB, appropriate 2nd-line regimen	0.020	[0.012-0.032]	
Mono-RIF or Mono-INH resistant → MDR-TB, inappropriate 2nd -regimen	0.230	[0.139-0.359]	
MDR-TB → MDR+/XDR-TB, appropriate 2nd -line regimen	0.020	[0.012-0.032]	
MDR-TB → MDR+/XDR-TB, inappropriate 2nd -line regimen	0.230	[0.139-0.359]	
Rate ratio of acquired resistance, pan-sensitive, non-DOTS regimen	3.0	[1.8-4.8]	[31]
Additional parameters related to HIV subdivisions			
HIV incidence	Time-varying	Annual change varied ±5%	UNAIDS unpublished estimates
Rate of HIV progression for individuals not on ART:			
CD4 >350 cells/μl to CD4 200–350 cells/μl	0.134	[0.08-0.21]	
CD4 200–350 cells/μl to CD4 <200 cells/μl	0.505	[0.30-0.81]	[59-62]
Historical ART coverage for treatment-eligible HIV-positive individuals	Time-varying	—	UNAIDS unpublished estimates
Future ART coverage for treatment-eligible HIV-positive individuals	0.8	[0.47-0.96]	[32]
Effectiveness of ART in reversing effect of HIV on TB natural history (all TB transition parameters subdivided by HIV status, excluding mortality)	0.7	[0.47-0.87]	[63-65]
Proportion of HIV-negative individuals with prior HIV test result	0.5	[0.25-0.75]	[66-68]

Table 2.5. Base-case parameter values and ranges (continued)

Description	Base-case value	Range*	Source
Additional parameters related to costs and health outcomes			
Per-test cost of Xpert	$20, $30, $40	Assumed fixed	[25,69,70]
Per-test cost of smear diagnosis:			
Botswana	$6.13	[4.18-8.68]	
Lesotho	$3.31	[2.26-4.68]	
Namibia	$5.31	[3.63-7.51]	
South Africa	$5.94	[4.06-8.39]	
Swaziland	$4.24	[2.90-5.99]	[24,71-77]
Per-test cost of culture:			
Botswana	$15.83	[13.07-18.99]	
Lesotho	$8.56	[7.07-10.27]	
Namibia	$13.72	[11.33-16.46]	
South Africa	$15.33	[12.66-18.39]	
Swaziland	$10.94	[9.04 -13.13]	[24,71,73,74,77]
Per-test cost of chest X-ray:			
Botswana	$16.69	[11.35-23.70]	
Lesotho	$9.03	[6.14-12.81]	
Namibia	$14.46	[9.83-20.52]	
South Africa	$16.16	[10.99-22.94]	
Swaziland	$11.54	[7.85-16.38]	[71,76,78]
Per-test cost of drug sensitivity testing:			
Botswana	$81.97	[61.44-107.17]	
Lesotho	$44.32	[33.22-57.94]	
Namibia	$71.02	[53.24-92.85]	
South Africa	$79.37	[59.50-103.77]	
Swaziland	$56.65	[42.47-74.07]	[79,80]
Cost of outpatient diagnostic visit:			
Botswana	$10.32	[6.09-16.40]	
Lesotho	$2.94	[1.73-4.67]	
Namibia	$7.99	[4.71-12.70]	
South Africa	$10.30	[6.08-16.39]	
Swaziland	$6.21	[3.66-9.87]	[81]

Table 2.5. Base-case parameter values and ranges (continued)

Description	Base-case value	Range*	Source
Cost of outpatient treatment visit:			
Botswana	$6.85	[4.04-10.89]	
Lesotho	$1.95	[1.15-3.10]	
Namibia	$5.31	[3.13-8.44]	
South Africa	$6.85	[4.04-10.89]	
Swaziland	$4.13	[2.44-6.57]	[81]
Cost of inpatient care, per day:			
Botswana	$38.99	[23.00-61.99]	
Lesotho	$8.78	[5.18-13.96]	
Namibia	$28.76	[16.97-45.73]	
South Africa	$39.38	[23.23-62.61]	
Swaziland	$21.91	[12.93-34.84]	[81]
Monthly TB regimen cost:			
First-line	$5.86	[3.46-9.32]	
Mono-INH resistant	$18.02	[10.63-28.65]	
Mono-RIF resistant	$33.91	[20.01-53.92]	
MDR-TB	$119.37	[70.43-189.79]	
MDR+/XDR-TB	$179.06	[105.64-284.7]	[41]
Monthly frequency of treatment activities, averaged over treatment course:			
Clinic visits (first-line)	5.9	[3.5-9.4]	
Clinic visits (second-line)	22.3	[13.2-35.4]	
Monitoring smears (first-line)	1.0	[0.6-1.6]	
Monitoring smears (second-line)	1.0	[0.6-1.6]	
Sputum cultures (second-line)	0.43	[0.25-0.68]	
Chest X-rays (second-line)	0.14	[0.08-0.22]	[1]
Number of months of inpatient care with MDR-TB treatment	4.0	[2.4-6.4]	[82]
Monthly cost of ART:			
Botswana	$104.97	[84-80-128.48]	
Lesotho	$69.63	[57.22-83.92]	
Namibia	$94.68	[76.78-115.52]	
South Africa	$102.53	[82.90-125.40]	
Swaziland	$81.20	[66.25-98.52]	[41,83-87]

Table 2.5. Base-case parameter values and ranges (continued)

Description	Base-case value	Range*	Source
Disability weights:			
Active TB	0.271	[0.151-0.422]	
HIV-pos, CD4 >350 cells/μl, no ART	0.135	[0.078-0.213]	
HIV- pos, CD4 200–350 cells/μl, no ART	0.320	[0.176-0.496]	
HIV- pos, CD4 <200 cells/μl, no ART	0.505	[0.252-0.757]	
HIV- pos, ART initiated at CD4 >350	0.135	[0.078-0.213]	
HIV- pos, ART initat CD4 200–350	0.151	[0.087-0.238]	
HIV- pos, ART initat CD4 <200	0.167	[0.096-0.262]	[43,44]
Discount rate	3.0%	[0-10%]	[88,89]

All costs are given in 2011 US dollars

* Ranges for parameters were derived from the literature where sufficient data existed, and otherwise were calculated as ± 50% of the point estimate value.

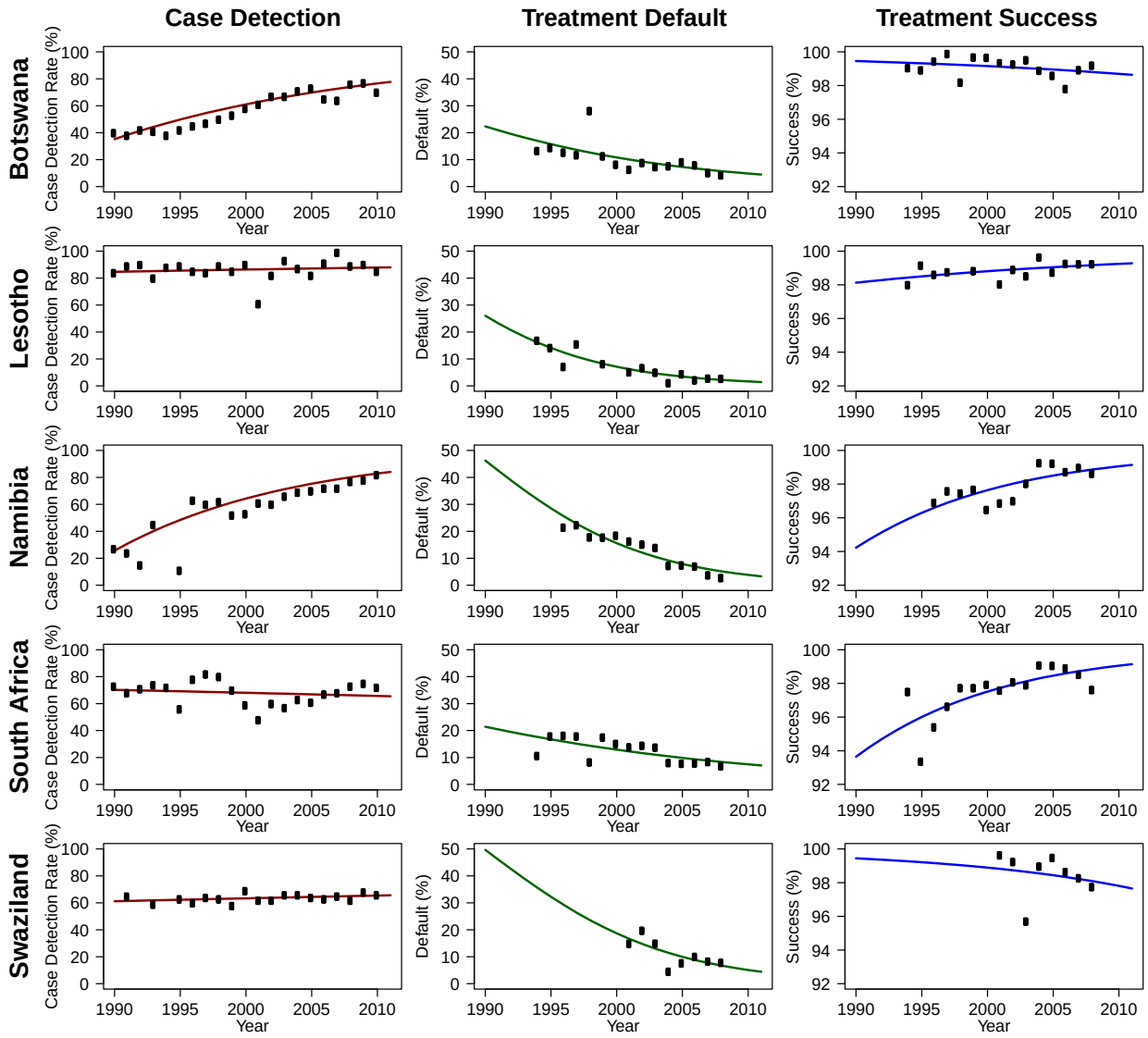

Figure 2.11. Time-varying parameter inputs for TB diagnosis and treatment

2.6.4. Model calibration

We adopted a Bayesian approach to calibrate the model, following the prior work of Raftery, Alkema and colleagues [90,91]. The approach enables the synthesis of multiple sources of information on the values of model outputs, and allows for characterization of the uncertainty in model results using Bayesian posterior intervals and similar metrics.

The disease model (M) can be considered a deterministic mapping from the parameter space of the model inputs ($\boldsymbol{\Theta}$) to that of the model outputs ($\boldsymbol{\Phi}$), such that M: $\theta \rightarrow \varphi$. For some of these outputs (φ_1) we have external data (X) related to φ_1 through a defined probability model. An example of φ_1 would be model projections of MDR-TB prevalence for 2010, and an example for X would be the estimate for MDR-TB prevalence obtained from a population-based survey conducted in the same year. For other outputs (φ_2) — generally those about we would like to make inferences — we have no external data, but can estimate their distribution based on the prior information about θ and φ_2, relying on the deterministic disease model to link these three sets of parameters. As we have probabilistic prior information on θ and φ_1, we can use this information to estimate the posterior density of θ:

$$p(\theta|X) \propto p(\theta) * L(X|\theta)$$

where $p(\theta)$ is the prior distribution of the model inputs, and $L(X|\theta)$ is the likelihood function for θ constructed with the external data X. While this likelihood function cannot be estimated directly, we can transform θ into the output parameter space to estimate the likelihood:

$$p(\theta|X) \propto p(\theta) * L\big(X\big|M(\theta)\big)$$

$$\propto p(\theta) * L(X|\varphi_1)$$

Having obtained a posterior distribution for the model inputs, we can then estimate the posterior density of φ_2 through the model, as $M(p(\theta|X))$. An analytic solution can be difficult or impossible to calculate for disease models of moderate or greater complexity, but the posterior distributions can be approximated using numerical methods. Following Alkema *et al*. [90], we used a sampling / importance resampling (SIR) algorithm [92]:

The prior uncertainty was quantified for each model parameter, expressed as the ranges given in Table 2.5. Each range was assumed to represent the 95% equal tailed interval for a log-normal distribution (for parameters defined over positive numbers, e.g., rates, costs) or logit-normal distribution (for parameters defined over the interval 0–1, e.g., probabilities, disability weights).

For each country, a likelihood function was constructed to calibrate the model, based on (a) WHO estimates [29] for TB prevalence and incidence in 1990 and 2009 (the earliest and most recent estimates available, respectively); and (b) results from a country-level drug resistance survey, where available [93]. The uncertainty around prevalence and incidence estimates was assumed to be distributed normally, with a variance calculated from the width of the uncertainty intervals reported with the WHO estimates. The sample size and MDR-TB prevalence reported by the drug resistance surveys were used to parameterize two beta distributions (one for treatment-experienced and one for treatment-naïve individuals), assuming a design effect of 2.0 for the survey sample. These likelihood functions were assumed to be mutually independent, and multiplied to create a joint likelihood function.

For each country 20,000 random parameter sets were drawn via Latin hypercube sampling, and a separate simulation conducted for each of these parameter sets. A likelihood statistic was calculated for each of these model runs by applying the joint likelihood function to the model outputs produced by a particular parameter set.

The 20,000 parameter sets from the first stage sample were then resampled with replacement to create a final array of parameter sets, using the likelihoods as sampling weights. A sample size of 100,000 was used for this second sample as this step is not computationally intensive.

Results were calculated by running the model for the resampled parameter sets. For each quantity of interest, the point estimate was calculated as the mean of the results for the second stage sample,

and 95% posterior intervals (the Bayesian equivalent of confidence intervals) calculated from the 2.5th and 97.5th percentiles of the simulation results for each quantity of interest.

This procedure was conducted separately for each country. Figure 2.12 shows the results of the calibration for TB prevalence, incidence and MDR-TB prevalence in South Africa, overlaid with the WHO estimates and drug resistance survey data. Posterior distributions for health outcomes and costs for the southern Africa region were calculated by summing the outcomes for each country.

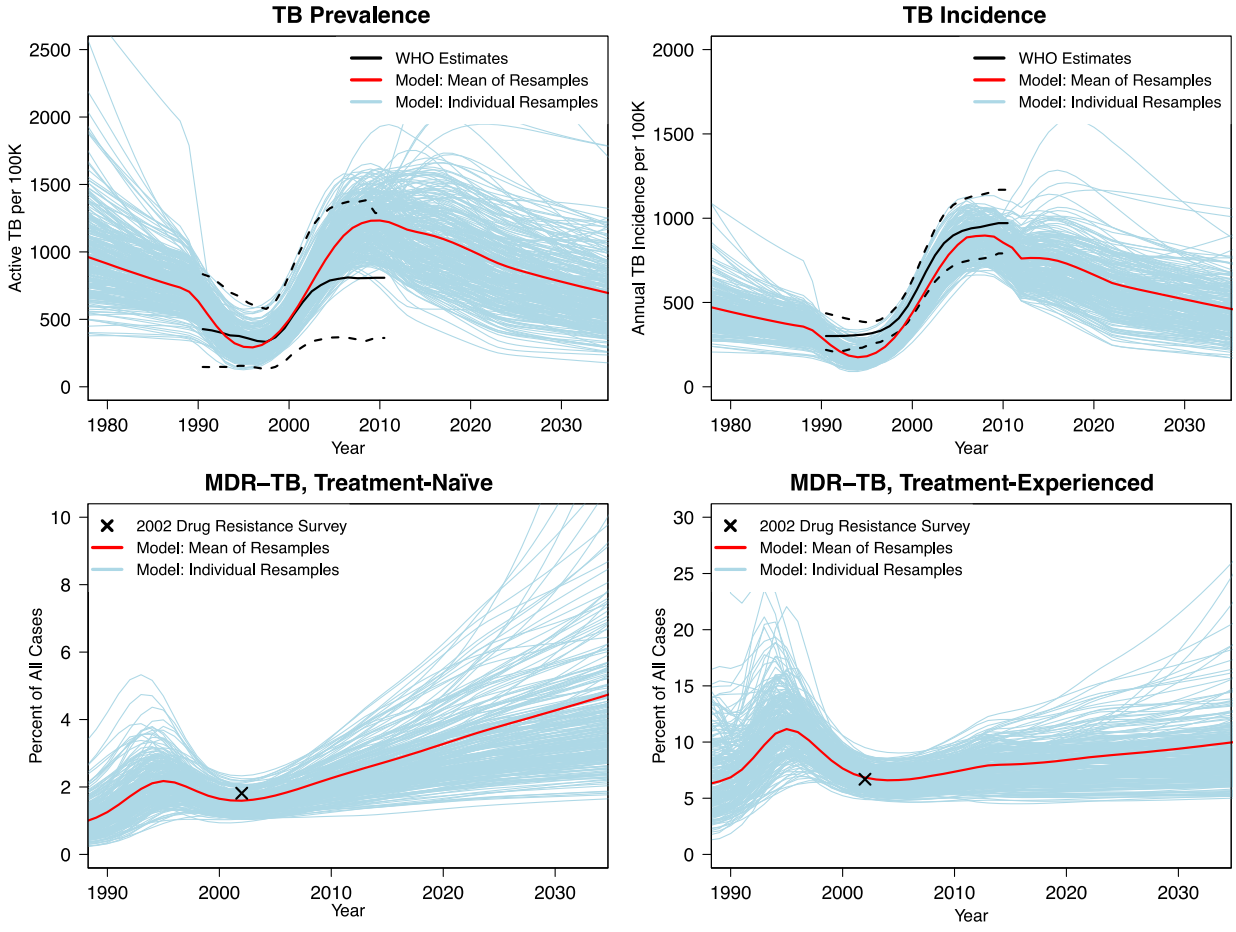

Figure 2.12. Calibrated outcomes for South Africa based on sampling / importance resampling

2.6.5. Sensitivity and uncertainty analyses

We adopted four approaches to investigate the sensitivity of results to changes in model inputs.

2.6.5.1. Deterministic one-way senstitivity analyses

Traditional deterministic one-way sensitivity analyses describe how the value of a model output responds to deliberate changes in the value of a particular input parameter, when all other variables are held at their expected values. For all input parameters, we evaluated how the 10-year incremental cost-effectiveness ratio for Xpert vs. the status quo changed as each individual parameter was varied ±1 standard deviation from the mean of its posterior distribution, while all other variables were held at their posterior mean values. The resulting information represents a set of 'what-if' analyses, useful for identifying situations where the optimal policy decision might change if the value of an individual parameter were found to differ substantially from prior expectations. The main paper (Figure 2.8) reported on results for the 10 most influential parameters identified through this process for South Africa. A full listing of results, by country, is shown here in Tables 2.6-2.10.

2.6.5.2. Analysis of partial rank correlation coefficients

Partial rank correlation coefficients (PRCCs) represent a complementary approach for investigating uncertainty, providing information on the relative influence that individual parameters have on model outcomes based on the results of a probabilistic sensitivity analysis [4,94,95]. We calculated PRCCs using the resampled parameter sets produced by the calibration proceedure. Results for the 10 parameters having the greatest influence on the cost-effectiveness ratio for Xpert in South Africa, under a 10-year time horizon, are shown in Figure 2.9.

Table 2.6. Univariate sensitivity analysis, Botswana (base-case ICER =$1,289)

Parameter description	Low par. value	High par. value	ICER w/ low value	ICER w/ high value
Transmission parameter for individuals with smear-pos TB in 1950	9.6	12.2	1,381	1,248
Annual percentage decline in transmission parameter	0.004	0.010	1,236	1,394
Infectivity of smear-neg TB, relative to smear-pos TB	0.17	0.30	1,447	1,167
Fitness cost for drug-resistant TB strains (% of base-case)	82%	134%	1,392	1,218
Rate of attending TB testing site, for individuals with active TB, DOTS, 1990 (% of base-case)	53%	174%	1,292	1,285
Rate of attending TB testing site, for individuals with active TB, DOTS, 2010 (% of base-case)	90%	191%	1,071	1,561
Rate of attending TB testing site, for individuals with active TB, non-DOTS, 1990 (% of base-case)	48%	136%	1,242	1,335
Rate of attending TB testing site, for individuals with active TB, non-DOTS, 2010 (% of base-case)	50%	140%	1,245	1,334
Rate ratio of TB testing, for individuals without active TB compared to those with active TB	0.011	0.019	1,203	1,374
Specificity of sputum smear microscopy	0.97	0.98	1,256	1,321
Specificity of sputum culture	0.98	0.99	1,284	1,293
Sensitivity of Xpert for TB, smear-neg TB	0.69	0.76	1,314	1,267
Sensitivity of Xpert for TB, smear-pos TB	0.98	0.99	1,295	1,282
Specificity of Xpert for TB	0.99	1.00	1,316	1,261
Sensitivity of Xpert for RIF resistance	0.96	0.99	1,280	1,297
Specificity of Xpert for RIF resistance	0.98	0.99	1,291	1,286
Probability of sputum culture following a negative sputum smear (status quo), tx-naïve patients	0.16	0.27	1,192	1,389
Probability of sputum culture following a negative sputum smear (status quo), tx-experienced patients	0.75	0.85	1,289	1,288
Probability of DST following a positive TB diagnosis (status quo), tx-experienced patients	0.75	0.85	1,324	1,253
Probability of loss to follow-up between initial presentation and tx initiation, with prompt diagnosis	0.12	0.19	1,281	1,298
Probability of loss to follow-up between initial presentation and tx initiation, with delayed diagnosis	0.18	0.30	1,343	1,238
Tx default rate, DOTS (% of base-case)	78%	129%	1,278	1,293
Tx default rate, non-DOTS	0.39	0.70	1,363	1,218
Probability of tx success, individuals with pan-sensitive TB completing 1st-line regimen (% of base-case)	77%	125%	1,304	1,283

Table 2.6. Univariate sensitivity analysis, Botswana (base-case ICER =$1289) (continued)

Parameter description	Low par. value	High par. value	ICER w/ low value	ICER w/ high value
Risk ratio of tx success, 1st-line regimen, semi-sensitive strain	0.79	0.87	1,296	1,282
Risk ratio of tx success, 1st-line regimen, non-sensitive strain	0.32	0.56	1,303	1,278
Risk ratio of tx success, 2nd-line regimen, sensitive strain	0.91	0.95	1,301	1,277
Risk ratio of tx success, 2nd-line regimen, non-sensitive strain	0.34	0.58	1,339	1,260
Risk ratio of tx success, non-DOTS regimen, non-MDR strain	0.65	0.81	1,287	1,290
Risk ratio of tx success, non-DOTS regimen, MDR strain	0.32	0.56	1,302	1,277
Excess mortality rate for active TB, smear-neg	0.20	0.23	1,282	1,295
Excess mortality rate for active TB, smear-pos	0.26	0.37	1,322	1,267
Excess mortality rate for HIV, CD4 >350 cells/µl, no ART	0.006	0.010	1,285	1,292
Excess mortality rate for HIV, CD4 200-350 cells/µl, no ART	0.023	0.038	1,287	1,290
Excess mortality rate for HIV, CD4 <200 cells/µl, no ART	0.17	0.28	1,285	1,291
Excess mortality rate for HIV, on ART initiated at CD4 >350 cells/µl	0.006	0.010	1,289	1,289
Excess mortality rate for HIV, on ART initiated at CD4 200-350 cells/µl	0.017	0.028	1,286	1,291
Excess mortality rate for HIV, on ART initiated at CD4 <200 cells/µl	0.038	0.062	1,275	1,302
Excess mortality rate for advanced HIV (CD4 <200 cells/µl) and active TB without ART	0.62	1.04	1,287	1,290
TB tx mortality rates (% of base-case)	77%	127%	1,308	1,271
Partial immunity afforded by prior infection, HIV-neg	0.60	0.81	1,283	1,303
Partial immunity afforded by prior infection, HIV-pos, CD4 >350 cells/µl, no ART	0.35	0.58	1,291	1,287
Partial immunity afforded by prior infection, HIV-pos, CD4 200-350 cells/µl, no ART	0.19	0.31	1,288	1,290
Partial immunity afforded by prior infection, HIV-pos, CD4 <200 cells/µl, no ART	0.18	0.32	1,288	1,289
Probability of fast breakdown to active TB, with new infection, HIV-neg	0.10	0.12	1,333	1,256
Probability of fast breakdown to active TB, with new infection, HIV-pos, CD4 >350 cells/µl, no ART	0.24	0.41	1,298	1,282

Table 2.6. Univariate sensitivity analysis, Botswana (base-case ICER =$1289) (continued)

Parameter description	Low par. value	High par. value	ICER w/ low value	ICER w/ high value
Probability of fast breakdown to active TB, with new infection, HIV-pos, CD4 200-350 cells/µl, no ART	0.59	0.77	1,290	1,287
Probability of fast breakdown to active TB, with new infection, HIV-pos, CD4 <200 cells/µl, no ART	0.87	1.00	1,289	1,288
Probability of smear-positivity, for incident TB cases, HIV-neg	0.56	0.74	1,190	1,428
Probability of smear-positivity, for incident TB cases, HIV-pos, CD4 >350 cells/µl, no ART	0.34	0.57	1,262	1,317
Probability of smear-positivity, for incident TB cases, HIV-pos, CD4 200-350 cells/µl, no ART	0.27	0.44	1,272	1,307
Probability of smear-positivity, for incident TB cases, HIV-pos, CD4 <200 cells/µl, no ART	0.26	0.44	1,273	1,305
Rate of breakdown, latent/recovered to active TB, HIV-neg	0.0006	0.0014	1,339	1,251
Rate of breakdown, latent/recovered to active TB, HIV-pos, CD4 >350 cells/µl, no ART	0.002	0.004	1,296	1,281
Rate of breakdown, latent/recovered to active TB, HIV-pos, CD4 200-350 cells/µl, no ART	0.08	0.11	1,305	1,275
Rate of breakdown, latent/recovered to active TB, HIV-pos, CD4 <200 cells/µl, no ART	0.14	0.22	1,314	1,273
Rate of conversion, smear-neg to smear-pos active TB	0.012	0.019	1,286	1,291
Rate of self-cure for active TB, HIV-neg	0.19	0.24	1,258	1,321
Rate of self-cure for active TB, HIV-pos, CD4 >350 cells/µl, no ART	0.08	0.13	1,284	1,292
Probability that failed tx cases are correctly identified and returned to tx	0.38	0.63	1,294	1,283
Rate of acquisition of TB drug resistance (% of base-case)	77%	127%	1,179	1,414
HIV incidence trend, post-2011 (% of base-case)	98%	103%	1,290	1,287
Rate of HIV progression for individuals not on ART, from CD4 >350 cells/µl to CD4 200-350 cells/µl	0.11	0.17	1,266	1,308
Rate of HIV progression for individuals not on ART, from CD4 200-350 cells/µl to CD4 <200 cells/µl	0.35	0.66	1,287	1,290
Future ART coverage for tx-eligible HIV-pos individuals	0.66	0.93	1,180	1,371
Effectiveness of ART in reversing effect of HIV on TB natural history	0.54	0.75	1,213	1,393
Per-test cost of smear diagnosis	4.9	7.5	1,334	1,243
Per-test cost of culture	14.4	17.4	1,301	1,276

Table 2.6. Univariate sensitivity analysis, Botswana (base-case ICER =$1289) (continued)

Parameter description	Low par. value	High par. value	ICER w/ low value	ICER w/ high value
Per-test cost of chest X-ray	13.5	19.8	1,288	1,289
Per-test cost of drug sensitivity testing	71.0	94.5	1,296	1,281
Cost of outpatient diagnostic visit	7.7	13.1	1,321	1,256
Cost of outpatient tx visit	5.0	9.0	1,281	1,296
Cost of inpatient care, per day	28.6	48.8	1,246	1,331
Monthly TB regimen costs (% of base-case)	0.74	1.27	1,267	1,310
Monthly frequency of tx activities, averaged over tx course, clinic visits (1st-line)	4.3	7.5	1,299	1,278
Monthly frequency of tx activities, averaged over tx course, clinic visits (2nd-line)	15.9	27.4	1,266	1,311
Monthly frequency of tx activities, averaged over tx course, monitoring smears (1st-line)	0.73	1.25	1,290	1,287
Monthly frequency of tx activities, averaged over tx course, monitoring smears (2nd-line)	0.74	1.26	1,288	1,289
Monthly frequency of tx activities, averaged over tx course, sputum cultures (2nd-line)	0.31	0.54	1,288	1,290
Monthly frequency of tx activities, averaged over tx course, chest X-rays (2nd-line)	0.11	0.18	1,288	1,289
Number of months of inpatient care with MDR-TB tx	3.0	5.1	1,246	1,331
Monthly cost of ART	93.3	116.0	1,227	1,350
Disability weight, active TB	0.20	0.34	1,366	1,219
Disability weight, HIV-pos, CD4 >350 cells/μl, no ART	0.10	0.17	1,285	1,292
Disability weight, HIV-pos, CD4 200-350 cells/μl, no ART	0.23	0.39	1,289	1,289
Disability weight, HIV-pos, CD4 <200 cells/μl, no ART	0.36	0.64	1,282	1,295
Disability weight, HIV-pos, ART initiated CD4 >350	0.10	0.17	1,278	1,300
Disability weight, HIV-pos, ART initiated CD4 200-350	0.12	0.19	1,284	1,293
Disability weight, HIV-pos, ART initiated CD4 <200	0.13	0.21	1,271	1,307
Annual discount rate	0	10%	1,265	1,348

Table 2.7. Univariate sensitivity analysis, Lesotho (base-case ICER =$1071)

Parameter description	Low par. value	High par. value	ICER w/ low value	ICER w/ high value
Transmission parameter for individuals with smear-pos TB in 1950	9.7	12.4	1,281	942
Annual percentage decline in transmission parameter	0.004	0.010	896	1,294
Infectivity of smear-neg TB, relative to smear-pos TB	0.18	0.30	1,254	933
Fitness cost for drug-resistant TB strains (% of base-case)	79%	131%	1,085	1,062
Rate of attending TB testing site, for individuals with active TB, DOTS, 1990 (% of base-case)	58%	185%	1,045	1,090
Rate of attending TB testing site, for individuals with active TB, DOTS, 2010 (% of base-case)	60%	139%	714	1,537
Rate of attending TB testing site, for individuals with active TB, non-DOTS, 1990 (% of base-case)	46%	139%	1,060	1,082
Rate of attending TB testing site, for individuals with active TB, non-DOTS, 2010 (% of base-case)	48%	152%	1,068	1,075
Rate ratio of TB testing, for individuals without active TB compared to those with active TB	0.012	0.019	931	1,212
Specificity of sputum smear microscopy	0.97	0.98	1,058	1,085
Specificity of sputum culture	0.98	0.99	1,070	1,073
Sensitivity of Xpert for TB, smear-neg TB	0.69	0.76	1,101	1,046
Sensitivity of Xpert for TB, smear-pos TB	0.98	0.99	1,077	1,067
Specificity of Xpert for TB	0.99	1.00	1,083	1,060
Sensitivity of Xpert for RIF resistance	0.97	0.99	1,070	1,073
Specificity of Xpert for RIF resistance	0.98	0.99	1,072	1,071
Probability of sputum culture following a negative sputum smear (status quo), tx-naïve patients	0.16	0.27	937	1,227
Probability of sputum culture following a negative sputum smear (status quo), tx-experienced patients	0.74	0.85	1,067	1,076
Probability of DST following a positive TB diagnosis (status quo), tx-experienced patients	0.75	0.85	1,078	1,065
Probability of loss to follow-up between initial presentation and tx initiation, with prompt diagnosis	0.11	0.18	1,060	1,085
Probability of loss to follow-up between initial presentation and tx initiation, with delayed diagnosis	0.18	0.32	1,141	1,008
Tx default rate, DOTS (% of base-case)	73%	120%	1,064	1,074
Tx default rate, non-DOTS	0.48	0.78	1,086	1,058
Probability of tx success, individuals with pan-sensitive TB completing 1st-line regimen (% of base-case)	76%	127%	1,067	1,073

Table 2.7. Univariate sensitivity analysis, Lesotho (base-case ICER =$1071) (continued)

Parameter description	Low par. value	High par. value	ICER w/ low value	ICER w/ high value
Risk ratio of tx success, 1st-line regimen, semi-sensitive strain	0.79	0.87	1,073	1,070
Risk ratio of tx success, 1st-line regimen, non-sensitive strain	0.36	0.58	1,071	1,072
Risk ratio of tx success, 2nd-line regimen, sensitive strain	0.91	0.95	1,074	1,069
Risk ratio of tx success, 2nd-line regimen, non-sensitive strain	0.35	0.57	1,078	1,067
Risk ratio of tx success, non-DOTS regimen, non-MDR strain	0.66	0.81	1,066	1,077
Risk ratio of tx success, non-DOTS regimen, MDR strain	0.32	0.56	1,073	1,070
Excess mortality rate for active TB, smear-neg	0.20	0.23	1,066	1,078
Excess mortality rate for active TB, smear-pos	0.27	0.39	1,046	1,104
Excess mortality rate for HIV, CD4 >350 cells/µl, no ART	0.006	0.010	1,063	1,080
Excess mortality rate for HIV, CD4 200-350 cells/µl, no ART	0.023	0.038	1,061	1,082
Excess mortality rate for HIV, CD4 <200 cells/µl, no ART	0.16	0.25	1,021	1,114
Excess mortality rate for HIV, on ART initiated at CD4 >350 cells/µl	0.006	0.010	1,071	1,071
Excess mortality rate for HIV, on ART initiated at CD4 200-350 cells/µl	0.017	0.029	1,070	1,073
Excess mortality rate for HIV, on ART initiated at CD4 <200 cells/µl	0.039	0.061	1,054	1,089
Excess mortality rate for advanced HIV (CD4 <200 cells/µl) and active TB without ART	0.61	1.00	1,033	1,103
TB tx mortality rates (% of base-case)	78%	130%	1,068	1,075
Partial immunity afforded by prior infection, HIV-neg	0.62	0.82	1,033	1,111
Partial immunity afforded by prior infection, HIV-pos, CD4 >350 cells/µl, no ART	0.33	0.57	1,069	1,074
Partial immunity afforded by prior infection, HIV-pos, CD4 200-350 cells/µl, no ART	0.18	0.31	1,069	1,074
Partial immunity afforded by prior infection, HIV-pos, CD4 <200 cells/µl, no ART	0.18	0.32	1,067	1,076
Probability of fast breakdown to active TB, with new infection, HIV-neg	0.10	0.12	1,159	1,000
Probability of fast breakdown to active TB, with new infection, HIV-pos, CD4 >350 cells/µl, no ART	0.25	0.43	1,109	1,036

Table 2.7. Univariate sensitivity analysis, Lesotho (base-case ICER =$1071) (continued)

Parameter description	Low par. value	High par. value	ICER w/ low value	ICER w/ high value
Probability of fast breakdown to active TB, with new infection, HIV-pos, CD4 200-350 cells/µl, no ART	0.58	0.76	1,077	1,066
Probability of fast breakdown to active TB, with new infection, HIV-pos, CD4 <200 cells/µl, no ART	0.85	1.00	1,078	1,067
Probability of smear-positivity, for incident TB cases, HIV-neg	0.53	0.72	1,043	1,120
Probability of smear-positivity, for incident TB cases, HIV-pos, CD4 >350 cells/µl, no ART	0.33	0.58	1,051	1,093
Probability of smear-positivity, for incident TB cases, HIV-pos, CD4 200-350 cells/µl, no ART	0.26	0.44	1,058	1,085
Probability of smear-positivity, for incident TB cases, HIV-pos, CD4 <200 cells/µl, no ART	0.27	0.44	1,060	1,084
Rate of breakdown, latent/recovered to active TB, HIV-neg	0.0005	0.00122	1,137	1,025
Rate of breakdown, latent/recovered to active TB, HIV-pos, CD4 >350 cells/µl, no ART	0.002	0.004	1,082	1,061
Rate of breakdown, latent/recovered to active TB, HIV-pos, CD4 200-350 cells/µl, no ART	0.08	0.11	1,099	1,048
Rate of breakdown, latent/recovered to active TB, HIV-pos, CD4 <200 cells/µl, no ART	0.15	0.24	1,140	1,025
Rate of conversion, smear-neg to smear-pos active TB	0.011	0.018	1,071	1,072
Rate of self-cure for active TB, HIV-neg	0.18	0.24	1,027	1,119
Rate of self-cure for active TB, HIV-pos, CD4 >350 cells/µl, no ART	0.07	0.13	1,065	1,078
Probability that failed tx cases are correctly identified and returned to tx	0.39	0.65	1,072	1,071
Rate of acquisition of TB drug resistance (% of base-case)	66%	108%	1,052	1,094
HIV incidence trend, post-2011 (% of base-case)	98%	102%	1,076	1,066
Rate of HIV progression for individuals not on ART, from CD4 >350 cells/µl to CD4 200-350 cells/µl	0.11	0.18	1,092	1,066
Rate of HIV progression for individuals not on ART, from CD4 200-350 cells/µl to CD4 <200 cells/µl	0.36	0.61	1,028	1,102
Future ART coverage for tx-eligible HIV-pos individuals	0.67	0.91	1,009	1,134
Effectiveness of ART in reversing effect of HIV on TB natural history	0.58	0.79	1,000	1,157
Per-test cost of smear diagnosis	2.7	3.8	1,091	1,052
Per-test cost of culture	7.7	9.4	1,078	1,065

Table 2.7. Univariate sensitivity analysis, Lesotho (base-case ICER =$1071) (continued)

Parameter description	Low par. value	High par. value	ICER w/ low value	ICER w/ high value
Per-test cost of chest X-ray	7.2	10.6	1,071	1,072
Per-test cost of drug sensitivity testing	37.9	51.1	1,075	1,068
Cost of outpatient diagnostic visit	2.2	3.8	1,080	1,063
Cost of outpatient tx visit	1.5	2.5	1,073	1,070
Cost of inpatient care, per day	6.6	10.9	1,068	1,075
Monthly TB regimen costs (% of base-case)	0.75	1.24	1,064	1,079
Monthly frequency of tx activities, averaged over tx course, clinic visits (1st-line)	4.3	7.4	1,074	1,069
Monthly frequency of tx activities, averaged over tx course, clinic visits (2nd-line)	16.9	28.0	1,069	1,074
Monthly frequency of tx activities, averaged over tx course, monitoring smears (1st-line)	0.76	1.29	1,072	1,071
Monthly frequency of tx activities, averaged over tx course, monitoring smears (2nd-line)	0.75	1.22	1,071	1,072
Monthly frequency of tx activities, averaged over tx course, sputum cultures (2nd-line)	0.32	0.54	1,071	1,072
Monthly frequency of tx activities, averaged over tx course, chest X-rays (2nd-line)	0.10	0.18	1,071	1,072
Number of months of inpatient care with MDR-TB tx	3.0	5.1	1,067	1,076
Monthly cost of ART	62.5	76.5	1,035	1,108
Disability weight, active TB	0.21	0.35	1,130	1,019
Disability weight, HIV-pos, CD4 >350 cells/µl, no ART	0.10	0.17	1,067	1,076
Disability weight, HIV-pos, CD4 200-350 cells/µl, no ART	0.24	0.40	1,071	1,071
Disability weight, HIV-pos, CD4 <200 cells/µl, no ART	0.36	0.64	1,064	1,079
Disability weight, HIV-pos, ART initiated CD4 >350	0.10	0.17	1,067	1,076
Disability weight, HIV-pos, ART initiated CD4 200-350	0.12	0.19	1,065	1,078
Disability weight, HIV-pos, ART initiated CD4 <200	0.12	0.21	1,053	1,091
Annual discount rate	0	10%	1,050	1,126

Table 2.8. Univariate sensitivity analysis, Namibia (base-case ICER =$863)

Parameter description	Low par. value	High par. value	ICER w/ low value	ICER w/ high value
Transmission parameter for individuals with smear-pos TB in 1950	10.0	12.8	955	811
Annual percentage decline in transmission parameter	0.003	0.007	803	942
Infectivity of smear-neg TB, relative to smear-pos TB	0.19	0.33	992	768
Fitness cost for drug-resistant TB strains (% of base-case)	79%	132%	916	828
Rate of attending TB testing site, for individuals with active TB, DOTS, 1990 (% of base-case)	52%	137%	864	862
Rate of attending TB testing site, for individuals with active TB, DOTS, 2010 (% of base-case)	42%	96%	688	1,088
Rate of attending TB testing site, for individuals with active TB, non-DOTS, 1990 (% of base-case)	47%	153%	839	887
Rate of attending TB testing site, for individuals with active TB, non-DOTS, 2010 (% of base-case)	44%	132%	838	890
Rate ratio of TB testing, for individuals without active TB compared to those with active TB	0.011	0.019	786	941
Specificity of sputum smear microscopy	0.97	0.98	848	879
Specificity of sputum culture	0.98	0.99	861	866
Sensitivity of Xpert for TB, smear-neg TB	0.69	0.76	883	846
Sensitivity of Xpert for TB, smear-pos TB	0.98	0.99	870	857
Specificity of Xpert for TB	0.99	1.00	878	849
Sensitivity of Xpert for RIF resistance	0.97	0.99	859	868
Specificity of Xpert for RIF resistance	0.98	0.99	865	862
Probability of sputum culture following a negative sputum smear (status quo), tx-naïve patients	0.15	0.25	804	928
Probability of sputum culture following a negative sputum smear (status quo), tx-experienced patients	0.75	0.86	864	863
Probability of DST following a positive TB diagnosis (status quo), tx-experienced patients	0.75	0.86	881	846
Probability of loss to follow-up between initial presentation and tx initiation, with prompt diagnosis	0.12	0.19	858	870
Probability of loss to follow-up between initial presentation and tx initiation, with delayed diagnosis	0.19	0.31	895	834
Tx default rate, DOTS (% of base-case)	74%	116%	858	866
Tx default rate, non-DOTS	0.45	0.75	908	822
Probability of tx success, individuals with pan-sensitive TB completing 1st-line regimen (% of base-case)	73%	129%	873	861

Table 2.8. Univariate sensitivity analysis, Namibia (base-case ICER =$863) (continued)

Parameter description	Low par. value	High par. value	ICER w/ low value	ICER w/ high value
Risk ratio of tx success, 1st-line regimen, semi-sensitive strain	0.79	0.87	866	861
Risk ratio of tx success, 1st-line regimen, non-sensitive strain	0.36	0.60	866	861
Risk ratio of tx success, 2nd-line regimen, sensitive strain	0.91	0.95	869	858
Risk ratio of tx success, 2nd-line regimen, non-sensitive strain	0.33	0.56	877	855
Risk ratio of tx success, non-DOTS regimen, non-MDR strain	0.67	0.81	861	865
Risk ratio of tx success, non-DOTS regimen, MDR strain	0.33	0.54	869	859
Excess mortality rate for active TB, smear-neg	0.19	0.23	851	876
Excess mortality rate for active TB, smear-pos	0.27	0.37	886	848
Excess mortality rate for HIV, CD4 >350 cells/µl, no ART	0.006	0.009	861	866
Excess mortality rate for HIV, CD4 200-350 cells/µl, no ART	0.022	0.036	861	866
Excess mortality rate for HIV, CD4 <200 cells/µl, no ART	0.16	0.26	858	870
Excess mortality rate for HIV, on ART initiated at CD4 >350 cells/µl	0.006	0.010	863	863
Excess mortality rate for HIV, on ART initiated at CD4 200-350 cells/µl	0.017	0.028	863	864
Excess mortality rate for HIV, on ART initiated at CD4 <200 cells/µl	0.037	0.061	855	873
Excess mortality rate for advanced HIV (CD4 <200 cells/µl) and active TB without ART	0.61	0.97	860	866
TB tx mortality rates (% of base-case)	78%	126%	871	857
Partial immunity afforded by prior infection, HIV-neg	0.61	0.83	847	885
Partial immunity afforded by prior infection, HIV-pos, CD4 >350 cells/µl, no ART	0.32	0.55	863	864
Partial immunity afforded by prior infection, HIV-pos, CD4 200-350 cells/µl, no ART	0.19	0.31	862	865
Partial immunity afforded by prior infection, HIV-pos, CD4 <200 cells/µl, no ART	0.18	0.31	861	866
Probability of fast breakdown to active TB, with new infection, HIV-neg	0.10	0.12	920	819
Probability of fast breakdown to active TB, with new infection, HIV-pos, CD4 >350 cells/µl, no ART	0.26	0.43	868	860

Table 2.8. Univariate sensitivity analysis, Namibia (base-case ICER =$863) (continued)

Parameter description	Low par. value	High par. value	ICER w/ low value	ICER w/ high value
Probability of fast breakdown to active TB, with new infection, HIV-pos, CD4 200-350 cells/µl, no ART	0.58	0.75	864	863
Probability of fast breakdown to active TB, with new infection, HIV-pos, CD4 <200 cells/µl, no ART	0.87	1.00	864	863
Probability of smear-positivity, for incident TB cases, HIV-neg	0.54	0.72	783	981
Probability of smear-positivity, for incident TB cases, HIV-pos, CD4 >350 cells/µl, no ART	0.35	0.58	855	873
Probability of smear-positivity, for incident TB cases, HIV-pos, CD4 200-350 cells/µl, no ART	0.27	0.47	858	869
Probability of smear-positivity, for incident TB cases, HIV-pos, CD4 <200 cells/µl, no ART	0.28	0.45	860	867
Rate of breakdown, latent/recovered to active TB, HIV-neg	0.0005	0.00141	911	826
Rate of breakdown, latent/recovered to active TB, HIV-pos, CD4 >350 cells/µl, no ART	0.002	0.004	866	861
Rate of breakdown, latent/recovered to active TB, HIV-pos, CD4 200-350 cells/µl, no ART	0.08	0.12	871	857
Rate of breakdown, latent/recovered to active TB, HIV-pos, CD4 <200 cells/µl, no ART	0.15	0.25	885	850
Rate of conversion, smear-neg to smear-pos active TB	0.012	0.018	862	865
Rate of self-cure for active TB, HIV-neg	0.18	0.24	831	898
Rate of self-cure for active TB, HIV-pos, CD4 >350 cells/µl, no ART	0.08	0.13	861	865
Probability that failed tx cases are correctly identified and returned to tx	0.37	0.64	866	861
Rate of acquisition of TB drug resistance (% of base-case)	70%	113%	812	921
HIV incidence trend, post-2011 (% of base-case)	97%	103%	863	864
Rate of HIV progression for individuals not on ART, from CD4 >350 cells/µl to CD4 200-350 cells/µl	0.12	0.19	860	870
Rate of HIV progression for individuals not on ART, from CD4 200-350 cells/µl to CD4 <200 cells/µl	0.35	0.61	858	868
Future ART coverage for tx-eligible HIV-pos individuals	0.65	0.92	816	911
Effectiveness of ART in reversing effect of HIV on TB natural history	0.50	0.71	824	917
Per-test cost of smear diagnosis	4.3	6.3	886	841
Per-test cost of culture	12.5	15.2	871	856

Table 2.8. Univariate sensitivity analysis, Namibia (base-case ICER =$863) (continued)

Parameter description	Low par. value	High par. value	ICER w/ low value	ICER w/ high value
Per-test cost of chest X-ray	11.7	17.0	863	864
Per-test cost of drug sensitivity testing	61.0	80.5	867	860
Cost of outpatient diagnostic visit	5.9	10.0	878	849
Cost of outpatient tx visit	3.9	6.6	854	873
Cost of inpatient care, per day	20.9	35.3	845	882
Monthly TB regimen costs (% of base-case)	0.73	1.25	850	877
Monthly frequency of tx activities, averaged over tx course, clinic visits (1st-line)	4.4	7.2	863	864
Monthly frequency of tx activities, averaged over tx course, clinic visits (2nd-line)	16.6	28.9	852	874
Monthly frequency of tx activities, averaged over tx course, monitoring smears (1st-line)	0.75	1.22	863	864
Monthly frequency of tx activities, averaged over tx course, monitoring smears (2nd-line)	0.76	1.25	863	864
Monthly frequency of tx activities, averaged over tx course, sputum cultures (2nd-line)	0.32	0.54	863	864
Monthly frequency of tx activities, averaged over tx course, chest X-rays (2nd-line)	0.11	0.18	863	864
Number of months of inpatient care with MDR-TB tx	3.0	5.2	845	882
Monthly cost of ART	84.6	104.0	829	898
Disability weight, active TB	0.21	0.34	912	820
Disability weight, HIV-pos, CD4 >350 cells/µl, no ART	0.10	0.17	863	864
Disability weight, HIV-pos, CD4 200-350 cells/µl, no ART	0.25	0.40	863	863
Disability weight, HIV-pos, CD4 <200 cells/µl, no ART	0.38	0.64	861	866
Disability weight, HIV-pos, ART initiated CD4 >350	0.10	0.17	860	867
Disability weight, HIV-pos, ART initiated CD4 200-350	0.12	0.19	861	866
Disability weight, HIV-pos, ART initiated CD4 <200	0.13	0.21	854	873
Annual discount rate	0	10%	843	915

Table 2.9. Univariate sensitivity analysis, South Africa (base-case ICER =$986)

Parameter description	Low par. value	High par. value	ICER w/ low value	ICER w/ high value
Transmission parameter for individuals with smear-pos TB in 1950	10.4	13.2	979	1,019
Annual percentage decline in transmission parameter	0.003	0.007	1,012	983
Infectivity of smear-neg TB, relative to smear-pos TB	0.17	0.28	1,087	907
Fitness cost for drug-resistant TB strains (% of base-case)	68%	106%	1,105	903
Rate of attending TB testing site, for individuals with active TB, DOTS, 1990 (% of base-case)	51%	159%	1,027	958
Rate of attending TB testing site, for individuals with active TB, DOTS, 2010 (% of base-case)	52%	126%	903	1,085
Rate of attending TB testing site, for individuals with active TB, non-DOTS, 1990 (% of base-case)	65%	178%	918	1,055
Rate of attending TB testing site, for individuals with active TB, non-DOTS, 2010 (% of base-case)	48%	165%	905	1,070
Rate ratio of TB testing, for individuals without active TB compared to those with active TB	0.011	0.019	959	1,013
Specificity of sputum smear microscopy	0.97	0.98	976	996
Specificity of sputum culture	0.98	0.99	985	987
Sensitivity of Xpert for TB, smear-neg TB	0.70	0.76	1,003	971
Sensitivity of Xpert for TB, smear-pos TB	0.98	0.99	994	978
Specificity of Xpert for TB	0.99	1.00	994	978
Sensitivity of Xpert for RIF resistance	0.97	0.99	979	993
Specificity of Xpert for RIF resistance	0.98	0.99	988	985
Probability of sputum culture following a negative sputum smear (status quo), tx-naïve patients	0.15	0.27	925	1,057
Probability of sputum culture following a negative sputum smear (status quo), tx-experienced patients	0.75	0.86	987	985
Probability of DST following a positive TB diagnosis (status quo), tx-experienced patients	0.76	0.85	1,011	961
Probability of loss to follow-up between initial presentation and tx initiation, with prompt diagnosis	0.11	0.20	987	987
Probability of loss to follow-up between initial presentation and tx initiation, with delayed diagnosis	0.20	0.32	1,014	960
Tx default rate, DOTS (% of base-case)	67%	119%	983	986
Tx default rate, non-DOTS	0.37	0.65	1,083	896
Probability of tx success, individuals with pan-sensitive TB completing 1st-line regimen (% of base-case)	71%	125%	1,025	973

Table 2.9. Univariate sensitivity analysis, South Africa (base-case ICER =$986) (continued)

Parameter description	Low par. value	High par. value	ICER w/ low value	ICER w/ high value
Risk ratio of tx success, 1st-line regimen, semi-sensitive strain	0.79	0.88	993	980
Risk ratio of tx success, 1st-line regimen, non-sensitive strain	0.32	0.54	1,029	959
Risk ratio of tx success, 2nd-line regimen, sensitive strain	0.91	0.95	998	975
Risk ratio of tx success, 2nd-line regimen, non-sensitive strain	0.32	0.56	1,041	950
Risk ratio of tx success, non-DOTS regimen, non-MDR strain	0.67	0.81	985	987
Risk ratio of tx success, non-DOTS regimen, MDR strain	0.33	0.55	1,016	961
Excess mortality rate for active TB, smear-neg	0.19	0.23	983	989
Excess mortality rate for active TB, smear-pos	0.26	0.37	1,072	922
Excess mortality rate for HIV, CD4 >350 cells/µl, no ART	0.006	0.010	985	987
Excess mortality rate for HIV, CD4 200-350 cells/µl, no ART	0.021	0.036	986	986
Excess mortality rate for HIV, CD4 <200 cells/µl, no ART	0.16	0.26	993	980
Excess mortality rate for HIV, on ART initiated at CD4 >350 cells/µl	0.006	0.010	986	986
Excess mortality rate for HIV, on ART initiated at CD4 200-350 cells/µl	0.018	0.029	986	986
Excess mortality rate for HIV, on ART initiated at CD4 <200 cells/µl	0.040	0.063	988	984
Excess mortality rate for advanced HIV (CD4 <200 cells/µl) and active TB without ART	0.60	1.02	983	987
TB tx mortality rates (% of base-case)	73%	125%	1,012	962
Partial immunity afforded by prior infection, HIV-neg	0.58	0.81	1,044	967
Partial immunity afforded by prior infection, HIV-pos, CD4 >350 cells/µl, no ART	0.33	0.54	988	985
Partial immunity afforded by prior infection, HIV-pos, CD4 200-350 cells/µl, no ART	0.18	0.30	985	987
Partial immunity afforded by prior infection, HIV-pos, CD4 <200 cells/µl, no ART	0.19	0.32	985	987
Probability of fast breakdown to active TB, with new infection, HIV-neg	0.10	0.13	988	997
Probability of fast breakdown to active TB, with new infection, HIV-pos, CD4 >350 cells/µl, no ART	0.27	0.42	986	988

Table 2.9. Univariate sensitivity analysis, South Africa (base-case ICER =$986) (continued)

Parameter description	Low par. value	High par. value	ICER w/ low value	ICER w/ high value
Probability of fast breakdown to active TB, with new infection, HIV-pos, CD4 200-350 cells/µl, no ART	0.58	0.76	984	988
Probability of fast breakdown to active TB, with new infection, HIV-pos, CD4 <200 cells/µl, no ART	0.88	1.00	985	987
Probability of smear-positivity, for incident TB cases, HIV-neg	0.57	0.74	876	1,134
Probability of smear-positivity, for incident TB cases, HIV-pos, CD4 >350 cells/µl, no ART	0.37	0.62	956	1,020
Probability of smear-positivity, for incident TB cases, HIV-pos, CD4 200-350 cells/µl, no ART	0.28	0.46	973	1,000
Probability of smear-positivity, for incident TB cases, HIV-pos, CD4 <200 cells/µl, no ART	0.28	0.48	970	1,003
Rate of breakdown, latent/recovered to active TB, HIV-neg	0.0005	0.00126	991	983
Rate of breakdown, latent/recovered to active TB, HIV-pos, CD4 >350 cells/µl, no ART	0.002	0.004	987	985
Rate of breakdown, latent/recovered to active TB, HIV-pos, CD4 200-350 cells/µl, no ART	0.08	0.11	984	988
Rate of breakdown, latent/recovered to active TB, HIV-pos, CD4 <200 cells/µl, no ART	0.14	0.23	979	995
Rate of conversion, smear-neg to smear-pos active TB	0.012	0.018	984	988
Rate of self-cure for active TB, HIV-neg	0.18	0.23	975	998
Rate of self-cure for active TB, HIV-pos, CD4 >350 cells/µl, no ART	0.08	0.12	983	989
Probability that failed tx cases are correctly identified and returned to tx	0.38	0.62	994	978
Rate of acquisition of TB drug resistance (% of base-case)	85%	123%	888	1,094
HIV incidence trend, post-2011 (% of base-case)	98%	103%	986	987
Rate of HIV progression for individuals not on ART, from CD4 >350 cells/µl to CD4 200-350 cells/µl	0.11	0.17	960	1,005
Rate of HIV progression for individuals not on ART, from CD4 200-350 cells/µl to CD4 <200 cells/µl	0.37	0.63	980	990
Future ART coverage for tx-eligible HIV-pos individuals	0.67	0.93	941	1,026
Effectiveness of ART in reversing effect of HIV on TB natural history	0.60	0.80	978	994
Per-test cost of smear diagnosis	4.8	7.0	998	974
Per-test cost of culture	14.2	17.1	990	982

Table 2.9. Univariate sensitivity analysis, South Africa (base-case ICER =$986) (continued)

Parameter description	Low par. value	High par. value	ICER w/ low value	ICER w/ high value
Per-test cost of chest X-ray	13.6	19.3	986	986
Per-test cost of drug sensitivity testing	66.7	89.5	989	983
Cost of outpatient diagnostic visit	7.9	12.6	997	975
Cost of outpatient tx visit	5.0	8.3	952	1,020
Cost of inpatient care, per day	28.9	49.9	938	1,034
Monthly TB regimen costs (% of base-case)	0.79	1.27	961	1,011
Monthly frequency of tx activities, averaged over tx course, clinic visits (1st-line)	4.3	7.5	977	995
Monthly frequency of tx activities, averaged over tx course, clinic visits (2nd-line)	16.0	27.9	956	1,016
Monthly frequency of tx activities, averaged over tx course, monitoring smears (1st-line)	0.77	1.21	985	987
Monthly frequency of tx activities, averaged over tx course, monitoring smears (2nd-line)	0.75	1.18	985	987
Monthly frequency of tx activities, averaged over tx course, sputum cultures (2nd-line)	0.32	0.52	985	987
Monthly frequency of tx activities, averaged over tx course, chest X-rays (2nd-line)	0.11	0.17	986	986
Number of months of inpatient care with MDR-TB tx	3.0	4.7	945	1,027
Monthly cost of ART	91.9	114.0	943	1,029
Disability weight, active TB	0.20	0.32	1,037	940
Disability weight, HIV-pos, CD4 >350 cells/μl, no ART	0.10	0.17	983	989
Disability weight, HIV-pos, CD4 200-350 cells/μl, no ART	0.23	0.38	986	986
Disability weight, HIV-pos, CD4 <200 cells/μl, no ART	0.38	0.63	982	990
Disability weight, HIV-pos, ART initiated CD4 >350	0.11	0.17	983	989
Disability weight, HIV-pos, ART initiated CD4 200-350	0.12	0.20	982	990
Disability weight, HIV-pos, ART initiated CD4 <200	0.13	0.21	973	999
Annual discount rate	0	10%	966	1,038

Table 2.10. Univariate sensitivity analysis, Swaziland (base-case ICER =$770)

Parameter description	Low par. value	High par. value	ICER w/ low value	ICER w/ high value
Transmission parameter for individuals with smear-pos TB in 1950	9.9	12.6	819	751
Annual percentage decline in transmission parameter	0.003	0.008	742	827
Infectivity of smear-neg TB, relative to smear-pos TB	0.18	0.32	880	695
Fitness cost for drug-resistant TB strains (% of base-case)	77%	130%	837	729
Rate of attending TB testing site, for individuals with active TB, DOTS, 1990 (% of base-case)	56%	182%	783	762
Rate of attending TB testing site, for individuals with active TB, DOTS, 2010 (% of base-case)	73%	193%	648	940
Rate of attending TB testing site, for individuals with active TB, non-DOTS, 1990 (% of base-case)	48%	143%	751	789
Rate of attending TB testing site, for individuals with active TB, non-DOTS, 2010 (% of base-case)	53%	153%	746	796
Rate ratio of TB testing, for individuals without active TB compared to those with active TB	0.011	0.019	731	810
Specificity of sputum smear microscopy	0.97	0.98	764	777
Specificity of sputum culture	0.98	0.99	770	771
Sensitivity of Xpert for TB, smear-neg TB	0.70	0.77	784	758
Sensitivity of Xpert for TB, smear-pos TB	0.98	0.99	774	767
Specificity of Xpert for TB	0.99	1.00	776	765
Sensitivity of Xpert for RIF resistance	0.96	0.99	767	774
Specificity of Xpert for RIF resistance	0.98	0.99	772	769
Probability of sputum culture following a negative sputum smear (status quo), tx-naïve patients	0.15	0.27	713	837
Probability of sputum culture following a negative sputum smear (status quo), tx-experienced patients	0.75	0.86	771	770
Probability of DST following a positive TB diagnosis (status quo), tx-experienced patients	0.75	0.85	785	756
Probability of loss to follow-up between initial presentation and tx initiation, with prompt diagnosis	0.12	0.19	767	775
Probability of loss to follow-up between initial presentation and tx initiation, with delayed diagnosis	0.18	0.31	797	746
Tx default rate, DOTS (% of base-case)	75%	125%	766	772
Tx default rate, non-DOTS	0.43	0.72	807	736
Probability of tx success, individuals with pan-sensitive TB completing 1st-line regimen (% of base-case)	73%	121%	784	765

Table 2.10. Univariate sensitivity analysis, Swaziland (base-case ICER =$770) (continued)

Parameter description	Low par. value	High par. value	ICER w/ low value	ICER w/ high value
Risk ratio of tx success, 1st-line regimen, semi-sensitive strain	0.79	0.87	774	767
Risk ratio of tx success, 1st-line regimen, non-sensitive strain	0.35	0.58	782	763
Risk ratio of tx success, 2nd-line regimen, sensitive strain	0.91	0.95	776	765
Risk ratio of tx success, 2nd-line regimen, non-sensitive strain	0.33	0.57	791	758
Risk ratio of tx success, non-DOTS regimen, non-MDR strain	0.65	0.81	769	772
Risk ratio of tx success, non-DOTS regimen, MDR strain	0.33	0.55	778	764
Excess mortality rate for active TB, smear-neg	0.20	0.23	765	776
Excess mortality rate for active TB, smear-pos	0.27	0.39	800	748
Excess mortality rate for HIV, CD4 >350 cells/µl, no ART	0.006	0.010	768	773
Excess mortality rate for HIV, CD4 200-350 cells/µl, no ART	0.023	0.038	769	772
Excess mortality rate for HIV, CD4 <200 cells/µl, no ART	0.16	0.26	772	769
Excess mortality rate for HIV, on ART initiated at CD4 >350 cells/µl	0.006	0.010	770	770
Excess mortality rate for HIV, on ART initiated at CD4 200-350 cells/µl	0.017	0.029	770	770
Excess mortality rate for HIV, on ART initiated at CD4 <200 cells/µl	0.039	0.062	769	773
Excess mortality rate for advanced HIV (CD4 <200 cells/µl) and active TB without ART	0.65	1.08	759	779
TB tx mortality rates (% of base-case)	77%	130%	784	758
Partial immunity afforded by prior infection, HIV-neg	0.60	0.81	766	778
Partial immunity afforded by prior infection, HIV-pos, CD4 >350 cells/µl, no ART	0.33	0.56	769	772
Partial immunity afforded by prior infection, HIV-pos, CD4 200-350 cells/µl, no ART	0.18	0.31	769	772
Partial immunity afforded by prior infection, HIV-pos, CD4 <200 cells/µl, no ART	0.18	0.33	768	773
Probability of fast breakdown to active TB, with new infection, HIV-neg	0.10	0.12	795	751
Probability of fast breakdown to active TB, with new infection, HIV-pos, CD4 >350 cells/µl, no ART	0.26	0.44	789	756

Table 2.10. Univariate sensitivity analysis, Swaziland (base-case ICER =$770) (continued)

Parameter description	Low par. value	High par. value	ICER w/ low value	ICER w/ high value
Probability of fast breakdown to active TB, with new infection, HIV-pos, CD4 200-350 cells/µl, no ART	0.58	0.76	771	770
Probability of fast breakdown to active TB, with new infection, HIV-pos, CD4 <200 cells/µl, no ART	0.88	1.00	772	770
Probability of smear-positivity, for incident TB cases, HIV-neg	0.54	0.72	715	842
Probability of smear-positivity, for incident TB cases, HIV-pos, CD4 >350 cells/µl, no ART	0.36	0.60	749	795
Probability of smear-positivity, for incident TB cases, HIV-pos, CD4 200-350 cells/µl, no ART	0.27	0.45	764	778
Probability of smear-positivity, for incident TB cases, HIV-pos, CD4 <200 cells/µl, no ART	0.27	0.45	763	779
Rate of breakdown, latent/recovered to active TB, HIV-neg	0.0005	0.00128	779	763
Rate of breakdown, latent/recovered to active TB, HIV-pos, CD4 >350 cells/µl, no ART	0.002	0.004	773	768
Rate of breakdown, latent/recovered to active TB, HIV-pos, CD4 200-350 cells/µl, no ART	0.08	0.12	773	769
Rate of breakdown, latent/recovered to active TB, HIV-pos, CD4 <200 cells/µl, no ART	0.14	0.24	777	769
Rate of conversion, smear-neg to smear-pos active TB	0.012	0.018	769	772
Rate of self-cure for active TB, HIV-neg	0.18	0.24	756	785
Rate of self-cure for active TB, HIV-pos, CD4 >350 cells/µl, no ART	0.07	0.13	765	775
Probability that failed tx cases are correctly identified and returned to tx	0.38	0.65	774	767
Rate of acquisition of TB drug resistance (% of base-case)	70%	116%	716	833
HIV incidence trend, post-2011 (% of base-case)	97%	102%	772	769
Rate of HIV progression for individuals not on ART, from CD4 >350 cells/µl to CD4 200-350 cells/µl	0.11	0.17	751	785
Rate of HIV progression for individuals not on ART, from CD4 200-350 cells/µl to CD4 <200 cells/µl	0.39	0.66	760	778
Future ART coverage for tx-eligible HIV-pos individuals	0.66	0.92	722	814
Effectiveness of ART in reversing effect of HIV on TB natural history	0.56	0.78	745	802
Per-test cost of smear diagnosis	3.4	5.0	780	761
Per-test cost of culture	10.0	11.9	773	767

Table 2.10. Univariate sensitivity analysis, Swaziland (base-case ICER =$770) (continued)

Parameter description	Low par. value	High par. value	ICER w/ low value	ICER w/ high value
Per-test cost of chest X-ray	9.4	13.5	770	771
Per-test cost of drug sensitivity testing	48.6	64.8	773	768
Cost of outpatient diagnostic visit	4.6	8.0	779	762
Cost of outpatient tx visit	3.1	5.4	757	784
Cost of inpatient care, per day	15.8	27.5	753	788
Monthly TB regimen costs (% of base-case)	0.72	1.20	755	786
Monthly frequency of tx activities, averaged over tx course, clinic visits (1st-line)	4.4	7.4	766	775
Monthly frequency of tx activities, averaged over tx course, clinic visits (2nd-line)	16.5	27.4	761	780
Monthly frequency of tx activities, averaged over tx course, monitoring smears (1st-line)	0.76	1.29	770	771
Monthly frequency of tx activities, averaged over tx course, monitoring smears (2nd-line)	0.71	1.24	770	771
Monthly frequency of tx activities, averaged over tx course, sputum cultures (2nd-line)	0.34	0.57	770	771
Monthly frequency of tx activities, averaged over tx course, chest X-rays (2nd-line)	0.10	0.18	770	771
Number of months of inpatient care with MDR-TB tx	2.9	5.2	753	788
Monthly cost of ART	73.7	89.6	733	808
Disability weight, active TB	0.21	0.35	814	731
Disability weight, HIV-pos, CD4 >350 cells/µl, no ART	0.10	0.17	767	774
Disability weight, HIV-pos, CD4 200-350 cells/µl, no ART	0.25	0.41	770	770
Disability weight, HIV-pos, CD4 <200 cells/µl, no ART	0.36	0.62	766	775
Disability weight, HIV-pos, ART initiated CD4 >350	0.11	0.17	767	774
Disability weight, HIV-pos, ART initiated CD4 200-350	0.12	0.19	767	774
Disability weight, HIV-pos, ART initiated CD4 <200	0.13	0.21	759	783
Annual discount rate	0	10%	758	802

2.6.5.3. Alternative scenarios relating to HIV treatment, TB diagnostic algorithms and MDR-TB treatment

In addition to the one-way sensitivity analyses described above, we defined a range of additional scenarios that included alternative assumptions regarding HIV treatment, TB diagnostic algorithms, and MDR-TB treatment components. In each of these further analyses, we adjusted the model inputs relating to each new scenario then re-ran the whole simulation, calculating point estimates and posterior 95% intervals as described for the main analysis.

The cost-effectiveness ratios from the main analysis aim to capture the major changes in health system resource use and health outcomes resulting from the adoption of the Xpert algorithm, including increases in TB treatment and HIV treatment volume. The increase in TB treatment volume is a direct consequence of better case-finding under the Xpert algorithm. The increase in ART volume is an indirect consequence of Xpert introduction, resulting from improved survival of TB-HIV coinfected individuals currently receiving ART or those who would go on to receive ART in the future. In order to disentangle the direct effect of Xpert from this secondary effect through HIV survival, we constructed a scenario in which access to ART under a scaled-up Xpert approach was constrained to be the same as in the status quo scenario (as might be the case if the future HIV treatment budget were fixed and did not increase as a function of HIV treatment need). While artificial, this scenario allowed us to estimate the cost-effectiveness of Xpert adoption separate from the effects on HIV treatment. In this scenario, incremental costs and DALYs averted dropped by 35-40% and 10-15%, respectively, compared to the main analysis, and the cost per DALY averted dropped to US$656 [386 - 1,115] over a 10-year analytic horizon (assuming a US$30 per-test cost for Xpert). While this analysis is informative, we emphasize that a policy-maker aiming to maximize the effectiveness of the entire health portfolio should use the ICER generated in the main analysis unless planning to limit ART enrollment without consideration of actual treatment need.

We also investigated the potential consequences of time-trends in ART prices. In the main analysis the per-patient costs of ART were assumed to be constant. Recent analyses have observed a net downward trend [86], although an upward trend might be possible, with the uncertainty reflecting a tradeoff between price reductions and increasing use of more expensive second-line therapies. We investigated the possible consequences of ART price reductions by recalculating the results under an assumption that ART costs would drop by 50% every 10 years. This change reduced the cost per DALY to US$812 [522-1,283] over the 10-year analytic horizon and to US$552 [320 - 1,023] over 20 years, reductions of 15% and 30% compared to the results in the main analysis.

Similar to ART, MDR-TB treatment is another expensive service with increased volume under the Xpert strategy, due to both better TB case-finding and better identification of drug resistance. Inpatient care adds substantially to MDR-TB treatment costs, yet there is limited evidence that it improves treatment outcomes [82,96]. We constructed a scenario to investigate how Xpert cost-effectiveness would change if inpatient care were no longer required for MDR-TB treatment, assuming this would produce no net change in health outcomes. This change was found to reduce incremental health system costs of the Xpert algorithm by 15%, and to reduce the cost per DALY averted by the same percentage, to US$812 [522 - 1,283] over a 10-year analytic horizon.

Our main analysis focused on an Xpert algorithm in which a negative Xpert diagnosis would be treated as definitive, whereas South Africa has developed local guidelines that call for more aggressive investigation (including culture, chest X-ray and antibiotic trial) for Xpert-negative individuals who have positive or unknown HIV status [97]. We compared this algorithm to the Xpert algorithm used in the main analysis, assuming that all truly HIV-positive individuals would be categorized as 'HIV-positive or unknown' at TB diagnosis, while 50% (range 25-75%) of all truly HIV-negative individuals would have a prior HIV test confirming this status, based on recent population based surveys [66-68]. In this comparison the South African Xpert algorithm was found

to increase incremental costs by 60% and incremental DALYs averted by 27%, which resulted in an incremental cost-effectiveness ratio of US$2,128 [1,215-3,954] per DALY averted (10-year analytic horizon, US$30 Xpert cost) for the more aggressive strategy compared to the base-case Xpert algorithm. We also conducted sensitivity analyses on how the cost-effectiveness of Xpert might change if all individuals with a positive Xpert RIF result receive empiric MDR-TB treatment while waiting for the DST result to be returned (a delay estimated at 80 days [98]). This change had a modest effect, raising incremental costs by 8%, and resulting in a cost per DALY averted of US$1,038 [683-1,584] (10-year analytic horizon, US$30 year Xpert cost).

In another set of sensitivity analyses we tested the robustness of the results to changes in the status quo algorithm. In the main analysis we assumed incomplete access to TB culture and DST. If instead we assumed 100% access to TB culture, such that all treatment-experienced patients testing negative with sputum smear received a confirmatory TB culture, incremental costs and DALYs averted by the Xpert algorithm both dropped by 3%, with little change in the cost per DALY averted, which was estimated as US$956 [628-1,491]. If we also assumed that 100% of treatment-experienced patients diagnosed with TB received DST, then incremental costs and DALYS averted by the Xpert algorithm dropped by 15% and 4%, respectively, compared to the main analysis, and the cost per DALY averted dropped marginally to US$851 [570-1,323]. We also conducted a three-way sensitivity analysis that considered a much wider range of estimates for culture and DST access, investigating the possibility of country-level differences in access to these diagnostic services. The results of these changes on incremental costs, incremental health benefits, and incremental cost-effectiveness ratios are shown in Figures 2.13-2.17. This figure shows that if use of culture under the status quo algorithm is higher than the value used in the main analysis, this would reduce the incremental costs and health benefits produced by adopting Xpert and result in a less favorable cost-effectiveness ratio. In some countries very high values of culture use would result in the status quo strategy dominating the Xpert strategy, i.e., having lower costs and greater

health benefits. The coverage levels that produce such a result (80% of all treatment- naïve and treatment-experienced patients diagnosed via culture), however, are unlikely to be in place at present given current infrastructure and program constraints. Higher than expected DST access under the status quo would produce modest reductions in incremental costs and minimal changes in cost-effectiveness ratios.

Similarly, allowing for the possibility of clinical diagnosis as part of the base case algorithm did not substantially alter the cost-effectiveness of Xpert. When we compared the Xpert algorithm to an altered status quo algorithm in which all individuals with suspected TB testing negative with sputum smear receive clinical diagnosis (which might include chest X-ray or antibiotic trial [49]) to confirm the negative diagnosis, this increased the incremental cost-effectiveness ratio for Xpert by approximately 10%, to US$1,052 [643 - 1,785], with both incremental costs and DALYs averted approximately one-third lower than estimated in the main analysis.

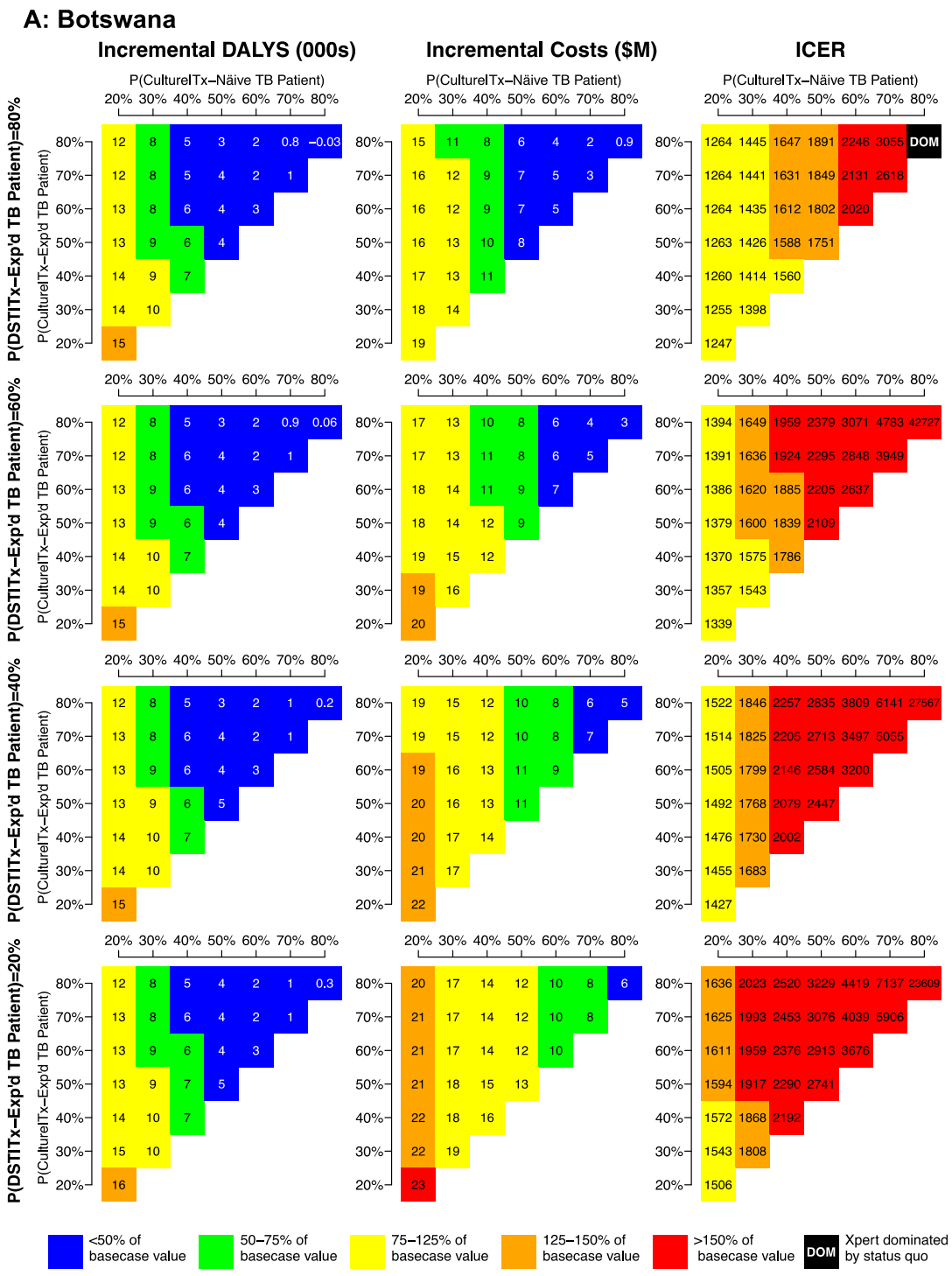

Figure 2.13. Three-way sensitivity analyses showing effects of changes in culture and DST coverage on major study outcomes in Botswana

* Costs, DALYs and ICERs assessed over a 10-year analytic horizon with a US$30 Xpert unit cost. All other parameters held at their mean posterior values.

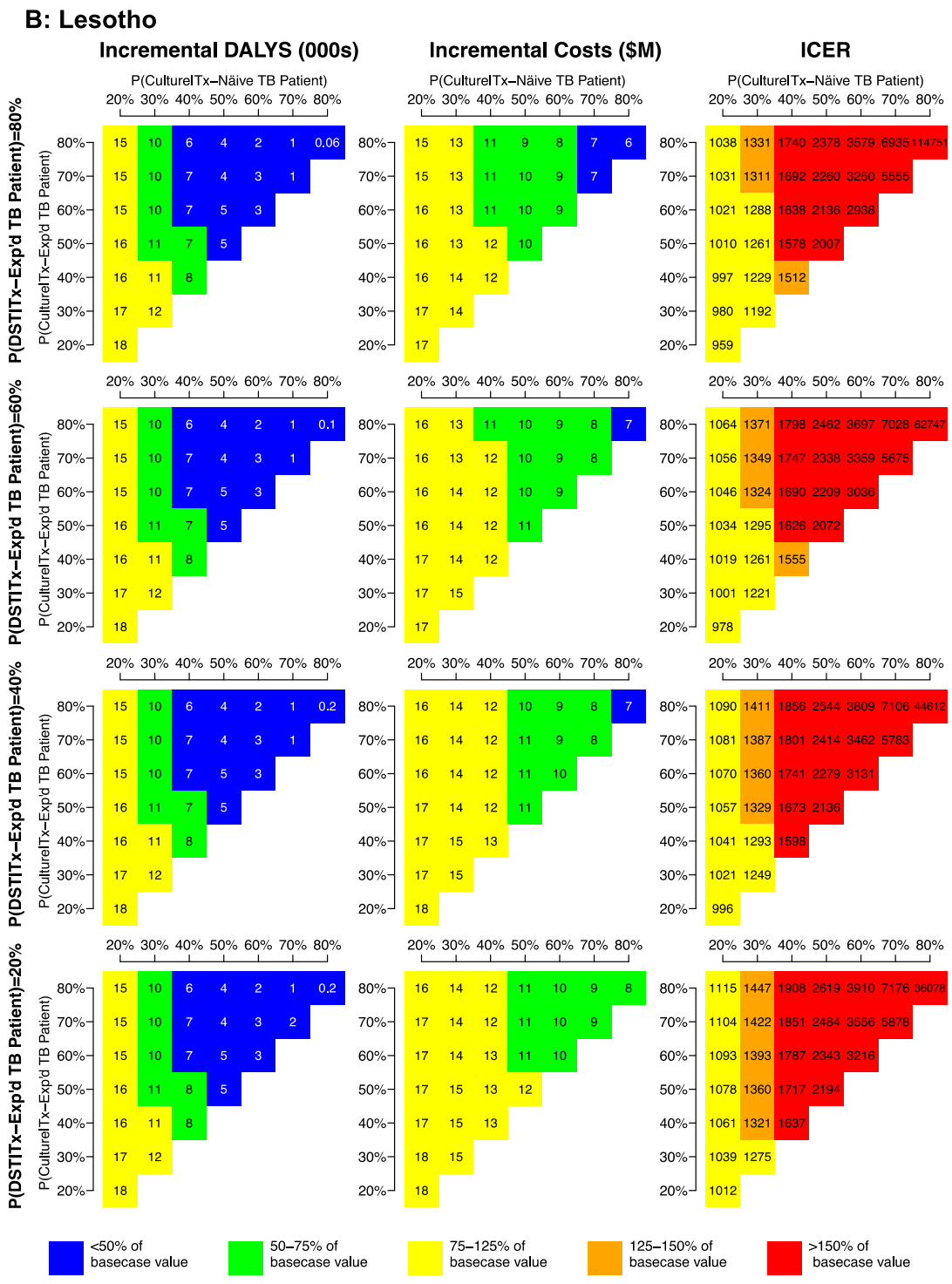

Figure 2.14. Three-way sensitivity analyses showing effects of changes in culture and DST coverage on major study outcomes in Lesotho

* Costs, DALYs and ICERs assessed over a 10-year analytic horizon with a US$30 Xpert unit cost. All other parameters held at their mean posterior values.

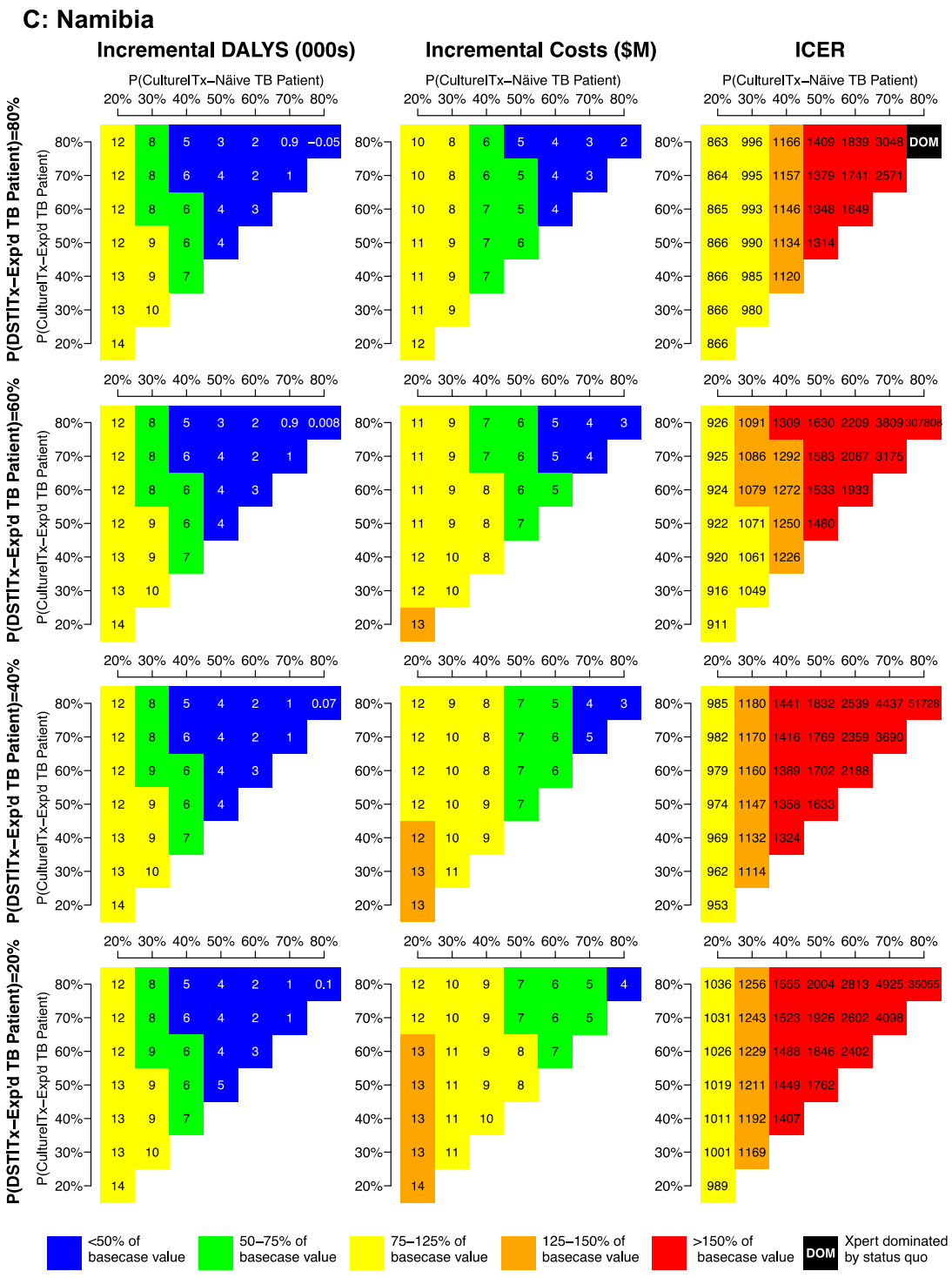

Figure 2.15. Three-way sensitivity analyses showing effects of changes in culture and DST coverage on major study outcomes in Namibia

* Costs, DALYs and ICERs assessed over a 10-year analytic horizon with a US$30 Xpert unit cost. All other parameters held at their mean posterior values.

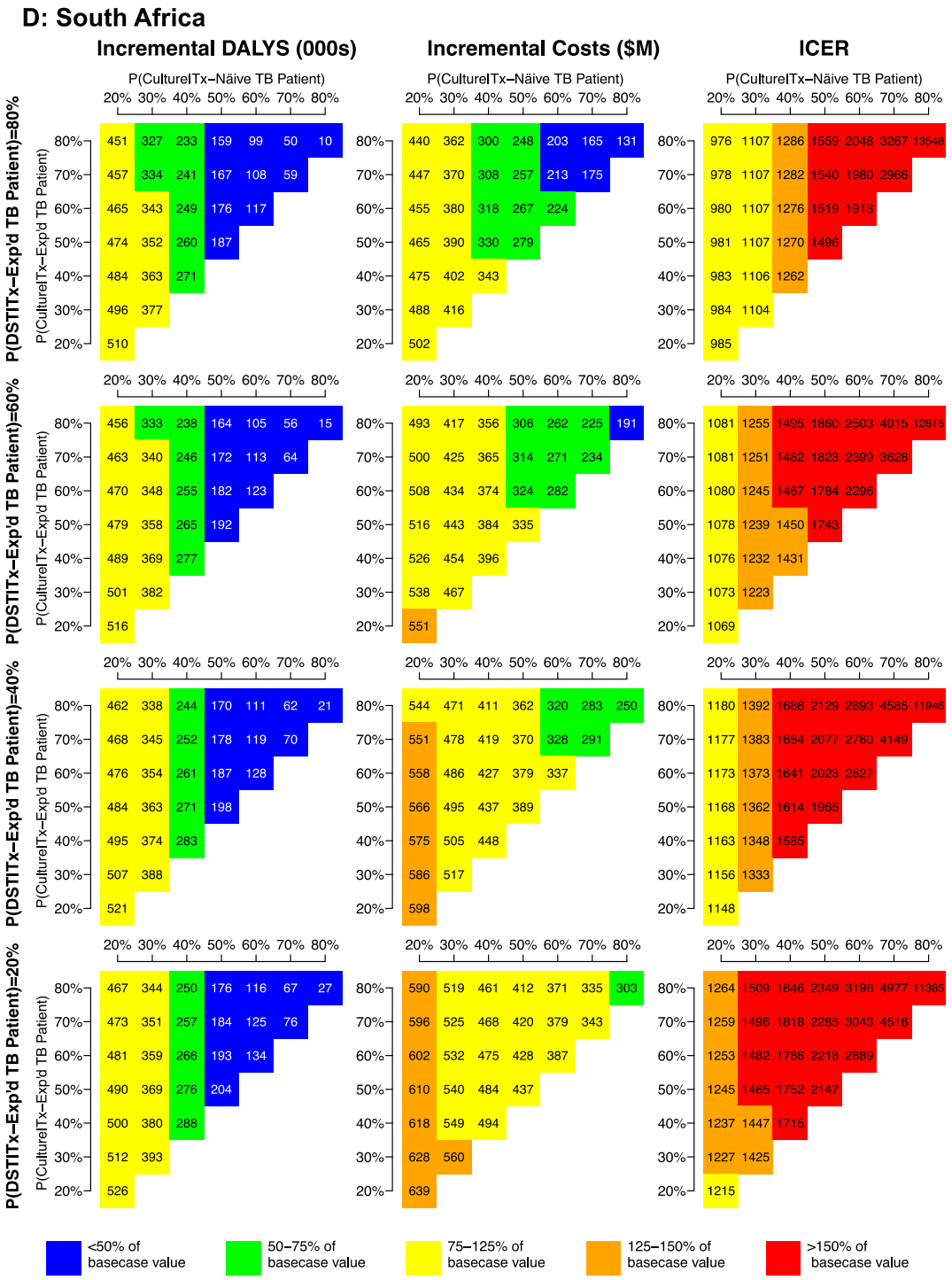

Figure 2.16. Three-way sensitivity analyses showing effects of changes in culture and DST coverage on major study outcomes in South Africa

* Costs, DALYs and ICERs assessed over a 10-year analytic horizon with a US$30 Xpert unit cost. All other parameters held at their mean posterior values.

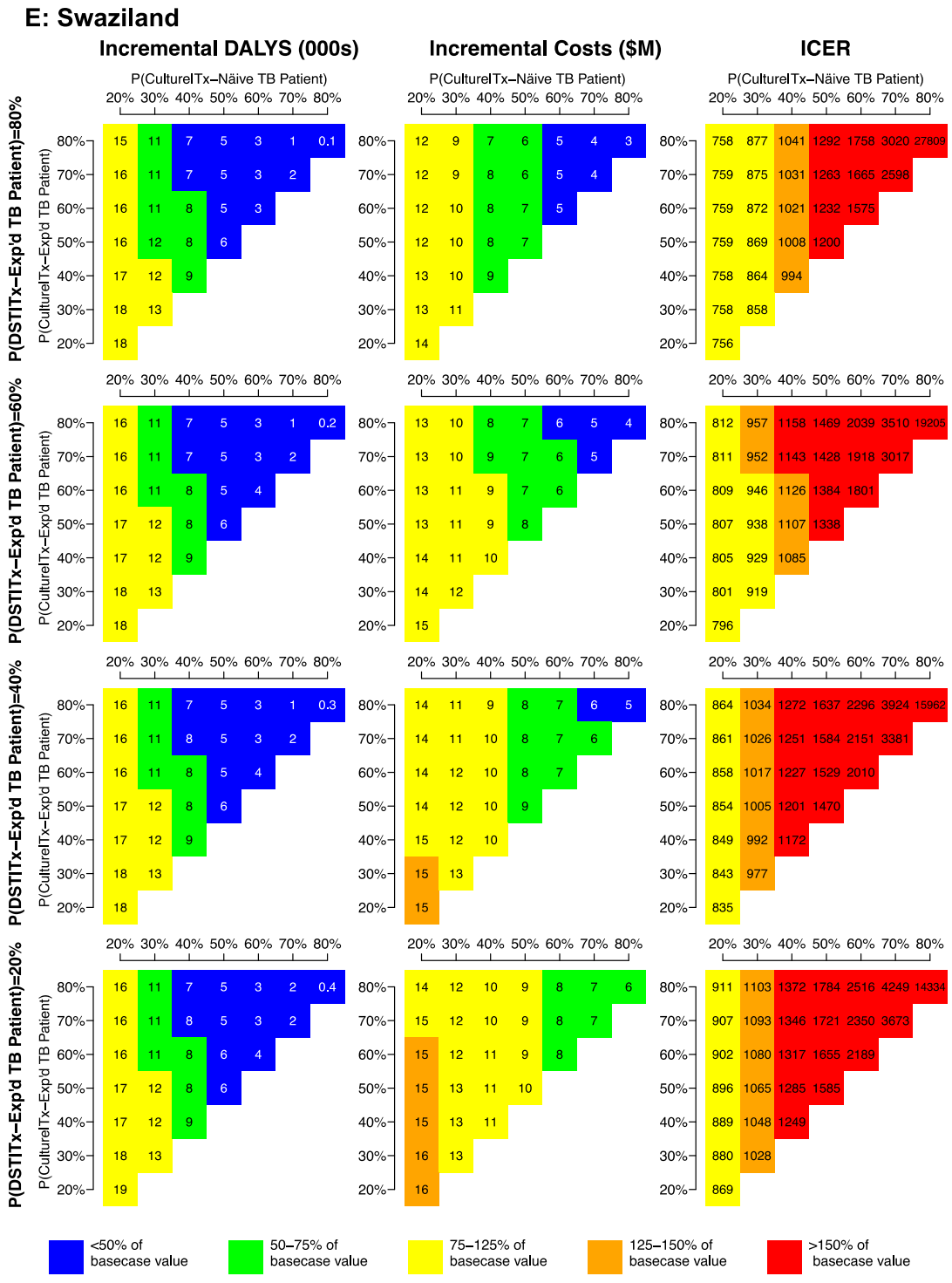

Figure 2.17. Three-way sensitivity analyses showing effects of changes in culture and DST coverage on major study outcomes in Swaziland

* Costs, DALYs and ICERs assessed over a 10-year analytic horizon with a US$30 Xpert unit cost. All other parameters held at their mean posterior values.

2.6.6. References

1. Baltussen R, Floyd K, Dye C (2005) Cost effectiveness analysis of strategies for tuberculosis control in developing countries. *BMJ* 331: 1364.

2. Cohen T, Lipsitch M, Walensky RP, Murray M (2006) Beneficial and perverse effects of isoniazid preventive therapy for latent tuberculosis infection in HIV-tuberculosis coinfected populations. *Proc Natl Acad Sci U S A* 103: 7042-7047.

3. Dowdy DW, Chaisson RE (2009) The persistence of tuberculosis in the age of DOTS: reassessing the effect of case detection. *Bull World Health Organ* 87: 296-304.

4. Dye C, Garnett GP, Sleeman K, Williams BG (1998) Prospects for worldwide tuberculosis control under the WHO DOTS strategy. Directly observed short-course therapy. *Lancet* 352: 1886-1891.

5. Dye C, Williams BG (2000) Criteria for the control of drug-resistant tuberculosis. *Proc Natl Acad Sci U S A* 97: 8180-8185.

6. Murray CJ, Salomon JA (1998) Modeling the impact of global tuberculosis control strategies. *Proc Natl Acad Sci U S A* 95: 13881-13886.

7. Salomon JA, Lloyd-Smith JO, Getz WM, Resch S, Sanchez MS, *et al*. (2006) Prospects for advancing tuberculosis control efforts through novel therapies. *PLoS Med* 3: e273.

8. Daley CL, Small PM, Schecter GF, Schoolnik GK, McAdam RA, *et al*. (1992) An outbreak of tuberculosis with accelerated progression among persons infected with the human immunodeficiency virus. An analysis using restriction-fragment-length polymorphisms. *N Engl J Med* 326: 231-235.

9. Shafer RW, Singh SP, Larkin C, Small PM (1995) Exogenous reinfection with multidrug-resistant Mycobacterium tuberculosis in an immunocompetent patient. *Tuber Lung Dis* 76: 575-577.

10. Bucher HC, Griffith LE, Guyatt GH, Sudre P, Naef M, *et al*. (1999) Isoniazid prophylaxis for tuberculosis in HIV infection: a meta-analysis of randomized controlled trials. *AIDS* 13: 501-507.

11. Corbett EL, Watt CJ, Walker N, Maher D, Williams BG, *et al*. (2003) The growing burden of tuberculosis: global trends and interactions with the HIV epidemic. *Arch Intern Med* 163: 1009-1021.

12. Elliott AM, Halwiindi B, Hayes RJ, Luo N, Tembo G, *et al*. (1993) The impact of human immunodeficiency virus on presentation and diagnosis of tuberculosis in a cohort study in Zambia. *J Trop Med Hyg* 96: 1-11.

13. Getahun H, Harrington M, O'Brien R, Nunn P (2007) Diagnosis of smear-negative pulmonary tuberculosis in people with HIV infection or AIDS in resource-constrained settings: informing urgent policy changes. *Lancet* 369: 2042-2049.

14. Manosuthi W, Tantanathip P, Chimsuntorn S, Eampokarap B, Thongyen S, *et al*. (2010) Treatment outcomes of patients co-infected with HIV and tuberculosis who received a nevirapine-based antiretroviral regimen: a four-year prospective study. *Int J Infect Dis* 14: e1013-1017.

15. van der Sande MA, Schim van der Loeff MF, Bennett RC, Dowling M, Aveika AA, *et al*. (2004) Incidence of tuberculosis and survival after its diagnosis in patients infected with HIV-1 and HIV-2. *AIDS* 18: 1933-1941.

16. Adam MA, Johnson LF (2009) Estimation of adult antiretroviral treatment coverage in South Africa. *S Afr Med J* 99: 661-667.

17. Granich RM, Gilks CF, Dye C, De Cock KM, Williams BG (2009) Universal voluntary HIV testing with immediate antiretroviral therapy as a strategy for elimination of HIV transmission: a mathematical model. *Lancet* 373: 48-57.

18. Stover J, Bollinger L, Avila C (2011) Estimating the Impact and Cost of the WHO 2010 Recommendations for Antiretroviral Therapy. *AIDS Res Treat* 2011: 738271.

19. UNAIDS Reference Group on Estimates Modelling and Projections (2011) *Technical Meeting to Review Spectrum 2011 and considering potential bias in DHS and ANC data*. Geneva: Joint United Nations Programme on HIV/AIDS.

20. Lipsitch M, Colijn C, Cohen T, Hanage WP, Fraser C (2009) No coexistence for free: neutral null models for multistrain pathogens. *Epidemics* 1: 2-13.

21. United Nations Population Division (2011) *World Population Prospects: The 2010 Revision, CD-ROM Edition*. Geneva: United Nations, Department of Economic and Social Affairs, Population Division.

22. Cohen T, Murray M (2004) Modeling epidemics of multidrug-resistant M. tuberculosis of heterogeneous fitness. *Nat Med* 10: 1117-1121.

23. Dowdy DW, Chaisson RE, Maartens G, Corbett EL, Dorman SE (2008) Impact of enhanced tuberculosis diagnosis in South Africa: a mathematical model of expanded culture and drug susceptibility testing. *Proc Natl Acad Sci U S A* 105: 11293-11298.

24. Dowdy DW, O'Brien MA, Bishai D (2008) Cost-effectiveness of novel diagnostic tools for the diagnosis of tuberculosis. *Int J Tuberc Lung Dis* 12: 1021-1029.

25. WHO (2011) *Rapid Implementation of the Xpert MTB/RIF diagnostic test: Technical and operational 'How-to'*. Geneva: WHO.

26. Boehme CC, Nabeta P, Hillemann D, Nicol MP, Shenai S, *et al*. (2010) Rapid molecular detection of tuberculosis and rifampin resistance. *N Engl J Med* 363: 1005-1015.

27. Frieden T (2004) *Toman's tuberculosis: case detection, treatment and monitoring: questions and answers (2nd edition)*. Geneva: WHO.

28. Levy H, Feldman C, Sacho H, van der Meulen H, Kallenbach J, *et al*. (1989) A reevaluation of sputum microscopy and culture in the diagnosis of pulmonary tuberculosis. *Chest* 95: 1193-1197.

29. WHO (2011) *Global TB Database* (http://www.who.int/tb/country/data/download/en/index.html, accessed September 30 2011). Geneva: WHO.

30. WHO (2009) *TB Impact Measurement: Policy and recommendations for how to assess the epidemiological burden of TB and the impact of TB control*. Stop TB policy paper; no 2. Geneva: WHO.

31. Lew W, Pai M, Oxlade O, Martin D, Menzies D (2008) Initial drug resistance and tuberculosis treatment outcomes: systematic review and meta-analysis. *Ann Intern Med* 149: 123-134.

32. UNAIDS (2010) *Towards universal access: Scaling up priority HIV/AIDS interventions in the health sector. Progress report 2010*. Geneva: UNAIDS.

33. WHO (2006) *Antiretroviral Therapy for HIV Infection in Adults and Adolescents: Recommendations for a public health approach. 2006 Revision*. Geneva: WHO.

34. WHO (2010) *Antiretroviral therapy for HIV infection in adults and adolescents: recommendations for a public health approach – 2010 Revision*. Geneva: WHO.

35. Anglaret X, Minga A, Gabillard D, Ouassa T, Messou E, *et al*. (2012) AIDS and non-AIDS morbidity and mortality across the spectrum of CD4 cell counts in HIV-infected adults before starting antiretroviral therapy in Cote d'Ivoire. *Clin Infect Dis* 54: 714-723.

36. Badri M, Lawn SD, Wood R (2006) Short-term risk of AIDS or death in people infected with HIV-1 before antiretroviral therapy in South Africa: a longitudinal study. *Lancet* 368: 1254-1259.

37. Egger M, May M, Chene G, Phillips AN, Ledergerber B, *et al*. (2002) Prognosis of HIV-1-infected patients starting highly active antiretroviral therapy: a collaborative analysis of prospective studies. *Lancet* 360: 119-129.

38. May M, Sterne JA, Sabin C, Costagliola D, Justice AC, *et al*. (2007) Prognosis of HIV-1-infected patients up to 5 years after initiation of HAART: collaborative analysis of prospective studies. *AIDS* 21: 1185-1197.

39. Phillips A, Pezzotti P, Cascade Collaboration (2004) Short-term risk of AIDS according to current CD4 cell count and viral load in antiretroviral drug-naive individuals and those treated in the monotherapy era. *AIDS* 18: 51-58.

40. When To Start Consortium, Sterne JA, May M, Costagliola D, de Wolf F, *et al*. (2009) Timing of initiation of antiretroviral therapy in AIDS-free HIV-1-infected patients: a collaborative analysis of 18 HIV cohort studies. *Lancet* 373: 1352-1363.

41. WHO (2011) *Global Price Reporting Mechanism* (http://www.who.int/hiv/amds/gprm/en/, accessed May 21 2011). Geneva: WHO.

42. Meyer-Rath G, Bistline K, Long L, MacLeod B, Sanne I, *et al*. (2011) *The incremental cost of introducing Xpert® MTB/RIF into the South African national tuberculosis programme: Results of the National TB Cost Model 2011/12 - 2016/17*. Johannesburg: University of Witwatersrand, Health Economics and Epidemiology Research Office.

43. Murray CJL, Lopez AD (1996) *The Global Burden of Disease: A comprehensive assessment of mortality and disability from diseases, injuries and risk factors in 1990 and projected to 2020*. Cambridge, MA: Harvard University Press.

44. WHO (2004) Gl*obal Burden of Disease 2004 Update: Disability Weights for Diseases and Conditions*. Geneva: WHO.

45. Flanagan W, McIntosh CN, Le Petit C, Berthelot JM (2006) Deriving utility scores for co-morbid conditions: a test of the multiplicative model for combining individual condition scores. *Popul Health Metr* 4: 13.

46. Mathers CD, R. S, Salomon JA, L. MCJ, Lopez AD (2000) *Estimates of DALE for 191 countries: methods and results*. Geneva: WHO.

47. Dye C, Espinal MA (2001) Will tuberculosis become resistant to all antibiotics? Proc Biol Sci 268: 45-52.

48. Luciani F, Sisson SA, Jiang H, Francis AR, Tanaka MM (2009) The epidemiological fitness cost of drug resistance in Mycobacterium tuberculosis. *Proc Natl Acad Sci U S A* 106: 14711-14715.

49. Vassall A, van Kampen S, Sohn H, Michael JS, John KR, *et al*. (2011) Rapid Diagnosis of Tuberculosis with the Xpert MTB/RIF Assay in High Burden Countries: A Cost-Effectiveness Analysis. *PLoS Med* 8: e1001120.

50. Espinal MA, Kim SJ, Suarez PG, Kam KM, Khomenko AG, *et al*. (2000) Standard short-course chemotherapy for drug-resistant tuberculosis: treatment outcomes in 6 countries. *JAMA* 283: 2537-2545.

51. Menzies D, Benedetti A, Paydar A, Royce S, Madhukar P, *et al*. (2009) Standardized treatment of active tuberculosis in patients with previous treatment and/or with mono-resistance to isoniazid: a systematic review and meta-analysis. *PLoS Med* 6: e1000150.

52. Migliori GB, Espinal M, Danilova ID, Punga VV, Grzemska M, *et al*. (2002) Frequency of recurrence among MDR-tB cases 'successfully' treated with standardised short-course chemotherapy. *Int J Tuberc Lung Dis* 6: 858-864.

53. Orenstein EW, Basu S, Shah NS, Andrews JR, Friedland GH, *et al*. (2009) Treatment outcomes among patients with multidrug-resistant tuberculosis: systematic review and meta-analysis. *Lancet Infect Dis* 9: 153-161.

54. Verma R, Khanna P, Prinja S (2010) A Comparative Study Between Dots & Non-Dots Patients In Two Districts Of Haryana, India. *Internet Journal of Epidemiology* 8: 246e.

55. Vynnycky E, Fine PE (1997) The natural history of tuberculosis: the implications of age-dependent risks of disease and the role of reinfection. *Epidemiol Infect* 119: 183-201.

56. Ferebee SH (1970) Controlled chemoprophylaxis trials in tuberculosis. A general review. *Bibl Tuberc* 26: 28-106.

57. Datiko DG, Lindtjorn B (2010) Cost and cost-effectiveness of smear-positive tuberculosis treatment by Health Extension Workers in Southern Ethiopia: a community randomized trial. *PLoS One* 5: e9158.

58. WHO (2008) *Guidelines for the programmatic management of drug-resistant tuberculosis: Emergency update 2008*. Geneva: WHO.

59. Mellors JW, Margolick JB, Phair JP, Rinaldo CR, Detels R, *et al*. (2007) Prognostic value of HIV-1 RNA, CD4 cell count, and CD4 Cell count slope for progression to AIDS and death in untreated HIV-1 infection. *JAMA* 297: 2349-2350.

60. Rodriguez B, Sethi AK, Cheruvu VK, Mackay W, Bosch RJ, *et al*. (2006) Predictive value of plasma HIV RNA level on rate of CD4 T-cell decline in untreated HIV infection. *JAMA* 296: 1498-1506.

61. Williams BG, Korenromp EL, Gouws E, Schmid GP, Auvert B, *et al*. (2006) HIV infection, antiretroviral therapy, and CD4+ cell count distributions in African populations. *J Infect Dis* 194: 1450-1458.

62. Wolbers M, Babiker A, Sabin C, Young J, Dorrucci M, *et al*. (2010) Pretreatment CD4 cell slope and progression to AIDS or death in HIV-infected patients initiating antiretroviral therapy--the CASCADE collaboration: a collaboration of 23 cohort studies. *PLoS Med* 7: e1000239.

63. Badri M, Wilson D, Wood R (2002) Effect of highly active antiretroviral therapy on incidence of tuberculosis in South Africa: a cohort study. *Lancet* 359: 2059-2064.

64. Golub JE, Saraceni V, Cavalcante SC, Pacheco AG, Moulton LH, *et al*. (2007) The impact of antiretroviral therapy and isoniazid preventive therapy on tuberculosis incidence in HIV-infected patients in Rio de Janeiro, Brazil. *AIDS* 21: 1441-1448.

65. Lawn SD, Kranzer K, Wood R (2009) Antiretroviral Therapy for Control of the HIVassociated Tuberculosis Epidemic in Resource- Limited Settings. *Clin Chest Med* 30: 685-699.

66. Central Statistical Office Swaziland, Macro International Inc (2008) *Swaziland Demographic and Health Survey 2006-07*. Swaziland: Central Statistical Office and Macro International Inc.

67. Ministry of Health and Social Welfare Lesotho, ICF Macro (2010) *Lesotho Demographic and Health Survey 2009*. Lesotho: Ministry of Health and Social Welfare Lesotho & ICF Macro.

68. Peltzer K, Matseke G, Mzolo T, Majaja M (2009) Determinants of knowledge of HIV status in South Africa: results from a population-based HIV survey. *BMC Public Health* 9: 174.

69. Meyer-Rath G, Schnippel K, Long L, MacLeod W, Sanne I, *et al*. (2012) The impact and cost of scaling up GeneXpert MTB/RIF in South Africa. *PLoS One* 7: e36966.

70. Schnippel K, Meyer-Rath G, Long L, Macleod W, Sanne I, *et al*. (2012) Scaling up Xpert MTB/RIF technology: the costs of laboratory- vs. clinic-based roll-out in South Africa. *Trop Med Int Health* 17(9): 1142-1151.

71. Albert H (2004) Economic analysis of the diagnosis of smear-negative pulmonary tuberculosis in South Africa: incorporation of a new rapid test, FASTPlaqueTB, into the diagnostic algorithm. *Int J Tuberc Lung Dis* 8: 240-247.

72. Floyd K, Skeva J, Nyirenda T, Gausi F, Salaniponi F (2003) Cost and cost-effectiveness of increased community and primary care facility involvement in tuberculosis care in Lilongwe District, Malawi. *Int J Tuberc Lung Dis* 7: S29-37.

73. Hausler HP, Sinanovic E, Kumaranayake L, Naidoo P, Schoeman H, *et al*. (2006) Costs of measures to control tuberculosis/HIV in public primary care facilities in Cape Town, South Africa. *Bull World Health Organ* 84: 528-536.

74. Hudson CP, Wood R, Maartens G (2000) Diagnosing HIV-associated tuberculosis: reducing costs and diagnostic delay. *Int J Tuberc Lung Dis* 4: 240-245.

75. Nganda B, Wang'ombe J, Floyd K, Kangangi J (2003) Cost and cost-effectiveness of increased community and primary care facility involvement in tuberculosis care in Machakos District, Kenya. *Int J Tuberc Lung Dis* 7: S14-20.

76. Samandari T, Bishai D, Luteijn M, Mosimaneotsile B, Motsamai O, *et al*. (2011) Costs and consequences of additional chest x-ray in a tuberculosis prevention program in Botswana. *Am J Respir Crit Care Med* 183: 1103-1111.

77. Suarez PG, Floyd K, Portocarrero J, Alarcon E, Rapiti E, *et al*. (2002) Feasibility and cost-effectiveness of standardised second-line drug treatment for chronic tuberculosis patients: a national cohort study in Peru. *Lancet* 359: 1980-1989.

78. van Cleeff MR, Kivihya-Ndugga LE, Meme H, Odhiambo JA, Klatser PR (2005) The role and performance of chest X-ray for the diagnosis of tuberculosis: a cost-effectiveness analysis in Nairobi, Kenya. *BMC Infect Dis* 5: 111.

79. Acuna-Villaorduna C, Vassall A, Henostroza G, Seas C, Guerra H, *et al*. (2008) Cost-effectiveness analysis of introduction of rapid, alternative methods to identify multidrug-resistant tuberculosis in middle-income countries. *Clin Infect Dis* 47: 487-495.

80. Resch SC, Salomon JA, Murray M, Weinstein MC (2006) Cost-effectiveness of treating multidrug-resistant tuberculosis. *PLoS Med* 3: e241.

81. Adam T, Evans DB, Murray CJ (2003) Econometric estimation of country-specific hospital costs. *Cost Eff Resour Alloc* 1: 3.

82. Loveday M, Wallengren K, Voce A, Margot B, Reddy T, *et al*. (2012) Comparing early treatment outcomes of MDR-TB in decentralised and centralised settings in KwaZulu-Natal, South Africa. *Int Journal of Tub Luncg Dis* 16: 209-215.

83. Bikilla AD, Jerene D, Robberstad B, Lindtjorn B (2009) Cost estimates of HIV care and treatment with and without anti-retroviral therapy at Arba Minch Hospital in southern Ethiopia. *Cost Eff Resour Alloc* 7: 6.

84. Bratt JH, Torpey K, Kabaso M, Gondwe Y (2011) Costs of HIV/AIDS outpatient services delivered through Zambian public health facilities. *Trop Med Int Health* 16: 110-118.

85. Harling G, Wood R (2007) The evolving cost of HIV in South Africa: changes in health care cost with duration on antiretroviral therapy for public sector patients. *J Acquir Immune Defic Syndr* 45: 348-354.

86. Menzies NA, Berruti AA, Berzon R, Filler S, Ferris R, *et al*. (2011) The cost of providing comprehensive HIV treatment in PEPFAR-supported programs. *AIDS* 25: 1753-1760.

87. Rosen S, Long L, Sanne I (2008) The outcomes and outpatient costs of different models of antiretroviral treatment delivery in South Africa. *Trop Med Int Health* 13: 1005-1015.

88. Tan Torres T, Baltussen R, Adam T, Hutubessy R, Acharya A, *et al*. (2003) *Making Choices in Health: WHO Guide to Cost Effectiveness Analysis*. Geneva: WHO.

89. Weinstein MC, Siegel JE, Gold MR, Kamlet MS, Russell LB (1996) Recommendations of the Panel on Cost-effectiveness in Health and Medicine. *JAMA* 276: 1253-1258.

90. Alkema L, Raftery AE, Clark SJ (2007) Probabilistic Projections of HIV Prevalence Using Bayesian Melding. *Ann Appl Stat* 1: 229-248.

91. Poole D, Raftery AE (2000) Inference for deterministic simulation models: The Bayesian melding approach. *J Am Stat Assoc* 95: 452.

92. Rubin D (1988) Using the SIR algorithm to simulate posterior distributions. In: Bernardo JM, DeGroot MH, Lindley DV, Smith AFM, editors. *Bayesian Statistics 3*. Oxford: Oxford University Press. pp 395–402

93. WHO (2010) *Multidrug and extensively drug-resistant TB (M/XDR-TB): 2010 global report on surveillance and response*. Geneva: WHO.

94. Iman RL, Helton JC, Campbell JE (1981) An approach to sensitivity analysis of computer models: part I—introduction, input variable selection and preliminary variable assessment. *J Qual Technol* 13: 174-183.

95. Iman RL, Helton JC, Campbell JE (1981) An approach to sensitivity analysis of computer models: part II—ranking of input variables, response surface validation, distribution effect, and technique synopsis variable assessment. *J Qual Technol* 13: 232-240.

96. Heller T, Lessells RJ, Wallrauch CG, Barnighausen T, Cooke GS, *et al*. (2010) Community-based treatment for multidrug-resistant tuberculosis in rural KwaZulu-Natal, South Africa. *Int J Tuberc Lung Dis* 14: 420-426.

97. National Health Laboratory Service (2012) *Xpert Testing Algorithm*. South Africa: National Health Laboratory Service.

98. Jacobson KR, Theron D, Kendall EA, Franke MF, Barnard M, *et al*. (2012) Implementation of GenoType MTBDRplus Reduces Time to Multidrug-Resistant Tuberculosis Therapy Initiation in South Africa. Manuscript Under Review.

99. Fenwick E, O'Brien BJ, Briggs A (2004) Cost-effectiveness acceptability curves--facts, fallacies and frequently asked questions. *Health Econ* 13: 405-415.

Chapter 3. Value of new research to inform HIV control policy in South Africa

Abstract

In this analysis I estimate the relative value of new research on various targets related to HIV control in South Africa. There has been growing enthusiasm for expanding HIV treatment programs in highly-affected settings, due to new evidence that antiretroviral therapy (ART) may reduce HIV transmission. Expanding ART programs would likely require substantial resources, and there is considerable uncertainty about the impact of such expansion on long-term outcomes. The best strategy for ART expansion is also unclear—policy debate has focused on relaxing ART eligibility criteria, but this must compete with efforts to increase enrollment among groups already eligible according to current guidelines. This uncertainty hinders the development of long-term HIV control strategy. In this analysis I used Value of Information (VOI) methods to identify the types of new research that would be most valuable to this policy debate, using South Africa as a case study. I implemented this analysis using a mathematical model of HIV epidemiology in the adult population. The model simulated HIV transmission through durable sexual partnerships and casual sexual contacts, disease progression for HIV-infected individuals, and initiation and receipt of ART. I used this model to project the costs and health outcomes resulting from various ART policies that might be adopted, and used Monte Carlo methods to quantify how uncertainty in epidemiology, programmatic performance, and costs translated into uncertainty about policy outcomes. These results were used to estimate VOI for individual parameters or groups of parameters. Issues found to have the highest potential value of information included issues of cost and implementation, relative infectiousness during late HIV and the reduction in infectiousness for individuals on ART, and the therapeutic health benefits of early ART initiation. These findings generally held up across different time horizons and other analytic assumptions. Another notable finding was the apparent unimportance of information about transmission during early HIV infection, despite earlier research suggesting that transmission during early HIV infection could substantially reduce the impact of ART expansion. This analysis also developed new methods for estimating VOI in the

context of numerically calibrated models, which may be of increasing relevance as a greater number of analyses adopt these calibration techniques.

3.1. Introduction

Policy decisions are made under conditions of uncertainty. While rational policy makers will adopt policies that appear to give the best expected outcomes given the current state of knowledge, better information may change policy choices and improve expected outcomes. As research can improve information before consequential policy decisions are made, the value of research can be can estimated from the expected improvement in policy choices and outcomes. This approach can be used to guide the magnitude and direction of new research investments.

This paper examines the value of new research related to HIV control in developing countries. In 2011, there was $US16.8 billion spent globally on HIV control, the majority in developing countries [1]. Most of this funding is devoted to providing care and antiretroviral therapy (ART), with over 8 million individuals in low and middle-income countries now receiving ART [1]. The progressive expansion of treatment services is seen as one of the successes of global HIV control, with many institutions promoting the goal of universal treatment access [2]. Despite these advances many countries are not yet providing treatment services to all who might benefit, and in 2011 there were an estimated 6.8 million individuals eligible for treatment according to current WHO guidelines who were not yet receiving ART [1]. Treatment programs continue to face constrained budgets, with both domestic and external HIV spending under increasing pressure [3].

While the therapeutic benefits of ART are well established [4], there has been increasing evidence that ART may also have a role to play in HIV prevention, building on the facts that ART reduces HIV viral load in treated individuals [5], and that a lower viral load is associated with reduced rates of HIV transmission [6]. Evidence from observational analyses supports this relationship [7,8], and results reported for a recent clinical trial (HPTN 052) confirm the effectiveness of ART for reducing transmission in serodiscordant couples, with transmission rates reduced by 96% (95% CI: 73-99%) [9].

These results have important implications for HIV control in the many highly-affected countries with ongoing generalized HIV epidemics. Analyses have used mathematical models to explore the potential of expanded ART eligibility as a policyfor reducing HIV incidence at a population-level [10,11], and policy makers are considering an increased prioritization of ART within the HIV control portfolio. Expansion of ART may come at the expense of other health interventions unless further funding is available [12], and policy changes to extend ART eligibility beyond current guidelines must compete with efforts to increase enrollment among groups already eligible according to current guidelines. A recent study by a consortium of HIV modeling groups found that in 4 highly affected settings (South Africa, Zambia, India, Vietnam) improving ART coverage (through improved HIV testing and linkage to care) and expanding eligibility both have the potential to generate substantial health gains, and would be considered cost-effective according to conventional benchmarks [13]. This study also revealed substantial uncertainty about the projected resource requirements and epidemic impact of competing policies. Uncertainty about the appropriate timing of treatment initiation has been highlighted as a barrier to developing long-term HIV control strategy [14].

Even if ART could be scaled up to high coverage with expanded eligibility criteria, it will not be possible to enroll individuals with early HIV infection. These are individuals who have recently acquired HIV, and are therefore unlikely to be aware of their HIV status. Given the short duration and difficult diagnosis of early HIV, it is unlikely that this group would be affected by a policy aiming to use treatment of infected individuals to reduce transmission. The extremely high levels of viral load observed during early infection has been linked to increased transmission risk [15], and an observational study from Uganda has estimated that each log increment in the viral load produces a 2-3 fold increase in transmission risk [6]. There are few additional studies to confirm this finding, and this is reflected in prior modelling studies that reveal substantial uncertainty about the proportion of all infections attributable to transmission during early HIV infection [16]. A recent

Malawian study used a mathematical model to examine the role of acute HIV infection in overall transmission dynamics, suggested that 38% (19-52%) of all transmissions could be attributed to individuals in the first 5 months following initial infection [17]. Uncertainty about the role of transmission during early HIV has relevance for the programmatic response to the HPTN 052 results – if the proportion of new infections coming from transmission during early HIV infection is low, efforts to scale-up ART programs may produce substantial incidence reductions. If the proportion of new infections coming from transmission during early HIV infection is high, the prevention benefits of aggressive treatment scale-up may be less, and the cost-effectiveness of ART may not differ substantially from analyses focused on the therapeutic benefits alone [18–20].

Other information gaps add to the uncertainty around optimal ART policy. While it now seems clear that ART can reduce transmission, the magnitude of this effect is still uncertain. The HPTN 052 trial is the only randomized study to date to report on the prevention benefits of ART, and while it identified a 20-fold reduction in transmission risk, these findings were estimated from only 28 transmission events within study couples [9]. There is also substantial uncertainty about the therapeutic benefits of early ART initiation for individuals with high CD4 cell count, with no randomized trials yet reported and conflicting evidence from analyses of observational data [21]. Finally, there is substantial uncertainty about the costs and difficulty of policy implementation, as ART scale-up will require identifying, enrolling, and retaining patients who may not currently know their HIV status or be experiencing HIV symptoms.

This study aims to estimate the potential value of new research on the various uncertainties related to ART policy. Understanding the relative value of different research investments will allow programs to identify and prioritize high-value research and improve expected outcomes.

This research approach—quantifying the value of research through its potential to improve decision-making—draws on a class of methods known as value of information (VOI) analysis [22–

24]. In the absence of further research, it is assumed that HIV control programs will allocate funding across the HIV control portfolio in a way that will maximize valued health outcomes *on expectation*, averaging over the joint distribution of possible costs and health outcomes for each possible intervention portfolio.. Given the substantial uncertainty that exists, it is possible that a portfolio will be chosen that achieves worse health outcomes than would be produced by other portfolios under consideration, but without further research this cannot be known *ex ante*. If new research is undertaken before the policy decision is made, this can reduce the uncertainty faced by policy-makers and reduce the probability that a suboptimal policy will be chosen. The incremental gains in expected outcomes (reductions in expected costs and/or improvement in expected health outcomes) that result from this improved policy choice can be used to estimate the value of undertaking the research.

The application of VOI methods to real-world policy problems is growing [25,26]. There has so far been little use of VOI methods to address HIV control questions, though some recent examples exist: Leelahavarong *et al*. [27] undertake a VOI analysis as part of an examination of HIV vaccine cost-effectiveness in Thailand, while Maheswara and Barton [28] estimate VOI in the context of an analysis of TB case-finding and prevention activities for HIV-infected populations.

In the present study the VOI analysis is operationalized in the context of a dynamic HIV transmission model of the South African epidemic, focusing on a decision currently facing policy makers: whether to expand HIV treatment services, given the growing evidence base that it may reduce transmission, and if so how this should be accomplished. With 5.6 million HIV-positive individuals [1], the HIV epidemic in South Africa is almost twice as large as in any other country, and represents one-sixth of the world's HIV-infected population. South Africa also reflects characteristics common to other highly-affected settings, with ongoing HIV transmission in the general community, limited success of conventional prevention approaches, and scarce resources

for increased HIV spending. For this reason, South Africa represents a focus of HIV research and policy dialogue, and insights learned in this setting will be relevant locally as well as in other similar settings.

In addition to providing guidance on a substantive question—how should new HIV research funding be directed to maximize health gains—this study also addresses a specific methodological question, that of how various VOI estimates can be obtained when the distribution of model parameters is not available in closed-form. This situation arises in the context of common model calibration techniques (such as used in this analysis), where the joint distribution of model parameters, after they have been calibrated, is represented by a sample of parameter sets rather than an equation. This situation poses no problem for calculating the expected value of perfect information (EVPI), as this outcome can be calculated directly using the sample of parameter sets. In contrast, published methods for estimating the expected value of partial perfect information (EVPPI) [22,29] require the expected value of model outcomes (specifically, net monetary benefit achieved by each policy) to be estimated conditional on the value of the parameter (or group of parameters) that is the subject of the analysis. This can be straight-forward if the parameter distribution is available in closed form (particularly if the parameters are uncorrelated). In contrast, it is not immediately clear how to estimate EVPPI when the parameter distribution is represented by a fixed sample of parameter sets, as there is no way to generate new samples from the conditional distribution of other parameters once the value of one parameter has been fixed. While a 'brute force' solution to this problem is possible—recalibrating the model for many different values of a given parameter—such an approach would likely be infeasible in many analysis, where the computational burden of a single calibration may be large. Formal calibration procedures are increasingly being used to improve the predictive validity of complex disease models, it is therefore useful to describe methods for estimating VOI in this class of analyses.

3.2. Methods

3.2.1. General approach

We assumed that the South African national HIV control program chooses between policies based on their potential costs and health benefits. The trade-off between these two goals can be operationalized as a willingness-to-pay (WTP) threshold, describing the maximum rate at which the program would be willing to expend resources in order to gain health benefits. For a given WTP threshold, the health and economic consequences of a policy can be summarized as net monetary benefit (NMB), a measure of the social welfare generated by health programs, combining both costs and health benefits [30]. In the absence of new research, we assumed a policy would be preferred if it maximizes NMB on expectation. The expected NMB (E(NMB)) obtained under this 'no research' scenario can be compared to alternative scenarios in which new research is commissioned in order to reduce decision uncertainty. We assumed that the national program would consistently apply the same decision rule, choosing the policy option that maximizes E(NMB) in light of new research findings. The potential benefits of research can then be quantified as the difference in E(NMB) between 'no research' and alternative scenarios.

3.2.2. Policy options

We characterized the policy decision facing the national program in terms of two dimensions: the criteria determining ART eligibility, and the intensity of HIV testing programs undertaken to identify HIV-positive individuals for care. This second dimension was operationalized as the rate of HIV testing in the general population. Three different eligibility criteria were considered:

A. ART eligibility for HIV-infected individuals with CD4 cell count <350 cells/μL (current eligibility).
B. ART eligibility for individuals with CD4 cell count <500 cells/μL.

C. ART eligibility for all HIV-positive individuals.

Five different HIV testing scenarios were considered:

1. Continuation of current HIV testing rates and restriction of total ART patient volume to current levels, such that any patients leaving ART cohorts are replaced, but no new patient slots are added.
2. Continuation of current HIV testing rates, with individuals initiating ART per eligibility guidelines.
3. Expanded HIV testing programs raising the average rate of testing to 1.5 times its current level, with individuals initiating ART per eligibility guidelines.
4. Expanded HIV testing programs raising the average rate of testing to 2.0 times its current level, with individuals initiating ART per eligibility guidelines.
5. Expanded HIV testing programs raising the average rate of testing to 3.0 times its current level, with individuals initiating ART per eligibility guidelines.

Each of these coverage scenarios was applied to each of the possible eligibility criteria, giving 15 possible policies[1]. We assumed any changes in ART eligibility and coverage would be introduced over a 12-month period starting in 2013 and then remain in force for the duration of the analysis.

[1] For convenience, the policies are labeled with a letter-number combination, such that "B1" denotes a policy combining the second eligibility policy and the first coverage policy.

3.2.3. Model overview

We used a mathematical model to project the costs and health outcomes resulting from the various policy options that might be adopted by the South African national HIV control program. The model was developed to represent an HIV epidemic in the South African adult population, simulating transmission of HIV infection through durable sexual partnerships and casual sexual contacts, the progression of HIV disease for HIV-infected individuals, and initiation and receipt of antiretroviral therapy. We parameterized the model to the South African epidemic, with probability distributions constructed for each model parameter to represent current uncertainty about these values. We used a Bayesian approach to calibrate these probability distributions to agree with empirical data on HIV prevalence trends, distribution across CD4 count categories, and survival following HIV infection. We used this calibrated model to estimate future outcomes of the policy options described in Section 3.2.2, and then used the results to estimate VOI for individual parameters or groups of parameters. Finally, we compared VOI estimates for different parameters to draw conclusions about high-priority research targets for informing ART policy.

3.2.4. Model structure

The structure of the model was based on approaches adopted by other published HIV transmission models [17,31–37]. The model distributes the adult population across compartments that distinguish HIV status, CD4 cell count categories, receipt of ART, sex, and sexual behavior characteristics. A schematic of the model is shown in Figure 3.1. A fraction of the population residing in one compartment may transition into another compartment at weekly timesteps, according to transition probabilities defined by model parameter values.

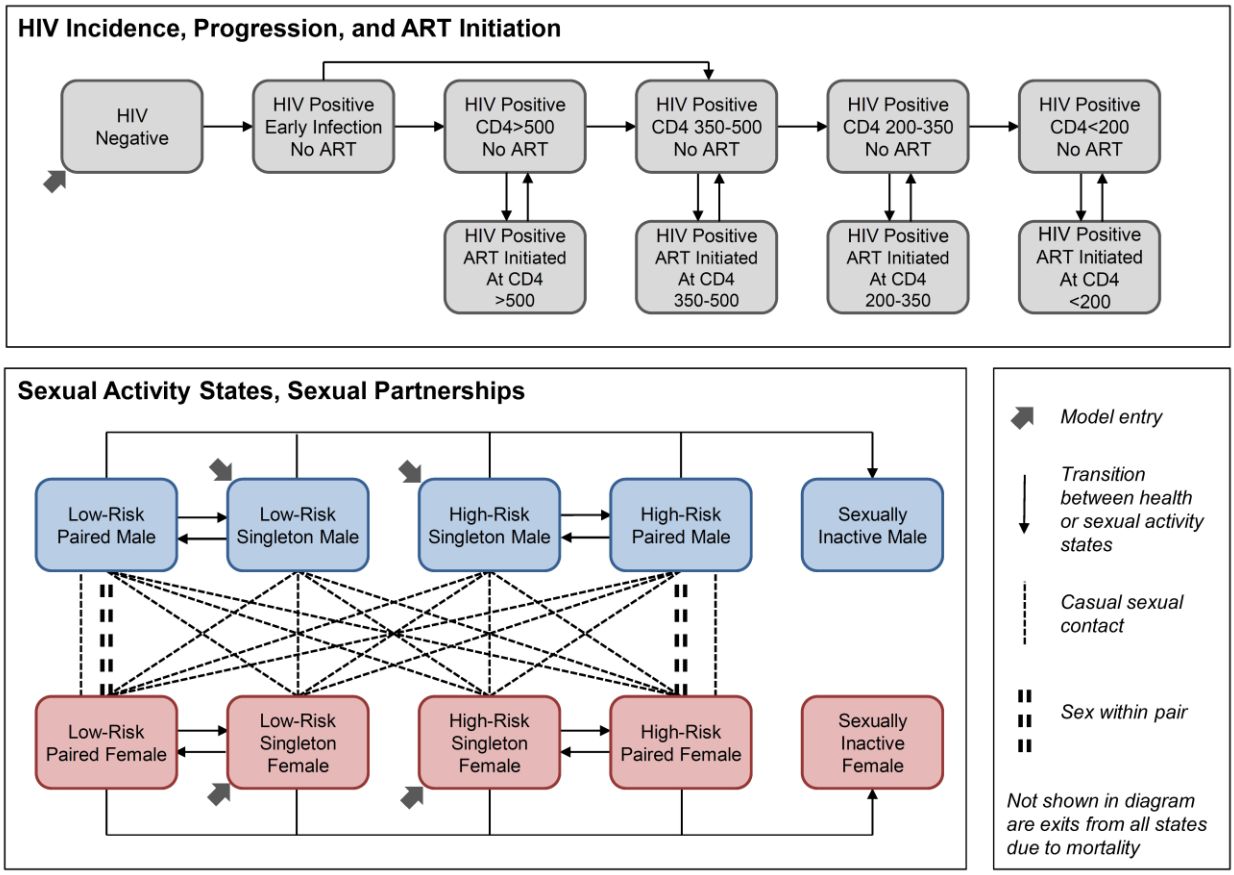

Figure 3.1. Schematic of model compartments, transitions, and sexual interactions

3.2.5. Sexual networks

Multiple studies have demonstrated that the nature of sexual interaction has important implications for the dynamics of generalized HIV epidemics [31–34,37–39]. This concern is particularly important when addressing the issue of early HIV infection, with Eaton and colleagues demonstrating that the role of early infection in HIV epidemics differs between models that assume random, instantaneous sexual contacts and those that capture more realistic patterns of sexual mixing [38]. Similarly, an earlier analysis by Kretzschmar and Dietz demonstrate that models that explicitly account for disease transmission within durable sexual partnerships (pair models) attribute a smaller fraction of overall transmission to early infection, compared to random mixing models [31]. A number of analyses have applied pair models to understand real epidemics, most

notably Xiridou and colleagues in a series of studies related to homosexual [32,33] and heterosexual [40,41] HIV transmission in the Netherlands, and more recently Powers *et al*. (hereafter 'Powers') in an analysis of heterosexual HIV transmission in Lilongwe, Malawi [17]. The Powers analysis is particularly relevant to the current study, in that the primary goal of the analysis was to understand the role of early infection in a generalized heterosexual HIV epidemic that bears some similarities to South Africa's. In developing the model for the current analysis we adopted many features of the Powers model, described in detail below.

3.2.5.1. Durable sexual partnerships

We modeled sexual interaction as occurring through either durable sexual partnerships or casual sex. Durable sexual partnerships (pairs) were modeled explicitly, with a distinct model compartment devoted to each allowed type of heterosexual pairing (e.g., an HIV-negative female paired with an HIV-positive male with CD4<200). Following earlier approaches, the population is divided into distinct sexual activity strata to capture, in a simplified form, the heterogeneity in risk behaviors across the population. Sexual risk strata differ in the rate of formation/dissolution of pairs as well as other sexual behaviors. Pairs are allowed to form within each risk stratum (high-risk and low-risk) but not across strata [17,35,37]. Within each pair, sexual activity is assumed to be constant over the duration of the partnership (conditional on HIV stage), and the rates of other model transitions (e.g., mortality, disease progression) are assumed to be unaffected by pair membership.

For each timestep, let q_{sri} be the total number of pairs formed by individuals in risk stratum *r* (high or low), HIV state *i* (as shown in the top section of Figure 3.1), and sex *s*, where *s*=*w* for women and *s*=*m* for men. Let q_{sr} represent the total number of pairs formed by a particular risk stratum and sex. The rate that an individual in model compartment *sri* attempts to enter a pair relationship is calculated as the product of the average rate for healthy individuals in the risk stratum a_r, and a

multiplier b_i that accounts for lower pair formation rates in individuals with advanced HIV infection. Empirical estimates of the pair formation rate a_r are unavailable, and following Powers we approximated a_r from the pair dissolution rate β_r, the fraction of the risk stratum in a steady pair relationship f_r, and the combined exit rate from the sexually active population (a combination of the background mortality rate μ_b and the rate at which individuals age out of the sexually active population g)[17]:

$$a_r = \frac{f_r\left(\beta_r + 2(g + \mu_b)\right)}{(1 - f_r)} \tag{1}$$

An estimate of the fraction of low-risk types in a pair relationship was derived from data on cohabiting couples reported in the 2001 South African census [42]. Estimates of the fraction of high-risk types in a pair relationship, partnership dissolution rates for high- and low-risk types, and relative partnership formation rate for individuals with advanced HIV infection were drawn from a detailed modeling study of sexual behavior and HIV risk in South Africa by Johnson and colleagues [34].

For a given sex and risk stratum, the total number of unpaired individuals attempting to enter a pair relationship can be calculated as the product of the pair formation rate for each HIV health state and the number of individuals in each HIV health state (n_{sri}), summed across HIV health states:

$$q_{sr} = \sum_{i \in I} a_r b_i n_{sri} \tag{2}$$

The value of q_{sr} as calculated for each sex will not necessarily match, and an adjustment factor is calculated within the model such that the total number of new pairs formed in risk stratum *r* is the

mean of q_{wr} and q_{mr}. The transition rate α for an unpaired individual in compartment *sri* to a paired compartment with an unpaired individual in compartment $\widehat{sri}$ can be then be expressed as[2]:

$$\alpha_{sri_{\widehat{sri}}} = a_r b_i * \frac{(q_{wr} + q_{mr})}{2 * q_{sr}} * \frac{a_{\hat{r}} b_{\hat{\imath}} n_{\widehat{sri}}}{\sum_{\hat{\imath}\in\hat{I}} a_{\hat{r}} b_{\hat{\imath}} n_{\widehat{sri}}} \qquad for\ s \neq \hat{s} \tag{3}$$

The rate of sexual contact within pair relationships (k_r^P) and the reduction in coital frequency associated with advanced HIV infection (l_i) were drawn from Johnson *et al*. [34].

3.2.5.2. Casual sex

Casual sex was modeled as instantaneous 'one-off' sexual contacts between males and females. The model allows for casual sex involving both paired and unpaired individuals, and across sexual risk strata, with individuals in each of these groups participating in casual sex at different rates. The Powers analysis assumed random mixing, whereby individuals exhibit no preference as to the characteristics of sexual partners [17]. However, other modeled analyses have shown that mixing patterns between subgroups with different characteristics can affect epidemic outcomes, suggesting that an assumption of random mixing may be inappropriate [43]. In our model the possibility of assortative mixing (i.e., allowing for unequal preferences regarding sexual partners of different types) is operationalized as a mixing matrix *M,* the cells of which describe the relative preference of an individual in a given subgroup for forming a partnership with members of other subgroups (Figure 3.2). Two parameters are used to specify mixing patterns: *d*, which determines the degree of assortativity between risk strata, and *e*, which determines the relative frequency of casual sex between paired individuals. The mixing matrix shown in Figure 3.2 can be understood as

[2] In other applications a geometric mean has been to correct the different estimates of q_{sr}. Sensitivity analysis using a geometric mean showed that the results are insensitive to this assumption.

a linear interpolation between 4 extremes: (a) random mixing (for d=e=1), (b) complete with-like assortative mixing within risk strata (for d=0, e=1), (3) random mixing except with no casual sex between two individuals both in pair relationships (for d=1, e=0), and (4) complete with-like assortative mixing within risk strata and no casual sex between two individuals both in pair relationships (for d=e=0) [35,37]. Consistent with this interpretation, the parameters d and e are assumed to fall within the range [0,1]. The value of d was drawn from Johnson *et al*. 2009 [34]. No estimates were available for e, and a weakly-informative probability distribution was specified centered at 0.5. While HIV health state was assumed to affect the rate at which individuals participate in casual sex, it was assumed not to affect mixing patterns[3].

[3] Of note, the restriction of the model to heterosexual sex can be seen as an assumption of complete 'with-unlike' mixing, ruling out sexual contact or pair formation between individuals of the same sex. Similarly, the assumption of pair formation within risk strata assumes complete 'with-like' mixing. To relax these assumptions would involve a substantial expansion of the state-space of the model.

		MALES			
		Low-risk, unpaired	Low-risk, paired	High-risk, unpaired	High-risk, paired
FEMALES	Low-risk, unpaired	1	1	d	d
	Low-risk, paired	1	e	d	d*e
	High-risk, unpaired	d	d	1	1
	High-risk, paired	d	d*e	1	e

Figure 3.2. Mixing matrix for casual sex (*M*)

The total number of sexual contacts $\tilde{h}_{sj}$ (where subscript *j* indicates one of the 4 categories created by high- vs. low-risk, unpaired vs. paired,) attempted by each group is calculated as:

$$\tilde{h}_{sj} = \sum_{i \in I} n_{sij} * k_j^c * l_i * m_t \tag{4}$$

In this equation, subscript *j* indicates one of the 4 categories created by high- vs. low-risk, unpaired vs. paired, and the tilde on $\tilde{h}_{sj}$ indicates these are attempted partnerships. As the number of attempted contacts for various groups will not automatically match (as described below) $\tilde{h}_{sj}$ is distinguished from h_{sj} , the number of realized contacts. In addition, k_j^c indicates the annualized rate of casual sex for healthy individuals in group *j*, l_i indicates the rate of casual sex for each HIV health state relative to healthy individuals, and m_t is a time-varying parameter allowing for time changes in the rate of risky sexual behavior, a phenomenon identified by earlier analyses [39,44]. For the purposes of this analysis risky sexual behavior was defined as including casual sex as well as any sex involving high-risk individuals. Values for k_j^c were drawn from the 2003 Demographic

and Health Survey [45], and values for l_i were drawn from Johnson *et al*. 2009 [34]. The parameter m_t is operationalized as a logistic curve with an initial value of 1.0 that declines to asymptote to a new, lower level at some point during the historical development of the epidemic. Values for the start year of this change, the time taken to reach the new level, and the magnitude of the reduction were drawn from Johnson *et al*. 2009 [34].

The total sexual contact attempts for each group can be distributed among the 4 groups of the opposite sex, where $M_{sj\_\hat{s}\hat{j}}$ represents cells of the mixing matrix:

$$\tilde{h}_{sj\_\hat{s}\hat{j}} = h_{sj} * \frac{\tilde{h}_{\hat{s}\hat{j}} * M_{sj\_\hat{s}\hat{j}}}{\sum_{\hat{j}\in\hat{j}} \tilde{h}_{\hat{s}\hat{j}} * M_{sj\_\hat{s}\hat{j}}} \qquad \text{for } s \neq \hat{s} \tag{5}$$

As the number of sexual contact attempts will not automatically match (e.g., the number of sexual contacts attempted by high-risk paired men with low-risk unpaired women will not automatically match the number of sexual contacts attempted by low-risk unpaired women with high-risk paired men), these two approaches must be balanced, with the actual number of casual sexual contacts between groups zj and $f\hat{j}$ calculated as:

$$h_{zj\_f\hat{j}} = \left(\tilde{h}_{zj\_f\hat{j}} * \tilde{h}_{f\hat{j}\_zj}\right)^{\frac{1}{2}} \tag{6}$$

3.2.6. HIV transmission

3.2.6.1. Transmission within discordant pairs

The rate of HIV acquisition by HIV-negative members of HIV discordant pairs is determined by the number of sexual contacts and the per-contact transmission risk. Both of these quantities are allowed to vary by risk stratum and by the health state of the HIV-positive member of the pair, and the per-contact risk is also allowed to differ depending on the sex of the HIV-negative member of

the pair, based on evidence of sex differentials in HIV acquisition risk [46,47]. Due to the potential for high numbers of sexual contacts within pairs the probability of transmission within a single timestep (γ_L^p and γ_H^p for low-risk and high-risk pairs respectively) is calculated with a Bernoulli model:

$$\gamma_L^p = 1 - (1 - o * p_s * p_r * p_i)^{k_r^p * l_i} \quad (7)$$

$$\gamma_H^p = 1 - (1 - o * p_s * p_r * p_i)^{k_r^p * l_i * m_t} \quad (8)$$

where o is the per-act transmission risk [47], $p_s$is the relative transmission risk related to the sex of the HIV-negative partner [47], p_r is the relative transmission risk related to risk stratum (proxying for unmodeled differences in the prevalence of other sexually transmitted infections that increase transmission risk [17,48,49]), p_i is the relative transmission risk related to HIV health state and ART status of the HIV-positive partner [50,51] , and k_r^p is the number of within-pair sex acts per timestep, by risk stratum [34].

3.2.6.2. Transmission through casual sex

The rate of HIV acquisition through casual sex for a particular HIV-negative group (γ_{sri}^c) is calculated as the sum of acquisition risk across all casual sexual partners, adjusted for individuals' risk factors:

$$\gamma_{sri}^c = \sum_{\hat{s}\in\hat{S}} \sum_{\hat{r}\in\hat{R}} \sum_{\hat{\imath}\in\hat{I}} \frac{h_{sri\_\hat{s}\hat{r}\hat{\imath}}}{n_{sri}} * o * p_s * \ p_{r+\hat{r}} * p_{\hat{\imath}} \quad (9)$$

Note that the subscript on p_s refers to the sex of the HIV-negative partner, the subscript on $p_{\hat{\imath}}$ refers to the HIV-positive partner, and $p_{r+\hat{r}}$ refers to both individuals, such that if either or both is high-risk then the risk-ratio for to the high-risk stratum is applied.

The total HIV acquisition rate for an individual model compartment is calculated as the sum of the rates from pairs and casual sex.

3.2.7. HIV progression

HIV progression is modeled as the transition between discrete CD4 categories, with transition rates $\xi_{i\_\hat{\imath}}$ for the transition between HIV state i and state $\hat{\imath}$. Following HIV acquisition, individuals enter the early HIV compartment, then transition rapidly to either the CD4>500 or CD4 350-500 compartment. The average duration of time spent with early HIV infection (and thus the sum of exit rates to subsequent CD4 cell count compartments) was based on a reanalysis of historical data on transmission during untreated HIV infection in Rakai, Uganda [50]. Following early infection, individuals transition to compartments representing progressively lower CD4 cell counts until they reach the CD4<200 compartment, in which they remain until death or ART uptake. Rates of transition between these CD4 compartments were based on data from observational cohorts [52–54].

3.2.8. Model entry, aging, and mortality

Individuals enter the model as unpaired HIV-negative adults (≥15 years). Time trends in new entrants were calculated from annual birth estimates obtained from the UN Population Division [55], lagged by 15 years and adjusted for intervening mortality. The model has a simplified age structure that distinguishes individuals 15-49 years of age from those aged 50 years and above. It was assumed for simplicity that sexual transmission of HIV occurs prior to age 50 years, consistent with earlier studies [17]. As pairs are only modeled to capture infection risks within sexual relationships, the model does not track pairs at ages above 50 years. Age-based background mortality rates [56] for 15-49 and ≥50 age groups were derived from the Actuarial Society of South Africa [56]. Disease-specific mortality rates for each HIV health state were derived from observational cohort data [57–61]. In the model, overall mortality rates are assumed to be the sum

of background and disease-specific mortality rates. Uncertainty in time varying parameters for model entry and background mortality is introduced by multiplying the time trend by random noise centered at 1.0.

3.2.9. HIV care and treatment

In the model, individuals can transition onto ART from any HIV health state except early HIV, as it is assumed that the difficulty of diagnosis during this period, in addition to delays in treatment initiation, will prevent individuals with early HIV from starting ART. The rate of treatment initiation for each HIV health state (ω_i) is determined by eligibility policy and the number of individuals in that health state receiving pre-ART care, as described below. Individuals receiving ART default from treatment at a fixed rate ς_i^{ART}. For individuals initiating ART with CD4<350, this rate is based on a recent systematic review [62]. There are few data on which to base the default rate for individuals initiating ART at higher CD4 counts, but a higher rate is plausible since these individuals will lack first-hand experience of the reduction in HIV symptoms associated with ART, and this rate was assumed to be double the rate for individuals initiating ART with CD4<350. Individuals defaulting from ART return to their original untreated health state.

Although pre-ART care (referred to simply as "pre-ART") is not represented by an explicit set of model compartments, it is an important component of the process of identifying individuals and linking them to ART, mediating the rate of ART initiation following a change in ART policy. The resources required to provide pre-ART also represent a non-trivial component of HIV treatment costs [63]. For these reasons the number of individuals receiving pre-ART is tracked in the model, and all individuals are assumed to pass through pre-ART before initiating ART. Individuals are initiated on pre-ART following identification in HIV testing programs. The average rate of HIV testing in the untreated population (i.e., all individuals not on ART or pre-ART) was specified as a time-varying policy input, with historical testing rates defined to be consistent with published

estimates of testing volume [64] and reproduce ART volume observed in prior years [65] in combination with historical ART eligibility criteria as described below. HIV-positive individuals are assumed to test at a higher rate than HIV-negative individuals based on consistent findings from population-based surveys [66]. Programmatic experience suggests that a substantial fraction of individuals testing HIV-positive will not initiate pre-ART, and the rate of primary default was derived from a systematic review by Rosen and Fox [67]. Individuals enrolled on pre-ART can subsequently default from care [67], die, or be initiated on ART. ART initiation rates prior to 2013 were based on historical ART eligibility criteria [68–71], which restricted general ART eligibility to individuals with CD4<200 cells/μL until 2010, then extended eligibility to include individuals with CD4<350 cells/μL by 2011 and maintained at this level until 2013. After 2013, modeled ART eligibility is determined by the policy scenario being modeled, as described in Section 3.2.2. Individuals who are enrolled on pre-ART and meeting CD4-based ART eligibility criteria are assumed to initiate ART on average one month after becoming eligible. Mortality rates, sexual behavior and other transitions are assumed to be unaffected by receipt of pre-ART.

3.2.10. Simulation

To undertake one simulation, the model is initiated in 1975, with individuals distributed across model compartments to represent an uninfected population. HIV is introduced into this population at a random point in time, centered at 1980 (Normally distributed with an equal-tailed 95% interval of +/- 5 years), and historical HIV eligibility guidelines and testing rates are modeled until the end of 2012. One of the policy options specified in Section 3.2.2 is introduced at the beginning of the year 2013 and assumed to be fully adopted by the end of 2013, then maintained at a constant level for a further 19 years, for a total analytic horizon of 20 years.

Simulations are limited to a 20-year analytic horizon as modeled epidemiology will be increasingly unreliable over longer time periods. However, restricting the analysis to this period ignores any

subsequent health benefits and costs, particularly the life-years gained through averted HIV mortality and averted transmission. These delayed costs and health outcomes may be of interest to decision-makers. For this reason, two sets of results were calculated: one set where only outcomes realized over the 20 years were included in the analysis ("truncated time horizon"), and one set where long-term outcomes were calculated for those individuals alive at the end of the initial 20-year simulation ("extended time horizon"). This second approach was operationalized by assuming no further HIV transmission, ART initiation[4] or population entry, and running the model for a further 100 years to capture the remaining life spans of both infected and uninfected persons of all ages, with outcomes being aggregated over the full 120 year period.

3.2.11. Parameter estimates and calibration

A Bayesian approach was used to calibrate model parameters to empirical data on HIV epidemiology in South Africa. . Under this approach, probability distributions were first specified to represent current uncertainty in model parameters (the 'prior'). A likelihood function (the 'likelihood') was then created to assess the level of agreement between modeled estimates and empirical data. This likelihood combined evidence from three sources (time trends in national HIV prevalence, survival in the absence of ART, and the CD4 cell count distribution in untreated HIV-positive individuals), with the overall likelihood calculated as the product of these three individual likelihoods. Finally, an iterative algorithm used to synthesis these various information sources via Bayes Theorem. Each of these steps is described in detail below.

[4] In sensitivity analyses we tested an alternate assumption in which all HIV-positive individuals were initiated on ART at the end of the initial 20-year period, with qualitatively similar results.

3.2.11.1. Parameter estimates

The estimates used to parameterize the model are shown in Table 3.1. There is substantial uncertainty about many of these parameters, and this uncertainty was operationalized as a prior probability distribution. For each parameter the prior distribution was centered at the mean shown in Table 3.1, with dispersion such that 2.5% of the distribution fell outside of the upper and lower bounds shown in the table (analogous to an equal-tailed 95% confidence interval). The functional form of the prior distributions was based on the range over which the parameter is defined: for parameters defined over the range [0,1] a logit-Normal prior was used (e.g., probabilities, disability weights), and for parameters defined over non-negative numbers a log-Normal prior was used (e.g., rates, costs)[5].

[5] While alternate functional forms might be considered, the logit-Normal and log-Normal were adopted as they were more easily adapted to the use with incremental mixture importance resampling (IMIS) calibration approach.

Table 3.1. Prior distributions for model parameters

Parameter Description	Value (Bounds)	Source
Sexual behavior parameters		
Rate of partnership dissolution, by risk stratum:		
Low-risk	0.017 [0.011, 0.025]	
High-risk	2.0 [1.3, 3.0]	[34]
Fraction of population in a pair, by risk stratum:		
Low-risk	0.63 [0.47, 0.77]	[42]
High-risk	0.88 [0.82, 0.92]	[34]
Relative partnership formation rate, by HIV health state:		
HIV-positive, CD4<200, no ART	0.25 [0.16, 0.37]	
HIV-positive, CD4 200-350, no ART	0.65 [0.42, 0.96]	
HIV-positive, CD4<350, ART	0.80 [0.52, 1.18]	
All others	1.00	[34]
Sexual mixing parameter for casual sex between risk strata	0.56 [0.13, 0.93]	[34]
Sexual mixing parameter for casual sex between paired individuals	0.50 [0.10, 0.90]	Assumed
Rate of sex acts within pairs, by risk stratum:		
Low-risk	42 [27, 63]	
High-risk	42 [27, 63]	[34]
Rate of casual sex acts, by risk stratum and pair status:		
Low-risk, in pair	4.4 [2.8, 6.5]	
Low-risk, not in pair	4.4 [2.8, 6.5]	
High-risk, in pair	4.4 [2.8, 6.5]	
High-risk, not in pair	4.4 [2.8, 6.5]	[45]
Relative frequency of sexual acts , by HIV health state:		
HIV-positive, CD4<200, no ART	0.65 [0.42, 0.96]	
HIV-positive, CD4 200-350, no ART	0.25 [0.16, 0.37]	
HIV-positive, CD4<350, ART	0.80 [0.52, 1.18]	
All others (reference)	1.0	[34]

Table 3.1. Prior distributions for model parameters (continued)

Parameter Description	Value (Bounds)	Source
Relative rate of risky sexual behavior over time, parameterized as a logistic curve (see Figure 3.3):		
Initial value (reference):	1.0	
Final value:	0.60 [0.42, 0.76]	
Start year of behavior change:	1995 [1990, 2000]	
Years to reach final value:	10.0 [5.9, 15.9]	[34]
Parameters related to HIV transmission risk		
Start year of modeled HIV epidemic	1980 [1975, 1985]	Assumed
Fraction of population HIV-positive at start year of epidemic (HIV seed)	0.0010 [0.0006, 0.0015]	Assumed
Per-act transmission risk for an individual with asymptomatic HIV, in the low-risk stratum, for male-to-female transmission	0.003 [0.001, 0.006]	[47]
Relative HIV transmission risk, by HIV health state:		
Early HIV	26.5 [5.1, 83.0]	
CD4>350, excl. early HIV (reference)	1.0	[50]
CD4<350	7.3 [1.6, 21.4]	
Relative transmission risk for individuals receiving ART, compared to untreated individuals	0.040 [0.006, 0.144]	[51]
Relative HIV transmission risk, by risk stratum:		
Low-risk (reference)	1.0	
High-risk	2.0 [1.3, 3.0]	[17]
Relative HIV transmission risk:		
Male-to-female (reference)	1.0	
Female-to-make	1.5 [1.2, 1.8]	[47]
Parameters related to HIV progression		
Transition rates between CD4 compartments:		
Early HIV to CD4>500 or 350-500	4.1 [1.5, 9.2]	[50]
Fraction exiting early HIV to CD4>500	0.70 [0.56, 0.81]	
CD4>500 to CD4 350-500	0.15 [0.10, 0.22]	
CD4 350-500 to CD4 200-350	0.41 [0.26, 0.61]	
CD4 200-350 to CD4>200	0.41 [0.26, 0.61]	[52–54]

Table 3.1. Prior distributions for model parameters (continued)

Parameter Description	Value (Bounds)	Source
Parameters related to model entry, aging and mortality		
Adult population in 1975 (millions)	14.9	[55]
Absolute number of new entrants to adulthood (age ≥15years)	Time-varying, see Figure 3.3	[55]
Fraction of new entrants female	0.51 [0.50, 0.52]	[55]
Fraction of new entrants entering low-risk stratum	0.70 [0.56, 0.81]	[34]
Rate at which individuals age out of the sexually active population	0.029	By construction
Background mortality by age group:		
Age 15-49 years	Time-varying,	
Age ≥50 years	see Figure 3.3	[56]
HIV specific mortality, by HIV health state:		
No ART, early HIV	0.006 [0.001, 0.020]	
No ART, CD4>500	0.006 [0.001, 0.020]	
No ART, CD4 350-500	0.016 [0.008, 0.030]	
No ART, CD4 200-350	0.042 [0.029, 0.058]	
No ART, CD4<200	0.31 [0.27, 0.35]	
ART, initiated at CD4>500	0.006 [0.001, 0.020]	
ART, initiated at CD4 350-500	0.006 [0.001, 0.020]	
ART, initiated at CD4 200-350	0.023 [0.014, 0.037]	
ART, initiated at CD4<200	0.050 [0.031, 0.076]	[57–61]
Parameters related to service delivery		
Rate of HIV testing in HIV-negative individuals as compared to HIV-positive individuals	0.63 [0.56, 0.71]	[66]
Probability of primary default between HIV diagnosis and pre-ART	0.42 [0.31, 0.53]	[67]
Rate of default from pre-ART care, by HIV health state:		
CD4<350	0.25 [0.15, 0.40]	
CD4>350	0.75 [0.53, 1.03]	[67]
Rate of default from ART, by health state at ART initiation:		
CD4<350 at ART initiation	0.10 [0.07, 0.15]	
CD4>350 at ART initiation	0.21 [0.13, 0.30]	[62]

Table 3.1. Prior distributions for model parameters (continued)

Parameter Description	Value (Bounds)	Source
Parameters related to cost and health state valuation		
Disability weights, by HIV health state:		
No ART, early HIV	0.053 [0.033, 0.081]	
No ART, CD4 200-350	0.22 [0.15, 0.31]	
No ART, CD4<200	0.55 [0.38, 0.71]	
ART	0.053 [0.034, 0.079]	[72]
Costs of health care received by individuals with symptomatic HIV, not on ART or pre-ART:		
No ART, CD4 350-500 (annual)	13 [7, 21]	
No ART, CD4 200-350 (annual)	46 [35, 60]	
No ART, CD4<200 (annual)	167 [160, 175]	[13]
Costs of pre-ART services (annual)	238 [161, 338]	[13]
Costs of ART services		[13]
ART initiation (per event)	95 [70, 127]	
Antiretroviral drugs (annual)	172 [127, 227]	
Non-ARV costs (annual)	422 [340, 517]	
Cost of HIV testing and counseling (per client)	20 [15, 27]	[13]
Cost of care during terminal illness	160 [88, 268]	[13]
Mark-up on direct service provision costs to account for program-level management and administrative support	0.50 [0.29, 0.79]	[13]
Discount rate	0.03	[73]

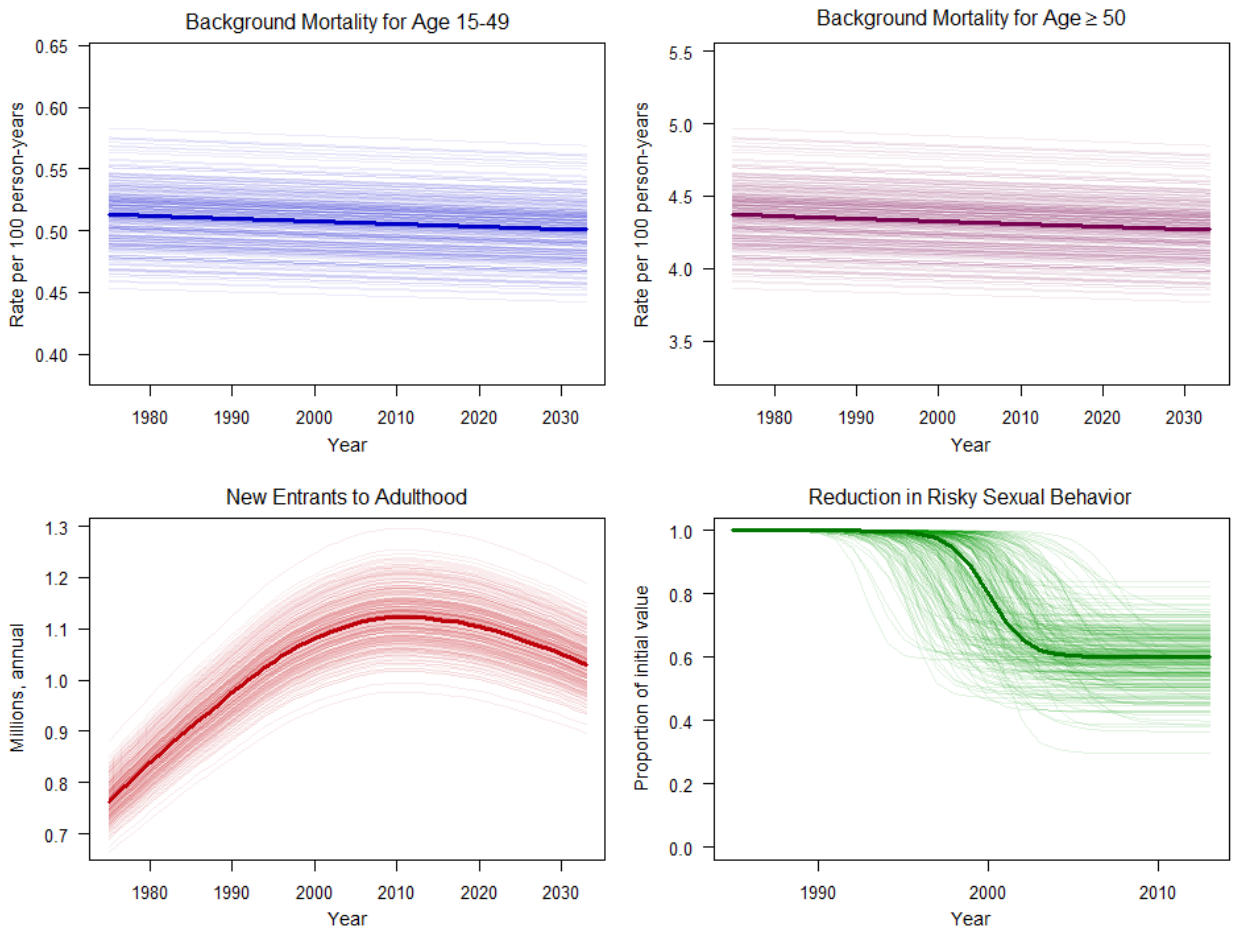

Figure 3.3. Prior distributions for time-varying model parameters

3.2.11.2. Likelihood for HIV prevalence

Two sources of HIV prevalence data were available: annual HIV prevalence estimates from sentinel surveillance at antenatal care (ANC) centers [74], and national population-based seroprevalence surveys conducted in 2002, 2005, and 2008 [75]. The estimates from population-based surveys were assumed to be unbiased but their small number provides limited information on long-term trends. In contrast, the estimates from ANC sites are generally based on a larger sample and are available as a complete annual time series 1990-2010. However, data from ANC sites are thought to provide biased estimates of general population prevalence, with pregnant women at higher relative risk of HIV compared to the general community [76]. As part of its Epidemic Projection Package for

estimating national HIV prevalence and incidence trends [77], the UNAIDS Reference Group on Estimates, Modelling and Projections has developed an approach for incorporating both surveys and ANC surveillance into a single likelihood, by assuming that the bias in the ANC data represents a constant additive term in probit space [78,79]. We adopt a modified version of this likelihood, expressed as the log-likelihood shown below:

$$ln\mathcal{L}_1(\theta_i|y,\mu,\sigma^2) = -\left(\frac{1}{2}ln(\sigma^2) + \frac{(\mu-b)^2}{2\sigma^2}\right) - \sum_{t\epsilon T}\left(\frac{1}{2}ln(\upsilon_t) + \frac{(y_t - b - \rho_{it})^2}{2\upsilon_t}\right) \quad (10)$$

where:

θ_i = parameter set *i,*

ρ_{it} = modeled HIV prevalence estimate for year *t* ($t \epsilon T$), produced by parameter set θ_i,

T = years in which ANC sentinel surveillance was conducted (1990-2010 inclusive),

y_t = probit-transformed ANC prevalence estimate in year *t*,

υ_t = variance for ANC prevalence estimate in year *t*, calculated as

$\upsilon_t = 2\pi\ exp(\Phi^{-1}(y_t)^2)y_t(1-y_t)/N_t$,

N_t = effective sample size of ANC survey in year *t*, calculated by dividing the reported sample size by a design effect of 2.0 to account for clustering[6],

b = constant term for bias in ANC prevalence estimates,

μ = prior mean for bias term *b*, calculated as $\mu = \frac{\sum_z(\eta_z - y_z)}{q}$,

σ^2 = prior variance for bias term *b*, calculated as $\sigma^2 = \frac{\sum_z(d\phi_z + \upsilon_z)}{q^2}$,

η_z = probit-transformed prevalence estimate from population-based survey in year *z*,

[6] While this design effect is assumed, 95% uncertainty intervals calculated using these variance estimates approximate the confidence intervals reported in the survey report [74].

z = year in which population-based survey was conducted ($z \epsilon$ 2002, 2005, 2008),

ϕ_z = variance estimate for population-based prevalence survey in year *z,*

d = multiplier on ϕ to account for selective non-participation in population-based prevalence surveys, and

q = number of population-based prevalence surveys conducted ($q = 3$ for South Africa).

By considering selective non-participation in population-based prevalence surveys (via the term d) the likelihood function shown in equation 10 differs from the likelihood described by Alkema and colleagues [78]. This change is motivated by recent re-analyses of national prevalence surveys using Heckman-type selection models [80,81]. In its review of the issue, the UNAIDS Reference Group on Estimates, Modelling and Projections concluded that appropriate consideration of this potential bias may extend reported confidence intervals by up to a factor of 4.5 [82]. In this analysis we assumed d = 2.0.

In addition, the assumption that the bias in the ANC data (operationalized as b) would be constant in probit space may not hold over a wide range of prevalence. As all the population-based prevalence surveys (used to estimate b) were conducted at a time of high prevalence (15.6-16.9%), we excluded from the likelihood all years where the maximum of the likelihood function would fall below 1% prevalence (1990-1992). Figure 3.4 summarizes the various data used for the prevalence likelihood.

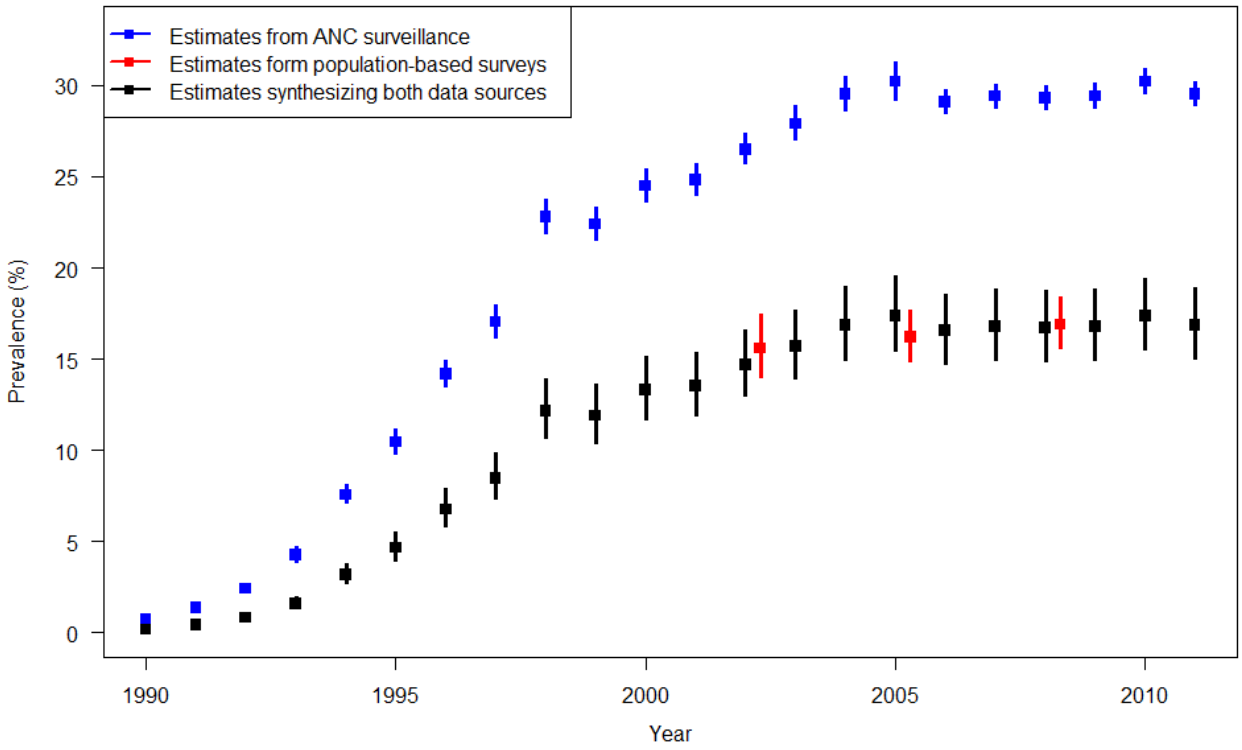

Figure 3.4. Data used for HIV prevalence likelihood

3.2.11.3. Likelihood for HIV-positive survival in the absence of ART

Glynn and colleagues report estimates of median survival from seroconversion to death in a retrospective cohort of South African mine workers [83]. As this study was conducted before ART became widely available, the results can be used to calibrate modeled estimates of survival for untreated HIV-positive individuals from the time of initial infection. In this study median survival was 10.5 years (95% CI: 10.0-10.8). As the raw data were unavailable, a Normal likelihood was constructed based on this summary estimate:

$$ln\mathcal{L}_2(\theta_i|\mu,\sigma^2) = -\frac{(\rho_i - u)^2}{2\sigma^2} \quad (11)$$

where:

θ_i = parameter set *i,*

ρ_i = modeled estimate of median survival following HIV seroconversion, produced by parameter set θ_i,

μ = median survival of 10.5 years reported by Glynn *et al*.,

d = factor to expand Normal likelihood to account for unobserved bias, value=2.0, and

σ^2 = variance of median survival estimate, calculated as $\left(\frac{10.8-10.0}{2*1.96}\right)^2 * d = 0.083$.

This study was conducted in a select population (mine workers) whose survival might differ from the general population. For this reason the variance of the likelihood function was expanded by a factor of 2.0 to account for the possibility of unobserved bias.

3.2.11.4. Likelihood for CD4 cell count distribution in untreated HIV-positive individuals

A number of studies report information on the distribution of CD4 cell counts in ART-naïve individuals. While some of these studies report on populations whose CD4 distribution will clearly differ from the general population[7], three studies report on groups whose CD4 distribution might be similar to the general population. These include data collected in 2002 from a single township with high HIV prevalence [84], data from a 2004 national survey of public school educators [85], and data collected in 2005 from health care workers in two public hospitals in Gauteng province [86]. These data are summarized in Figure 3.5.

[7] For example, Holmes *et al*. report on a population of ART-naïve patients attending an HIV treatment clinic [53]. As a consequence of attending the clinic, these individuals are more likely to be experiencing HIV symptoms and have lower CD4 cell counts compared to HIV-positive individuals in the general population.

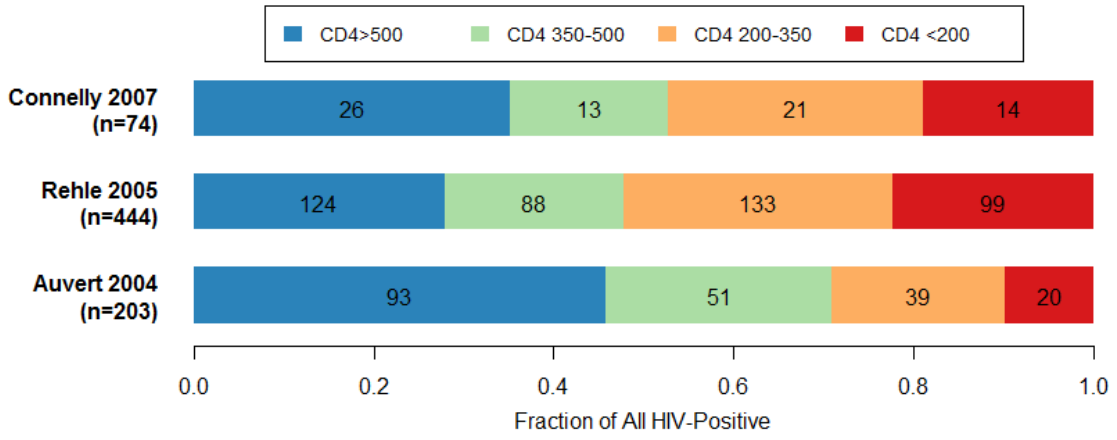

Figure 3.5. Data used for CD4 cell count distribution likelihood

These data were summarized in the following multinomial likelihood:

$$ln\mathcal{L}_3(\theta_i|y) = \sum_j \sum_k \frac{y_{jk}}{d} ln(\rho_{jk}) \tag{12}$$

where:

θ_i = parameter set *i*,

ρ_{jk} = modeled estimate of the fraction of the untreated HIV-positive population in CD4 stratum k in the year in which data were collected for study j, produced by parameter set θ_i,

y_{jk} = number of individuals in CD4 stratum k in study j, and

d = factor to expand multinomial likelihood to account for unobserved bias, value=2.0.

The study populations on which this likelihood is based represent specific groups (a single township, educators, health care workers) whose CD4 distributions might differ from the general population. As with the survival likelihood, an additional term (d) was included in order to increase the dispersion of the likelihood to account for the possibility of unobserved bias.

The likelihoods for prevalence, survival, and CD4 distribution were assumed to be independent, and consequently the overall log-likelihood was calculated as the sum of the individual log-likelihoods:

$$ln\mathcal{L}_{all} = ln\mathcal{L}_1 + ln\mathcal{L}_2 + ln\mathcal{L}_3 \quad (13)$$

3.2.11.5. Calibration approach

The posterior distribution of the model parameters was approximated using Incremental Mixture Importance Sampling (IMIS) [87]. Similar to the Markov chain Monte Carlo methods conventionally used for Bayesian inference, IMIS produces a table of parameter sets that represent independent draws from the joint posterior parameter distribution, which are obtained by updating the joint prior distribution *p(θ)* with the information contained in the likelihood function described in Sections 3.2.11.2-3.2.11.4. The algorithm proceeds by drawing a sample from the prior distribution of the model parameters, similar to Rubin's Sampling Importance Resampling approach [88] on which IMIS is based, and then iteratively adds extra draws to this sample in regions of the parameter space that the likelihood suggests are under-sampled with respect to the posterior distribution. The following description closely follows the exposition provided by Raftery and Bao 2010 [87]:

Initial stage:

a. Draw a large number (N_0) of parameter sets from the prior distribution $p(\theta)$.
b. For each of these parameter sets, θ_i , run the model and estimate the outcomes needed to evaluate the likelihood function (HIV prevalence, HIV survival, CD4 distribution in untreated individuals).
c. For each parameter set θ_i calculate the likelihood, $\mathcal{L}(\theta_i)$, and use these to calculate importance weights w_i^0:

$$w_i^0 = \frac{\mathcal{L}(\theta_i)}{\sum_i \mathcal{L}(\theta_i)} \tag{14}$$

Importance sampling stage: for k=1,2,… repeat the following steps

d. Choose the parameter set with the highest importance weight, θ^k, and use this parameter set as the center of a new multivariate Normal distribution, H^k, created to sample underrepresented parts of the parameter space. Estimate the variance-covariance matrix of this distribution, Σ^k, as the weighted covariance of the **B** parameter sets with the smallest Mahalonobis distance to θ^k, where distances are calculated with respect to the covariance of the prior distribution.

e. Sample *B* new parameter sets from H^k.

f. Run the model and calculate the likelihood for each of these new parameter sets.

g. Combine all parameter sets and calculate importance weights for the new parameter sets:

$$w_i^k = c\frac{\mathcal{L}(\theta_i)p(\theta_i)}{q^k(\theta_i)} \tag{15}$$

where *c* is a constant chosen so that the weights sum to 1, and $q^k(\theta_i)$ is the mixture distribution calculates as a mixture of the prior and the new multivariate Normal distribution:

$$q^k(\theta) = \frac{N_0 p(\theta) + B\sum_{s=1}^{k} H^s}{N_k} \tag{16}$$

where $N_k = N_0 + Bk$.

h. Evaluate the stopping criterion: that the expected fraction of unique parameter sets in the resample is greater or equal to $1 - \frac{1}{\mathrm{e}}$ (i.e., 0.632, which is the expected fraction when the

importance weights are all equal). The expected fraction of unique parameter sets is calculated as $\sum_{i=1}^{N_k}\left(1-\left(1-w_i^k\right)^J\right)$.

i. If the stopping criterion is not met, repeat steps d to h. If the stopping criterion is met, resample *J* parameter sets with replacement from the set of all N_k parameter sets, using the importance weights as sampling weights. These *J* parameter sets represent a draw from the posterior distribution.

N_0 (the size of the initial sample), *B* (the size of each additional importance sample) , and *J* (the number of resample in the final draw), are user specified inputs, set to 5 million, 50,000, and 100,000 respectively in this analysis.

The stopping criterion described above is difficult to obtain for a problem with a high-dimensional posterior, and for this reason an alternative approach was adopted, whereby the algorithm was stopped after 20 iterations and all parameter sets were retained whose likelihood was statistically indistinguishable from the maximum likelihood[8]. The resulting sample of 70,840 parameter sets was used for all subsequent analyses. Figure 3.6 compares the results produced by the calibrated model against the calibration data.

[8] This included all parameter sets *i* where $-2 * ln\left(\frac{w_i}{\max_i w_i}\right) \leq 65.2$, and where the 65.2 threshold for the test statistic is derived from a χ^2 distribution with 48 degrees of freedom and α = 0.05.

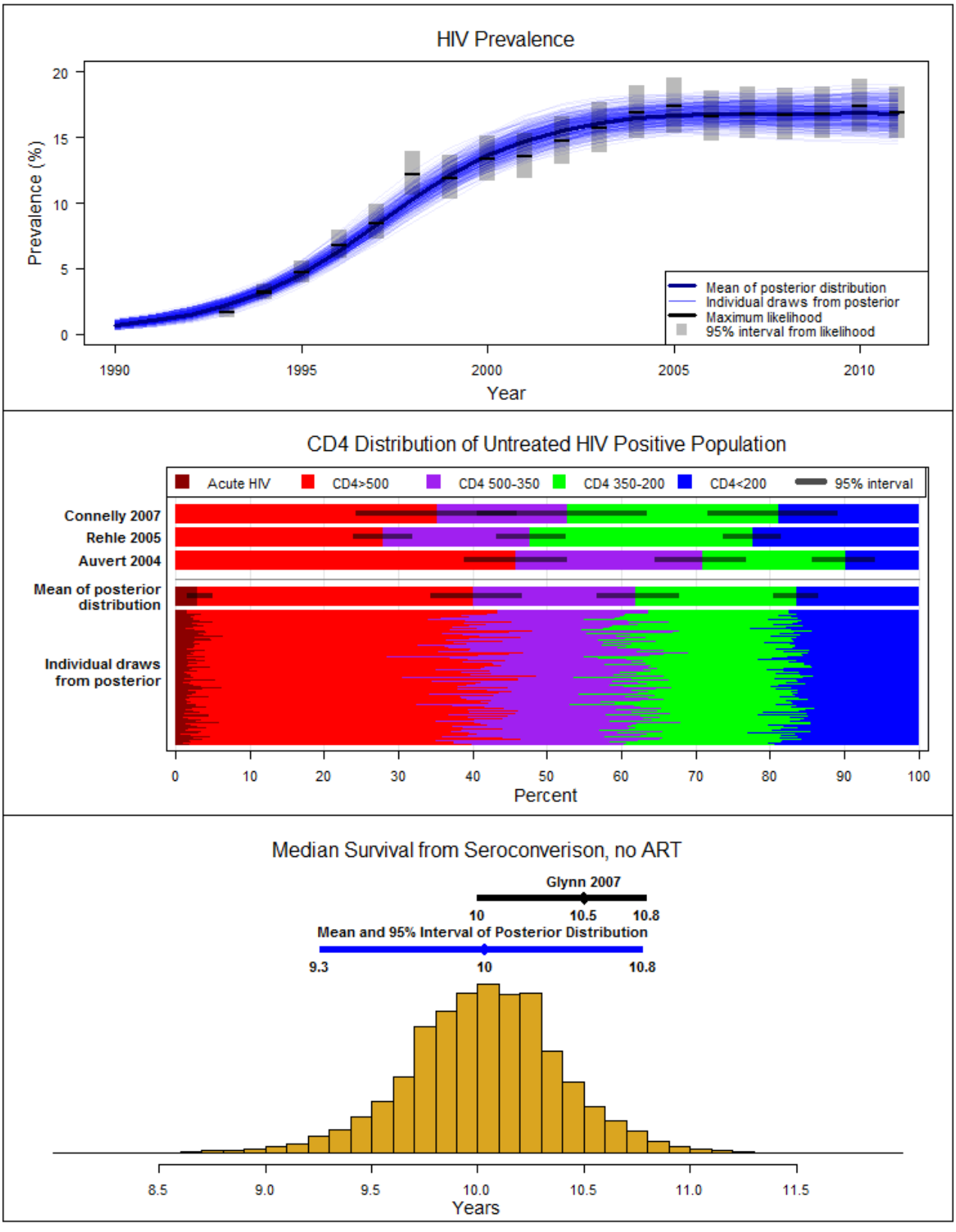

Figure 3.6. Results of calibrated model vs. calibration data

3.2.12. Estimating costs

We adopted a health system perspective for the analysis and costs were assessed incrementally, such that any cost categories unaffected by the changes in ART policy examined in this analysis were omitted from the costing. All costs are expressed in 2012 US dollars. Costs were assessed for the following categories:

(a) direct costs of care received by ART patients,
(b) direct costs of care received by pre-ART patients,
(c) direct costs of programs to identify and link HIV-positive individuals to care,
(d) averted costs due to reduced health care utilization outside of the HIV program, and
(e) costs of higher-level programmatic support.

3.2.12.1. ART costs

ART costs were subdivided into ARV drug costs and non-ARV costs. The total cost of ARV drugs in a given year was calculated by multiplying the number of person-years of ART in that year by the annual ART regimen unit cost. The ART regimen unit cost represents the average annual cost of the current distribution of ART regimens in South Africa, estimated as part of a recent analysis of WHO guideline changes [13]. This and other unit costs are shown in Table 3.1.

Nnon-ARV costs were subdivided into ART initiation costs and established patient costs. ART initiation costs—accounting for the additional laboratory tests and clinic visits incurred during a patient's initial months on ART [63]—were calculated by multiplying the number of individuals initiating ART in a given year by the ART initiation unit cost, which was obtained from an evidence synthesis of available costing data [13]. Established patient costs—accounting for the regular clinical care and laboratory monitoring received by ART patients, as well as all other site-level activities required for the functioning of the ART program—were calculated by multiplying the number of person-years of ART in a given year by the established ART patient unit cost, obtained

from the earlier evidence synthesis. Total ART costs were calculated as the sum of ARV costs, ART initiation costs, and established patient costs.

3.2.12.2. Pre-ART costs

Pre-ART patients receive regular clinical and laboratory monitoring of ART eligibility, as well as routine care and prophylaxis / treatment of opportunistic infections [89]. Pre-ART costs for a given year were calculated by multiplying the number of patient-years of pre-ART in that year (tracked in the model, as described in Section 3.2.9) by the pre-ART unit cost, obtained from the earlier evidence synthesis.

3.2.12.3. HIV testing costs

HIV testing costs in a given year were calculated as the product of the number of people receiving HIV tests in that year (as described in Section 3.2.9) and the unit cost of HIV testing and counseling, obtained from the earlier evidence synthesis.

3.2.12.4. Averted costs outside of the HIV program

Individuals with symptomatic HIV who are not receiving care or treatment in a dedicated HIV program may exhibit greater utilization of care within the routine health system. These other care costs were subdivided into annual health care utilization costs and end-of-life care costs.

Annual health care utilization costs were estimated for HIV-positive individuals not on pre-ART or ART with a CD4 count <500 cells/μL. For each CD4 count category (350-500, 200-350, <200), health care utilization costs in a given year were calculated as the product of the number of person-years spent in that state and the health care utilization unit cost for that state, obtained from the earlier evidence synthesis.

End-of-life care costs were assumed to be the same for all individuals, and total end-of-life care costs for a given year were estimated as the number of deaths in that year multiplied by the unit cost per death, reflecting the additional utilization and inpatient care received during terminal illness.

3.2.12.5. Programmatic support

Program costs—the costs of management, administration, supervision, training, M&E and other activities undertaken to support direct service provision—are frequently omitted from empirical costing exercises, but can represent a non-trivial fraction of total costs. Estimates of program costs for PMTCT services suggest that these costs can represent 4–18% of total costs, and for HIV education services this percentage has been estimated as 34–97% [90]. For this analysis the mark-up on direct service provision to take account of program costs was based on the input of costing and programmatic experts participating in the WHO guidelines analysis described previously [13]. In that analysis, program costs were divided into a fixed component, invariant to changes in program scale, and a variable component that scaled linearly with total direct costs (excluding ARVs). As this was an incremental costing the fixed costs could be ignored. The variable component represents a fixed multiple of direct costs, and this multiple was estimated at 50% (with a wide uncertainty interval), such that program costs would represent 33% of total service provision costs (excluding ARVs) [13].

3.2.13. Estimating health outcomes

Health consequences were summarized as incremental DALYs averted. For each year the total number of DALYs averted was calculated by summing the number of person-years lived in each HIV health state, multiplying this total by one minus the disability weight for that state (zero unless listed in Table 3.1), and summing across all HIV health states. The same basic estimation approach was used for truncated and extended time horizons, though the period over which results were

aggregated differed (20 years and 120 years respectively). No age-weighting was used, consistent with the approach used in the most recent iteration of the Global Burden of Disease (GBD) study [91]. However, unlike the current GBD approach, future health gains (and costs) were discounted, using a rate of 3% per year [73].

3.2.14. Value function and decision rule

It was assumed that:

- Policy makers are rational in their choice of policy options (i.e., hold preferences over any set of policy options that are complete and transitive),
- Faced with uncertain outcomes, policy makers value each outcome proportional to its probability of occurring, consistent with Von Neumann–Morgenstern Expected Utility Theory, and
- Policy makers hold preferences consistent with a utility function that is linearly increasing in health benefits (as operationalized in Section 3.2.13) and linearly decreasing in costs (as operationalized in Section 3.2.12), that these arguments exhibit additive independence, and that these outcomes (health system costs and DALYS averted) summarize all relevant consequences of the policies in question.

If these conditions hold, relative preference for different policy options can be summarized as Net Monetary Benefit (NMB) [30], where for a policy *i* the expected value of Net Monetary Benefit is given by:

$$E(NMB_i) = E(\lambda B_i - C_i) = \frac{1}{J}\sum_{j\in J}\sum_{t\in T}\left(\lambda B_{ijt} - C_{ijt}\right)(1+d)^{-t} \quad (17)$$

In equation 17 *j* indexes for parameter sets randomly drawn from the posterior parameter distribution, *t* indexes for year following policy introduction[9], *B* represents total health benefits (in DALYs averted), *C* represents total costs, *d* represents the discount rate, and λ represents the policy makers' rate of exchange between health benefits and cost savings.

As a consequence of the assumptions described above, decision makers will choose the policy that maximizes NMB on expectation, obtaining $NMB_{max} = \underset{i}{\text{MAX}}\ E(NMB_i)$. For the purposes of this analysis we also assumed that the preferences expressed by policy makers are consistent with general societal preferences, such that by making optimal choices according to the choice function described above policy makers are also maximizing social welfare.

The NMB framework also provides a direct measure of the welfare loss from sub-optimal decision-making, with $NMB_{max} - NMB_i$ representing the monetized value of the welfare loss through choosing policy *i* instead of the optimal policy, and the maximum value we should be willing to pay to switch from *i* to the optimal policy.

3.2.15. Value of information analysis

To assess the relative value of new research investments we followed the general framework described by earlier authors for estimating VOI [22,23,29,92,93].

[9] Note that T=20 for the truncated time horizon and T=120 for the extended time horizon, as discussed in Section 3.2.9.

3.2.15.1. Expected value of perfect information

The expected value of perfect information (EVPI) represents the additional welfare that would be gained if all decision uncertainty were resolved before a policy is chosen, as compared to a scenario where no new information is collected:

$$\begin{aligned} EVPI &= E\left(NMB_{perf\ info}\right) - \mathrm{E}\left(NMB_{no\ info}\right) \\ &= E_{\theta}\left(\underset{i}{\mathrm{MAX}}\ NMB_i\right) - \underset{i}{\mathrm{MAX}}\, E_{\theta}(NMB_i) \end{aligned} \tag{18}$$

Within the context of the calibrated model, this can be operationalized as:

$$EVPI = \left[\frac{1}{J}\sum_{j\in J} \underset{i}{\mathrm{MAX}}\ NMB_{ij}\right] - \left[\underset{i}{\mathrm{MAX}}\ \frac{1}{J}\sum_{\substack{j\in J \\ i}} NMB_{ij}\right] \tag{19}$$

where *j* indexes for parameter set drawn from the posterior parameter distribution.

Results are presented for EVPI as a function of WTP per DALY averted (λ), to understand the upper bound of the possible value of new research. However, this metric gives little insight as to the absolute or relative value of new information on specific research targets.

3.2.15.2. Expected value of partial perfect information

The expected value of partial perfect information (EVPPI) represents the expected value of the additional welfare that would be gained if the decision uncertainty around an individual parameter or subset of parameters were resolved before a policy is chosen, as compared to the 'no new information' scenario:

$$\begin{aligned} EVPPI_Z &= E\left(NMB_{perf\ info\ on\ z}\right) - \mathrm{E}\left(NMB_{no\ info}\right) \\ &= E_{\theta_Z}\left(\underset{i}{\mathrm{MAX}}\, E_{\theta_{Z^c}}(NMB_i|\theta_Z)\right) - \underset{i}{\mathrm{MAX}}\, E_{\theta}(NMB_i) \end{aligned} \tag{20}$$

where z represents the parameter or set of parameters on which perfect information is gained, and z^c represents the complement of z. $EVPPI_Z$ would typically be calculated by (i) drawing a single realization of θ_Z, (ii) drawing a large sample from θ_{Z^c} conditional on the realized value of θ_Z , (iii) finding the maximum average NMB in this sample that can be achieved by choosing between the different policy options i, (iv) repeating steps i-iii for a large sample from θ_Z and averaging the results, and finally (v) subtracting $\mathrm{E}\left(NMB_{no\ info}\right)$ from this total [22]. The first step in this algorithm is difficult to operationalize in the context of the calibrated model, as for each realization of θ_Z in the posterior parameter distribution (the set of 70,840 parameter sets described in Section 3.2.11.5), we have only a single realization of θ_{Z^c}, and no obvious way of generating new samples (aside from recalibrating the model with this parameter fixed). As all parameters are sampled from a continuous prior distribution, this issue remains even if a very large number of samples are obtained from the posterior parameter distribution. To resolve this problem, it is assumed that $E_{\theta_{Z^c}}(NMB_i|\theta_Z)$ will be similar to $E_{\theta_{Z^c}}\left(NMB_i|\theta_{Z_k}\right)$ for those parameter sets that lie close to θ_{Z_k} in $\mathbb{R}_Z$ (where k indexes a single realization of θ_Z), such that:

$$\lim_{\mathcal{E}\to 0} E_{\theta_{Z^c}}\left(NMB_i|\left(\theta_{Z_k}+\mathcal{E}\right)\right) = E_{\theta_{Z^c}}\left(NMB_i|\theta_{Z_k}\right) \quad for\ all\ i \in I \tag{21}$$

This property (that the change in $E_{\theta_{Z^c}}(NMB_i|\theta_Z)$ as a function of θ_Z is continuous) is not an inherent property of decision problems[10], yet it is true by construction for the model developed for this analysis. It is also true (due to the structure of the model) that the change in $E_{\theta_{Z^c}}(NMB_i|\theta_Z)$ as

[10] For example, this continuity property may not hold in decision problems that feature sequential decisions made by different actors, as when θ_Z crosses a threshold such that the first actor changes their optimal policy there may then be a step change in the outcomes for other actors.

a function of θ_Z is smooth (i.e., the first derivative of $E_{\theta_{Z^c}}(NMB_i|\theta_Z)$ with respect to any parameter in z is continuous). Based on these properties, we can approximate $E_{\theta_{Z^c}}(NMB_i|\theta_Z)$ by fitting a smooth curve (or smooth surface if there is more than one parameter in z) through $NMB_i|\theta_Z$, as calculated from the 70,840 posterior draws from the calibration. The resulting function, $\hat{E}_{\theta_{Z^c}}(NMB_i|\theta_Z)$, allows us to estimate $E(NMB_i|\theta_Z)$ for any policy and for any specific values of θ_Z in the range of those represented in the posterior parameter distribution[11]. For each policy, this function is created using locally-weighted polynomial regression (LOESS), an approach to estimating smooth curves or surfaces by fitting low-order polynomial functions to local subsets of data [94,95], operationalized using the *loess* function in **R**'s *stats* package [96]**.**

The following algorithm was used to estimate $EVPPI_Z$:

(i) For each policy *i*, the function $\hat{E}_{\theta_{Z^c}}(NMB_i|\theta_Z)$ was estimated by fitting a LOESS regression for NMB_i as a function of the parameters in z. For most analyses z consisted of a single parameter, but when z represented multiple parameters all interaction terms were included in the LOESS regression.

(ii) For each parameter set in J, the optimal policy given perfect information about z was identified as the policy that maximizes the function $\hat{E}_{\theta_{Z^c}}(NMB_i|\theta_Z)$ at θ_j. The rational decision maker should chose this policy, and obtain the actual value of NMB produced by this policy (i.e., not the value predicted by the function).

(iii) These actual values are averaged across all $j \in J$, and $\mathrm{E}(NMB_{no\ info})$ was subtracted from the result, with this difference representing $EVPPI_Z$.

[11] $\hat{E}_{\theta_{Z^c}}(NMB_i|\theta_Z)$ actually represents a set of functions, one for each policy *i.*

EVPPI results were calculated as a function of the WTP threshold, and used to make judgments about the relative value of perfect information for each parameter. EVPPI represents an upper bound of the value of new research, because the information obtained from research studies will not be perfect. In addition, as research on relative infectiousness might plausibly provide information on multiple phases of infection, EVPPI was calculated for the group of parameters determining relative transmission risk during early infection, late stage disease, and for those on ART.

As it examines the value of perfect information on a particular parameter, EVPPI provides an upper bound on the value of empirical research, which only provides sample information. While the expected value of partial sample information (EVPSI) can be calculated, to do so requires an explicit description of the practical research design that would be used to collect new information, the expected sampling variance, and any biases that might affect the relationship between research results and the population-level variables of interest. As many research approaches are possible for a given subject, with differing costs and informational value, one could generate a function that describes EVPSI for each research target as a function of the level of investment, then choose the level of expenditure that maximizes EVPSI minus research costs. As the EVPSI of different parameters may not be independent (or if the opportunity cost of increased research spending is not fixed), optimizing the overall research portfolio would require simultaneously choosing a level of investment for all research targets so as to maximize the overall NMB generated by research minus the total costs of this research. Such an analysis—requiring estimates of the informational value and costs of many different research designs on different targets— is not feasible in the context of the current study. Instead, the relative magnitude of EVPPI for different research targets was used to draw conclusions about the relative urgency of new research in different areas, and identify areas where new research could meaningfully influence policy.

3.2.16. Sensitivity analyses

3.2.16.1. Health benefits attributable to the therapeutic effects of ART

Sensitivity analyses were undertaken to estimate the fraction of health benefits that were attributable to the therapeutic effects of ART (*c.f.* the effects of reduced HIV transmission by ART patients). For each policy option, this fraction was calculated by comparing the number of DALYs averted by that policy in the main analysis (i.e., including both therapeutic and preventive benefits of ART) to the number of DALYs averted by that policy in an analysis in which future HIV infection risk is unaffected by ART policy, with all scenarios following the same HIV incidence trend as the current policy (policy A2, with ART eligibility of CD4 <350, and continuation of current testing rates).

3.2.16.2. Different assumptions about discount rates

Sensitivity analyses were undertaken to test the robustness of policy choices to changes in the discount rate applied to costs and health benefits. Three analyses were undertaken: one in which the discount rate for both costs and health benefits was set to 0% (i.e., no discounting), one in which this rate was set to 6%, and one in which costs were discounted at 3% (as in the main analysis) but health benefits were not discounted.

3.2.16.3. Changes in the choice set

For the value of information analysis, a sensitivity analysis was undertaken to understand the sensitivity of the VOI results to changes in the choice set. In this sensitivity analysis, the VOI results were recalculated under the assumption that the choice of coverage policy was already determined, representing continuation of current testing policy and continued ART enrollment (i.e., the choice set only includes policies A2, B2, and C2).

3.2.16.4. Fraction of transmission attributable to early infection

A sensitivity analysis was undertaken to test whether the VOI results obtained for the parameter for increased transmission risk during early infection was sensitive to changes in the fraction of all transmission occurring during early infection. This sensitivity analysis was undertaken using a Bayesian melding approach [97], by adding an additional prior on this outcome (i.e., the fraction of all transmission attributable to individuals with early infection). This additional prior was operationalized as a Normal distribution with mean and standard deviation based on the estimate reported by Powers (38% (19-52) of all transmission attributable to early infection). This sensitivity analysis was implemented by reweighting the parameter sets, with weights proportional to the density of this additional prior when evaluated at the value of this outcome (fraction of transmission attributable to early infection) generated by each parameter set. The result of this reweighting was a 70% increase in the fraction of transmission attributable to early infection, to 25% (15-39%).

3.3. Results

3.3.1. Epidemiological estimates and projections

Figure 3.7 presents modeled results for various epidemiological outcomes over the period 1985-2032, with future projections calculated under the assumption that current ART access and eligibility policies would be maintained (corresponding to policy A2, as described in Section 3.2.2).

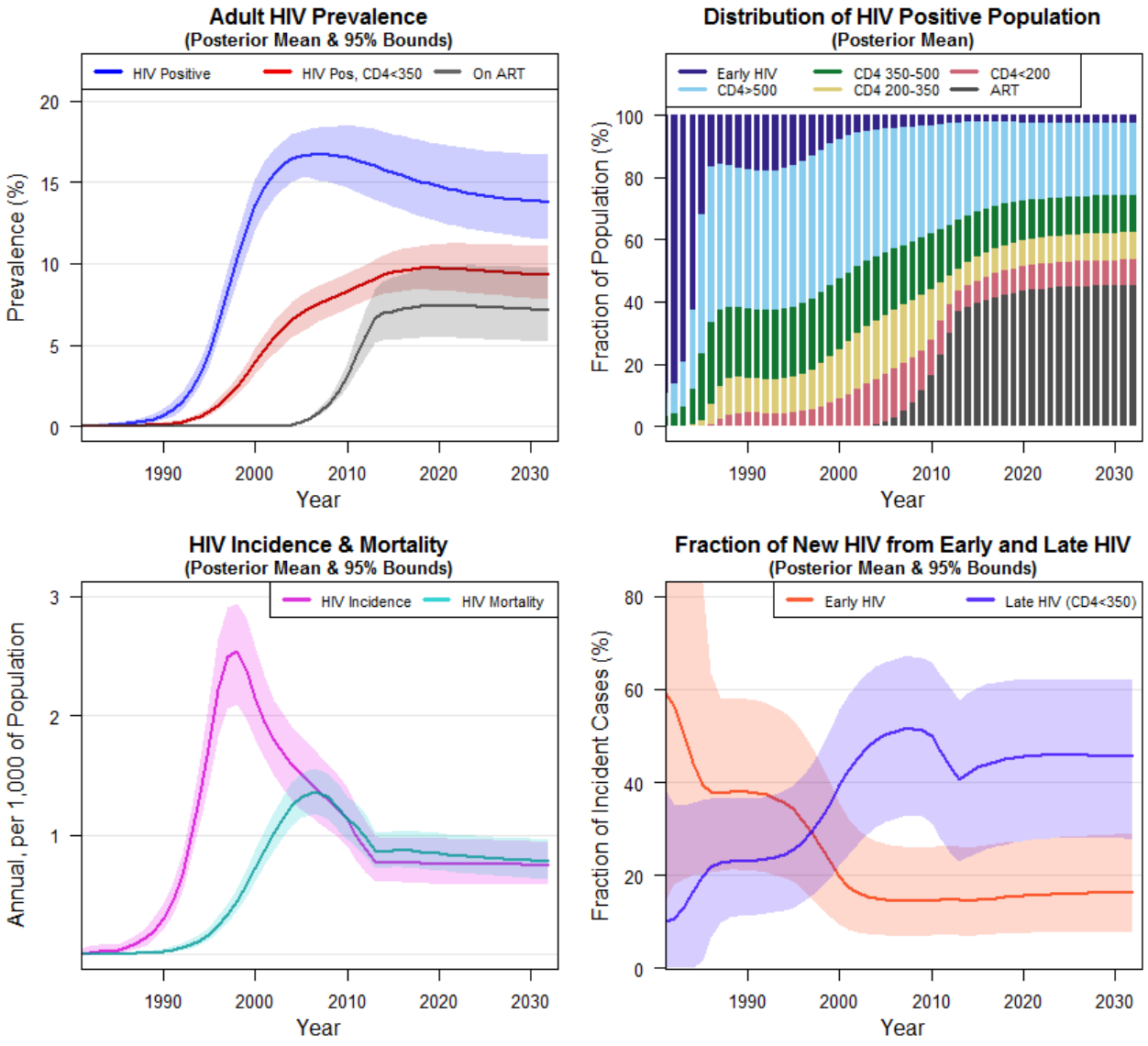

Figure 3.7. Epidemiological outcomes, 1985-2032, with current ART eligibility and coverage policy

The top left panel of this figure shows the rapid increase in HIV prevalence between 1990 and 2005, followed by a delayed and more gradual rise in the HIV population with CD4 cell count <350 cells/μL, the current ART eligibility threshold. The numbers of individuals receiving ART rises rapidly from 2005 to 2012 but subsequently plateaus as the majority of eligible individuals are initiated on treatment. The top right panel shows time changes in the distribution of the HIV-

positive population across CD4 cell count categories, initially dominated by early HIV during the early exponential growth of the epidemic, then with increasing numbers of individuals with low CD4 cell count as the epidemic matures. The bottom left panel shows HIV incidence and HIV mortality (defined as deaths of HIV-positive individuals), revealing the large lag in HIV mortality until 2005, after which the two curves move together, matching the rapid rise and subsequent plateau in HIV prevalence seen in the top right panel. The lower right panel explores the contributions of early and late HIV infection to overall HIV transmission, revealing a transition from early in the epidemic where most transmission is from individuals with early HIV, to late in the epidemic where almost half of all transmission is from individuals with CD4<350 (transmission from individuals in other disease stages not shown). This panel also reveals substantial uncertainty in this distribution of transmission across disease states, suggesting that a wide variety of values are compatible with the calibration data. These results—with 15% (7-26)[12] of all current transmission from individuals with early HIV—can be compared to the analysis of Powers and colleagues, who found 38% (19-52) of all transmission in 2010 in Lilongwe Malawi to derive from individuals in their first 5 months following infection. The other modeled results for sub-Saharan Africa summarized by Cohen *et al*. [16] provide additional points of comparison, with the fraction of new infections attributable to early HIV ranging from 10-30% when the Powers result is excluded.

Figure 3.8 shows summary epidemiological outcomes after 5 and 20 years for each of the 15 policy options assessed in the analysis. The policies are labeled with a letter-number combination, with the letter indicating ART eligibility threshold ("A" for CD4<350, "B", for CD4<500, and "C" for all HIV-positive) and the number indicating coverage scenario ("1" for testing at current rates with fixed ART volume, "2" for testing at current rates, "3" for testing at 1.5x current rates, "4" for testing

[12] Ranges in parentheses represent equal-tailed 95% posterior intervals.

at 2x current rates, and “5” for testing at 3x current rates). Both cumulative incidence and cumulative mortality are seen to drop as coverage is expanded (holding eligibility constant), and as eligibility is expanded (holding coverage constant). The one exception to this relationship is in the set of policies where the number of ART slots is constrained to its 2012 level (policies A1, B1, C1). For these policies that assume a fixed capacity constraint on ART volume, an eligibility policy that expands ART eligibility to all HIV-positive individuals (policy C1) will reduce cumulative HIV incidence over 20 years to 5.9 (4.5-7.5) million individuals compared to 6.2 (4.8-7.8) new infections with current eligibility (policy A1), a 5.1% (1.9-10.1) reduction. However, this policy change would marginally increase cumulative HIV mortality over the same period, from 6.9 (5.5-8.4) to 7.0 (5.6-8.6) million, a 1.9% (-0.2-3.9) increase in total deaths, due to relatively healthy individuals crowding out symptomatic individuals from limited ART slots.

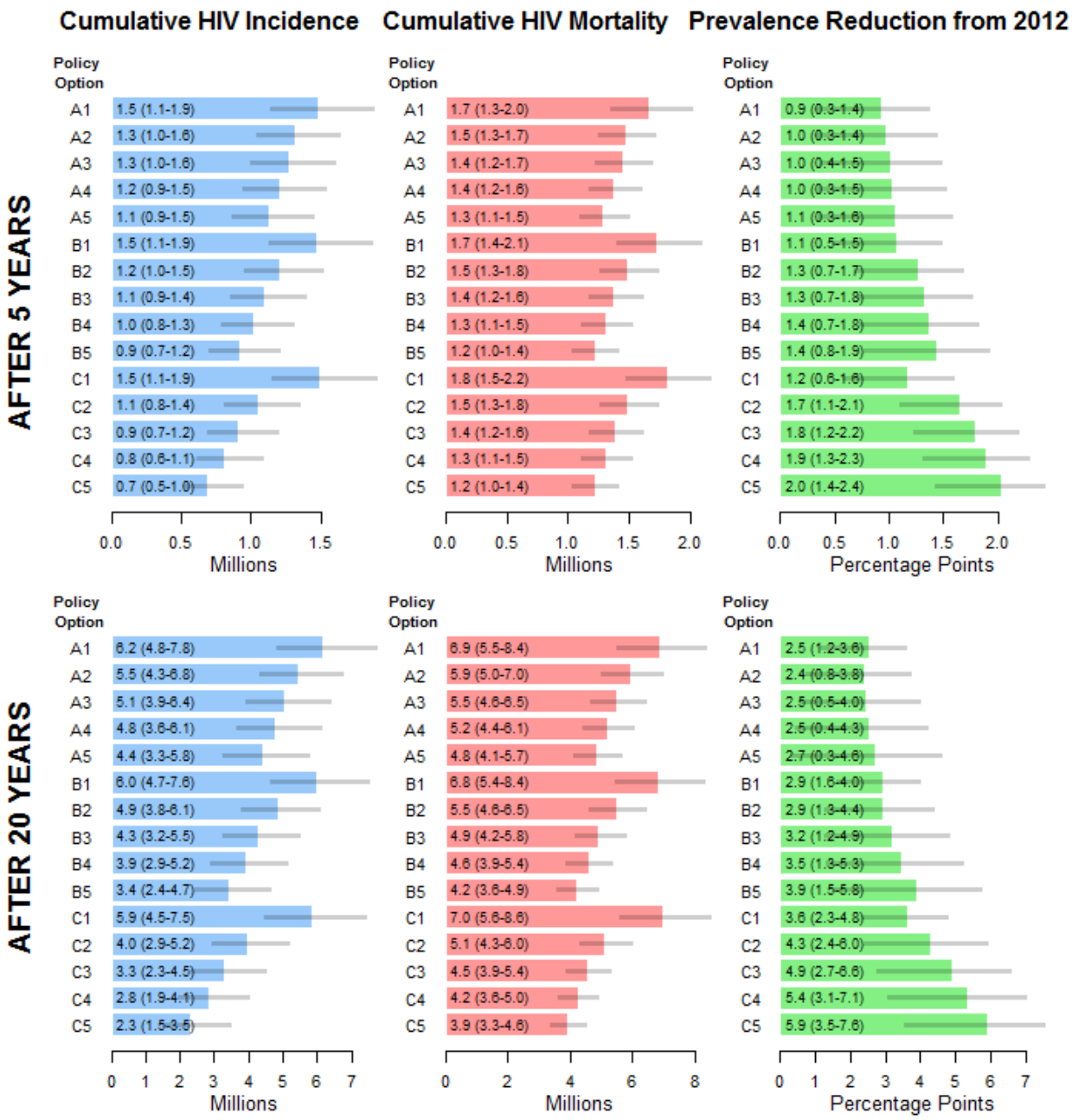

Figure 3.8. Major epidemiological outcomes at 5 and 20 years after policy introduction*

* Policies are labeled with a letter-number combination, with the letter indicating ART eligibility threshold ("A" for CD4<350, "B", for CD4<500, and "C" for all HIV-positive) and the number indicating coverage scenario ("1" for testing at current rates with fixed ART volume, "2" for testing at current rates, "3" for testing at 1.5x current rates, "4" for testing at 2x current rates, and "5" for testing at 3x current rates.

Over 20 years, compared to continuation of current eligibility and ART coverage (policy A2), the policy with most aggressive ART expansion (policy C5) is estimated to reduce cumulative HIV incidence by 3.1 million (2.4-3.9) new infections, a reduction of 58% (44-68), and reduce cumulative HIV mortality by 2.0 million (1.6-2.6), a reduction of 34% (29-38). The reductions in incidence and mortality that result from more aggressive eligibility and coverage policy will have countervailing effects on HIV prevalence. The third column of Figure 3.8, which shows the reduction in HIV prevalence compared to 2012 levels[13], suggests there would be a net reduction in prevalence as both ART eligibility and coverage are expanded, despite the improved survival of HIV-positive individuals initiated on ART. The most aggressive ART expansion policy (policy C5) is projected to reduce prevalence by 5.9% (3.5-7.6) between 2012 and 2032, as compared to 2.5% (1.2-3.6) for the current policy (policy A2).

Figure 3.9 shows the total DALYs averted by each policy, as compared to the status quo (policy A2). This figure presents results for the main analysis, when both preventive and therapeutic benefits of ART are taken into account, compared to a sensitivity analysis that considers only therapeutic health benefits by artificially holding HIV incidence equal for all policies. The fraction of total health benefits attributable to the therapeutic effects of ART are substantially higher under the truncated time horizon (representing all DALYs averted within the 20 year following policy introduction) as compared to the extended time horizon, which also includes lifetime health consequences for those alive at the end of the 20-year time horizon. This finding is consistent with the benefits of ART in averting transmission being substantially delayed relative to other outcomes, as newly infected individuals may live for many years (especially in an environment of good ART access) before the onset of substantial morbidity or early death. However, if these delayed health benefits are

[13] Prevalence in 2012 is estimated to be 16.2% [14.2-18.4].

considered, these results suggest the prevention benefits of ART are substantial compared to the therapeutic benefits. It is also notable that the fraction of total health benefits attributable to the therapeutic effect of ART are lower in policies that expand ART eligibility alone (e.g., under the truncated time horizon 63% of DALYs averted by policy C2 are attributable to therapeutic effects, and 34% under the extended time horizon), as compared to policies that expand coverage alone (e.g., under the truncated time horizon 89% of DALYs averted by policy A5 are attributable to therapeutic effects, and 49% under the extended time horizon). This suggests that the ratio of prevention benefits to therapeutic benefits will be higher for individuals initiating ART at higher CD4 cell counts, as compared to individuals initiating ART at low CD4 cell counts (i.e., early initiation of ART may be more important for preventing transmission than extending survival).

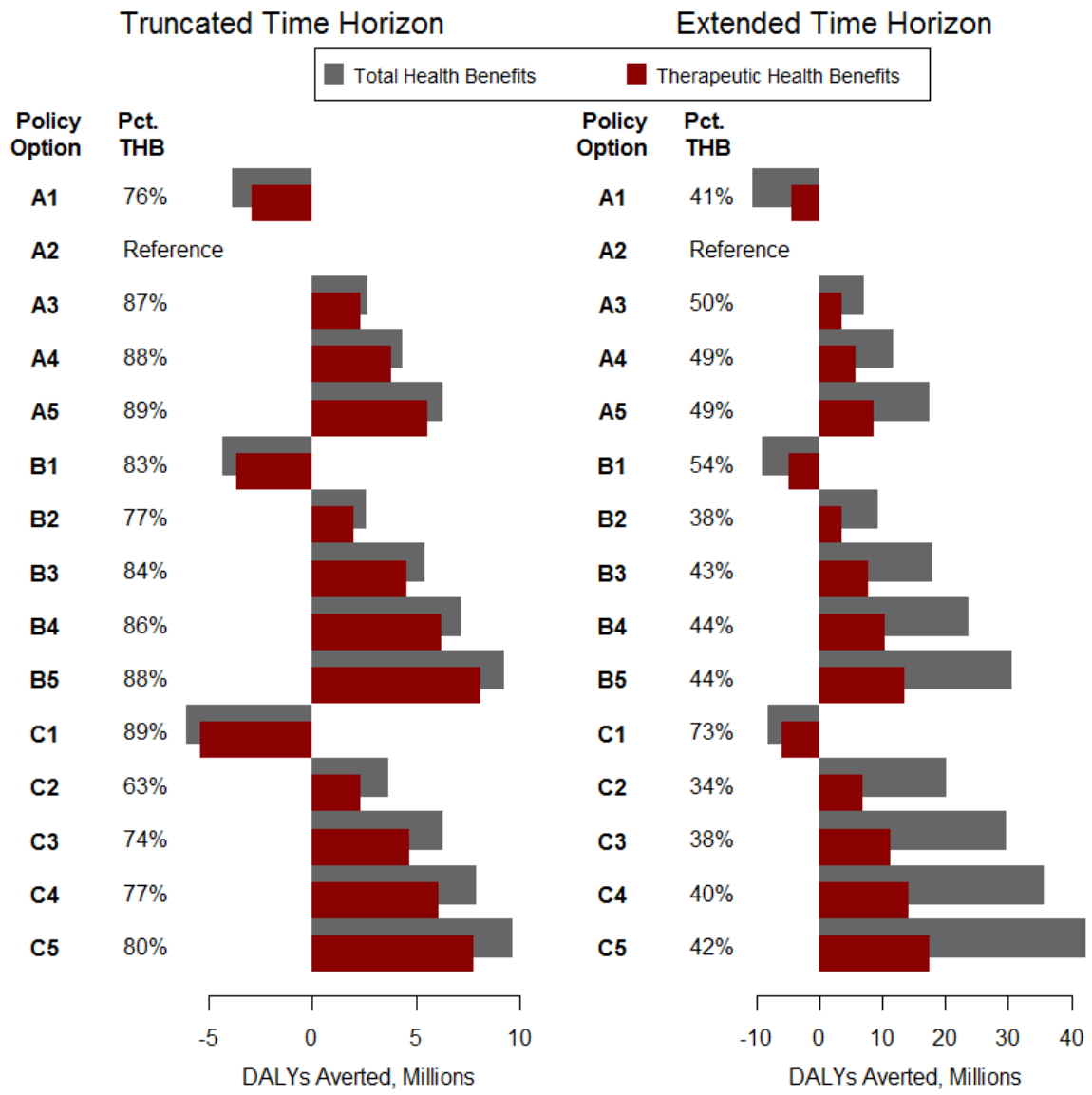

Figure 3.9. Total DALYs averted, and DALYs averted by therapeutic effects alone (i.e., excluding prevention benefits) for each policy compared to to policy A2*

* Policies are labeled with a letter-number combination, with the letter indicating ART eligibility threshold ("A" for CD4<350, "B", for CD4<500, and "C" for all HIV-positive) and the number indicating coverage scenario ("1" for testing at current rates with fixed ART volume, "2" for testing at current rates, "3" for testing at 1.5x current rates, "4" for testing at 2x current rates, and "5" for testing at 3x current rates. Estimates for DALYs averted from therapeutic health benefits alone are based on analyses where HIV infection risk is held constant at values generated by policy A2. 'Pct. IHB' represents the percentage of DALYs averted from therapeutic health benefits as compared to total health benefits (as calculated in the main analysis). Policy A2 used as the reference category.

3.3.2. Cost projections

The effect of changing policy on costs differed across cost categories. Figure 3.10 shows the incremental difference in mean annual costs over the period 2012-2032 for a subset of four policy options, in order to illustrate the effects of different types of policy as compared to continuation of current policy (A2).

Policy A1, in the top left panel of Figure 3.10, represents a very conservative approach to ART scale-up, with ART eligibility held at CD4<350 (as in the status quo), and with ART volume capped at 2012 levels. The cap on ART volume results in lower ART costs compared to the status quo (from both ARVs and non-ARV services), which are partially offset by increased pre-ART and other care costs (other care being care received outside of the HIV program). Policy C2, in the top right panel, is identical to the status quo except with greatly expanded ART eligibility (to all HIV-positive individuals), while policy A5, in the bottom left panel, is identical to the status quo except with greatly expanded ART coverage. Both changes result in higher overall costs. For policy C2, increased ART costs are partially offset by savings in pre-ART. In contrast, policy A5 results in increases in both ART and pre-ART costs, as well as large increases in testing costs, only modestly offset by savings in costs outside of the HIV program. These cost savings are realized because individuals with symptomatic HIV, who had previously been receiving care in the routine health system, would instead receive care through the HIV program (ART or pre-ART depending on eligibility). The combined effect of these factors is that the overall incremental costs under policy A5 appear much higher than policy C2 over all years (all panels use the same vertical scale). The lower right panel of Figure 3.8 shows the consequences of expanding HIV eligibility to include all HIV-positive individuals as well greatly expanded HIV testing programs (policy C5). Cumulative incremental costs are highest under this policy scenario, though the time trend in incremental costs

decreases after the initial years, potentially due to decreased long-term incidence trends compared to current policy.

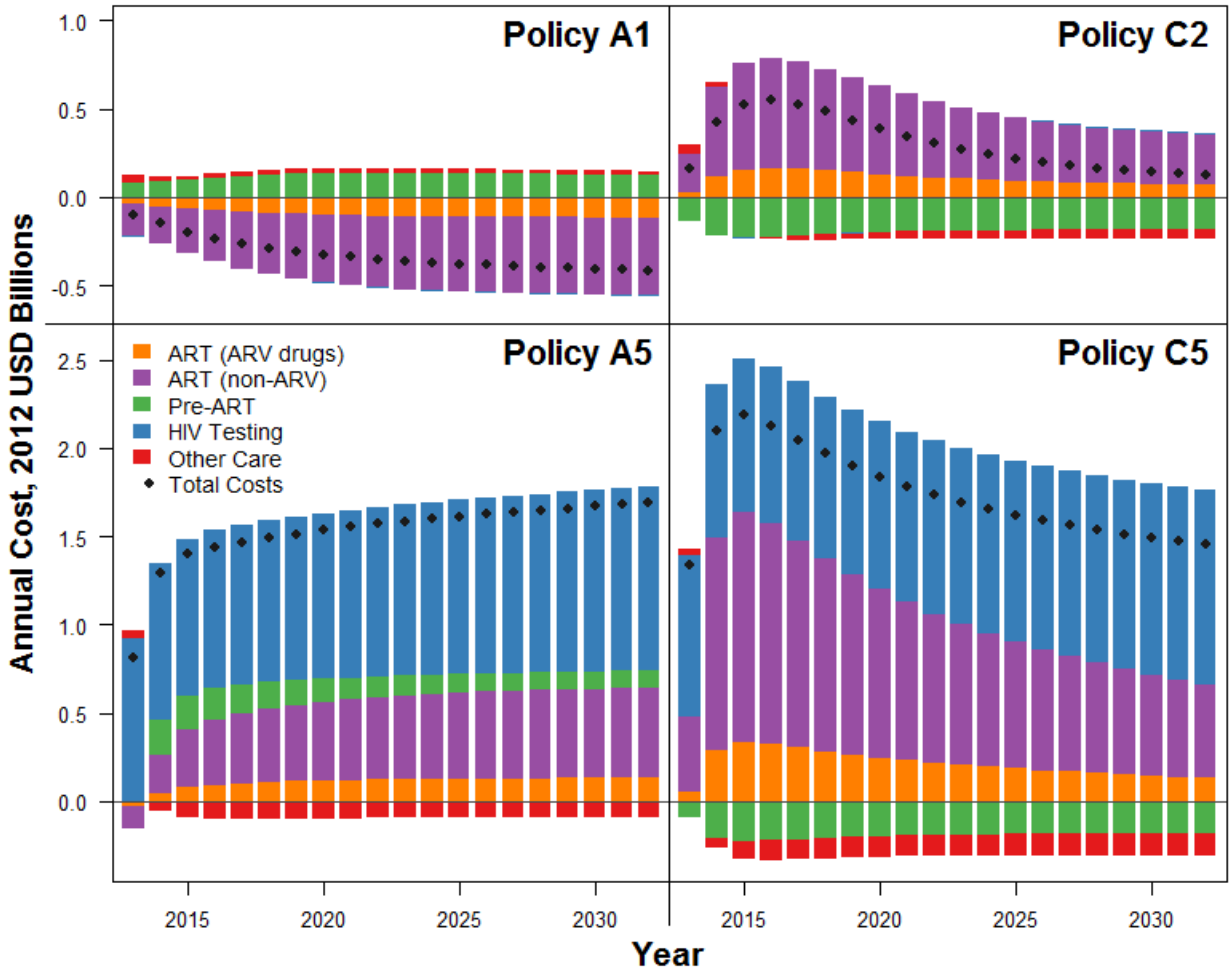

Figure 3.10. Disaggregation of total incremental costs by year and by cost category, for four policy options as compared to continuation of current eligibility and coverage (policy A2)*

* Policies are labeled with a letter-number combination, with the letter indicating ART eligibility threshold ("A" for CD4<350, "B", for CD4<500, and "C" for all HIV-positive) and the number indicating coverage scenario ("1" for testing at current rates with fixed ART volume, "2" for testing at current rates, "3" for testing at 1.5x current rates, "4" for testing at 2x current rates, and "5" for testing at 3x current rates.

Figure 3.11 presents summary estimates of total undiscounted costs for all policies over the 20 years since policy introduction, as compared to continuation of current eligibility and coverage (policy A2). As can be seen in the figure, those policies that assume ART volume is constrained at 2012 levels (policies A1, B1, and C1) produce cost-savings compared to the status quo, while policies that involve expanding eligibility and coverage result in higher overall costs. This is particularly true for increases in coverage (e.g., policy A5, lower left), whereas expansions in ART eligibility (e.g., policy C2, upper right) produce relatively modest increases in total costs over the whole 20 years.

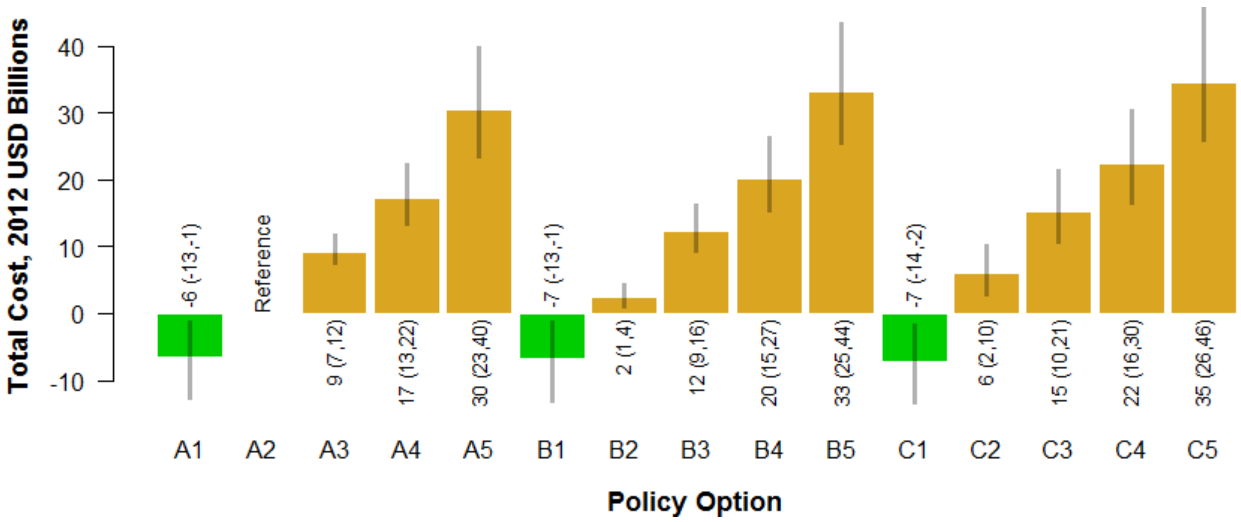

Figure 3.11. Summary estimates of total incremental costs over 20 years for competing policies, compared to continuation of current ART eligibility and coverage (policy A2)*

* Policies are labeled with a letter-number combination, with the letter indicating ART eligibility threshold ("A" for CD4<350, "B", for CD4<500, and "C" for all HIV-positive) and the number indicating coverage scenario ("1" for testing at current rates with fixed ART volume, "2" for testing at current rates, "3" for testing at 1.5x current rates, "4" for testing at 2x current rates, and "5" for testing at 3x current rates.

3.3.3. Decision-making with no new information

Absent the opportunity to seek or act on new information, decision uncertainty can be ignored and policy choices made based on the expected values of uncertain outcomes[14] [92,98–100]. Expected incremental costs (2012 US dollars, millions), health benefits (DALYs averted, millions) and incremental cost-effective ratios (ICERs) for competing ART policies are presented in Table 3.2, and cost-effectiveness results summarized graphically in Figure 3.12. All outcomes are discounted at 3% per year.

Results are presented for two time horizons: a truncated time horizon including only those costs and health outcomes realized within 20 years following policy introduction, and a extended time horizon that includes lifetime outcomes for all individuals alive at the end of the 20 year time horizon, in order to fully capture the value of reductions in mortality and HIV incidence (as described in Section 3.2.10).

[14] Following the assumptions described under Section 3.2.14.

Table 3.2. Incremental costs, DALYs averted, and cost-effectiveness ratios (US dollars per DALY averted) of competing policy options, assessed over both extended and truncated time horizons*

	Truncated time horizon: excludes health benefits and costs realized after 20 year horizon					Extended time horizon: includes health benefits and costs realized after 20 year horizon				
Policy Option	Cost	Inc. Cost	DALYs Averted	Inc. DALYs Averted	ICER	Cost	Inc. Cost	DALYs Averted	Inc. DALYs Averted	ICER
C1	---	---	---	---	---	---	---	---	---	---
B1	196	196	2.04	2.04	96	575	575	0.30	0.30	[1]
A1	407	211	2.60	0.56	380	1,135	1,135	-0.90	-0.90	[2]
A2	5,074	4,667	8.48	5.88	793	7,447	7,447	13.93	13.93	[1]
B2	6,897	1,823	10.30	1.82	1,004	9,063	9,063	22.15	22.15	[1]
C2	9,854	2,957	11.37	1.08	[1]	11,830	11,830	33.17	33.17	357
A3	11,800	4,903	10.88	0.59	[2]	15,010	3,176	21.28	-11.89	[2]
B3	14,320	7,421	13.65	3.36	2,210	17,110	5,279	32.06	-1.11	[2]
C3	16,840	2,522	14.55	0.90	2,805	19,110	7,284	43.85	10.68	682
A4	17,760	923	12.86	-1.69	[2]	21,450	2,339	26.66	-17.19	[2]
B4	20,220	3,379	15.70	1.15	[1]	23,290	4,181	38.37	-5.48	[2]
C4	22,350	5,515	16.45	1.90	2,902	24,700	5,585	50.35	6.50	859
A5	27,680	5,326	15.15	-1.30	[2]	31,870	7,169	33.08	-17.28	[2]
B5	30,030	7,672	18.04	1.59	[1]	33,310	8,611	45.86	-4.50	[2]
C5	31,640	9,281	18.59	2.13	4,350	33,950	9,253	57.75	7.40	1,251

[1] Dominated by extended dominance [2] Dominated by strong dominance

* Costs represent 2012 US dollars, both costs and outcomes are discounted at 3%. Policies are labeled with a letter-number combination, with the letter indicating ART eligibility threshold ("A" for CD4<350, "B", for CD4<500, and "C" for all HIV-positive) and the number indicating coverage scenario ("1" for testing at current rates with fixed ART volume, "2" for testing at current rates, "3" for testing at 1.5x current rates, "4" for testing at 2x current rates, and "5" for testing at 3x current rates.

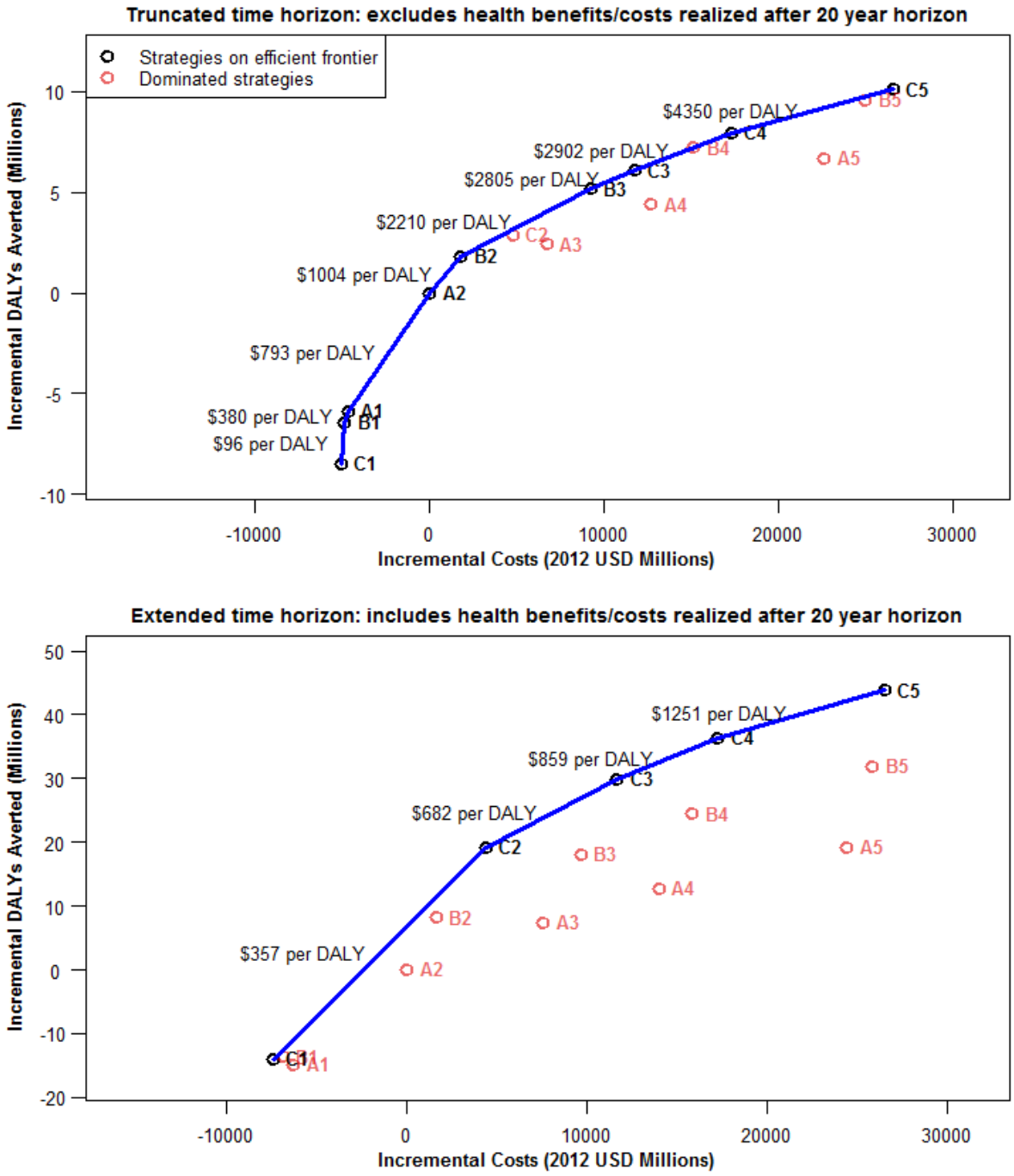

Figure 3.12. Cost-effectiveness of competing policies, assessed over extended and truncated time horizons*

* Policies are labeled with a letter-number combination, with the letter indicating ART eligibility threshold ("A" for CD4<350, "B", for CD4<500, and "C" for all HIV-positive) and the number indicating coverage scenario ("1" for testing at current rates with fixed ART volume, "2" for testing at current rates, "3" for 1.5x current rates, "4" for 2x current rates, and "5" for 3x current rates.

Figure 3.12 shows that, under the truncated time horizon (top panel), a large number of eligibility-coverage combinations lie on the efficient frontier. However, under the extended time horizon (bottom panel) it appears that policies that allow ART eligibility for all HIV-positive individuals (policies C1-C5) together dominate the other policies. The relative impacts of expanding coverage and expanding eligibility are shown in Figure 3.13, which plots the progression of costs and health benefits as eligibility is expanded under each coverage policy (top panels), and as coverage is expanded under each eligibility policy (bottom panels). For example, the base of the blue arrow in the lower panels represents a policy with ART eligibility at CD4<500 and a fixed cap on ART volume (policy B1). Following the arrow towards the tip represents the change in costs and health outcomes as coverage policy is progressively expanded while eligibility policy is fixed at CD4<500, to the point where the tip of the arrow represents policy B5, with ART eligibility still at CD4<500 but with very aggressive HIV testing programs.

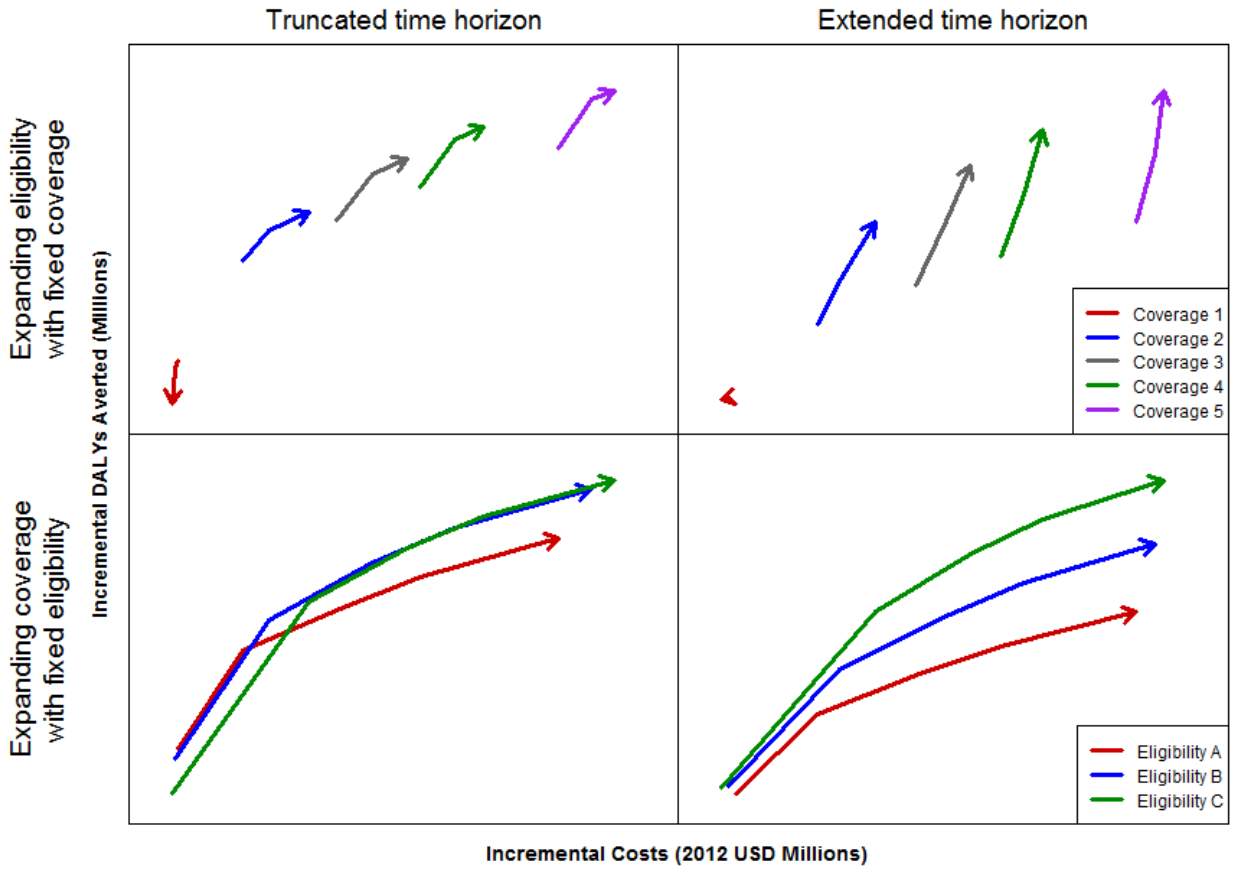

Figure 3.13. Change in costs and health benefits as one policy dimension is expanded while the other is held fixed, for both truncated and extended time horizons*

* Policy dimensions are labeled with letters and numbers, with the letter indicating ART eligibility threshold ("A" for CD4<350, "B", for CD4<500, and "C" for all HIV-positive) and the number indicating coverage scenario ("1" for testing at current rates with fixed ART volume, "2" for testing at current rates, "3" for 1.5x current rates, "4" for 2x current rates, and "5" for 3x current rates.

Under the truncated time horizon (panels on left), expansions in both eligibility and coverage have approximately similar slopes, and both exhibit decreasing returns to continued expansion, though

the magnitude of effects is greater with coverage expansion[15]. In contrast, under the extended time horizon (panels on right) expansions in coverage appear to produce substantially greater health gain per unit expenditure, without evidence of decreasing returns. The difference in results between the two time horizons can be linked back to the 20-year prevalence results shown in Figure 3.8, where policies expanding ART eligibility to all HIV-positive individuals (policies C1-C5) appear most effective at reducing prevalence relative to the other policies, mainly as a result of the incidence reductions associated with these policies. Reducing incidence is particularly influential in this extended time horizon, with each averted HIV infection producing substantial benefits in both cost savings and DALYs averted. The exact magnitude of these benefits will depend on the eligibility and coverage policy in place, but at one extreme in a scenario with no access to HIV-specific care or treatment the consequence would be 17.0 (16.1-17.7) DALYs averted and $825 (680-1019) in cost savings for each infection averted (discounted from the time the infection is averted). At the other extreme, in a scenario with immediate access to ART for all HIV-positive individuals, the consequences of preventing one HIV infection would be 3.5 (2.3-5.6) DALYs averted and $15,400 (12,000-19,400) in cost-savings for each infection averted[16]. In either case the benefits of incidence reduction are substantial, and only fully realized under the extended time horizon. This reinforces the findings shown in Figure 3.9, which compares the therapeutic and total benefits of ART under different time horizons.

---

[15] Expanding eligibility with constrained ART volume (policies A1, B1, and C1) behaves differently, with results reflecting the increased competition for ART slots as increasingly health individuals become ART-eligible.

[16] These results are obtained by comparing discounted lifetime costs and health benefits for a newly infected HIV-positive individual with the same outcomes calculated for an HIV-negative individual, under different health care access scenarios.

Given that the consequences of ART policy change accumulate over many years, the choice of discount rate could be influential for decision-making. Figure 3.14 shows the cost-effectiveness of competing policies under different discounting schemes. In the top panel, the use of a 0% discount rate implies that equal weight is given to all outcomes independent of when they occur. In contrast, the middle panel shows results calculated with a 6% discount rate, greatly down-weighting the value of consequences occurring many years in the future. Perhaps surprisingly, there is little change in the policies appearing on the efficient frontier under either scenario, or their ordering. However, the cost-effectiveness ratios for a given policy comparison are substantially higher as the discount rate increases (for example, under the extended time horizon the ICER for moving to policy C3 from policy C2 is 3.7 times larger with the 6% discount rate as compared to no discounting). This finding results from the health benefits of expanded ART access being experienced substantially later than the costs incurred to produce them. For a decision maker with a high rate of time preference, these results suggest that a more conservative approach to ART expansion will be optimal for a given willingness-to-pay for health benefits.

The lower panel of Figure 3.14 describes the cost-effectiveness of competing policies in a scenario where costs are discounted at a conventional 3% discount rate while health benefits are undiscounted. To present health benefits undiscounted is consistent with recent methodological changes made by the Global Burden of Disease Study that developed DALYs [91]. Perhaps more importantly, to discount costs but not health benefits implies that the relative value of averting a DALY increases by 3.1% each year. While this assumption might be implausible in a stable economy, it can be justified in the context of economic growth [101]. If one accepts that the marginal utility of averting DALYs is constant as the overall level of health increases, while the marginal utility of other consumption is decreasing, an increasing share of overall consumption should be devoted to averting DALYs as an economy grows (in per-capita terms). Per-capita GDP in South Africa rose at an average annual rate of 6% between 1960 and 2012, and 12% over the last

10 years [102]. It is not clear that the potential continuation of these growth rates supports a 3.1% annual increase in the value of averting DALYs, but it is not impossible. As with other sensitivity analyses shown in this figure, this discounting approach leads to little change in the identity and ordering of the policies on the efficient frontier, but does produce a substantial reduction in the ICERs for a given policy comparison. If a decision maker were to hold beliefs and preferences consistent with this discounting scheme, these results suggest that a more aggressive approach to ART expansion will be optimal for a given willingness-to-pay for health benefits.

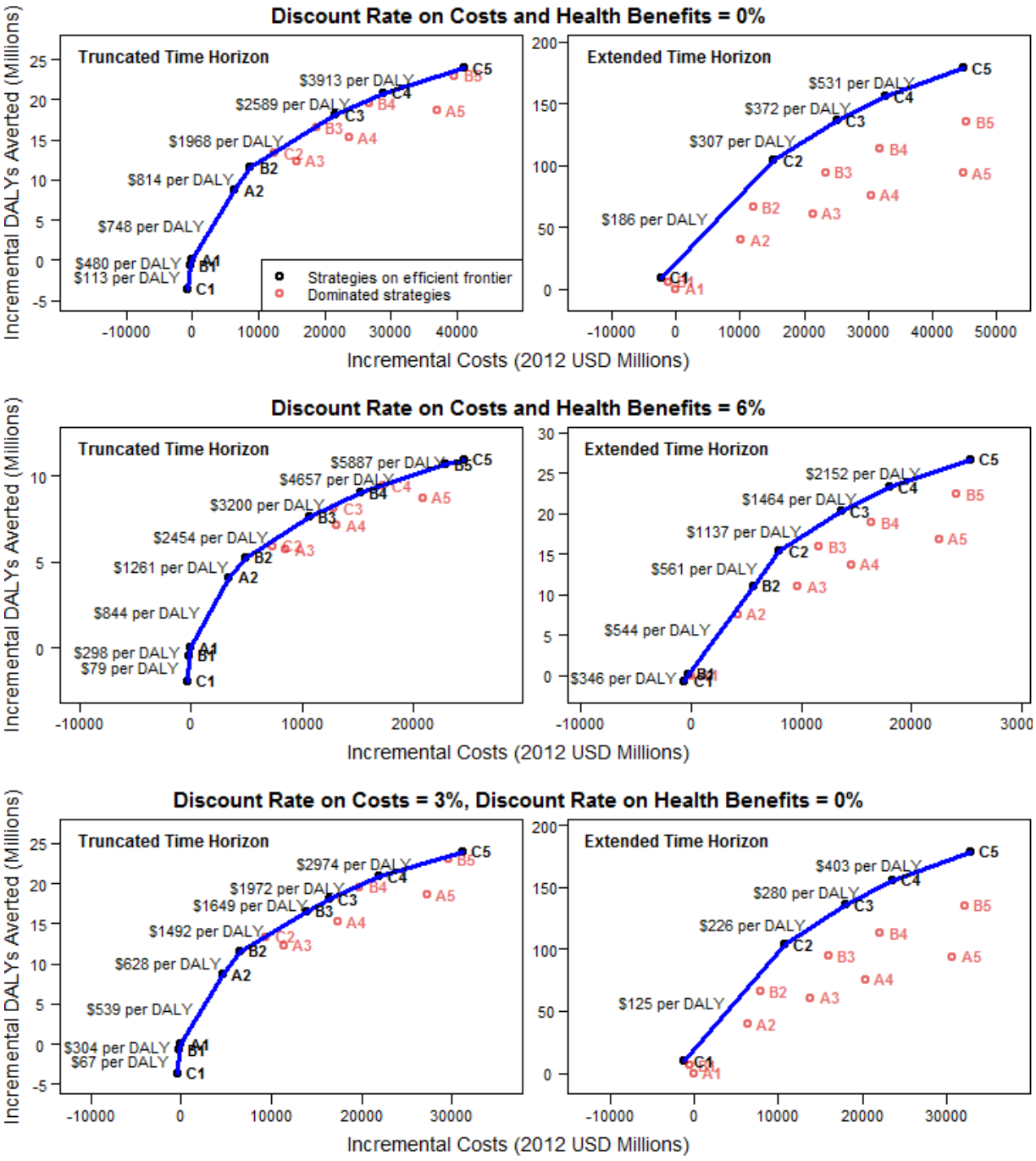

Figure 3.14. Cost-effectiveness of competing policies with different discount rates applied to future costs and health benefits*

* Policies are labeled with a letter-number combination, with the letter indicating ART eligibility threshold ("A" for CD4<350, "B", for CD4<500, and "C" for all HIV-positive) and the number indicating coverage scenario ("1" for testing at current rates with fixed ART volume, "2" for testing at current rates, "3" for 1.5x current rates, "4" for 2x current rates, and "5" for 3x current rates.

3.3.4. Decision uncertainty

The cost-effectiveness results described above specify the optimal policy choice for a given WTP threshold. Cost-effectiveness acceptability curves (CEACs) are one approach to understanding the uncertainty in these results, plotting the probability that each policy is optimal as a function of the WTP threshold [103]. Figure 3.15 presents CEACs for both truncated and extended time horizons. These plots reinforce the finding of Section 3.3.3 – that while a multitude of policies have non-negligible probability of being optimal under the truncated time horizon, the policies with eligibility for all HIV-positive individuals appear to be optimal with high probability under the extended time horizon.

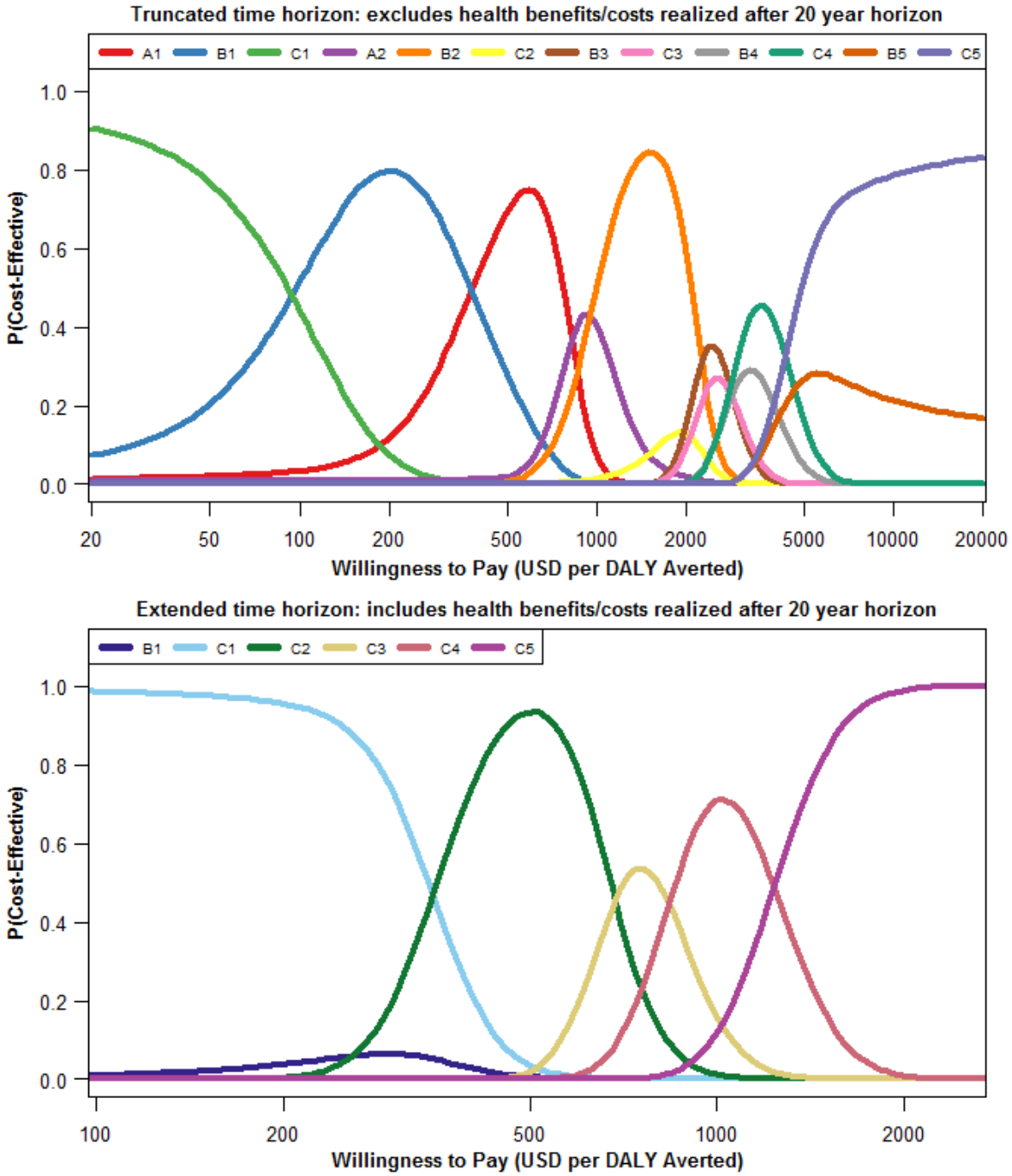

Figure 3.15. Cost-effectiveness acceptability curves for competing policies*

* Policies with P(Cost-Effective)<0.05 are not shown. Policies are labeled with a letter-number combination, with the letter indicating ART eligibility threshold ("A" for CD4<350, "B", for CD4<500, and "C" for all HIV-positive) and the number indicating coverage scenario ("1" for testing at current rates with fixed ART volume, "2" for testing at current rates, "3" for 1.5x current rates, "4" for 2x current rates, and "5" for 3x current rates.

The CEACs also provide information relevant to the value of information. Under the framework adopted for the VOI analysis, information is only valuable to the extent that it allows decision makers to choose a policy that they would previously have avoided, such that a policy appearing sub-optimal with prior information is proven optimal once new information is obtained. If, based on prior information, we know that there is no chance that collecting new information will lead us to change our policy decision, then there is no value to new research. This appears to be the case for all but a narrow band of WTP values under the extended time horizon, where if WTP is less than ~$100 per DALY averted, or greater than ~$2,000 per DALY averted, the policy deemed optimal based on expected values is almost certain to be cost-effective were full information available. In contrast, under the truncated time horizon there is substantial uncertainty as to the optimal policy over a wide range of WTP values.

3.3.5. Value of information

3.3.5.1. Expected value of perfect information

Figure 3.16 plots the expected value of perfect information—the net monetary benefit that would be obtained through complete resolution of all decision uncertainty—as a function of WTP. While not providing information on how to direct new research, the EVPI results show that there is potential for substantial value from new research that would reduce decision uncertainty. As noted earlier, under the extended time horizon this possibility is limited to situations where WTP is less than $2,000 per DALY averted.

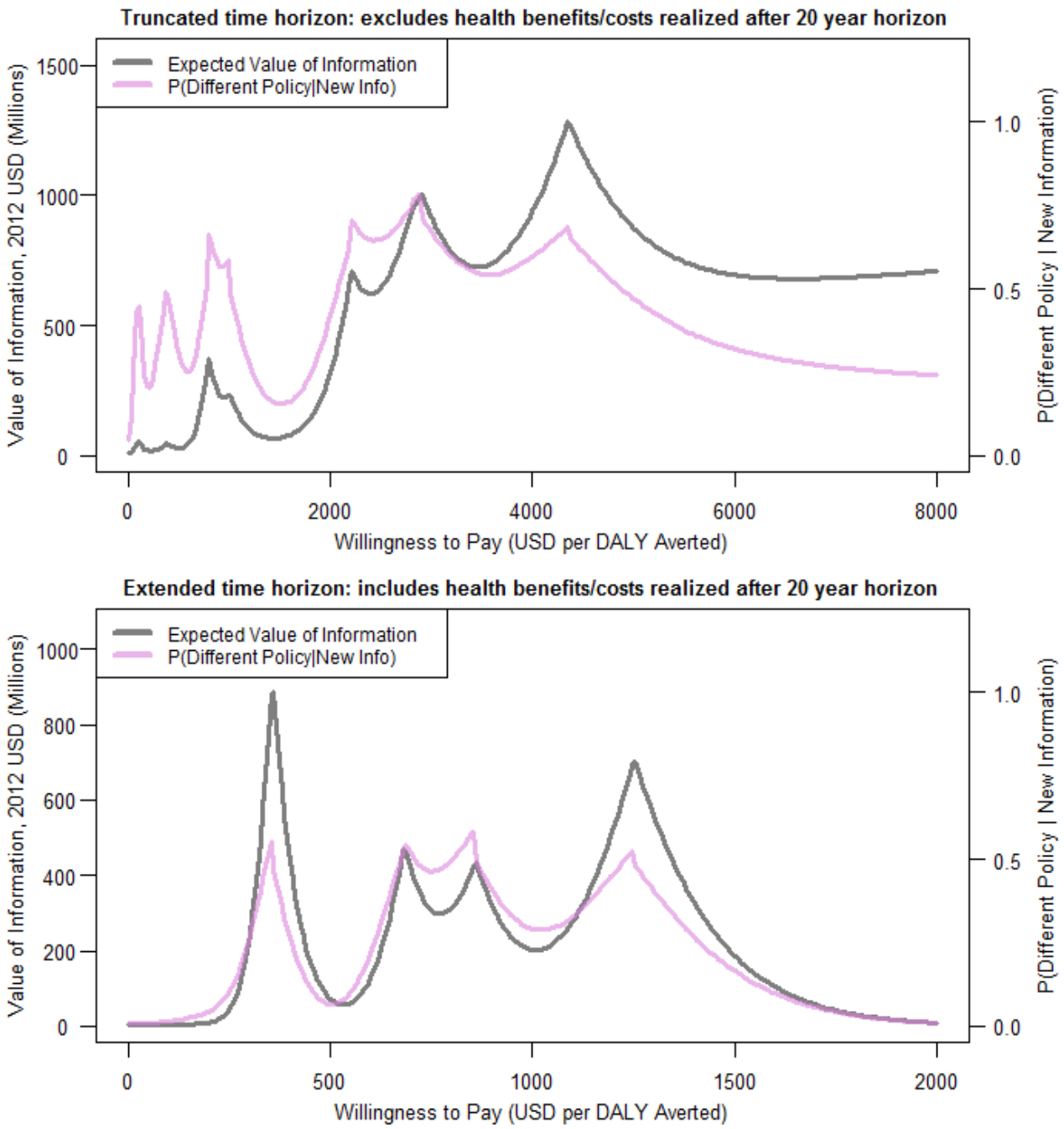

Figure 3.16. Value of perfect information, and probability that new information will lead to a different policy being chosen, as a function of willingness-to-pay and under truncated and extended time horizons

3.3.5.2. Expected value of partial perfect information

Figure 3.17 presents the expected value of partial perfect information (EVPPI) for selected individual model parameters. The figure shows the ten parameters with the highest EVPPI values as well as the relative transmission risk for early HIV (not in the top 10), given pre-specified interest in this parameter. EVPPI provides information on the value of resolving all uncertainty around a particular parameter, and in this analysis is used to understand the relative value of competing research targets. Though findings differ depending on the time horizon, parameters related to service provision (unit costs, default rates) are prominent. Parameters relating to HIV transmission risks do appear in the top ten, though the relative transmission risk associated with early HIV does not (but is included in the figure for purposes of comparison). Also notable from these results is the critical importance of the WTP threshold both for the absolute VOI as well as the relative ranking of different parameters. This feature results from characteristics of the policies that have non-zero probability of being optimal at a given WTP threshold (these probabilities are plotted in Figure 3.16). The local maxima observed in Figure 3.17 generally correspond to WTP values where two policies are equally optimal on expectation. For example the first major set of peaks under the extended time horizon occur at a WTP of $357, which is the threshold between policies C1 and C2 (representing a change in policy from fixed ART volume to a policy of continued ART scale-up based on current testing volume, with all individuals eligible for ART) being optimal (on expectation). At this point, EVPPI is highest for non-ARV ART costs, the relative transmission risk associated with ART, and pre-ART costs, suggesting the incremental difference between E(NMB) for C1 and C2 is most sensitive to these parameters. In contrast, the choice between policy C4 and C5 (raising the rate of HIV testing to very high levels, with all individuals eligible for ART), represented by the peaks at $1,251, appears most sensitive to HIV testing costs, the multiplier on costs to account for programmatic support, and the probability of primary default following HIV testing.

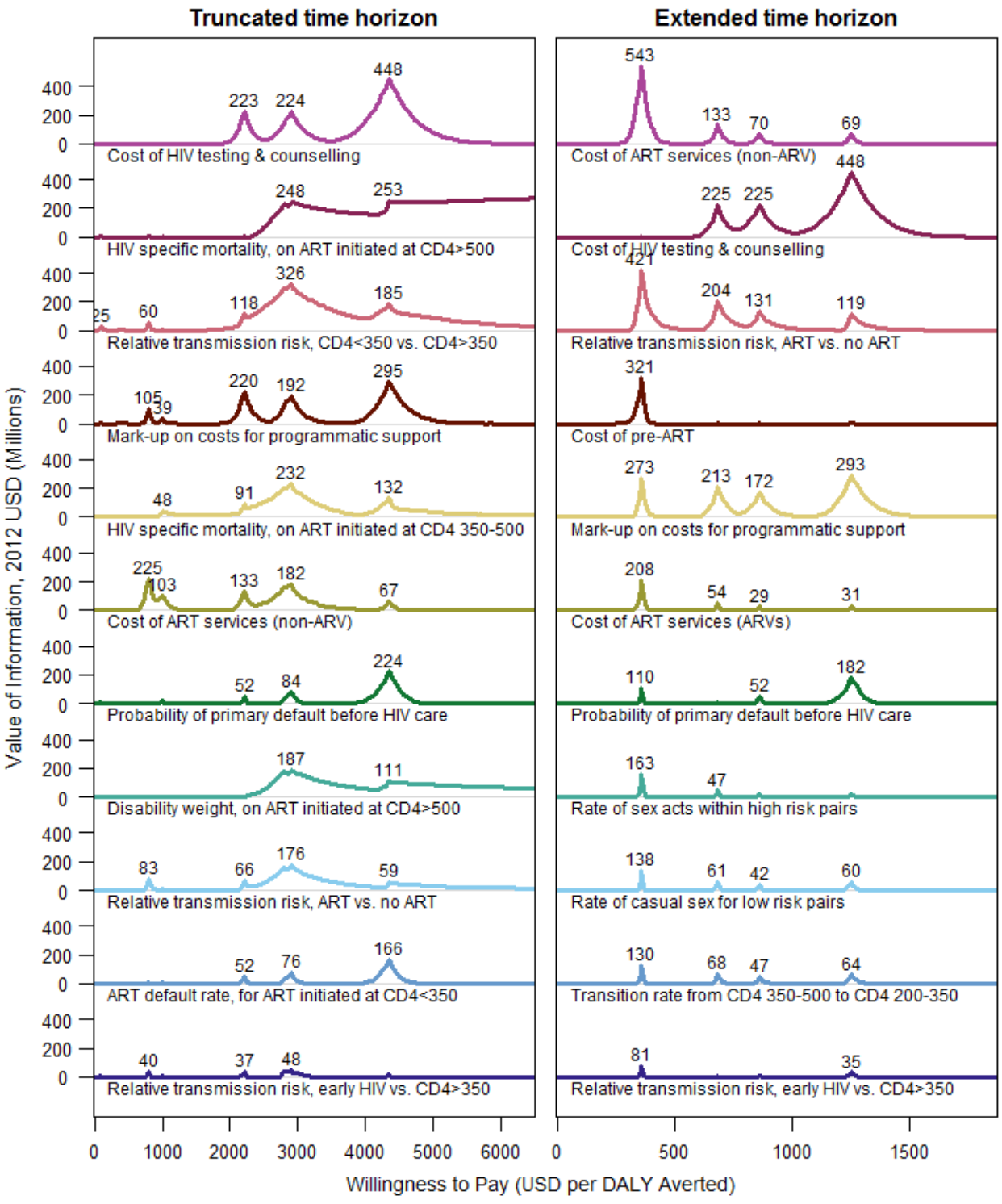

Figure 3.17. Expected value of partial perfect information for individual model parameters

While Figure 3.17 describes VOI for individual parameters, it is likely that some research designs would inform multiple parameters simultaneously. This is particularly true of research on relative infectiousness during different disease stages. Earlier work has described how the sum of VOI calculated for individual parameters is not necessarily equal to the joint VOI for the group of parameters [22], which could be either sub- or super-additive depending on the context. For this reason further analyses were undertaken to estimate EVPPI for the group of parameters relating to relative infectiousness during different disease stages (relative transmission risk for early HIV vs. CD4>350, relative transmission risk for CD4<350 vs. CD4>350, and relative transmission risk for ART vs. no ART). These results are shown in Figure 3.18, along with VOI results for these parameters individually. The joint EVPPI for all three parameters is superimposed on top of the naïve sum of EVPPI for the three parameters individually, showing that VOI of the individual parameters is approximately additive, though appears to be super-additive for WTP values where two policies are equally optimal on expectation (and decision uncertainty high), and sub-additive otherwise. It is also clear from the figure that while there would be substantial VOI from resolving uncertainty around relative transmission risk during later-stage HIV (CD4<350) and while on ART, there is comparatively little value in further improving our understanding of relative infectiousness during early HIV.

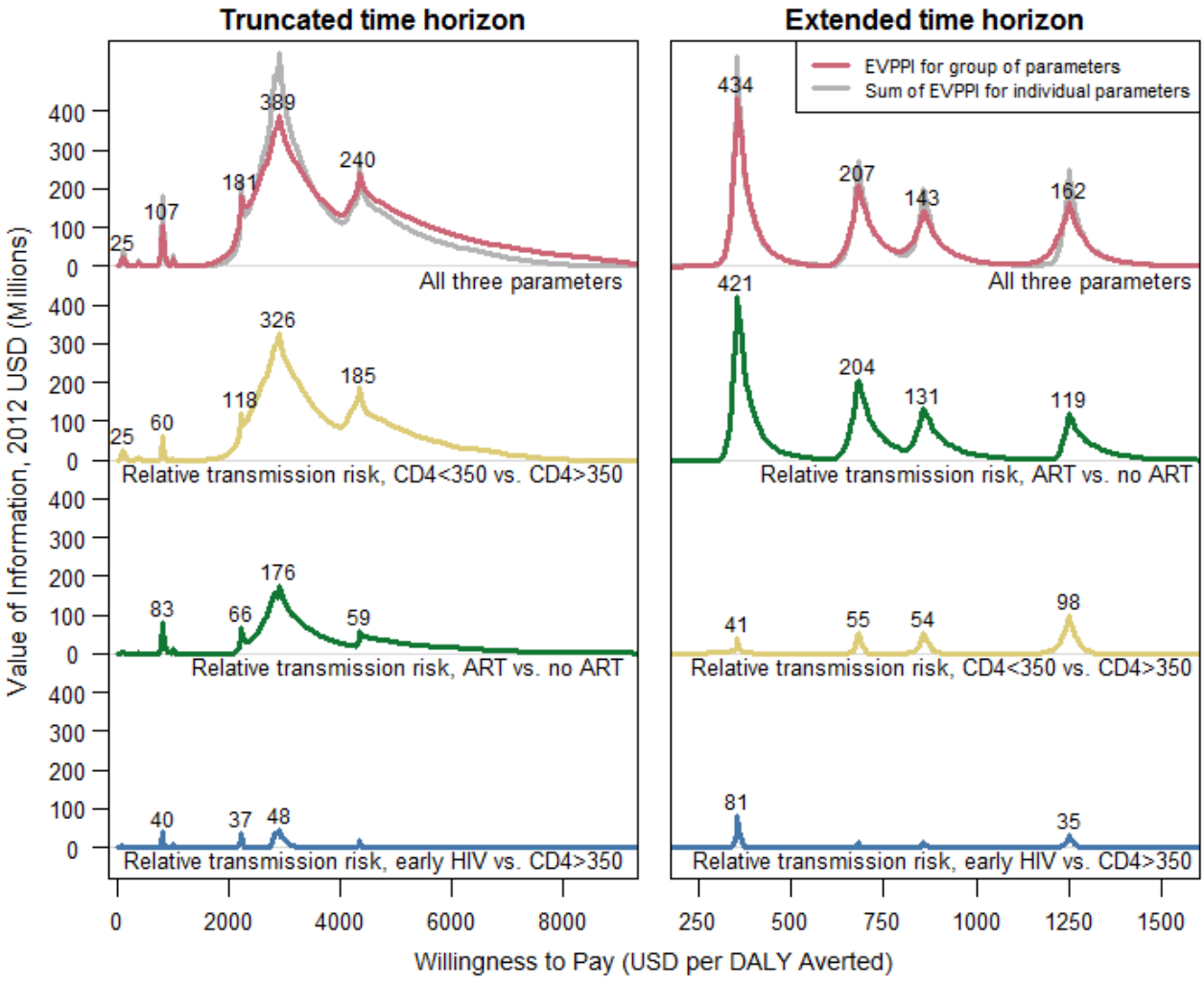

Figure 3.18. Expected value of partial perfect information on relative infectiousness by disease stage

Describing VOI as a function of WTP provides insight into the relationship between VOI and the specific policies with a positive probability of being optimal at a given WTP threshold, and highlights the importance of WTP to both absolute VOI and the relative importance of different parameters. However, it is also useful to summarize results based on current understanding of WTP in this setting. There is currently a poor understanding about WTP for health gains in developing countries such as South Africa, and active discussion is occurring regarding the criteria upon which WTP estimates should be based [104]. If WTP estimates are based on our understanding about

what countries *should* be willing to pay to improve health, a number of international agencies suggest thresholds based on small multiples of per capita GDP or GNI [105–107]. The most commonly cited of these are the thresholds proposed by the WHO-CHOICE initiative, suggesting 1x per capita GDP per DALY averted as an upper bound for interventions to be described as '*very cost-effective*', and 3x per capita GDP per DALY averted as an upper bound for interventions to be described as '*cost-effective*' [107]. For South Africa, these thresholds would be $7,500 and $22,500 respectively, based on per capita GDP in 2012 [108][17]. In contrast, thresholds motivated by concepts of affordability tend to be lower, reflecting that fact that total spending on health is often less than might be suggested by the GDP based thresholds described above [109]. Earlier World Bank and WHO publications have suggested thresholds of US$100 per DALY averted as an upper bound for describing '*highly attractive interventions*', and US$500 per DALY averted for describing '*attractive interventions*' in middle-income countries such as South Africa [110,111]. While inflation, economic growth, and the expansion of donor-funded health aid would suggest a threshold based on affordability concerns may be higher today, it is still likely that affordability and budgetary concerns will impose additional constraints, and dictate a lower WTP than that suggested by the WHO-CHOICE per-capita GDP approach. Given this uncertainty, summary results were calculated by assuming WTP would fall somewhere between $0 and $7,500 per DALY averted, with all values within this region being equally probable. The ten parameters for which EVPPI is highest by this approach are shown in Figure 3.19, for both truncated and extended time horizons. Included in this ranking is the joint EVPPI for the three parameters for relative transmission risk by disease stage.

[17] The WHO-CHOICE thresholds were originally described in terms of *international* dollars per DALY averted, reflecting concerns about purchasing power parity when regional thresholds are used. However, within a single country setting the calculation of both threshold and ICERs in US dollars (or other monetary unit) represents a simple currency conversion and does not affect the decision-making in any way.

While absolute values are shown in this figure, these values should be interpreted as upper bounds to the value of any research, given the impossibility of resolving all uncertainty around a particular parameter.

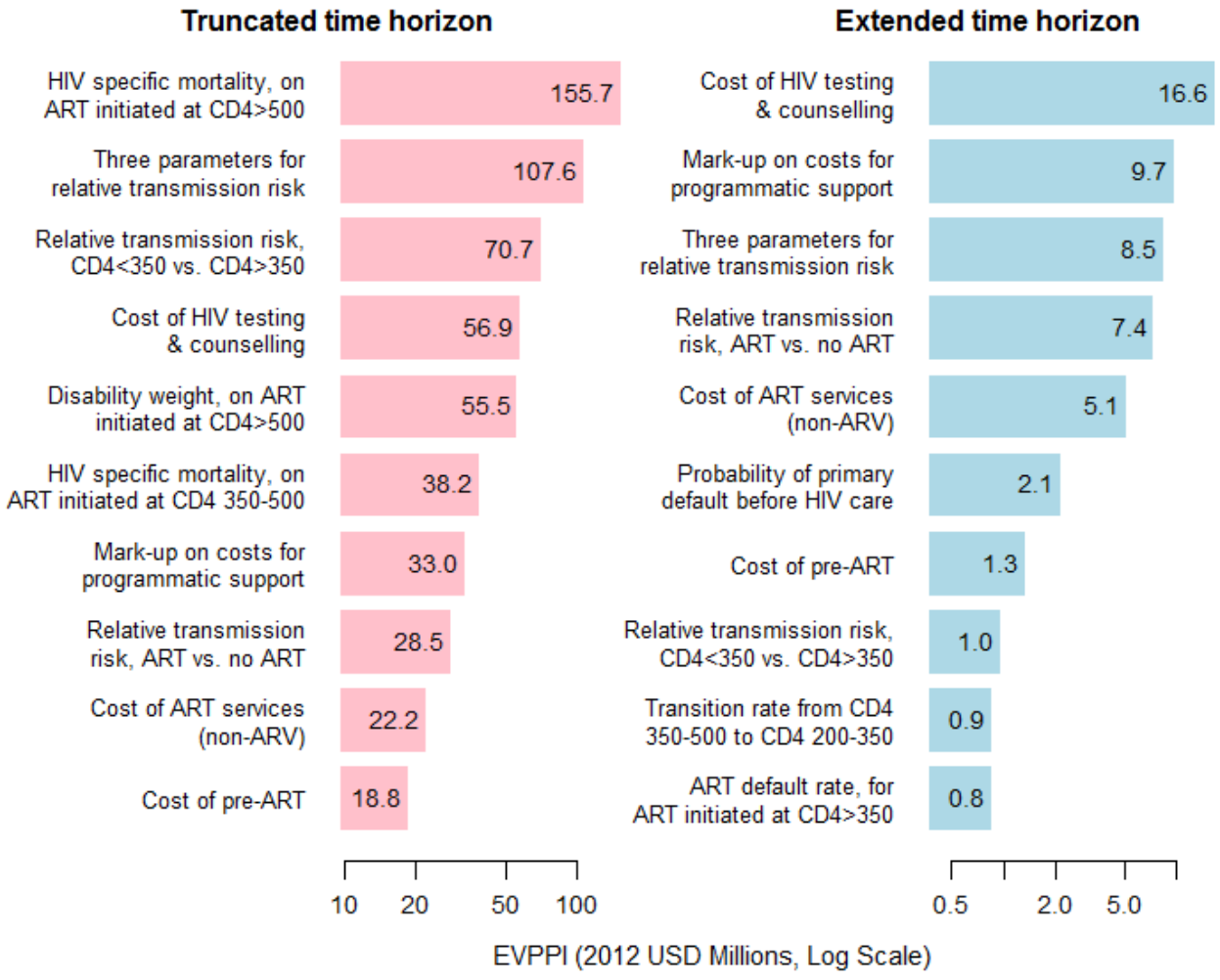

Figure 3.19. Expected value of partial perfect information, summary rankings

The results shown in Figure 3.19 generally confirm the findings reported in earlier figures, with parameters related to cost and service provision figuring prominently. The relative importance of resolving uncertainty around the three transmission risk parameters appears to be high (rank 2nd under the truncated time horizon, 3rd under the extended time horizon), though given the results

shown in Figure 3.15, this value stems largely from the resolution of uncertainty around transmission risk during later HIV and while on ART, rather than during early HIV. For the individual parameter for relative transmission risk during early HIV, the ranking is 46 out of 71 under the truncated time horizon, and 27 out of 71 under the extended time horizon. In both cases this parameter accounts for approximately 1% of the value of information estimated for the most valuable research targets shown in Figure 3.19.

It is possible that the low EVPPI estimated for relative transmission risk during early HIV is a consequence of the relatively small fraction of new infections estimated to come from early HIV, as described under Figure 3.7. To test this possibility, a sensitivity analysis was undertaken in which the fraction of transmission attributable to early infection was increased to 25% (15-39%), approximately 1.7 times its value in the main analysis[18]. When the VOI results are recalculated for this new scenario, EVPPI for the relative transmission risk during early HIV increases by 50-100%. However, this change is not sufficient to change the overall finding that EVPPI of relative transmission risk during early HIV is comparatively low, and the higher value obtained in this sensitivity analysis is still 50 times smaller than the highest values shown in Figure 3.19.

Additional sensitivity analyses were undertaken to assess the robustness of the results to changes in the choice set, by rerunning the cost-effectiveness analysis and VOI analysis under the assumption that testing policy was fixed (i.e., the current approach would be continued), and that the only policy changes being considered involved expansions in eligibility (i.e., policies A2, B2, and C2).

---

[18] This change was achieved by recalibrating the model with an additional calibration target specified for the fraction of transmission attributable to early infection, as described in Section 3.2.16.4.

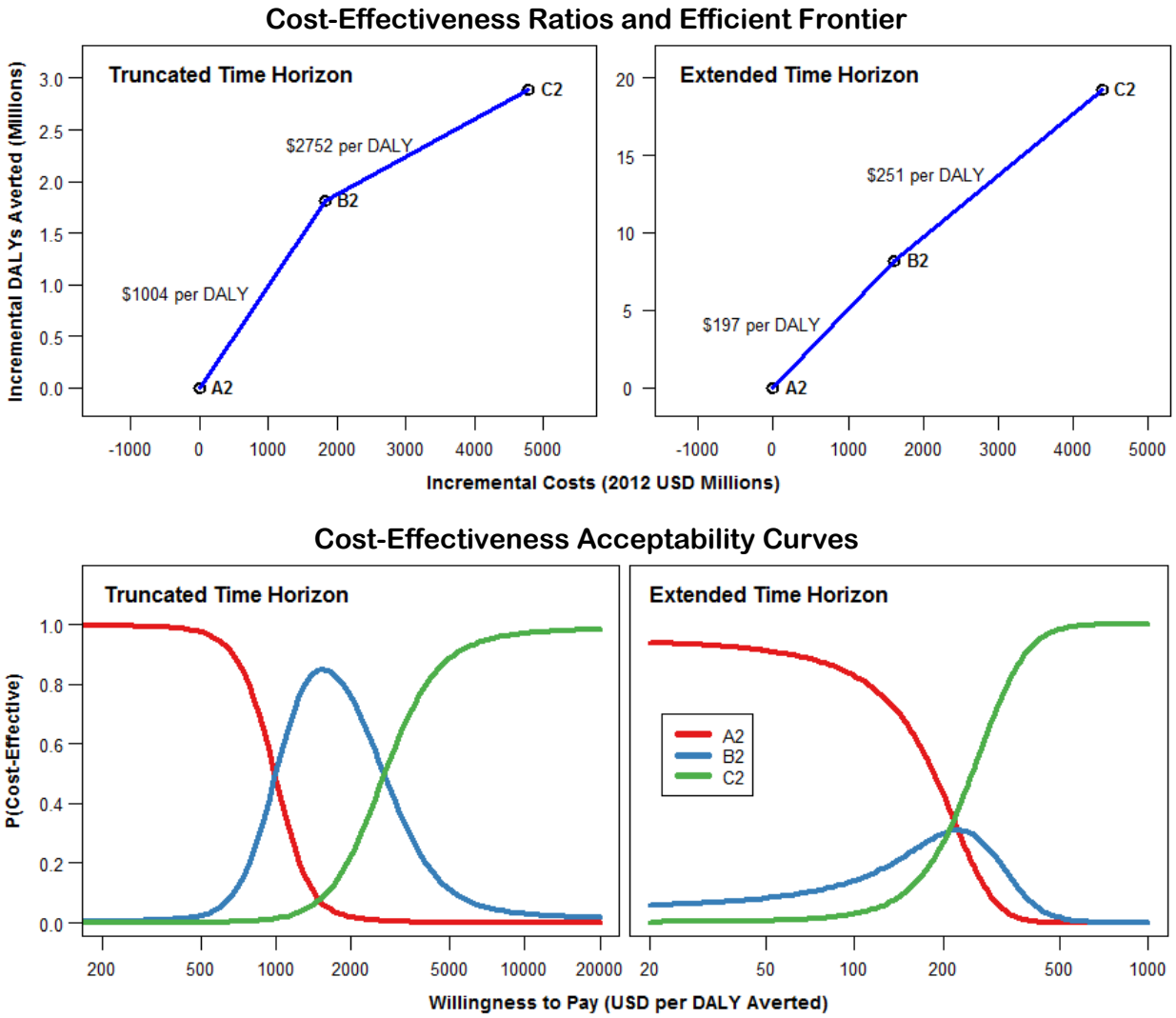

Figure 3.20. Cost-effectiveness results for a choice set including only policies A2, B2 and C2

The cost-effectiveness results obtained in this new analysis are shown in Figure 3.20, and the qualitative findings generally mirror those of the main analysis, though with all three policies now on the efficient frontier. EVPI results for this restricted choice set are shown in Figure 3.21 plotted as a function of WTP, and compared to the EVPI results obtained in the main analysis. As in that analysis, the local maxima coincide with WTP values where two policies appear equally optimal based on current information, and where new information would be most valuable for discerning

which policy is truly optimal. EVPI is generally lower if the choice set is restricted in this way (compared to the main analysis), and this can be understood by comparing the cost-effectiveness acceptability curves shown in Figures 3.15 and 3.20. In the main analysis (Figure 3.15) the range of WTP values where there is uncertainty as to the optimal policy is much wider, and the number of policies with a non-trivial probability of being optimal is larger. The VOI approach adopted for this analysis assumes that information is more valuable if it helps us resolve uncertainty about which policy will provide the best outcomes. A consequence of this approach is that greater decision uncertainty will lead to greater value of information, and this is relationship is reflected in the results of this sensitivity analysis. It should be noted that EVPI is not universally lower for the restricted choice set, as EVPI with the restricted choice set is higher under the extended time horizon if WTP is less than approximately $300 per DALY averted. In the main analysis under the extended time horizon, policy C1 (a fixed cap on ART scale-up with eligibility for all) is found to be optimal with high probability if WTP is less than $300 per DALY averted (Figure 3.15). In contrast, policy C1 is not available with the restricted choice set, and there is non-trivial uncertainty as to which of the three policies is optimal, particularly at a WTP of $200 per DALY averted, where all three policies have an approximately equal probability of being optimal. Thus the higher EVPI for the restricted choice in this particular context reinforces the relationship between decision uncertainty and VOI.

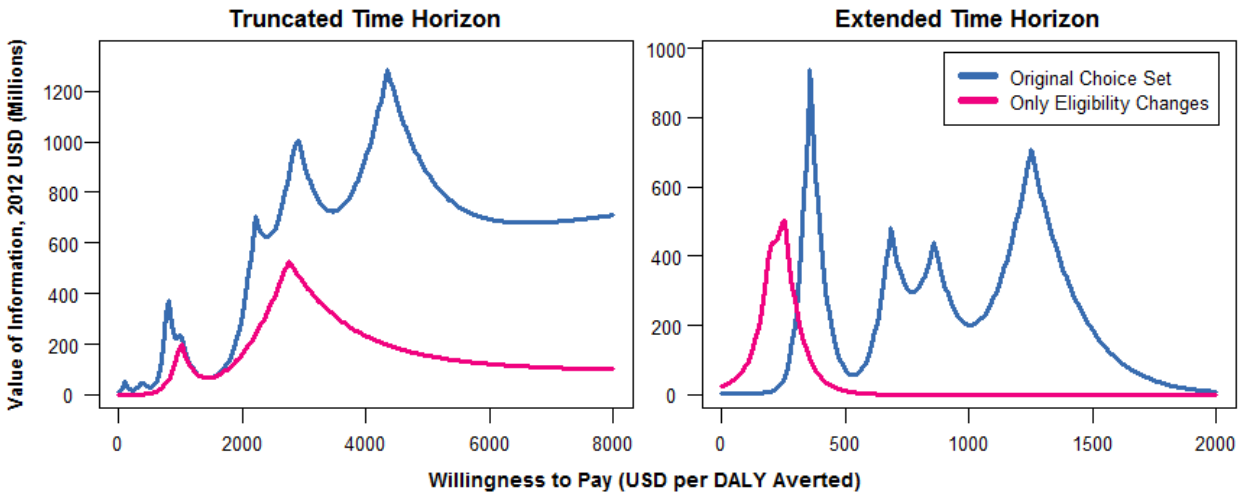

Figure 3.21. EVPI for a choice set including only policies A2, B2 and C2, compared to EVPI calculated for the original choice set

Figure 3.22 presents EVPPI estimates for the same 11 parameters shown in Figure 3.17, now calculated for the restricted choice set in which testing intensity is fixed. The EVPPI estimates from the main analysis are shown in grey for purposes of comparison. The qualitative findings from the comparison of EVPI results also apply here, with EVPPI generally lower in the analysis with the restricted choice set, though not universally so. It is notable that EVPPI for better information on HIV testing costs, found to be substantial in the main VOI analysis, appears to be zero with the restricted choice set. This is consistent with the idea that the value of information on HIV testing programs will be substantially reduced whren changes in HIV testing policy are no longer being considered.

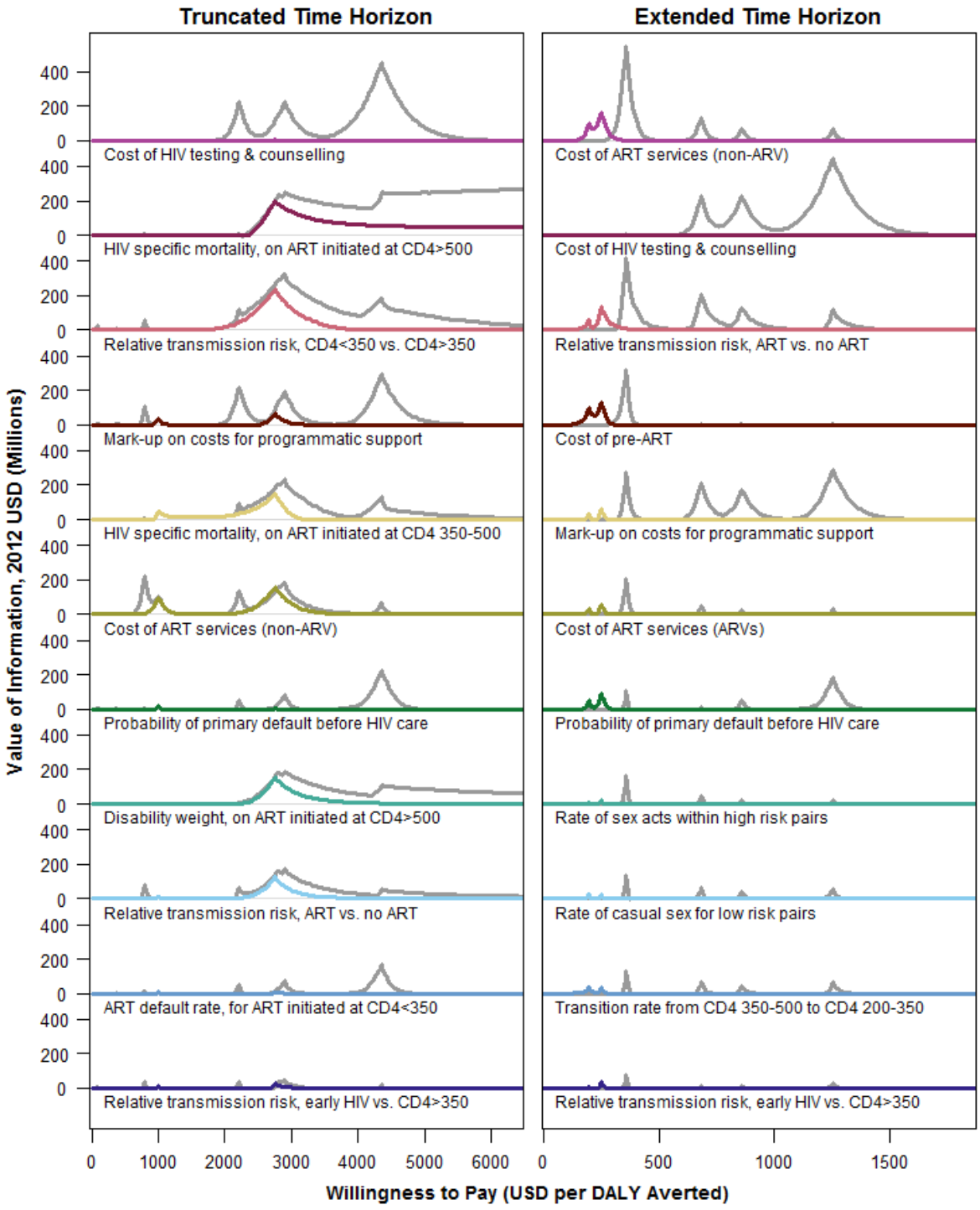

Figure 3.22. EVPPI for a choice set including only policies A2, B2 and C2, compared to EVPI calculated for the original choice set*

* Parameters shown in figure are those with the highest EVPPI estimated in the main analyses (Figure 3.17). Grey lines represent the EVPPI estimates from the main analysis, for purposes of comparison.

3.4. Discussion

This analysis finds that scaling-up ART in South Africa, either through expanded ART eligibility criteria or through more aggressive HIV testing programs, would lead to substantial reductions in the burden of disease associated with HIV. Expanded ART provision is shown to substantially reduce HIV-associated mortality, and absent other effects the improved survival of HIV-positive individuals would lead to increased HIV prevalence. However, results suggest that the net effect of expanded ART will be to reduce HIV prevalence over the long term, as the increase in prevalence due to reduced HIV mortality is outweighed by reductions in transmission. Over a extended time horizon, the DALYs averted through the preventative effects of ART represent over half of the total health benefits generated by ART. These prevention-related health benefits—representing the gains in quality and length of life among HIV-negative individuals who would otherwise be infected with HIV—are a delayed consequence of expanded ART, and might be incompletely captured by analyses that aggregate results over a truncated time horizon. In an analysis where health outcomes experienced after 20 years are ignored, the therapeutic effects of ART are the major driver of health impact, and the overall health benefits of expanded ART are substantially smaller.

Expanded ART also requires large increases in health system costs, with higher costs within HIV programs being only modestly offset by savings in routine health services. Policies involving more aggressive HIV testing programs appear to add substantially to overall costs. These cost increases come not only from the HIV testing programs but also from higher pre-ART costs for the larger cohort of individuals in care but not yet eligible for ART, as well as higher ART costs. In contrast, under policies involving expanded ART eligibility, higher ART costs are partially offset by reductions in pre-ART costs, as previously enrolled pre-ART patients are shifted onto ART.

The cost-effectiveness findings of this analysis suggest that expanding ART access in some way, either through raising CD4 cell count-based eligibility criteria or through more aggressive testing

programs, would be cost-effective under a wide range of assumptions. This finding appears robust, despite substantial uncertainties about important features of the epidemic and intervention policies. Over a extended time horizon, policies involving expanded ART eligibility criteria appear particularly effective at producing health benefits at comparatively low cost. This result is surprising, given that the therapeutic benefits of early ART initiation will be lower than providing ART to symptomatic individuals who otherwise would not receive it (as might be accomplished by expanded HIV testing programs). This result reflects the importance of HIV prevention to long-term health outcomes, as well as the comparatively lower costs of this ART scale-up approach, as discussed above. One condition under which this finding—that expanding ART access is cost-effective—may not apply is where policy makers operate under time horizons far shorter than those adopted here. Because spending on ART programs precedes the benefits it generates, the health benefits of ART may not accumulate sufficiently under a short time horizon to justify the costs in an acutely resource-constrained setting. Of course, in this situation the demand for new research will also likely be low, as the lag between investment and pay-off may be even longer for research.

The results describing epidemiologic and economic outcomes are broadly consistent with other analyses investigating the long-term costs and population health outcomes of ART expansion in South Africa [11,13,112,113], though not finding the possibility of long-term cost-savings suggested by some authors [112]. These results form the basis of a value-of-information analysis to identify priority targets for new HIV research.

Perhaps the most notable finding of the VOI results is the apparent unimportance of information about transmission during early HIV infection. Resolving uncertainty for this parameter (the relative risk of transmission during early HIV infection) accounts for approximately 1% of the value of information estimated for the most valuable research targets under both truncated and extended

time horizons. One possible explanation for this finding is that the estimated fraction of all new infections attributable to individuals with early HIV infection is smaller in our analysis than in some other analyses, particularly Powers *et al.* [17], who also adopted a pair model. In the Powers analysis, the majority of HIV transmission occurred within high-risk pairs with very high rates of partner turnover, so the potential for newly-infected individuals to be sequestered within pair relationships (a defining feature of pair models) may not have been realized. In addition, the Powers model had an average duration of early HIV of 4.8 months, while our analysis used a mean value of 2.9 months from Hollingsworth *et al*. [50], and these differences in the definition of early HIV could also affect the fraction of total infections coming from this group. In sensitivity analyses that increased the fraction of transmission attributable to early infection by 70%, to a point approximately half way between the original value and that reported by the Powers analysis, the VOI of information about transmission during early HIV infection rose by 50-100% of its original value. While confirming the intuition that this VOI would rise as the fraction of transmission attributable to early infection increased, this new value was insufficient to produce any meaningful change in the relative importance of this parameter relative to other model parameters. Even if this analysis were adjusted to obtain a fraction of transmission attributable to early infection similar to that reported by Powers, it is unlikely the VOI analysis would find information about transmission during early HIV infection to be a priority research target.

While there are important differences between this analysis and that conducted by Powers *et al.*, it is possible that the conclusion of the VOI analysis—that relative infectiousness during early HIV is effectively irrelevant for ART policy—might be a general feature of HIV epidemics. A heuristic approach to motivate this idea is to consider transmission during early HIV as a multiplier applied to any new HIV transmission – thus if an intervention is able to avert one primary infection, it might end up averting 1.5 infections in total if one counts the subsequent secondary transmissions that occur while the primarily infected individual is experiencing early HIV. In a scenario where

transmission during early HIV represents a large fraction of all new infections, the fraction of all transmission that could be averted by treatment of individuals in other disease stages will be smaller, and so ART would prevent fewer primary transmissions. However, the number of secondary transmissions averted for each primary transmission will be higher (e.g., instead of 1.5 the multiplier might be 1.8). Conversely, if early HIV contributes a small fraction of all infections, then although a greater fraction of all transmissions could be averted by expanding ART access to individuals in later disease stages, the number of secondary infections averted will be smaller (e.g., instead of 1.5 the multiplier might be 1.3). In sum the total change in HIV incidence following a change in ART policy may be different between these two scenarios, but this difference will be smaller than originally anticipated.

In contrast to early HIV infection, the issues found to have the highest potential value of information include (1) issues of cost and implementation, (2) relative infectiousness during late HIV and the reduction in infectiousness for individuals on ART, and (3) the therapeutic health benefits of ART for individuals with CD4 cell counts above current eligibility guidelines. The prevention benefits of ART are the subject of an increasing volume of research. The most notable trial reported thus far is the HPTN 052 trial, which found compelling reductions in HIV transmission for individuals initiated on ART [9]. A number of similar trials and observational studies are planned or ongoing, investigating different population groups and aspects of implementation [114,115], and for this reason we are likely to have improved information about the relative infectiousness of ART patients in the near future. These and other trials [116,117] will also provide information on the therapeutic benefits of early ART initiation. There has been less systematic investigation of HIV intervention costs beyond small single-center studies, though examples exist [118], particularly focused on the costs of HIV treatment [63,119–121]. One challenge for new research on HIV costs is generalizability: while the knowledge generated by trials of ART effectiveness may generalize broadly, the costs of service provision are a consequence of

complex social and institutional interactions, and might change substantially across settings or as intervention approaches change. Despite these difficulties, the findings of this analysis—that reducing uncertainty around the costs of competing policies is a high priority relative to other concerns—suggest that greater investment in understanding HIV intervention costs may be warranted. Similarly, operational issues—such as improved understanding of the pathways for diagnosis and treatment initiation—will also likely differ substantially across settings, yet may benefit from greater research funding.

The decision to highlight comparative VOI results (as opposed to the absolute dollar values) reflects the belief that that comparative findings will be more robust to some the limitations of the analysis. Among the limitations of using the absolute EVPPI estimates is the fact that the analysis was conducted in a single setting (South Africa), yet the information generated by new research would likely aid decision-making in other settings, and therefore the total global value may be much higher than the absolute values estimated in this analysis. Even within South Africa, there are likely a large number of policy decisions, big and small, to which new information might be applied. While likely not simply additive, the more decisions for which research might be relevant (and the more influential those decisions), the greater will be the value of that information. It is important to consider those research targets—such as an improved understanding of the population growth rate—that will be relevant to a large number of decision problems but have a small impact on any single decision. Research targets with these characteristics will be systematically undervalued by the approach adopted for this analysis, which by necessity focused on a single policy decision in great detail. For this reason, the VOI estimates for broadly applicable issues like population growth or background mortality rates should be interpreted with caution. In addition, the fact that these VOI results focus on perfect information means that any new research is likely to produce lower-value information, and the absolute EVPPI estimated reported in this study will not be attainable.

The application of VOI methods requires a formal description of the mechanism by which information about candidate policies is translated into a single policy choice. This choice function is a mathematical summary of the policy-making process, yet while the choice function adopted for this analysis reflects presumably reasonable assumptions—that policy makers will favor policies that improve health outcomes, and avoid policies that increase costs, that they will pay more attention to near term outcomes than outcomes realized in the distant future, that they will respond rationally to new information by updating their beliefs about policy outcomes—the relative weighting of different concerns has a central impact on the VOI results. This can be seen in the sensitivity of the VOI findings to changes in policy parameters such as the WTP threshold, the discount rate, and the time horizon. Because different policy makers might adopt different values of these parameters, results are presented for a range of different values for these parameters. Even where findings appear robust to a range of different assumptions about these values, there may be complex features of the 'true' choice function that are not explored by changing these values. For example, a concern for equity—which might be expressed as equity in total experience of health, equity in the distribution of health gains, or equitable access to care—would require different inputs from those currently considered in the choice function, as well as explicit mathematical specifications of how these equity concerns would be traded off against concerns for aggregate health gains and costs. Another example relates to WTP, which is operationalized as a single value, ignoring the possibility that the opportunity cost of spending may depend on the purpose to which spending is devoted (major donors may have preferences for certain health interventions, and funding may not be entirely fungible across budget categories), or on the absolute value of total spending, with progressively more valuable interventions forgone as total ART spending is increased. While not reflected in the results shown here, these concerns will impact actual decision-making.

Another simplification made to operationalize this analysis is the focus on a single policy decision. In reality the pattern of possible decisions may be more complicated than allowed for in this analysis. For example, it is likely that major policy decisions could be delayed, with a country like South Africa learning from the experience of other countries more willing to pursue aggressive ART scale-up. Similarly, even once a policy is chosen, this decision could be revised in the future as accumulating surveillance data and routine program reports provide empirical evidence of policy outcomes. Such sequential decision-making could be operationalized within the VOI approach used here, but would require additional assumptions about the rate at which programs generate evidence useful for decision makers, the points at which policy choices might be reviewed, and the implementation costs of policy change.

Just as importantly, it is clear that a technocratic representation of health care resource allocation—that policies are chosen based on a single social welfare function, and that policy makers are sensitive to the changing state of knowledge about competing policies—is a crude approximation of the real policy-making process in many settings, and that explanations focusing on structural elements of the decision process, such as the interaction of key stakeholder groups, as well as a broader understanding of the priorities that motivate decision makers, may have greater explanatory power. This is exemplified by the unprecedented investment in global HIV control by western donors since 2000. It is difficult to interpret this as the outcome of a cost-effectiveness analysis, and contemporary accounts, both critical and supportive, emphasis political explanations for these policy choices [122,123]. If real-world decision-making differs substantially from a normative model of decision-making such as used in this analysis, then the implications for VOI are unclear. One possibility is that VOI will fluctuate over the course of time, with research much more valuable if it is available during those windows of opportunity when major policy change can be considered [124], and less valuable otherwise. In this circumstance, conventional VOI analyses may still give reasonable estimates of the long-term average value of research. Another possibility is that

conventional analyses will systematically overestimate the overall value of research: if it is accepted that sub-optimal policy-making is only partly attributable to inadequate information, such that sub-optimal policies will still be chosen or retained after decision uncertainty is resolved, then the value of resolving that decision uncertainty may well be lower. It is important to note that this is not a necessary consequence: one can conceive of a situation where factors promoting sub-optimal decision-making (such as a policy maker's desire to please narrowly focused interest groups) play a much greater role in decisions when there is a poor understanding of policy outcomes. Essentially, when it is unclear which policy will best improve social welfare, the policy maker has greater liberty to adopt policies that promote other objectives. In contrast, when decision uncertainty is resolved, the task of justifying sub-optimal policy becomes more difficult. In this circumstance, the improvement in social welfare generated by research may be greater than predicted by conventional VOI approaches, as the discrepancy between actual decision-making and optimal decision-making (measured in relevant units of social welfare loss) may be smaller once decision-uncertainty is reduced.

In addition to addressing substantive questions about relative value of new research targets, this analysis also developed methods for the application of VOI methods in the context of calibrated models. These methods are more demanding than conventional approaches, yet will be of increasing relevance as a greater number of analyses adopt numerical methods to calibrate complex disease models, as it is the lack of an analytic representation of this calibrated parameter distribution that necessitates these new methods. While this analysis did not calculate measures of partial sample information (EVPSI), as would be required to understand the value of new information produced by realistic study designs, it is anticipated that the approach used in this analysis could be extended to estimate these quantities, by reweighting the parameter sets in light of the anticipated distribution of new information (as described in Section 3.2.16.4), and this extension will be addressed in future work.

3.5. Citations

1 UNAIDS. *World AIDS Day Report 2012*. Geneva: UNAIDS; 2012.

2 United Nations General Assembly. *Political Declaration on HIV/AIDS*. New York: United Nations; 2006. http://www.unhcr.org/refworld/docid/453781490.html

3 Leach-Kemon K, Chou DP, Schneider MT, Tardif A, Dieleman JL, Brooks BP, *et al.* The global financial crisis has led to a slowdown in growth of funding to improve health in many developing countries. *Heal Aff* 2012; 31:228–235.

4 Wandel S, Egger M, Rangsin R, Nelson KE, Costello C, Lewden C, *et al.* Duration from seroconversion to eligibility for antiretroviral therapy and from ART eligibility to death in adult HIV-infected patients from low and middle-income countries: collaborative analysis of prospective studies. *Sex Transm Infect* 2008; 84 Suppl 1:i31–i36.

5 Kilby JM, Lee HY, Hazelwood JD, Bansal A, Bucy RP, Saag MS, *et al.* Treatment response in acute/early infection versus advanced AIDS: equivalent first and second phases of HIV RNA decline. *AIDS* 2008; 22:957–62.

6 Quinn TC, Wawer MJ, Sewankambo N, Serwadda D, Li C, Wabwire-Mangen F, *et al.* Viral load and heterosexual transmission of human immunodeficiency virus type 1. Rakai Project Study Group. *New Engl J Med* 2000; 342:921–929.

7 Castilla J, Del Romero J, Hernando V, Marincovich B, Garcia S, Rodriguez C. Effectiveness of highly active antiretroviral therapy in reducing heterosexual transmission of HIV. *JAIDS* 2005; 40:96–101.

8 Donnell D, Baeten JM, Kiarie J, Thomas KK, Stevens W, Cohen CR, *et al.* Heterosexual HIV-1 transmission after initiation of antiretroviral therapy: a prospective cohort analysis. *Lancet* 2010; 375:2092–2098.

9 Cohen MS, Chen YQ, McCauley M, Gamble T, Hosseinipour MC, Kumarasamy N, *et al.* Prevention of HIV-1 infection with early antiretroviral therapy. *New Engl J Med* 2011; 365:493–505.

10 Granich RM, Gilks CF, Dye C, De Cock KM, Williams BG. Universal voluntary HIV testing with immediate antiretroviral therapy as a strategy for elimination of HIV transmission: a mathematical model. *Lancet* 2009; 373:48–57.

11 Hontelez JA, de Vlas SJ, Tanser F, Bakker R, Barnighausen T, Newell ML, *et al.* The impact of the new WHO antiretroviral treatment guidelines on HIV epidemic dynamics and cost in South Africa. *PLoS One* 2011; 6:e21919.

12 Lancet Editors. HIV treatment as prevention--it works. *Lancet* 2011; 377:1719.

13 Eaton J, Menzies N, Stover J, Cambiano V, Chindelevitch L, Cori A, *et al.* Health benefits, costs, and cost-effectiveness of earlier eligibility for adult antiretroviral therapy and expanded treatment coverage: a combined analysis of 12 mathematical models. *Lancet Glob Heal* 2014; 2:e23–34.

14 De Cock KM, El-Sadr WM. When to start ART in Africa — an urgent research priority. *New Engl J Med* 2013; 368:886–9.

15 Wawer MJ, Gray RH, Sewankambo NK, Serwadda D, Li X, Laeyendecker O, *et al.* Rates of HIV-1 transmission per coital act, by stage of HIV-1 infection, in Rakai, Uganda. *J Infect Dis* 2005; 191:1403–1409.

16 Cohen MS, Shaw GM, McMichael AJ, Haynes BF. Acute HIV-1 infection. *New Engl J Med* 2011; 364:1943–1954.

17 Powers KA, Ghani AC, Miller WC, Hoffman IF, Pettifor AE, Kamanga G, *et al.* The role of acute and early HIV infection in the spread of HIV and implications for transmission prevention strategies in Lilongwe, Malawi: a modelling study. *Lancet* 2011; 378:256–268.

18 Goldie SJ, Yazdanpanah Y, Losina E, Weinstein MC, Anglaret X, Walensky RP, *et al.* Cost-effectiveness of HIV treatment in resource-poor settings--the case of Cote d'Ivoire. *New Engl J Med* 2006; 355:1141–1153.

19 Badri M, Maartens G, Mandalia S, Bekker LG, Penrod JR, Platt RW, *et al.* Cost-effectiveness of highly active antiretroviral therapy in South Africa. *PLOS Med* 2006; 3:e4.

20 Cleary SM, McIntyre D, Boulle AM. The cost-effectiveness of antiretroviral treatment in Khayelitsha, South Africa--a primary data analysis. *Cost Eff Resour Alloc* 2006; 4:20.

21 Sabin C, Cooper D, Collins S, Schechter M. Rating evidence in treatment guidelines: a case example of when to initiate combination antiretroviral therapy (cART) in HIV positive asymptomatic persons. *AIDS* 2013; 27:1839–46.

22 Groot Koerkamp B, Myriam Hunink MG, Stijnen T, Weinstein MC. Identifying key parameters in cost-effectiveness analysis using value of information: a comparison of methods. *Heal Econ* 2006; 15:383–392.

23 Claxton K, Neumann PJ, Araki S, Weinstein MC. Bayesian value-of-information analysis. An application to a policy model of Alzheimer's disease. *Int J Technol Assess Heal Care* 2001; 17:38–55.

24 Claxton K, Cohen JT, Neumann PJ. When is evidence sufficient? *Heal Aff* 2005; 24:93–101.

25 Steuten L, van de Wetering G, Groothuis-Oudshoorn K, Retèl V. A systematic and critical review of the evolving methods and applications of value of information in academia and practice. *Pharmacoeconomics* 2013; 31:25–48.

26 Claxton KP, Sculpher MJ. Using value of information analysis to prioritise health research: some lessons from recent UK experience. *Pharmacoeconomics* 2006; 24:1055–68.

27 Leelahavarong P, Teerawattananon Y, Werayingyong P, Akaleephan C, Premsri N, Namwat C, *et al.* Is a HIV vaccine a viable option and at what price? An economic evaluation of adding HIV vaccination into existing prevention programs in Thailand. *BMC Public Health* 2011; 11:534.

28 Maheswaran H, Barton P. Intensive case finding and isoniazid preventative therapy in HIV infected individuals in Africa: economic model and value of information analysis. *PLoS One* 2012; 7:e30457.

29 Ades AE, Lu G, Claxton K. Expected value of sample information calculations in medical decision modeling. *Med Decis Mak* 2004; 24:207–227.

30 Stinnett AA, Mullahy J. Net health benefits: a new framework for the analysis of uncertainty in cost-effectiveness analysis. *Med Decis Mak* 1998; 18:S68–80.

31 Kretzschmar M, Dietz K. The effect of pair formation and variable infectivity on the spread of an infection without recovery. *Math Biosci* 1998; 148:83–113.

32 Xiridou M, Geskus R, Wit J de. Primary HIV infection as source of HIV transmission within steady and casual partnerships among homosexual men. *AIDS* 2004; 18:1311–20.

33 Xiridou M, Geskus R, Wit J De. The contribution of steady and casual partnerships to the incidence of HIV infection among homosexual men in Amsterdam. *AIDS* 2003; 17:1029–38.

34 Johnson L, Dorrington R, Bradshaw D, Pillay-Van Wyk V, Rehle T. Sexual behaviour patterns in South Africa and their association with the spread of HIV: insights from a mathematical model. *Demogr Res* 2009; 21:289–340.

35 Dodd PJ, Garnett GP, Hallett TB. Examining the promise of HIV elimination by "test and treat" in hyperendemic settings. *AIDS* 2010; 24:729–35.

36 Eaton JW, Johnson LF, Salomon J a, Bärnighausen T, Bendavid E, Bershteyn A, *et al.* HIV treatment as prevention: systematic comparison of mathematical models of the potential impact of antiretroviral therapy on HIV incidence in South Africa. *PLOS Med* 2012; 9:e1001245.

37 Garnett GP, White PJ, Ward H. Fewer partners or more condoms? Modelling the effectiveness of STI prevention interventions. *Sex Transm Infect* 2008; 84 Suppl 2:ii4–11.

38 Eaton JW, Hallett TB, Garnett GP. Concurrent sexual partnerships and primary HIV infection: a critical interaction. *AIDS Behav* 2011; 15:687–92.

39 Hallett TB, Aberle-Grasse J, Bello G, Boulos L-M, Cayemittes MPA, Cheluget B, *et al.* Declines in HIV prevalence can be associated with changing sexual behaviour in Uganda, urban Kenya, Zimbabwe, and urban Haiti. *Sex Transm Infect* 2006; 82 Suppl 1:i1–8.

40 Xiridou M, van Veen M, Coutinho R, Prins M. Can migrants from high-endemic countries cause new HIV outbreaks among heterosexuals in low-endemic countries? *AIDS* 2010; 24:2081–8.

41 Xiridou M, van Veen M, Prins M, Coutinho R. How patterns of migration can influence the heterosexual transmission of HIV in The Netherlands. *Sex Transm Infect* 2011; 87:289–91.

42 Statistics South Africa. *Census 2001: stages in the life cycle of South Africans*. Pretoria South Africa: Statistics South Africa; 2005.

43 Garnett GP, Anderson RM. Sexually transmitted diseases and sexual behavior: insights from mathematical models. *J Infect Dis* 1996; 174 Suppl:S150–61.

44 Johnson LF, Hallett TB, Rehle TM, Dorrington RE. The effect of changes in condom usage and antiretroviral treatment coverage on human immunodeficiency virus incidence in South Africa: a model-based analysis. *J R Soc Interface* 2012; 9:1544–54.

45 Department of Health. *South Africa demographic and health survey 2003*. Pretoria South Africa: South African Department of Health; 2007.

46 European Study Group on Heterosexual Transmission of HIV. Comparison of female to male and male to female transmission of HIV in 563 stable couples. European Study Group on Heterosexual Transmission of HIV. *BMJ* 1992; 304:809–13.

47 Boily M-C, Baggaley RF, Wang L, Masse B, White RG, Hayes RJ, *et al.* Heterosexual risk of HIV-1 infection per sexual act: systematic review and meta-analysis of observational studies. *Lancet Infect Dis* 2009; 9:118–29.

48 Chen L, Jha P, Stirling B, Sgaier SK, Daid T, Kaul R, *et al.* Sexual risk factors for HIV infection in early and advanced HIV epidemics in sub-Saharan Africa: systematic overview of 68 epidemiological studies. *PLoS One* 2007; 2:e1001.

49 Sexton J, Garnett G, Røttingen J-A. Metaanalysis and metaregression in interpreting study variability in the impact of sexually transmitted diseases on susceptibility to HIV infection. *Sex Transm Dis* 2005; 32:351–7.

50 Hollingsworth TD, Anderson RM, Fraser C. HIV-1 transmission, by stage of infection. *J Infect Dis* 2008; 198:687–93.

51 Anglemyer A, Rutherford GW, Hovarth T, Baggaley RC, Egger M, Siegfried N. Antiretroviral therapy for prevention of HIV transmission in HIV-discordant couples. *Cochrane DB Syst Rev* 2013; 4:CD009153.

52 Mellors JW, Margolick JB, Phair JP, Rinaldo CR, Detels R, Jacobson LP, *et al.* Prognostic value of HIV-1 RNA, CD4 cell count, and CD4 Cell count slope for progression to AIDS and death in untreated HIV-1 infection. *JAMA* 2007; 297:2349–50.

53 Holmes CB, Wood R, Badri M, Zilber S, Wang B, Maartens G, *et al.* CD4 decline and incidence of opportunistic infections in Cape Town, South Africa: implications for prophylaxis and treatment. *JAIDS* 2006; 42:464–9.

54 Wolbers M, Babiker A, Sabin C, Young J, Dorrucci M, Chêne G, *et al.* Pretreatment CD4 cell slope and progression to AIDS or death in HIV-infected patients initiating antiretroviral therapy--the CASCADE collaboration: a collaboration of 23 cohort studies. *PLOS Med* 2010; 7:e1000239.

55 Population Division. *World population prospects: the 2010 revision*. New York: Population Division of the Department of Economic and Social Affairs of the United Nations Secretariat; 2011.

56 Actuarial Society of South Africa. *ASSA 2008 AIDS and demographic models: user guide*. Pretoria South Africa: Actuarial Society of South Africa; 2010.

57 Anglaret X, Minga A, Gabillard D, Ouassa T, Messou E, Morris B, *et al.* AIDS and non-AIDS morbidity and mortality across the spectrum of CD4 cell counts in HIV-infected adults before starting antiretroviral therapy in Cote d'Ivoire. *Clin Infect Dis* 2012; 54:714–723.

58 Badri M, Lawn SD, Wood R. Short-term risk of AIDS or death in people infected with HIV-1 before antiretroviral therapy in South Africa: a longitudinal study. *Lancet* 2006; 368:1254–9.

59 May M, Sterne JAC, Sabin C, Costagliola D, Justice AC, Thiébaut R, *et al.* Prognosis of HIV-1-infected patients up to 5 years after initiation of HAART: collaborative analysis of prospective studies. *AIDS* 2007; 21:1185–97.

60 Egger M, May M, Chêne G, Phillips AN, Ledergerber B, Dabis F, *et al.* Prognosis of HIV-1-infected patients starting highly active antiretroviral therapy: a collaborative analysis of prospective studies. *Lancet* 2002; 360:119–29.

61 Sterne JAC, May M, Costagliola D, de Wolf F, Phillips AN, Harris R, *et al.* Timing of initiation of antiretroviral therapy in AIDS-free HIV-1-infected patients: a collaborative analysis of 18 HIV cohort studies. *Lancet* 2009; 373:1352–63.

62 Rosen S, Fox MP, Gill CJ. Patient retention in antiretroviral therapy programs in sub-Saharan Africa: a systematic review. *PLOS Med* 2007; 4:e298.

63 Menzies NA, Berruti AA, Berzon R, Filler S, Ferris R, Ellerbrock T V, *et al.* The cost of providing comprehensive HIV treatment in PEPFAR-supported programs. *AIDS* 2011; 25:1753–60.

64 Republic of South Africa. *Global AIDS response progress report 2012: South Africa*. Pretoria, South Africa: Republic of South Africa; 2012.

65 Johnson LJ. Access to antoretroviral treatment in South Africa, 2004-2011. *S Afr J HIV Med* 2012; 13:22–27.

66 ICF International. *Demographic and Health Surveys (multiple, 2003-2011)*. Calverton, MD: ICF International; 2012.

67 Rosen S, Fox MP. Retention in HIV care between testing and treatment in Sub-Saharan Africa: a systematic review. *PLOS Med* 2011; 8:e1001056.

68 Department of Health. *The South African antiretroviral treatment guidelines 2013*. Pretoria, South Africa: South African Department of Health; 2013.

69 Department of Health. *The South African antiretroviral treatment guidelines 2010*. Pretoria, South Africa: South African Department of Health; 2010.

70 Department of Health. *National antiretroviral treatment guidelines*. Pretoria, South Africa: South African Department of Health; 2004.

71 Pillay Y, White C, McCormick N. How times have changed – HIV and AIDS in South Africa in 2011. *S Afr Med J* 2012; 102:77–78.

72 Salomon JA, Vos T, Hogan DR, Gagnon M, Naghavi M, Mokdad A, *et al.* Common values in assessing health outcomes from disease and injury: disability weights measurement study for the Global Burden of Disease Study 2010. *Lancet* 2012; 380:2129–43.

73 Weinstein MC, Siegel JE, Gold MR, Kamlet MS, Russell LB. Recommendations of the Panel on Cost-Effectiveness in Health and Medicine. *JAMA* 1996; 276:1253–1258.

74 Department of Health. *The 2011 national antenatal sentinel HIV & syphilis prevalence survey in South Africa*. Pretoria, South Africa: South African Department of Health; 2012.

75 Shisana O, Rehle T, Simbayi LC, Zuma K, Jooste S, Pillay-van-Wyk V, *et al. South African national HIV prevalence, incidence, behaviour and communication survey, 2008*. Cape Town, South Africa: HSRC Press; 2009.

76 Gouws E, Mishra V, Fowler TB. Comparison of adult HIV prevalence from national population-based surveys and antenatal clinic surveillance in countries with generalised epidemics: implications for calibrating surveillance data. *Sex Transm Infect* 2008; 84 Suppl 1:i17–i23.

77 Brown T, Salomon JA, Alkema L, Raftery AE, Gouws E. Progress and challenges in modelling country-level HIV/AIDS epidemics: the UNAIDS Estimation and Projection Package 2007. *Sex Transm Infect* 2008; 84 Suppl 1:i5–i10.

78 Alkema L, Raftery AE, Clark SJ. Probabilistic projections of HIV prevalence using Bayesian melding. *Ann Appl Stat* 2007; 1:229–248.

79 Alkema L, Raftery AE, Brown T. Bayesian melding for estimating uncertainty in national HIV prevalence estimates. *Sex Transm Infect* 2008; 84 Suppl 1:i11–i16.

80 Hogan DR, Salomon JA, Canning D, Hammitt JK, Zaslavsky AM, Bärnighausen T. National HIV prevalence estimates for sub-Saharan Africa: controlling selection bias with Heckman-type selection models. *Sex Transm Infect* 2012; 88 Suppl 2:i17–23.

81 Bärnighausen T, Bor J, Wandira-Kazibwe S, Canning D. Correcting HIV prevalence estimates for survey nonparticipation using Heckman-type selection models. *Epidemiology* 2011; 22:27–35.

82 UNAIDS Reference Group on Estimates Modelling and Projections. *Use of Heckman-type selection models to account for selective non-participation in HIV testing surveys: Recommendations from a meeting of the UNAIDS Reference Group on Estimates, Modelling and Projections held in Boston, MA, USA, 3 April 2012*. Geneva: UNAIDS; 2012.

83 Glynn JR, Sonnenberg P, Nelson G, Bester A, Shearer S, Murray J. Survival from HIV-1 seroconversion in Southern Africa: a retrospective cohort study in nearly 2000 gold-miners over 10 years of follow-up. *AIDS* 2007; 21:625–32.

84 Auvert B, Males S, Puren A, Taljaard D, Caraël M, Williams B. Can highly active antiretroviral therapy reduce the spread of HIV?: A study in a township of South Africa. *JAIDS* 2004; 36:613–21.

85 Rehle TM, Shisana O. Estimates of eligibility for antiretroviral treatment (ART) and projected ART impact on AIDS mortality among South African educators. *J Soc Asp H* 2005; 2:304–10.

86 Connelly D, Veriava Y, Roberts S, Tsotetsi J, Jordan A, DeSilva E, *et al.* Prevalence of HIV infection and median CD4 counts among health care workers in South Africa. *S Afr Med J* 2007; 97:115–20.

87 Raftery AE, Bao L. Estimating and projecting trends in HIV/AIDS generalized epidemics using Incremental Mixture Importance Sampling. *Biometrics* 2010; 66:1162–73.

88 Rubin D. Using the SIR algorithm to simulate posterior distributions. *Bayesian Stat* 1988; 3:395–402.

89 Filler SJ, Berruti AA, Menzies N, Berzon R, Ellerbrock T V, Ferris R, *et al.* Characteristics of HIV care and treatment in PEPFAR-supported sites. *JAIDS* 2011; 57:e1–6.

90 Johns B, Baltussen R, Hutubessy R. Programme costs in the economic evaluation of health interventions. *Cost Eff Resour Alloc* 2003; 1:1–10.

91 Murray CJL, Ezzati M, Flaxman AD, Lim S, Lozano R, Michaud C, *et al.* GBD 2010: design, definitions, and metrics. *Lancet* 2012; 380:2063–6.

92 Claxton K. The irrelevance of inference: a decision-making approach to the stochastic evaluation of health care technologies. *J Heal Econ* 1999; 18:341–64.

93 Claxton K, Posnett J. An economic approach to clinical trial design and research priority-setting. *Heal Econ* 1996; 5:513–24.

94 Cleveland W, Devlin S. Locally weighted regression: an approach to regression analysis by local fitting. *J Am Stat Assoc* 1988; 83:596–610.

95 Cleveland W. Robust locally weighted regression and smoothing scatterplots. *J Am Stat Assoc* 1979; 74:829–836.

96 R Core Team. R: A language and environment for statistical computing. 2013. doi:ISBN 3-900051-07-0

97 Poole D, Raftery AE. Inference for deterministic simulation models: The Bayesian melding approach. *J Am Stat Assoc* 2000; 95:452.

98 Griffin SC, Claxton KP, Palmer SJ, Sculpher MJ. Dangerous omissions: the consequences of ignoring decision uncertainty. *Heal Econ* 2011; 20:212–24.

99 Eckermann S, Willan AR. The option value of delay in health technology assessment. *Med Decis Mak* 2008; 28:300–5.

100 Palmer S, Smith PC. Incorporating option values into the economic evaluation of health care technologies. *J Heal Econ* 2000; 19:755–66.

101 Claxton K, Paulden M, Gravelle H, Brouwer W, Culyer AJ. Discounting and decision making in the economic evaluation of health-care technologies. *Heal Econ* 2011; 20:2–15.

102 World Bank. *World Development Indicators 2013*. Washington DC: World Bank; 2013.

103 Fenwick E, O'Brien BJ, Briggs A. Cost-effectiveness acceptability curves--facts, fallacies and frequently asked questions. *Heal Econ* 2004; 13:405–415.

104 Shillcutt SD, Walker DG, Goodman CA, Mills AJ. Cost effectiveness in low- and middle-income countries: a review of the debates surrounding decision rules. *Pharmacoeconomics* 2009; 27:903–17.

105 Garber AM, Phelps CE. Economic foundations of cost-effectiveness analysis. *J Heal Econ* 1997; 16:1–31.

106 Sachs J. *Macroeconomics and health: investing in health for economic development*. Geneva: World Health Organization; 2001.

107 Tan Torres T, Baltussen R, Adam T, Hutubessy R, Acharya A, Evans D, *et al. Making choices in health: WHO guide to cost effectiveness analysis*. Geneva: WHO; 2003.

108 World Bank. *World Development Indicators 2012*. New York: World Bank; 2012.

109 Ssengooba F. Uganda's minimum package for health care: rationing within the minimum? *Heal Pol Devel* 2004; 2.

110 World Bank. *World Development Report 1993*. Washington DC: World Bank; 1993.

111 WHO. *Investing in health research and development: report of the ad hoc committee on health research relating to future intervention options*. Geneva: World Health Organization; 1996.

112 Granich R, Kahn JG, Bennett R, Holmes CB, Garg N, Serenata C, *et al.* Expanding ART for treatment and prevention of HIV in South Africa: estimated cost and cost-effectiveness 2011-2050. *PLoS One* 2012; 7:e30216.

113 Bärnighausen T, Bloom DE, Humair S. Economics of antiretroviral treatment vs. circumcision for HIV prevention. *P Natl Acad Sci USA* 2012; 109:21271–6.

114 HIV Prevention Trials Network. Antiretroviral Therapy Research (TasP and PrEP) (website, accessed October 20 2013). 2013.http://www.hptn.org/prevention_science/art.asp

115 Granich R, Gupta S, Suthar AB, Smyth C, Hoos D, Vitoria M, *et al.* Antiretroviral therapy in prevention of HIV and TB: update on current research efforts. *Curr HIV Res* 2011; 9:446–69.

116 French National Agency for Research on AIDS and Viral Hepatitis. Early antiretroviral treatment and/or early isoniazid prophylaxis against tuberculosis in HIV-infected adults

(ANRS 12136 TEMPRANO) (website, accessed October 8 2013). 2013.http://clinicaltrials.gov/ct2/show/NCT00495651

117 US National Institutes of Health. Strategic Timing of Antiretroviral Treatment (START) (website, accessed February 20 2013). 2013.http://clinicaltrials.gov/ct2/show/NCT00867048

118 Marseille E, Dandona L, Marshall N, Gaist P, Bautista-Arredondo S, Rollins B, *et al.* HIV prevention costs and program scale: data from the PANCEA project in five low and middle-income countries. *BMC Heal Serv Res* 2007; 7:108.

119 Menzies NA, Berruti AA, Blandford JM. The determinants of HIV treatment costs in resource limited settings. *PLoS One* 2012; 7:e48726.

120 Tager E. The cost of scaling-up antiretroviral treatment: a costing study in 161 representative facilities in Ethiopia, Malawi, Rwanda, and Zambia. In: *7th International AIDS Economics Network Pre-Conference Meeting, July 20-21*. Washington DC: ; 2012.

121 Marseille E, Giganti MJ, Mwango A, Chisembele-Taylor A, Mulenga L, Over M, *et al.* Taking ART to scale: determinants of the cost and cost-effectiveness of antiretroviral therapy in 45 clinical sites in Zambia. *PLoS One* 2012; 7:e51993.

122 Shiffman J. A social explanation for the rise and fall of global health issues. *B World Heal Organ* 2009; 87:608–13.

123 Whiteside A, Smith J. Exceptional epidemics: AIDS still deserves a global response. *Glob Heal* 2009; 5:15.

124 Balabanova D, Mills A, Conteh L, Akkazieva B, Banteyerga H, Dash U, *et al.* Good health at low cost 25 years on: lessons for the future of health systems strengthening. *Lancet* 2013; 381:2118–33.

Chapter 4. Estimating the health impact of recent changes in state-level cigarette taxes

Abstract

Cigarette smoking causes out of every five deaths in the U.S., and both state and federal governments have introduced cigarette excise taxes to limit cigarette consumption. Many states have raised these taxes in recent years, with the real value of the average state cigarette tax rising by over 200% between 1996 and 2013.

In this study we developed a mechanistic model of smoking behavior and associated health outcomes in the 50 U.S. states and District of Columbia, and used this model to assess the impact of state cigarette taxes introduced over the 17 years from 1996 to 2013. This analysis allowed separate effects on smoking initiation, smoking intensity, and quitting behavior, and estimated these effects in the context of a demographic model directly linking smoking behavior with mortality risks. Causal effects of cigarette taxes were estimated with data from the 1996-2012 rounds of the CDC's Behavioral Risk Factor Surveillance System. Our analyses made use of inter-state variation in the timing and magnitude of new cigarette taxes to identify causal effects.

Our analyses suggest that average national cigarette consumption by the beginning of 2013 was 4.4% (95% posterior interval: 3.7, 5.3) lower among men, and 3.6% (2.6, 4.2) lower among women, compared to a counterfactual scenario in which no new state cigarette taxes were introduced after 1996, for an overall reduction of 4.0% (3.3,4.6). The behavioral effects of tax increases were projected to be larger over a longer time horizon, with the average number of years spent smoking estimated to drop by 10 (7, 12) months for the 2013 birth cohort if exposed to 2013 vs. 1996 tax levels, for a 6.1% (4.5, 7.8) reduction in overall consumption. Estimates of the price elasticity of demand implied by these results varied from -0.14 to -0.39 depending on sex and the time horizon. These elasticities are smaller than conventional estimates for cigarette taxes and cigarette consumption, but are in line with other studies of inter-state tax variation.

Our analyses suggest 27 thousand (22, 34) deaths have been averted by state cigarette taxes introduced over the period 1996-2013, for an extra 119 thousand (92, 151) life-years lived. While these mortality reductions are relatively small, projections of future health outcomes under scenarios that compared 2013 and 1996 tax levels suggest that health benefits will largely accrue in future decades, with over a million extra life-years lived in the decade 2020-2029. We estimate a 2.0 (1.4, 2.7) month overall gain in life expectancy for the 2013 birth cohort due to state tax increases since 1996, with larger gains for men.

These analyses provide further evidence about the magnitude and distribution of effects of recent state cigarette taxes on smoking behavior and related mortality. Our analytic approach closely integrates the task of causal inference about cigarette taxation with the task of estimating final health outcomes. We hope that this analysis contributes to the knowledge base about cigarette taxation by providing a more nuanced understanding of the long-term consequences of cigarette tax policy.

4.1. Background

Both the federal government and individual U.S. states impose excise taxes on the sale of cigarettes. These taxes are assessed at the point of sale as a fixed mark-up on the quantity of cigarettes sold. Levying taxes on tobacco products serves multiple objectives for states, but a primary goal is to reduce smoking rates and in so doing reduce the risks of lung cancer and other adverse health effects associated with smoking [1,2]. Since 1995, individual states have raised the excise tax on cigarettes in 136 instances, with the average state excise tax rising from $0.31 (interquartile range = $0.19-$0.41) at the beginning of 1995 to $1.49 ($0.61-$2.00) by the end of 2012, more than four times its 1995 level. Over this same period, the federal excise tax rose from $0.24 to $1.01. State excise taxes produce the majority of tax revenue from cigarette sales in the United States, with $17.3 billion collected in the year ending June 30, 2011, as compared to $15.5 billion for federally imposed taxes and $0.4 billion for taxes imposed by municipalities [3].

Cigarette smoking is known to cause or aggravate a large number of health problems, leading to substantial mortality and morbidity [4–6]. In the United States, smoking is estimated to cause one quarter of all deaths between the ages of 35 and 70 [7], with smokers facing a life expectancy shortened by more than 10 years compared to individuals who have never smoked [4]. Individuals who quit smoking have been shown to regain much of this loss in life expectancy, especially those who quit at younger ages [4,8], and reduced smoking intensity is also associated with health benefits [5].

A large body of research suggests that raising cigarette taxes will reduce cigarette consumption [9], either through reducing smoking initiation, increasing quitting, or reduced smoking frequency. Many studies have investigated the relationship between taxation and smoking behavior, and the price elasticity of demand is generally found to be in the range of -0.4, implying that a 10% price increase would produce a 4% reduction in demand, with greater elasticity estimated for younger

age groups [10]. A number of studies have focused on state excise taxes in the U.S., with variation in these taxes between states and over time used to separate the causal effect of excise taxes from other influences on smoking behavior [11–20]. There is also reason to believe that the effects of these state-level tax changes may differ from changes in the federal tax, given the greater opportunity for smokers to avoid the effect of state-level tax increases by shifting purchasing to states with lower tax rates [21,22]. Evidence on the impact of state cigarette taxes on smoking behavior is mixed, with effect sizes estimated by previous studies smaller and less robust [11–20] than would be predicted from the broader evidence base on tax effects.

In general, analyses of state excise taxes focus on individual aspects of smoking behavior (e.g., smoking initiation, smoking prevalence, smoking intensity) and do not directly estimate the change in health outcomes resulting from changes in tax policy. Where these health impacts are estimated, it is commonly through simple multiplicative calculations used to explore possible ramifications of changes in smoking behavior, with a lower level of rigor than is applied to the analysis of behavioral outcomes. One exception to this is in the context of the California Tobacco Control Program, where Fichtenberg and Glantz were able to identify statistically significant reductions in the mortality associated with heart disease following the introduction of the program in 1989 [17]. The California program combined a $0.25 per pack increase in the state tobacco tax with an aggressive anti-smoking media campaign and additional programs fostering a smoke-free environment, and it is difficult to attribute the changes in cardiovascular mortality to tax changes alone. This is especially true given the partial rebound in cardiovascular mortality observed after the non-tax elements of the program were cut back in 1992 [17].

The present analysis takes a different approach to estimating the effects of cigarette excise taxes on mortality risks. The causal effects of cigarette excise taxes on smoking behavior are quantified in the context of a mechanistic population model, which directly relates individual age, sex, and

smoking behavior to mortality rates. This model simulates the distribution of smoking behaviors across the U.S. population, and calibrates the parameters determining this model—including parameters describing the effect of tax changes on smoking behavior—to observed patterns of smoking behavior reported by the Behavioral Risk Factor Surveillance System (BRFSS) between 1996 and 2013 [23]. With this analytic approach, it is possible to distinguish the separate effects of state cigarette taxes on smoking initiation, cessation, and smoking intensity, and to estimate the consequences for summary health outcomes such as mortality and life expectancy. These outcomes are available for individual states as well as individual sex and age groups. This analysis is used to estimate the effects of recent increases in state cigarette taxes on smoking behavior and on smoking-related mortality over the period 1996-2013, and to predict changes in long-term trends in smoking behavior and related mortality attributable to the state cigarette taxes.

4.2. Methods

4.2.1. General approach

A mathematical model was constructed to predict changes in smoking behavior as a function of individual characteristics and multiple state-level predictors. Model parameters were estimated using a likelihood function that summarized BRFSS survey data collected between 1996 and 2013, with the estimation approach designed to identify the causal effect of state-level cigarette tax changes on smoking behavior. The fitted model was then used to predict changes in smoking behavior and related mortality under various tax scenarios, in order to describe the health consequences of changes in state-level cigarette tax policy.

4.2.2. Identification strategy

States with higher cigarette excise taxes tend to have a lower prevalence of smoking behavior. However, this empirical relationship cannot be interpreted as causal, given the possibility of other state characteristics that determine both tax policy and smoking behavior. Randomized experiments allow stronger identification of causal effects, yet experiments to address issues of tax policy are rare, and the more rigorous studies of cigarette policy within the U.S. generally adopt quasi-experimental designs to estimate the causal effects of tax policy from observed variation in cigarette taxation. A common approach is to include state and year fixed effects as part of a regression of some indicator of smoking behavior on tax rates and other predictors [11,15,24,25]. This identification strategy assumes that the average year-on-year change in the smoking outcome would be the same in states that introduce cigarette taxes as those that do not, were no taxes introduced. If these trends are found to systematically differ in states that raise cigarette taxes, as compared to those that do not, this difference is attributed to the tax change.

While appealing the inclusion of state and year fixed effects can introduce challenges, due to the shear number of predictors used to fit the model. Arguing that state anti-smoking sentiment is the key confounder of the observed relationship between tax policy and smoking behavior, DeCicca *et al.* proposed a new indicator of state-level anti-smoking sentiment [12] as an alternative to state and year fixed effects. They calculated this measure from a factor analysis of attitudes towards tobacco control and smoking behavior reported in the Community Population Survey. They found that inclusion of this anti-smoking indicator in regression equations performs similarly to the state and years fixed effects specification, and use this identification strategy to investigate the relationship between cigarette prices and smoking behavior among youths [12] and older adults [11]. The present analysis adopts the identification approach developed by DeCicca *et al.*, by including a measure of state-level anti-smoking behavior in the model equations used to predict

smoking initiation, smoking intensity, and quitting behavior. Figure 4.1 shows a directed acyclic graph describing the causal relationships assumed in this analysis.

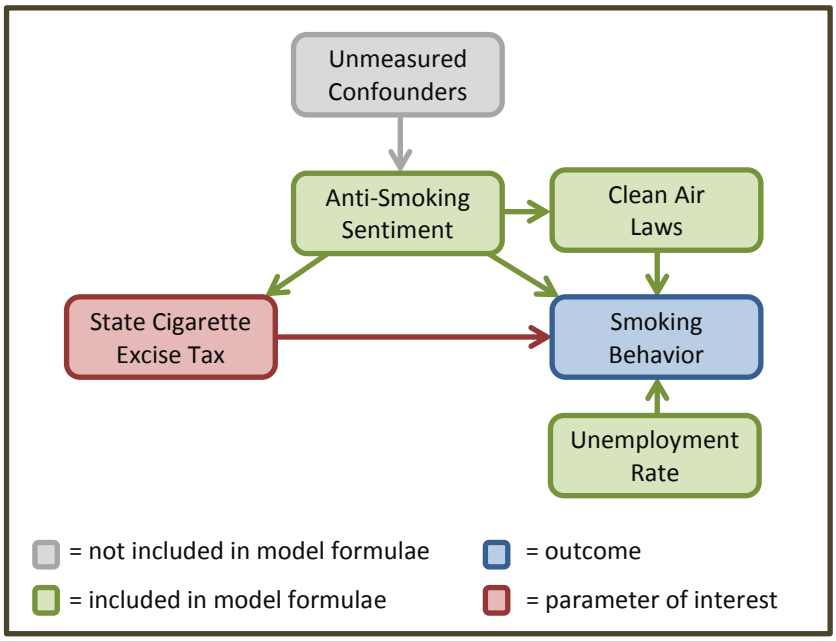

Figure 4.1. Directed acyclic graph describing causal relationships assumed in this analysis

4.2.3. Simulation model

A mathematical model was developed to represent successive cohorts of the total U.S. population (distinguished by sex, year of age, and state of residency), and describe how the smoking behavior of each cohort changes over time. A schematic of the compartments and transitions of this model is shown in Figure 4.2. These compartments are structured to match the categorization of smoking behavior in the BRFSS, as well categories used by Thun *et al.* [5] to define smoking-attributable mortality risks. The use of an approach that allows for different effects on various aspects of smoking behavior expands on work by DeCicca *et al.*, who report analyses that explicitly allow for changes in smoking initiation and cessation behavior to explain overall changes in smoking participation as a result of tax changes [13]. The model developed for this analysis also bears

similarities to simulation models used to estimate health outcomes based on exogenous estimates of tax effects [14,26–28].

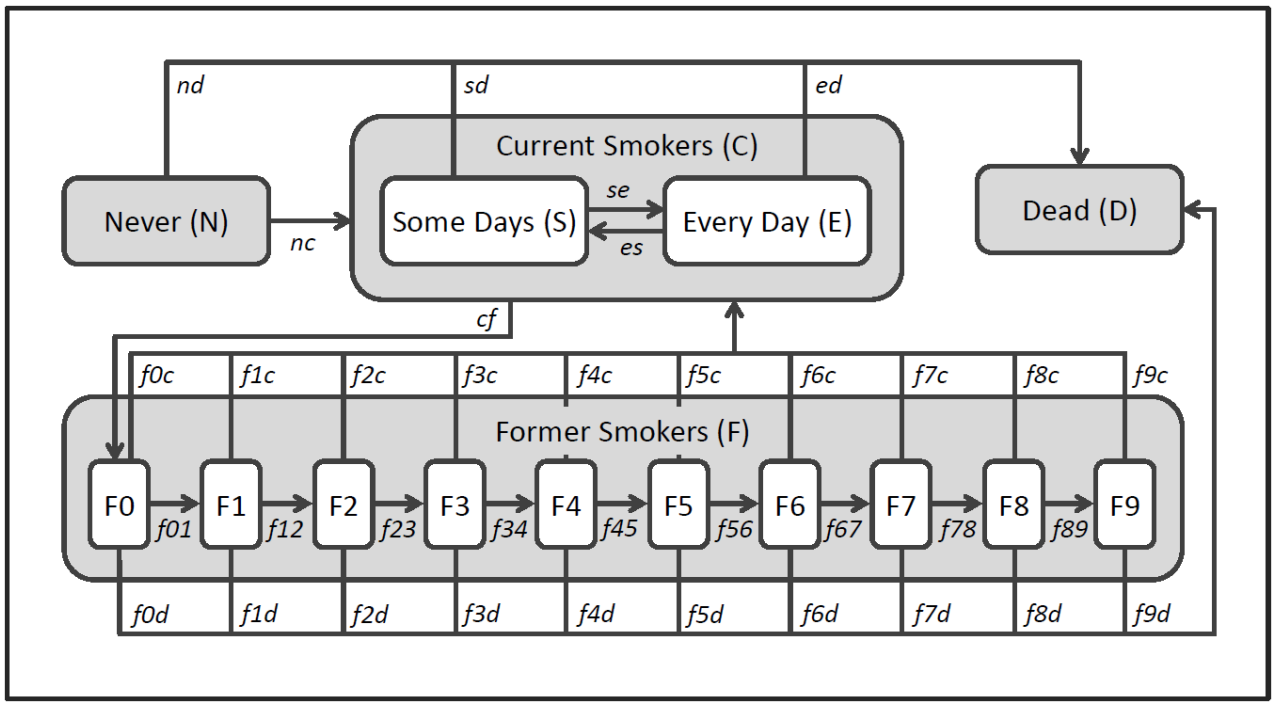

Figure 4.2. Schematic of simulation model, showing model compartments and transitions for a single cohort*

* Capital letters (e.g., N) indicate the number of individuals in each model compartment. Lower case letters (e.g., *nc*) indicate transition probabilities. Former smokier compartments 0 though 9 represent time since quitting.

The analysis is initiated with individuals distributed across the different model compartments to reflect the existing distribution in the population at the beginning of 1996. The distribution of individuals across model compartments is then updated each quarter, with individuals transitioning to different compartments based on transition probabilities which are themselves updated each quarter. Individuals in the 'Never' compartment remain in this compartment unless

they begin smoking. Those who start smoking transition to the 'Current' smoker compartments. Current smokers are divided in those who smoke 'Some Days' those who smoke 'Every Day', to allow for differences in smoking intensity within the smoking population. Current smokers can transition between these two intensity levels or quit smoking, with those who quit transitioning to the first 'Former' compartment. Former smokers progress through Former compartments 0 through 9 to track time since quitting (representing <1, 1, 2-4, 5-9, 10-14, 15-19, 20-29, 30-39, 40-49, and ≥50 years since quitting, respectively). Individuals in any of the Former smoker compartments can relapse, returning to the Current smoker compartments. In addition, individuals in any compartment can die and transition to the 'Dead' compartment, with mortality risks determined by age and smoking behavior, as well as by time trends in background mortality.

A separate cohort is formed to represent each year of age for all individuals alive in 1996 (ages 0-99, for 100 age categories), each state (including the District of Columbia, for 51 state categories), and each sex, producing a total of 100 x 51 x 2 = 10,200 cohorts. The distribution of individuals in each cohort across smoking behavior categories is updated every quarter from the beginning of 1996 to early 2013 (70 quarters in total), representing the total time period during which survey responses were being collected for BRFSS rounds 1996 to 2012.

4.2.4. Parameterization

The outcomes of the model (changes in smoking prevalence and related mortality) are determined by transition probabilities that describe the rates at which individuals move between different model compartments. These transition probabilities are described in detail below. In Figure 4.2 and in the description below, the number of individuals in each compartment is specified by capital letters (N for never smokers, S for current smokers who smoke some days, E for current smokers who smoke every day (C representing the sum of all current smokers), and F0 through F9 for former smokers categorized by time since smoking), with subscripts *atgi* for age *a* (in whole years),

calendar time *t* (in quarters since the beginning of 1996), sex *g*, and state *i*. The transition probability between two compartments is specified as a lower case combination of the first letter of the names of each compartment. For example, es_{atgi} indicates the transition probability from the Every compartment to the Some compartment for a particular age, time, sex and state.

4.2.4.1. Smoking initiation

The probability of smoking initiation is determined by the parameter nc_{atgi}. This parameter is assumed to be a function of individual age, calendar time, sex, and the state in which an individual resides. The effects of age and time on the smoking initiation probability are allowed to vary smoothly, each operationalized as a penalized B-spline with knots every 10 years[1] [29,30]. The effect of state of residence is assumed to operate through a set of independent variables, including a measure of state-level unemployment, indicators for the presence or absence of state-level clean air laws (for workplaces, bars, and restaurants separately), the indicator of anti-smoking sentiment described by DeCicca *et al.* [12], and the state cigarette tax, in 2013 constant dollars. Unemployment, clean air laws, and tax rates are all time-varying variables, while anti-smoking sentiment is assessed in 1995-1996, the year before the BRFSS time series begins. For each state, the tax variable is set equal to zero in 1995, such that the variable represents absolute increases in

---

[1] These splines are operationalized with cubic basis splines and a 2nd degree difference penalty. For age, a total of 10 knots are used (every 10 years from age 0 to age 100) requiring 13 basis splines and thus 13 spline parameters. For calendar time, a total of 3 knots are used (every 10 years at 1996, 2006, and 2016), requiring 5 basis splines. As two independent splines are used, a model thus specified would effectively have two intercept terms. To resolve this issue, the value of the year spline is fixed at zero at the beginning of the time series in 1996, by specifying the first spline parameter α_{21} as function of the 2nd and 3rd spline parameters: $\alpha_{21} = 4 * \alpha_{22} + \alpha_{23}$.

the state cigarette tax since this time point. As transition probabilities are defined over the interval [0, 1], the logit of the transition probability is modeled as a linear function of these predictors. The model is estimated separately for each sex.

$$logit(nc_{atgi}) = f_{\text{age}}(\alpha_{1\text{g}}, a) + f_{\text{time}}(\alpha_{2\text{g}}, t) + \alpha_{3\text{g}} * UN_{ti} + \alpha_{4\text{g}} * WP_{ti} + \alpha_{5\text{g}} * RST_{ti} + \alpha_{6\text{g}} * BAR_{ti} + \alpha_{7\text{g}} * ANTI_i + \alpha_{8\text{g}} * TX_{ti} \quad [1]$$

nc_{atgi} : quarterly probability of smoking initiation for individuals with age *a* in quarter *t*, sex *g,* and state *i*

a : age (in quarters)

y : calendar time (in quarters)

UN_{ti} : unemployment rate, in quarter *t* and state *i*

WP_{ti} : indicator variable for laws restricting smoking in workplaces, in quarter *t* and state *i*

RST_{ti} : indicator variable for laws restricting smoking in restaurants, , in quarter *t* and state *i*

BAR_{ti} : indicator variable for laws restricting smoking in bars, , in quarter *t* and state *i*

$ANTI_i$: measure of state anti-smoking sentiment for state *i*

TX_{ti} : cigarette excise tax in quarter *t* in state *i*, in dollars per pack

f_{age}, f_{time} : a set of penalized B-splines allowing smooth curves to be fitted to age and time

As the survey data used to fit the model are collected from individuals >18 years of age, age-related changes in smoking initiation risks will be poorly identified in younger age groups. To prevent implausible results, smoking initiation probabilities are set to zero for all individuals younger than

10 years old. In addition, given the cross-sectional nature of the BRFSS data, it is impossible to distinguish whether newly initiating individuals begin smoking with higher or lower intensity relative to other smokers. For this reason new smokers are assumed to enter the Some and Every compartments proportionally to the distribution of individuals already in those compartments, operationalized as the parameters ne_{atgi} and ns_{atgi} for the transition probabilities from Never to Some and Never to Every respectively:

$$ne_{atgi} = nc_{atgi} \frac{E_{atgi}}{E_{atgi}+S_{atgi}} \quad [2]$$

$$ns_{atgi} = nc_{atgi} \left(1 - \frac{E_{atgi}}{E_{atgi}+S_{atgi}}\right) \quad [3]$$

4.2.4.2. Smoking intensity

Individuals transition between Some and Every compartments as determined by the parameters es_{atgi} and se_{atgi} (transition probabilities for Every to Some, and from Some to Every respectively). The rate at which individuals move between levels of smoking intensity (i.e., the true values of es_{atgi} and se_{atgi}) is not identifiable from the BRFSS data, which only provides information on overall changes in distribution between these two categories[2]. Instead, these transition probabilities are operationalized as a function of the distribution across the two compartments, for a particular age, year, and state. Where $P(E_{atgi} | C_{atgi})$ represents the probability of being in the Every compartment, conditional on being in one of the Current smoker compartments, the values of es_{atgi} and se_{atgi} were calculated using the following equations:

[2] In addition, there is no evidence that this information would be relevant to subsequent smoking behavior or mortality risks.

$$se_{atgi} = P\left(E_{atgi} \mid C_{atgi}\right) \quad [4]$$

$$es_{atgi} = \left(1 - P\left(E_{atgi} \mid C_{atgi}\right)\right) \quad [5]$$

These equations implicitly assume that any changes in the predictors of smoking intensity will have an instantaneous effect on the distribution between Some Day and Every Day smokers[3].

As with nc_{atgi} , the logit of $P\left(E_{atgi} \mid C_{atgi}\right)$ is estimated as a linear function of age, calendar time, and multiple state-level predictors:

$$logit\left(P\left(E_{atgi} \mid C_{atgi}\right)\right) = f_{\text{age}}(\beta_{1\text{g}}, a) + f_{\text{time}}(\beta_{2\text{g}}, t) + \beta_{3\text{g}} * UN_{ti} + \beta_{4\text{g}} * WP_{ti} + \beta_{5\text{g}} * RST_{ti} + \beta_{6\text{g}} * BAR_{ti} + \beta_{7\text{g}} * ANTI_{i} + \beta_{8\text{g}} * TX_{ti} \quad [6]$$

$P\left(E_{atgi} \mid C_{atgi}\right)$: the fraction of current smokers in the who smoke every day, for individuals with age *a* in quarter *t*, sex *g,* and state *i*

a : age (in quarters)

y : calendar time (in quarters)

UN_{ti} : unemployment rate, in quarter *t* and state *i*

WP_{ti} : indicator variable for laws restricting smoking in workplaces, in quarter *t* and state *i*

RST_{ti} : indicator variable for laws restricting smoking in restaurants, , in quarter *t* and state *i*

BAR_{ti} : indicator variable for laws restricting smoking in bars, , in quarter *t* and state *i*

[3] While it is plausible that smoking intensity could change slowly in response to these determinants, it is unlikely that such effects could be identified with the cross-sectional data used for this analysis.

$ANTI_i$: measure of state anti-smoking sentiment for state *i*

TX_{ti} : cigarette excise tax in quarter *t* in state *i*, in dollars per pack

f_{age}, f_{time} : a set of penalized B-splines allowing smooth curves to be fitted to age and time

4.2.4.3. Smoking cessation and relapse

Individuals transition between the Current smoking compartments and the Former smoking compartments as determined by the parameters $cf0_{atgi}$ (which describes the probability of quitting for current smokers) and $f0c_{atgi}$ through $f9c_{atgi}$ (which describe probabilities of relapse for former smokers as a function of time since quitting). The parameters $cf0_{atgi}$ and $f0c_{atgi}$ are calculated using a similar approach to that used to model changes in smoking intensity, with the parameter $P\left(C_{atgi} | F0_{atgi} \cup C_{atgi}\right)$ defined as the number of current smokers (for a particular combination of age, time, sex and state), divided by the number of current smokers plus those who have quit within the last 12 months[4].

$$f0c_{atgi} = P\left(C_{atgi} | F0_{atgi} \cup C_{atgi}\right) \quad [7]$$

$$cf0_{atgi} = \left(1 - P\left(C_{atgi} | F0_{atgi} \cup C_{atgi}\right)\right) \quad [8]$$

These equations implicitly assume that any changes in the predictors of smoking cessation will have an instantaneous effect on the distribution between the Current compartment and the first Former compartment. Lower values of $P\left(C_{atgi} | F0_{atgi} \cup C_{atgi}\right)$ will indicate higher rates of quitting and transition out of the Current compartments. As the Current compartments are

[4] This can be thought of as the fraction who elected not to quit, of those smoking 12 months ago.

subdivided into Some and Every, the transition parameters for these compartments need to be defined:

$$f0e_{atgi} = f0c_{atgi} \frac{E_{atgi}}{E_{atgi} + S_{atgi}} \quad [9]$$

$$f0s_{atgi} = f0c_{atgi} \left(1 - \frac{E_{atgi}}{E_{atgi} + S_{atgi\,ayi}}\right) \quad [10]$$

$$ef0_{atgi} = sf0_{atgi} = cf0_{atgi} \quad [11]$$

This assumes that individuals who reinitiate smoking are distributed across the Some and Every compartments based on the current distribution between these compartments, and that individuals in the Some and Every compartments share the same probability of transition to the first Former compartment.

As with other transition probabilities, the logit of $P\left(C_{atgi} | F0_{atgi} \cup C_{atgi}\right)$ is estimated as a linear function of age, calendar time, and multiple state-level predictors:

$$logit\left(P\left(C_{atgi} | F0_{atgi} \cup C_{atgi}\right)\right) = f_{\text{age}}(\delta_{1\text{g}}, a) + f_{\text{time}}(\delta_{2\text{g}}, t) + \delta_{3\text{g}} * UN_{ti} + \delta_{4\text{g}} * WP_{ti} + \delta_{5\text{g}} * RST_{ti} + \delta_{6\text{g}} * BAR_{ti} + \delta_{7\text{g}} * ANTI_{i} + \delta_{8\text{g}} * TX_{ti} \quad [12]$$

$P\left(C_{atgi} | F0_{atgi} \cup C_{atgi}\right)$: the fraction of current smokers, out of all individuals who smoke or quit within the last 12 months for individuals with age *a* in quarter *t*, sex *g,* and state *i*

a : age (in quarters)

y : calendar time (in quarters)

UN_{ti} : unemployment rate, in quarter *t* and state *i*

WP_{ti} : indicator variable for laws restricting smoking in workplaces, in quarter *t* and state *i*

RST_{ti} : indicator variable for laws restricting smoking in restaurants, , in quarter *t* and state *i*

BAR_{ti} : indicator variable for laws restricting smoking in bars, , in quarter *t* and state *i*

$ANTI_i$: measure of state anti-smoking sentiment for state *i*

TX_{ti} : cigarette excise tax in quarter *t* in state *i*, in dollars per pack

f_{age}, f_{time} : a set of penalized B-splines allowing smooth curves to be fitted to age and time

Probabilities of smoking relapse for individuals who have quit for >12 months (Former compartments 1 - 9) are estimated using a proportional hazards assumption, whereby the rate of reinitiating smoking is assumed to represent a fixed multiple of the rate estimated for those who have quit in the last 12 months (this rate being a transformation of the probability $f0c_{atgi}$). The decline in the rate of smoking relapse as a function of time is modeled using a Weibull distribution (previously used by other analyses to model hazards of smoking relapse [31]). The survival function associated with the Weibull distribution, $S(t)$, can be used to compute $p(a, b)$, the probability of relapse between the time when an individual enters a particular Former compartment (a), and the time when an individual moves to the next Former compartment (b).

$$p(a,b) = \frac{S(a)-S(b)}{S(a)} = \frac{e^{-\left(\frac{a}{\lambda}\right)^k} - e^{-\left(\frac{b}{\lambda}\right)^k}}{e^{-\left(\frac{a}{\lambda}\right)^k}} = 1 - e^{-(a^k - b^k)\lambda^{-k}} \quad [13]$$

This probability can be used to calculate the average relapse rate for the compartment, $\bar{h}(a, b)$:

$$\bar{h}(a,b) = \frac{-ln(1-p(a,b))}{b-a} = \frac{-ln\left(1-\left(1-e^{-\left(a^k-b^k\right)\lambda^{-k}}\right)\right)}{b-a} = \frac{b^k-a^k}{(b-a)\lambda^k} \quad [14]$$

The ratio of these average relapse rates (where rr_j represents the rate ratio of relapse for Former compartment *j* relative to the first Former compartment) can be used to calculate the transition probabilities for smoking relapse for all Former compartments as a function of $f0c_{atgi}$ and the Weibull parameter *k* (note that Weibull parameter λ drops out of the equation).

$$rr_j = \frac{b_j^k - a_j^k}{(b_j - a_j)\lambda^k} \Big/ \frac{b_0^k - a_0^k}{(b_0 - a_0)\lambda^k} = \frac{\left(b_j^k - a_j^k\right)(b_0 - a_0)}{(b_0^k - a_0^k)(b_j - a_j)} \quad [15]$$

$$fjc_{atgi} = 1 - e^{ln(1 - f0c_{atgi})\, rr_j} = 1 - e^{ln(1 - f0c_{atgi})\frac{\left(b_j^k - a_j^k\right)(b_0 - a_0)}{(b_0^k - a_0^k)(b_j - a_j)}} \quad \text{for } j \in [1, 2 \ldots 9] \quad [16]$$

4.2.4.4. Progression through former smoker states

Former smokers who do not die or relapse will progress through Former compartments 0 to 9 in sequence. The transition probabilities for this progression are defined deterministically as the inverse of the number of quarters each state represents. Thus the transition probability from the first to the second Former compartment (*f01*) is equal to ¼, producing an average sojourn time of 1 year for individuals in the first Former compartment who do not die or relapse.

4.2.4.5. Mortality

Mortality risks are operationalized as a function of age, calendar time, sex, and smoking behavior compartment:

$$jd_{atg} = 1 - e^{-\frac{1}{4}\mu^b_{atg}\tau_{gj}} \quad \text{for } j \in [n, s, e, f0, f1, f2, f3, f4, f5, f6, f7, f8, f9] \quad [17]$$

jd_{ay} : quarterly mortality risk for individuals in compartment *j*, age *a,* quarter *t,* and sex *g*

μ^b_{atg} : smoking-deleted background mortality rate for age *a,* quarter *t*, and sex *g*

τ_{gj} : mortality rate ratio for sex *g* and compartment *j,* relative to a never smoking population of the same sex (i.e., $\tau_{gn} = 1.0$)

4.2.4.6. Model formulae

The model is implemented as a set of difference equations. These formulae operationalize the description given above[5].

$$N_{z+1} = N_z(1 - nd_{atg})(1 - ns_{atgi} - ne_{atgi}) \quad [18]$$

$$S_{z+1} = z(1 - sd_{atgi})(1 - sf0_{atgi})(1 - se_{atgi}) + N_z(1 - nd_{atg})ns_{atgi} + E_z(1 - ed_{atg})(1 - ef0_{atgi})es_{atgi} + \sum_{j=0}^{9} Fj_z\ (1 - fjd_{atg})fjs_{atgi} \quad [19]$$

$$E_{z+1} = E_z(1 - ed_{atg})(1 - ef0_{atgi})(1 - es_{atgi}) + N_z(1 - nd_{atg})ne_{atgi} + S_z(1 - sd_{atg})(1 - sf0_{atgi})se_{atgi} + \sum_{j=0}^{9} Fj_z\ (1 - fjd_{atg})fje_{atgi} \quad [20]$$

$$F0_{z+1} = F0_z(1 - f0d_{atg})(1 - f0s_{atgi} - f0e_{atgi})(1 - f01) + S_z(1 - sd_{atg})sf0_{atgi} + E_z(1 - ed_{ay})ef0_{atgi} \quad [21]$$

$$F1_{z+1} = F1_z(1 - f1d_{atg})(1 - f1s_{atgi} - f1e_{atgi})(1 - f12) + F0_z(1 - f0d_{atg})(1 - f0s_{atgi} - f0e_{atgi})f01 \quad [22]$$

$$F2_{z+1} = F2_z(1 - f2d_{atg})(1 - f2s_{atgi} - f2e_{atgi})(1 - f23) + F1_z(1 - f1d_{atg})(1 - f1s_{atgi} - f1e_{atgi})f12 \quad [23]$$

$$F3_{z+1} = F3_z(1 - f3d_{atg})(1 - f3s_{atgi} - f3e_{atgi})(1 - f34) + F2_z(1 - f2d_{atg})(1 - f2s_{atgi} - f2e_{atgi})f23 \quad [24]$$

$$F4_{z+1} = F4_z(1 - f4d_{atg})(1 - f4s_{atgi} - f4e_{atgi})(1 - f45) + F3_z(1 - f3d_{atg})(1 - f3s_{atgi} - f3e_{atgi})f34 \quad [25]$$

$$F5_{z+1} = F5_z(1 - f5d_{atg})(1 - f5s_{atgi} - f5e_{atgi})(1 - f56) + F4_z(1 - f4d_{atg})(1 - f4s_{atgi} - f4e_{atgi})f45 \quad [26]$$

[5] These equations implicitly assume a single value for each transition probability for all individuals of a given age/time/sex/state subgroup, while in reality we would expect that individuals within a particular subgroup might differ in their propensity to begin smoking, to quit smoking, to relapse, etc. For this reason the model can be seen as an approximation that calculates subgroup-level averages for each of the model parameters, but that individual level outcomes (for example, the change in smoking initiation risk associated with a change in cigarette tax rates) may differ from these group-level averages.

$$F6_{z+1} = F6_z(1 - f6d_{atg})(1 - f6s_{atgi} - f6e_{atgi})(1 - f67) + F5_z(1 - f5d_{atg})(1 - f5s_{atgi} - f5e_{atgi})f56 \quad [27]$$

$$F6_{z+1} = F6_z(1 - f6d_{atg})(1 - f6s_{atgi} - f6e_{atgi})(1 - f67) + F5_z(1 - f5d_{atg})(1 - f5s_{atgi} - f5e_{atgi})f56 \quad [28]$$

$$F7_{z+1} = F7_z(1 - f7d_{atg})(1 - f7s_{atgi} - f7e_{atgi})(1 - f78) + F6_z(1 - f6d_{atg})(1 - f6s_{atgi} - f6e_{atgi})f67 \quad [29]$$

$$F8_{z+1} = F8_z(1 - f8d_{atg})(1 - f8s_{atgi} - f8e_{atgi})(1 - f89) + F7_z(1 - f7d_{atg})(1 - f7s_{atgi} - f7e_{atgi})f78 \quad [30]$$

$$F9_{z+1} = F9_z(1 - f9d_{atg})(1 - f9s_{atgi} - f9e_{atgi}) + F8_t(1 - f8d_{atg})(1 - f8s_{atgi} - f8e_{atgi})f89 \quad [31]$$

$$D_{z+1} = D_z + N_z nd_{atg} + S_z sd_{atg} + N_z nd_{atg} + F0_z f0d_{atg} + F1_z f1d_{atg} + F2_z f2d_{atg} + F3_z f3d_{atg} + F4_z f4d_{atg} + F5_z f5d_{atg} + F6_z f6d_{atg} + F7_z f7d_{atg} + F8_z f8d_{atg} + F9_z f9d_{atg} \quad [32]$$

In these equations, subscript *z* indicates a particular subgroup *atgi*, and *z+1* indicates the next quarter for the same subgroup (i.e., where both *a* and *t* have been incremented up by 1).

4.2.5. Data sources

4.2.5.1. Data on smoking behavior

The CDC's Behavioral Risk Factor Surveillance Survey (BRFSS) is a large telephone survey of Americans aged >18 years, conducted annually to monitor national and state-level prevalence of behavioral risk factors for premature morbidity and mortality [23]. Since being initiated in 1984, the BRFSS has asked respondents several questions related to smoking behavior, including current smoking status, past smoking status, time since quitting, and smoking intensity. A major change in the question about smoking intensity occurred between 1995 and 1996 surveys, and for this reason the analysis is restricted to the period 1996-2013, over which smoking-related survey questions were largely unchanged.

Current smoking status: one set of questions allows respondents to be categorized by current smoking status, specifically those who report having never smoked, current smokers who report smoking "some days", current smokers who report smoking "every day", and former smokers. This set of questions has been asked each year from 1996 to 2013. The data from these questions were

used to construct a likelihood function for the distribution of individuals across compartments N, S, E, and the sum of compartments F0-F9.

Smoking intensity: differences in smoking intensity are associated with differences in smoking attributable mortality risks, and Thun *et al*. report mortality risk ratios for current smokers as a function of the number of cigarettes smoked per day [5]. While the categorization of current smokers in the BRFSS (those who smoke "some days" vs. those who smoke "every day") indicates qualitative differences in smoking intensity, these descriptions need to be mapped to a quantitative measure of cigarette consumption in order to calculate the appropriate mortality risks. To provide a cross-walk from the survey responses to the Thun *et al*. mortality estimates we use additional data from survey questions on the number of cigarettes smoked each day. These questions were posed to individuals who reported smoking "every day" in survey years 1996 to 2000. Figure 4.3 shows the relationship between the average number of cigarettes smoked each day for individuals reporting smoking every day, as a function of age, sex, and survey year.

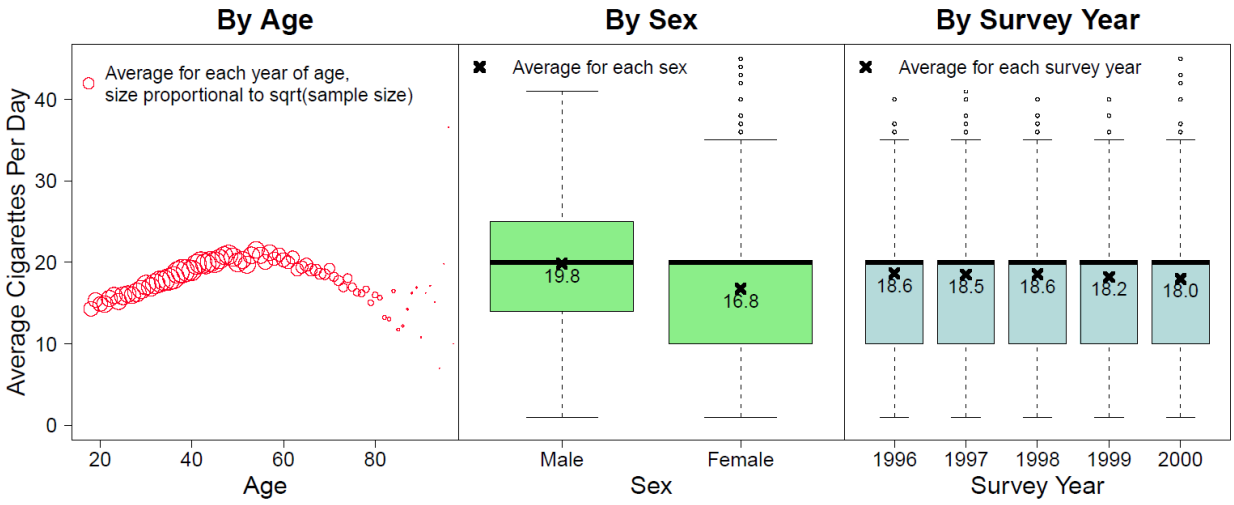

Figure 4.3. Average number of cigarettes smoked each day for individuals reporting smoking every day, as a function of age, sex, and BRFSS survey year

As can be seen in Figure 4.3, smoking intensity varies somewhat between different ages, and also between men and women. However, these differences are relatively minor, and were ignored for the purposes of calculating the fraction of "every day" smokers who fell into different categories of cigarettes smoked per day. These percentages were calculated as 13% smoking <10 cigarettes per day, 32% smoking 10-19 cigarettes per day, 47% smoking 20-39 cigarettes per day, and 8% smoking ≥40 cigarettes per day. No such questions was asked for individuals reporting smoking only "some days", and these individuals were assumed to smoke <10 cigarettes per day (the lowest risk category) for the purposes of estimating smoking mortality rate ratios for each model compartment.

Time since quitting: an additional set of questions allows former smokers to be categorized according to time since quitting. These questions have changed over the years, allowing the following categorization:

Survey years 1996-2000	<1 year[6], 1-4 years, 5-14 years, and 15+ years since quitting
Survey years 2001-2005	<1 year, 1-4 years, 5-9 years, and 10+ years since quitting
Survey years 2006-2008	Question not asked
Survey years 2009-2013	As in 2001-2005

For the years when these questions were asked, data were used to construct a likelihood function for the distribution of individuals across former smoker states, with modelled former smoker categories grouped to fit the categorization used in the survey questions.

[6] The survey questions allow the group reporting <1 year since quitting to be broken up into several smaller categories, but this level of granularity was ignored for the analysis.

Survey weighting: the BRFSS publishes weights to be used to adjust for known biases in the BRFSS sampling frame, such that summary estimates calculated using these weights should be representative of the adult U.S. population. Using probability weights will have consequences for the uncertainty represented by the likelihood, and although these issues have been apparent for many years [32,33], the methodological difficulties have not yet been fully resolved [34]. While regression methods for the analysis of weighted data are better developed, the appropriate use of weights in an analysis such as required for the present study is not immediately apparent. If weights are used directly when constructing a likelihood, the implied sample size (and hence the relative dispersion of the likelihood) may not reflect the strength of information in the data[7]. If these weights are not used, the likelihood may not be reflective of the general U.S. population and parameter estimates will be biased. A revised weighting scheme was developed to satisfy these two concerns:

(i) For each combination of age (in whole years), quarter, sex, and state, the distribution of survey respondents across smoking behavior categories (never, current some days, current every day, and former) was calculated using the published weights.

(ii) For each combination of age (in whole years), quarter, sex, and state, the effective sample size (ESS) was calculated, where $ESS = (\sum_{i \in I} w_i)^2 / (\sum_{i \in I} w_i^2)$ for the vector of survey weights w and observations $i \in I$.

(iii) The distribution across smoking behavior categories calculated in (i) was scaled by a common factor such that the sum matched the ESS calculated in (ii). For each combination of age,

[7] With unequal weights, the effective sample size will always be less than the original sample size. At the extreme, a set of probability weights equal to 1.0 for one observation and 0.0 otherwise will always have an effective sample size of 1.0, irrespective of the original sample size.

quarter, sex, and state, this adjustment can be considered as a new weight $\widehat{w}_i$ applied to the raw survey data:

$$\widehat{w}_i = \frac{w_i(\sum_{i\in I} w_i)^2}{(\sum_{i\in I} w_i)(\sum_{i\in I} w_i^2)} \quad [33]$$

The survey dataset, once processed in this way, preserves the weighted distribution across smoking behavior categories while also reflecting the reduction in effective sample size associated with non-equal weights. The same approach was used to adjust the survey data describing time since quitting among former smokers.

Finally, the respondent-level data were summarized into total counts by age, sex, state, quarter, and smoking behavior category. This allowed the large datasets to be manipulated more efficiently during analysis while retaining the same informational content.

4.2.5.2. Data on smoking-related mortality risks

Several recently published studies summarize smoking-related mortality risks in different populations [4–6]. The present analysis utilizes estimates reported by Thun *et al*., who synthesize data from multiple large observational cohorts to estimate relative risks of smoking mortality as a function of sex, current smoking behavior, smoking frequency, and time since quitting [5].

4.2.5.3. Data on smoking-deleted background mortality

Smoking is known to cause a non-trivial fraction of total U.S. mortality [35,36]. For this reason, the background mortality estimates used for this analysis must have smoking-attributable mortality removed, to prevent double counting of this mortality risk and overestimation of total mortality rates. While the National Center for Health Statistics publishes cause-deleted life tables for various

health concerns [37], smoking is not included in these estimates. Smoking-deleted mortality estimates were created for this analysis following an approach described by Levy *et al.* [27].

For a given age (a), sex (g), and time (t), the all-cause mortality rate (μ_{atg}^{all}) can be related to the smoking-deleted mortality rate (μ_{atg}^{b}), the relative risks associated with each smoking behavior category (τ_{gj} for smoking category *j*), and the distribution of smoking behavior in the population (where m_{atgj} represents the fraction of the population in smoking state *j* for a particular age, sex, and time):

$$\mu_{atg}^{all} = \sum_j \tau_{gj} * \mu_{atg}^{b} * m_{atgj} \quad [34]$$

This can be rearranged to express smoking-deleted mortality as a function of the other terms:

$$\mu_{atg}^{b} = \frac{\mu_{atg}^{all}}{\sum_j \tau_{gj} * m_{atgj}} \quad [35]$$

This relationship was used to estimate smoking-deleted mortality rates for both men and women, for each single year of age, for years 1996-2013. To do so, yearly all-cause mortality estimates were derived from life tables published by the U.S. Centers for Disease Control [38,39]. As single-year life tables were not available for the year 1996 and had not yet been published for years 2009-2013, mortality rates for these years were obtained by extrapolating time trends during the period 1997-2008. Data on relative mortality risks for different smoking categories were taken from Thun *et al.* [5] as described above, and estimates of the prevalence of smoking behaviors by age, year, and sex were created by fitting smooth curves[8] to the BRFSS survey data described earlier. The BRFSS does not collect information on individuals <18 years old, and it was assumed that smoking behavior

[8] These curves were estimated using local polynomial regression via **R**'s LOESS package.

imparted no excess mortality risk in this population. Calculations described under Section 4.2.5.1 (smoking intensity) were used to provide a crosswalk between descriptions of smoking intensity found in the BRFSS and those used by Thun *et al*. For former smokers, the categories used by the BRFSS and Thun *et al*. do not completely align in terms of time since quitting, and the mortality rates for each of these former smoking categories was calculated as the average across the relevant categories in the Thun *et al.* estimates. Table 4.1 summarizes the approach used to calculate relative risks for each BRFSS smoker category, and also shows the relative mortality risks produced.

Table 4.1. Crosswalk between smoking categories used in the BRFSS and those reported in Thun *et al*., for the purposes of estimating smoking deleted mortality rates

Category from BRFSS	Smoking category from Thun *et al.* used to estimate relative mortality risk (vs. never smokers)	Relative mortality risk calculated from Thun *et al.*	
Current smoker, smoke some days	Current smoker, smoke <10 cigarettes per day	Male: 2.21	Female: 2.27
Current smoker, smoke every day	Weighted average across current smoker categories, with weight based on distribution in BRFSS: <10 cigarettes per day (wt=0.13) 10-19 cigarettes per day (wt=0.32) 20-39 cigarettes per day (wt=0.47) ≥40 cigarettes per day (wt=0.08)	Male: 3.00	Female: 3.14
Former smoker, quit 0-1 months	<2 years since quitting	Male: 2.77	Female: 2.34
Former smoker, quit 1-3 months	<2 years since quitting	Male: 2.77	Female: 2.34
Former smoker, quit 3-6 months	<2 years since quitting	Male: 2.77	Female: 2.34
Former smoker, quit 6-12 months	<2 years since quitting	Male: 2.77	Female: 2.34
Former smoker, quit 1-5 years	2-4 years since quitting	Male: 2.65	Female: 2.02
Former smoker, quit 5-15 years*	Average of 5-9 and 10-19 years since quitting	Male: 2.08	Female: 2.02
Former smoker, quit 15+ years*	Average of 20-29, 30-39, 40-49, and ≥50 years since quitting	Male: 1.18	Female: 1.11
Former smoker, quit 5-10 years**	5-9 years since quitting	Male: 2.16	Female: 2.25
Former smoker, quit 10+ years**	Average of 10-19, 20-29, 30-39, 40-49, and ≥50 since quitting	Male: 1.34	Female: 1.24

*BRFSS question format used until 2000. ** BRFSS question format used from 2000 onwards.

These various data were combined using equation 35 to estimate smoking-deleted background mortality rates for each sex, age, and calendar year, which were then used in the main analysis.

Cohorts were modeled from the age at which they started in the model until 100 years of age, at which point a mortality risk of 1.0 was imposed.

While not required for parameter estimation, projections of future smoking-deleted mortality rates are needed to estimate health consequences realized in future years. Mortality rates for future years were obtained by adjusting the historical estimates described above for anticipated trends in all-cause mortality for each sex and year of age derived from future life tables published by the U.S. Social Security Administration [40].

4.2.5.4. Data on population size and distribution in 1996

Estimates of the 1996 population, disaggregated by age, sex, state, and smoking behavior category were required to initially populate the model (i.e., for t=0). These values were estimated by obtaining U.S. Census Bureau data on population size for each year of age, sex, and state in January 1996 [41]. These population totals were distributed across smoking behavior categories based on 1996 data from the BRFSS.

4.2.5.5. Data on births from 1996 onwards

While not required for parameter estimation, data on births from 1996 onwards are required to reconstruct a full cross-section of the population for estimating total changes in smoking behavior and mortality outcomes. Historical data on births by sex, year, and state were obtained from the National Vital Statistics System [42]. Estimates for future years were obtained from the U.S. Census Bureau's 2012 National Population Projections [43]. As these projections are only available at a national level, they were used to calculate the projected percentage change in total births over future years, which were then applied to the historical state-level births data in order to estimate annual state-level births for future years.

4.2.5.6. Data on predictors of smoking behavior

State cigarette taxes: Data on time changes in state cigarette excise taxes were obtained from a historical compilation of tobacco tax data [3]. For each state the value of the tax at the beginning of 1996 was subtracted from the time series, so that the variable represented absolute changes in the state cigarette tax since this time point. All values were converted to 2013 constant dollars using the CPI [44].

State unemployment rates: Data on seasonally-adjusted state-level unemployment rates were obtained from the U.S. Bureau of Labor Statistics [45].

State clean air laws: Summary data on state clean air regulations were obtained from the American Non-Smokers' Rights Foundation's Tobacco Control Laws Database [46]. These summaries categorize the strength of clean air regulation on a 4 point scale from no coverage to 100% smoke-free. For each type of clean air regulation, a variable was created by dichotomizing this scale at its midpoint, equal to 1.0 if a state's regulations were 100% smoke-free, or smoke-free with minor qualifications, and 0.0 otherwise.

State anti-smoking sentiment: estimates of state-level anti-smoking sentiment in 1995-96 were drawn from DeCicca *et al*. [12]. This measure is a synthetic index created from a factor analysis of multiple TUS-CPS survey questions describing an individual's level of support for various anti-smoking measures, promotion of tobacco products, and household rules about smoking in the home. More negative values on this index represent stronger state-level anti-smoking sentiment. The values used in the present analysis (i.e., estimates for 1995-96) had a mean of -0.01 and a standard deviation of 0.16. Values for each state are shown in Table 4.2.

Table 4.2. Value of anti-smoking sentiment index for each state*

State	$ANTI_i$	State	$ANTI_i$	State	$ANTI_i$
Utah	0.40	New Hampshire	0.06	Illinois	-0.06
California	0.32	North Dakota	0.04	Louisiana	-0.08
Maine	0.19	Iowa	0.04	Delaware	-0.08
Idaho	0.19	South Dakota	0.04	Pennsylvania	-0.09
Oregon	0.18	New York	0.03	Arkansas	-0.10
Vermont	0.17	Nebraska	0.03	Michigan	-0.11
Washington	0.17	Rhode Island	0.02	Oklahoma	-0.11
Hawaii	0.16	DC	0.02	Virginia	-0.12
Arizona	0.12	Colorado	0.00	Tennessee	-0.16
Minnesota	0.09	Montana	0.00	Indiana	-0.18
Connecticut	0.07	New Jersey	0.00	Ohio	-0.22
Florida	0.07	Georgia	-0.03	Missouri	-0.23
Massachusetts	0.07	Mississippi	-0.04	South Carolina	-0.23
Texas	0.07	Alabama	-0.05	Nevada	-0.26
Maryland	0.06	Kansas	-0.05	West Virginia	-0.27
New Mexico	0.06	Wyoming	-0.06	North Carolina	-0.38
Alaska	0.06	Wisconsin	-0.06	Kentucky	-0.45

* States ordered by values of the index. More negative values on this index represent stronger state-level anti-smoking sentiment.

All independent variables were standardized (demeaned and scaled to a standard deviation of 1.0) prior to analysis to allow more efficient estimation of results.

4.2.6. Parameter estimation

A Bayesian approach was used to estimate the parameters determining smoking behavior, which include all parameters in equations 1, 6, and 12, and parameter *k* from equation 16. Prior distributions were specified for all model parameters and a likelihood function created for the BRFSS data. A modified version of the incremental mixture importance sampling (IMIS) algorithm

[47] was used to estimate the posterior parameter distribution. All analyses were undertaken using the **R** statistical computing environment [48], with the model itself coded in C++ using the Rcpp package [49].

4.2.6.1. Prior distributions for model parameters

Prior distributions were specified for parameters describing smoking behavior (Table 4.3). For coefficients on unemployment rates, anti-smoking sentiment, clean air laws and cigarette taxes (this includes parameters α_{qg}, β_{qg}, δ_{qg}, and q, which appear in equations 1, 6 and 12), weakly-informative priors were adopted, based on a Normal distribution with mean zero and standard deviation of 10. The smoothness penalties on the age and year splines were calculated using an approach described by Lang and Brezger [50], whereby a Normal prior distribution was adopted for the 2nd difference of the spline coefficients, with mean zero and the standard deviation itself estimated as part of the analysis. The hyper-prior for this standard deviation was based on a half-Cauchy distribution [51] with mean zero and standard deviation 5. The 2nd differences used to assess smoothness were calculated directly from the spline coefficients. For example, for the spline on age used to model the parameter nc_{atgi} (equation 1), these 2nd differences are calculated as $abs(\alpha_{1j} - 2\alpha_{1j+1} + \alpha_{1j+2})$ for j ∈ [1,2,…11]. A non-informative prior was assumed for parameter k, which is used to estimate the decline in relapse risk as a function of time since quitting (equation 16). This prior was operationalized as a Beta distribution with both parameters equal to 1 (equivalent to a uniform distribution over the interval [0,1])[9]. Priors for mortality rate ratios for different smoking behavior compartments were based on the Gamma distribution. The parameters

[9] By construction the domain of k is restricted to real positive numbers. However, this domain is further restricted to the [0,1] interval to reflect the empirical finding that smoking relapse hazards decrease over time [31,61], consistent with values of k<1.0.

for these distributions were estimated from the Thun *et al*. results described earlier [5], by identifying Gamma distribution parameters that recreated published means and confidence intervals. These mortality rate ratios were held constant at their mean estimate during parameter estimation, but allowed to vary when projecting outcomes under different cigarette tax scenarios[10]. Table 4.2 summarizes prior distributions for all model parameters.

[10] It is conventional to allow all uncertain parameters to vary during parameter estimation, as even parameters with informative priors may be updated by the likelihood. However, when these mortality rate ratios were allowed to vary as part of parameter estimation, it was found that the posterior modes for these parameters were shifted far from their original values. While this might be appropriate in some circumstances, it is unlikely that the information available in BRFSS data provides evidence to update our current understanding of smoking-related mortality risks. Further investigation revealed that these changes were related to the likelihood for time since quitting among former smokers. In effect, the number of individuals represented in the BRFSS data was so large, and the likelihood so strong, that the estimation procedure was obtaining a better fit to the survey data via changes in the mortality rates, despite the relatively strong prior. This bias would likely be resolved by introducing further flexibility to the model, yet to do so could threaten the feasibility of the estimation approach as well as the identification strategy. Instead, this bias to the mortality rate ratios was resolved by holding them fixed during parameter estimation. This approach implicitly assumes (i) that the BRFSS data provide no evidence for updating the information on smoking mortality risks estimated by Thun *et al.*, and (ii) there is no important dependence between these parameters and the other model parameters.

Table 4.3. Prior distributions for model parameters

Name	Description	Functional form	Parameterization			Implied mean and 95% bounds
α_{qg}, β_{qg}, and δ_{qg}, for q in [3 - 8] and g in [men , women]	Coefficients on variables for unemployment rate, clean air laws, anti-smoking sentiment, and tax rates	Normal		Mu	Sigma	Mean (bounds)
				0.0	10.0	0.0 (±19.6)
α_{1g}, β_{1g}, δ_{1g}, for g in [men , women]	Spline parameters for age. Each represents a vector of 13 values. Prior constructed around vector of 2nd differences (11 values)	Normal		Mu	Sigma	Mean (bounds)
			α_{1g},	0.0	$\sigma_{\alpha_{1g}}$	0.0 ($\pm 1.96 * \sigma_{\alpha_{1g}}$)
			β_{1g}	0.0	$\sigma_{\beta_{1g}}$	0.0 ($\pm 1.96 * \sigma_{\beta_{1g}}$)
			δ_{1g}	0.0	$\sigma_{\delta_{1g}}$	0.0 ($\pm 1.96 * \sigma_{\delta_{1g}}$)
α_{2g}, β_{2g}, δ_{2g}, for g in [men , women]	Spline parameters for year. Each represents a vector of 5 values. Prior constructed around vector of 2nd differences (3 values)	Normal		Mu	Sigma	Mean (bounds)
			α_{2g},	0.0	$\sigma_{\alpha_{2g}}$	0.0 ($\pm 1.96 * \sigma_{\alpha_{2g}}$)
			β_{2g}	0.0	$\sigma_{\beta_{2g}}$	0.0 ($\pm 1.96 * \sigma_{\beta_{2g}}$)
			δ_{2g}	0.0	$\sigma_{\delta_{2g}}$	0.0 ($\pm 1.96 * \sigma_{\delta_{2g}}$)
$\sigma_{\alpha_{1g}}$, $\sigma_{\beta_{1g}}$, $\sigma_{\delta_{1g}}$, $\sigma_{\alpha_{2g}}$, $\sigma_{\beta_{2g}}$, and $\sigma_{\delta_{2g}}$, for g in [men , women]	Standard deviation of 2nd differences of spline parameters	Half-Cauchy		Mu	Scale	Mean (bounds)
				0.0	5.0	Undefined (0.2, 127)
k_g , for g in [men , women]	Parameter determining relative hazard of smoking relapse in former smokers	Beta		Alpha	Beta	Mean (bounds)
				1.0	1.0	0.5 (0.025, 0.975)

Table 4.3 Prior distributions for model parameters (continued)

Name	Description	Functional form	Parameterization				Implied mean and 95% bounds	
			MEN		**WOMEN**		**MEN**	**WOMEN**
			Scale	Rate	Scale	Rate	Mean (bounds)	Mean (bounds)
ρ_{gj} for j in [n, s, e, $f0$-$f9$] and g in [men , women]	Mortality rate ratios for smoking behavior compartments	Gamma						
			ρ_s	1303	589	2740	1207	2.21 (2.09, 2.33)	2.27 (2.19, 2.36)
			ρ_e	1468	488	1001	318	3.01 (2.86, 3.17)	3.14 (2.95, 3.34)
			ρ_{f0}	307	111	821	351	2.77 (2.47, 3.09)	2.34 (2.18, 2.50)
			ρ_{f1}	307	111	821	351	2.77 (2.47, 3.09)	2.34 (2.18, 2.50)
			ρ_{f2}	510	192	1185	587	2.65 (2.42, 2.89)	2.02 (1.91, 2.14)
			ρ_{f3}	796	369	1470	653	2.16 (2.01, 2.31)	2.25 (2.14, 2.37)
			ρ_{f4}	2105	1058	4023	2260	1.99 (1.91, 2.08)	1.78 (1.73, 1.84)
			ρ_{f5}	2105	1058	4023	2260	1.99 (1.91, 2.08)	1.78 (1.73, 1.84)
			ρ_{f6}	2489	1778	3255	2485	1.40 (1.35, 1.46)	1.31 (1.27, 1.36)
			ρ_{f7}	2287	1874	2905	2641	1.22 (1.17, 1.27)	1.10 (1.06, 1.14)
			ρ_{f8}	1536	1397	2012	1954	1.10 (1.05, 1.16)	1.03 (0.99, 1.08)
			ρ_{f9}	1088	1078	909	909	1.01 (0.95, 1.07)	1.00 (0.94, 1.07)

4.2.6.2. Likelihood function

The survey data, weighted and summarized into total counts for each age, sex, quarter, state, and smoking category (as described in Section 4.2.5.1) were used to create likelihood functions for the modeled distribution of the population across smoking behavior categories. Likelihood functions were constructed for each age, sex, quarter, and state for which data were available, with each individual likelihood function summarizing the distribution of surveyed individuals across smoking

behavior categories in a given age/sex/year/state subgroup. A generalized multinomial likelihood[11] was used, and constant terms of the log-likelihood dropped to allow more efficient computation. The functional form for this log-likelihood is shown below, for modeled outcomes φ_{atgi}, given survey data Y_{atgi}.

$$ln\mathcal{L}(\varphi_{atgi}|Y_{atgi}) \propto \sum_{j\in J} ln\left(\varphi_{atgi}^{j}\right) * y_{atgi}^{j} \quad [36]$$

In this equation φ represents modeled outcomes produced by a parameter set θ (i.e., $M(\theta) \rightarrow \varphi$), y_{atgi}^{j} represents the observed count in smoking behavior category *j* for the model subgroup with age *a*, time *t*, sex *g* and state *i*, and φ_{atgi}^{j} represents the fraction of the cohort in compartment *j*, for that same subgroup, as estimated by the model. Separate log-likelihoods were constructed for the different data sources described in Section 4.2.5.1, with $ln\mathcal{L}_1$ describing the distribution across current smoking compartments (4 categories: N ,S, E and the sum of F0 to F9), $ln\mathcal{L}_{2a}$ describing the distribution of former smokers by time since quitting according to the BRFSS question format used before 2000 (four categories: F0, F1+F2, F3+F4, and the sum of F5 to F9), and $ln\mathcal{L}_{2b}$ describing the distribution of former smokers by time since quitting according to the BRFSS question format used from 2000 onwards (four categories: F0, F1+F2, F3, and the sum of F4 to F9). All these separate likelihoods were assumed to be independent, conditional on a given set of parameter values. As a parameter set defines a unique value for every model outcome, the overall log-likelihood for a

[11] The conventional multinomial likelihood is restricted to positive integers. However, following survey weighting adjustment (Section 4.2.5.1) the data for this analysis included fractions, and consequently the likelihood needed to be defined for all positive real numbers. The likelihood used here represents a generalization of the standard Multinomial likelihood, though the functional form of the log-likelihood is identical to the log-likelihood of the conventional multinomial once constant terms have been dropped.

particular parameter set was calculated as the sum across the three likelihoods for all age/time/state subgroups (note: as parameters are estimated separately for men and women, no single likelihood was constructed across both sexes).

$$ln\mathcal{L}(\theta_g|Y_g) = \sum_{h\in[1,2_a,2_b]}\sum_{a\in A}\sum_{t\in T}\sum_{i\in I} ln\mathcal{L}_h(\varphi_{atgi}|Y_{atgi}) \text{ for } g \text{ in [male, female]} \quad [37]$$

4.2.6.3. Computation

The posterior parameter distribution was estimated using a modified IMIS algorithm [47]. As originally described, this algorithm begins by drawing a first sample from the prior distribution. Next, further samples are drawn from new importance sampling distributions iteratively created to explore under-sampled regions of the parameter space. This iterative creation of and sampling from new importance sampling distributions proceeds until the total set of samples approximates the posterior distribution of interest. This approach is particularly useful in situations where it is expected that parameters will be correlated in the posterior (these situations have been found to impair the performance of conventional Markov chain Monte Carlo approaches).

One complication for the present analysis is that the prior is sufficiently diffuse, and the likelihood sufficiently strong, that a random sample from the prior (even if very large) is unlikely to fall anywhere near the mode of the posterior distribution. While the published version of IMIS would likely still succeed in this situation, the algorithm would be very slow in locating and sampling from the region of maximum likelihood. In order to more efficiently operationalize this analysis, a revised version of IMIS was implemented whereby an optimization approach was used to identify the mode of the posterior, and then the curvature of the log-posterior at this location used to create the variance-covariance matrix of the first importance sampling distribution (which is based on a

multivariate Normal)[12]. Using an optimization approach to identify the posterior mode brings with it a risk of being caught in a local maximum, and for this reason the optimization was undertaken 10 times, each time initialized at randomly chosen starting points. A new importance sampling distribution was constructed around the results of each of these optimizations, similar to the 'IMIS-opt' approach described by Raftery and Bao [47]. The analysis then followed the IMIS algorithm as originally described, until stable estimates were achieved. Figure 4.4 presents the progression of estimates for the mean and posterior intervals of key parameters and outcomes for successive iterations of the IMIS algorithm, and shows no systematic change in mean estimates or width of posterior intervals. Study results were estimated following 27 iterations of the algorithm.

[12] This revision to the IMIS algorithm was discussed with Adrian Raftery (Adrian Raftery, personal communication, October 27th 2013).

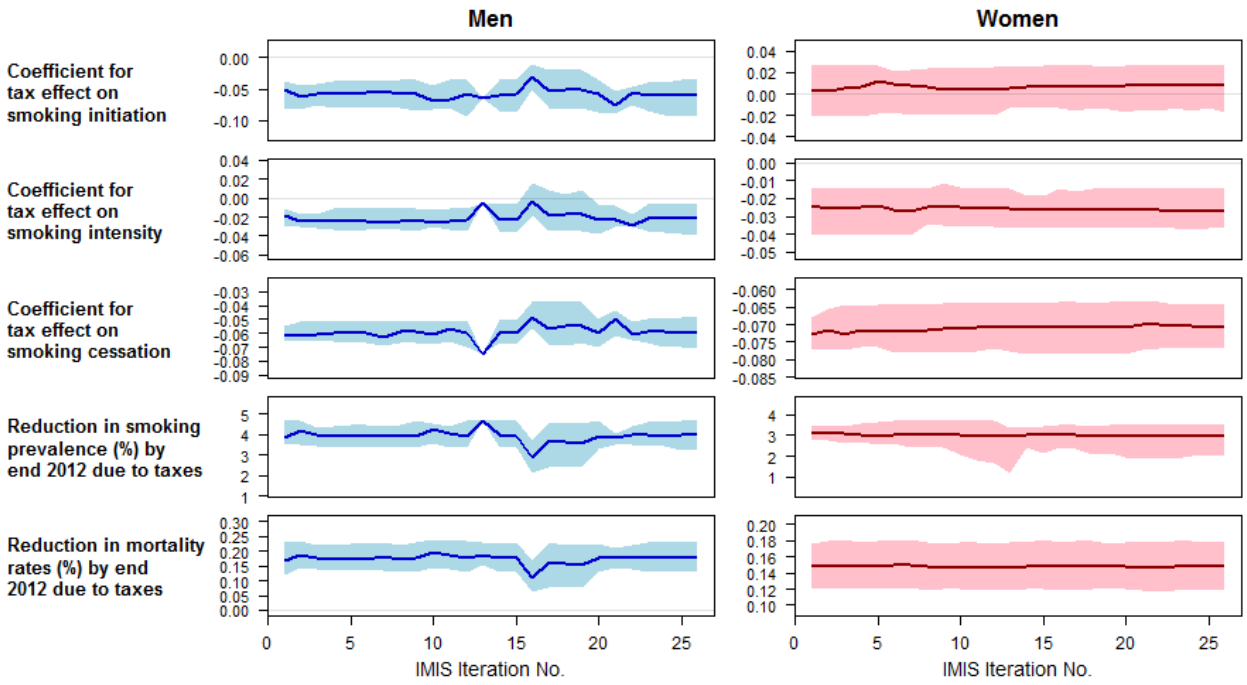

Figure 4.4. Estimates for the mean and posterior intervals of major parameters and outcomes for successive iterations of the IMIS algorithm

4.2.7. Validation

Smoking behaviors and health outcomes estimated by the fitted model were compared to a number of independent datasets to ensure the analysis was consistent with available evidence. The distribution of smoking behavior at different time points, as estimated by the model, was compared to estimates derived from the Current Population Survey's Tobacco Use Supplement (TUS-CPS). The TUS-CPS is an occasional supplement to Current Population Survey that uses a similar question format to the BRFSS to collect information on cigarette smoking and related behaviors [52]. Population demographics, describing the distribution of the population by state, age, and sex, were compared to estimates from the 2010 U.S. Census [53]. Modeled estimates for total mortality were compared to 2010 estimates produced by the CDC's National Vital Statistics System [54].

4.2.8. Comparison of alternative cigarette tax scenarios

Two cigarette taxation scenarios were compared using the fitted model. These comparisons were used to estimate the causal effect of recent state cigarette tax increases during the period of the analysis 1996-2013.

Status quo scenario (taxes introduced): under this scenario, cigarette taxes in each state follow their historical trajectory, as described previously.

Counterfactual scenario (no new state taxes since 1996): under this counterfactual scenario, state cigarette taxes are assumes to stay at their 1996 values.

In both scenarios, all other determinants of smoking behavior were assumed to follow their historical trajectory, as in the main analysis. This implicitly assumes that changes in state cigarette taxes have no causal effect on other determinants of smoking behavior. The comparison of these two scenarios allows us to explore the implications of increased state cigarette taxes on smoking behavior, total cigarette consumption[13], and health outcomes realized between 1996 and 2013.

Additional analyses were undertaken to explore the long-term consequences of these tax changes beyond 2013. In the first of these analyses the scenarios described above were extended for a further four decades into the future, to understand how the changes in smoking behavior and

[13] Calculations for total consumption required estimates of the relative cigarette consumption of Some Day vs. Every Day smokers. For this analysis it was assumed that Some Day smokers consumed cigarettes at 0.21 the rate of Every Day smokers, based on the distributions of smoking intensity for Some Day and Every Day smokers described in Table 4.1. Estimates of total consumption were robust to different assumptions about this value. It was also assumed that any change in smoking intensity induced by tax changes was fully captured by the change in distribution between Some Day vs. Every Day smokers.

health outcomes associated with the 1996-2013 tax increases would accumulate over time. For these analyses, background mortality rates and birth rates were assumed to follow long-term secular trends based on published estimates [40,43] , but all other variables were held at their final values, and taxes were fixed at their 2013 values under both status quo and counterfactual scenarios. As these assumptions require the value of the tax to be fixed in 2013 constant dollars, these scenarios can be thought of as including ongoing minor tax increases to offset the effect of inflation in reducing the real value of the tax.

A third set of analyses calculated life expectancy for the 2013 birth cohort if exposed to status quo or counterfactual tax scenarios. For this analysis, a single birth cohort was simulated from birth to death under the two competing tax regimes, with all other variables, including background mortality rates, held constant at their 2013 values (consistent with conventional approaches for estimating life expectancy). Taxes were assumed fixed in 2013 constant dollars, so that the real value is maintained over the lifetime.

In addition to producing estimates of behavioral and health outcomes, analyses were undertaken to estimate the price elasticity of demand associated with the tax increases. For a particular comparison, these elasticity estimates (e) were calculated as shown in equation 38, where A indicates the status quo scenario (taxes introduced), B represents the counterfactual scenario (taxes fixed at 1996 levels), Q represents total national consumption estimated under a particular scenario, and P represents average pack price for that same scenario. P_A was taken to be the 2013 average national pack price net of sales taxes[14], equal to $5.74 [55], and P_B was taken to be

[14] For the large majority of states, sales taxes on tobacco products are applied as a percentage mark-up after state and federal excise taxes have been added, thus the absolute price increase produced by an increase in

P_A minus the national average value for state cigarette taxes imposed since 1996, which was calculated as part of the analysis. This approach assumes that cigarette prices, net of taxes, are not affected by the taxes themselves. In sensitivity analyses we tested an alternate assumption whereby the pass-through of taxes to prices was assumed to be 1.11 [56].

$$e = \frac{Q_A - Q_B}{Q_B} \Big/ \frac{P_A - P_B}{P_B} \quad [38]$$

Elasticity estimates were calculated for men and women as well as overall, for the period 1996-2013. Long-run elasticity estimates were also calculated in the context of the life-expectancy analysis, given that decreased smoking initiation behavior, if this were a consequence of tax increases, would have a delayed effect on overall smoking prevalence. These delayed effects could result in long-run elasticity estimates that are greater than those estimated over a shorter time horizon.

4.3. Results

4.3.1. Fit to BRFSS smoking data

Figures 4.5-4.7 compare modeled estimates of smoking behavior to the BRFSS data used to fit the model. Figure 4.5 presents the distribution of the national population across smoking behaviors as a function of age, year, and sex, and there appears to be a close calibration to the BRFSS data. Figure

---

the excise tax will be larger than the tax itself. For this reason the correct elasticity estimates are obtained by removing the sales taxes before the elasticities are computed.

4.6 further disaggregates these estimates by state, and while in general there is close agreement with the survey data, there are a small number of states where modeled estimates diverge from those estimated directly from the BRFSS data. For example, for men in both Georgia and Oklahoma, the model fails to capture observed reductions in the fraction of never smokers, as well as increases in former smokers, over the early 2000s. These discrepancies indicate that estimated outcomes for some individual states should be interpreted with caution, but in general the fit to the observed distribution across smoking behaviors is good.

Figure 4.7 disaggregates former smokers by time since quitting. Again, the fit to the survey data appears acceptable, despite changes in question format following 2000, and despite survey data on time since quitting not being collected in 2006-2008.

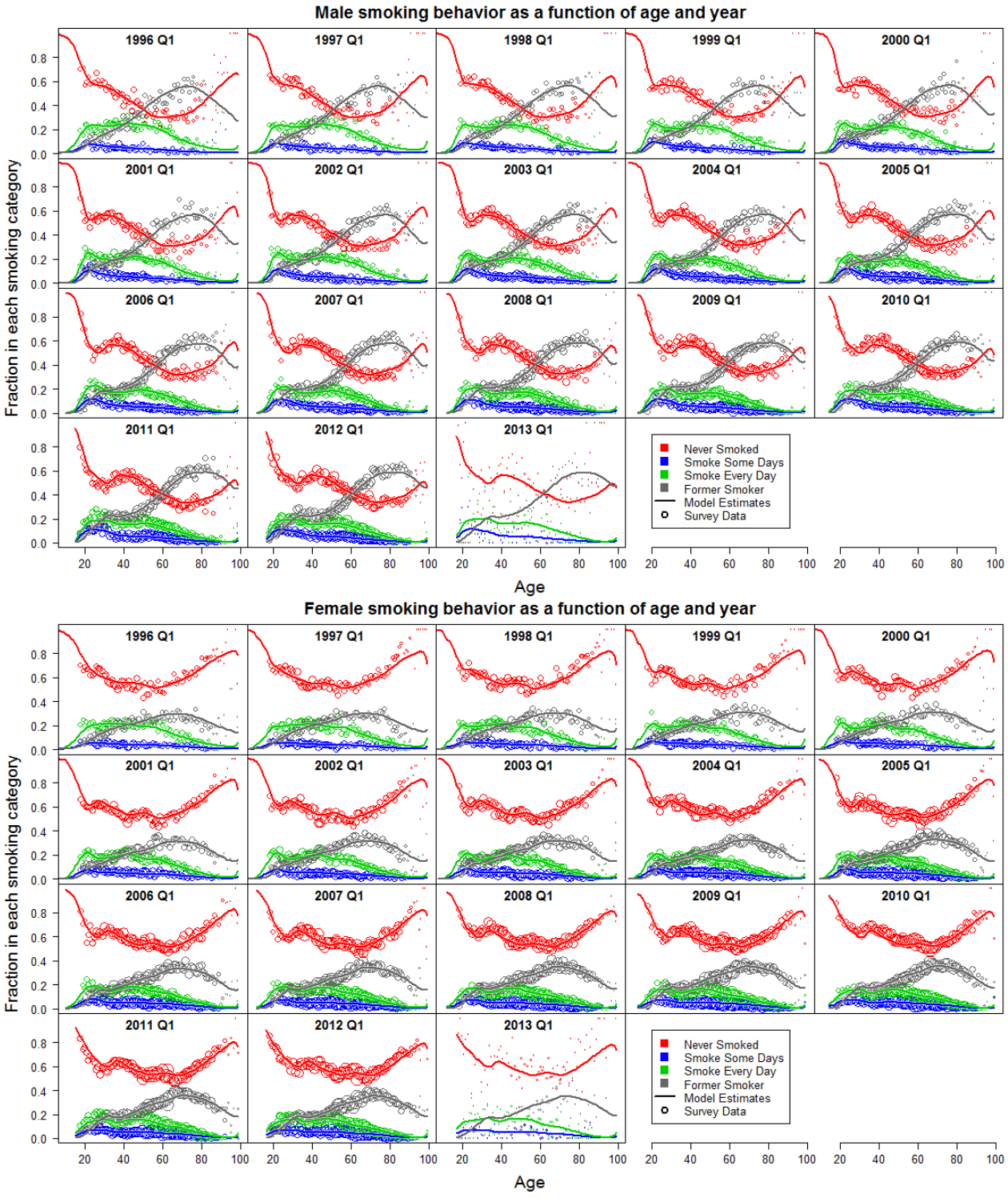

Figure 4.5. Comparison of modeled estimates to BRFSS data on smoking behavior, as a function of age and year*

* Size of plotting symbols for survey data proportional to square root sample size. Estimates shown for 2013 Q1 represent data collected during the 2012 round of the BRFSS.

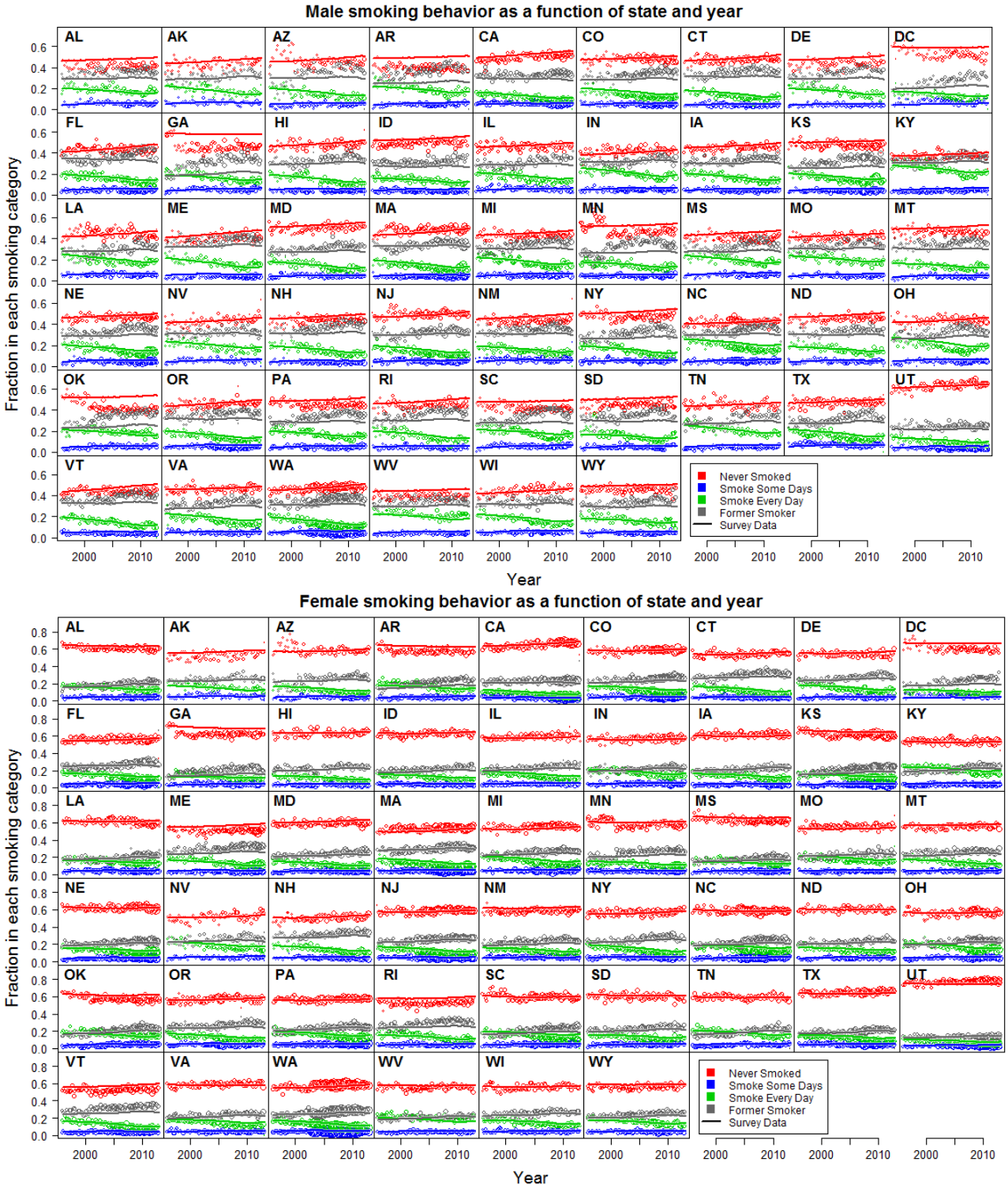

Figure 4.6. Comparison of modeled estimates to BRFSS data on smoking behavior, as a function of year and state*

* Size of plotting symbols for survey data proportional to square root sample size. Survey data and modeled estimates for state populations aged ≥18 years old.

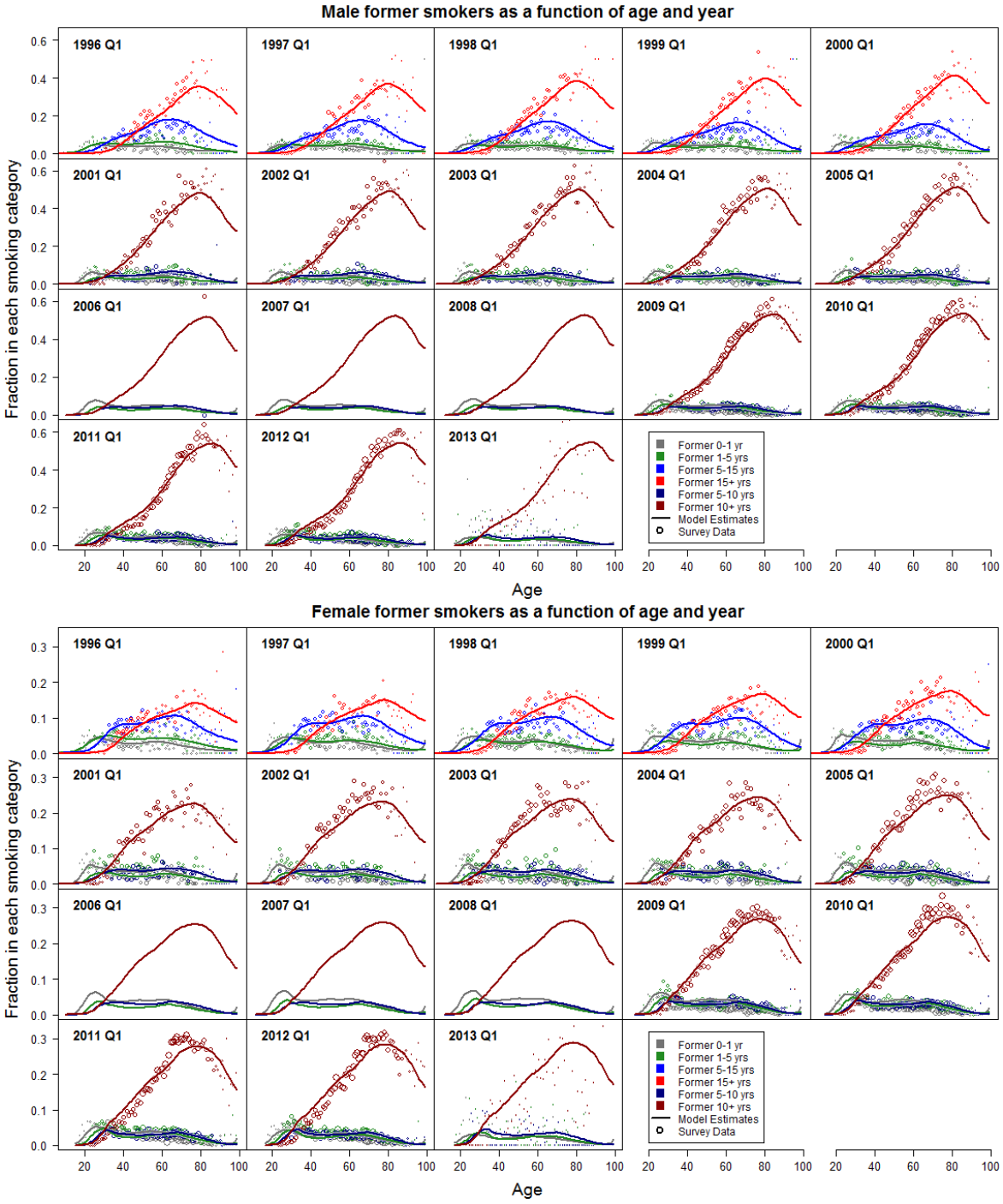

Figure 4.7. Comparison of modeled estimates to BRFSS data on time since quitting in former smokers, as a function of age and year*

* Size of plotting symbols for survey data proportional to square root sample size. Survey question categorization for time since quitting revised in 2001 (indicated by different plotting color). Questions on time since quitting not asked 2006-2008. Estimates shown for 2013 Q1 represent data collected during the 2012 round of the BRFSS.

4.3.2. Validation

Model projections were compared to several independent data sources. To validate smoking prevalence estimates, modeled results were compared to data from successive rounds of the TUS-CPS collected between 1999 and 2011. These comparisons are shown in Figure 4.8. Compared to the model estimates, the TUS-CPS data generally show a similar prevalence of current smoking behavior, but a lower prevalence of individuals reporting former smoking, with this difference made up by an increased fraction reporting having never smoked. The differences between modeled estimates and TUS-CPS data are largest in younger age groups, where the modeled estimates predict higher fractions of both current and former smokers. Given the close fit of model estimates to the BRFSS data, these discrepancies likely reflect differences associated with the instruments or the sampling frame of these two surveys.

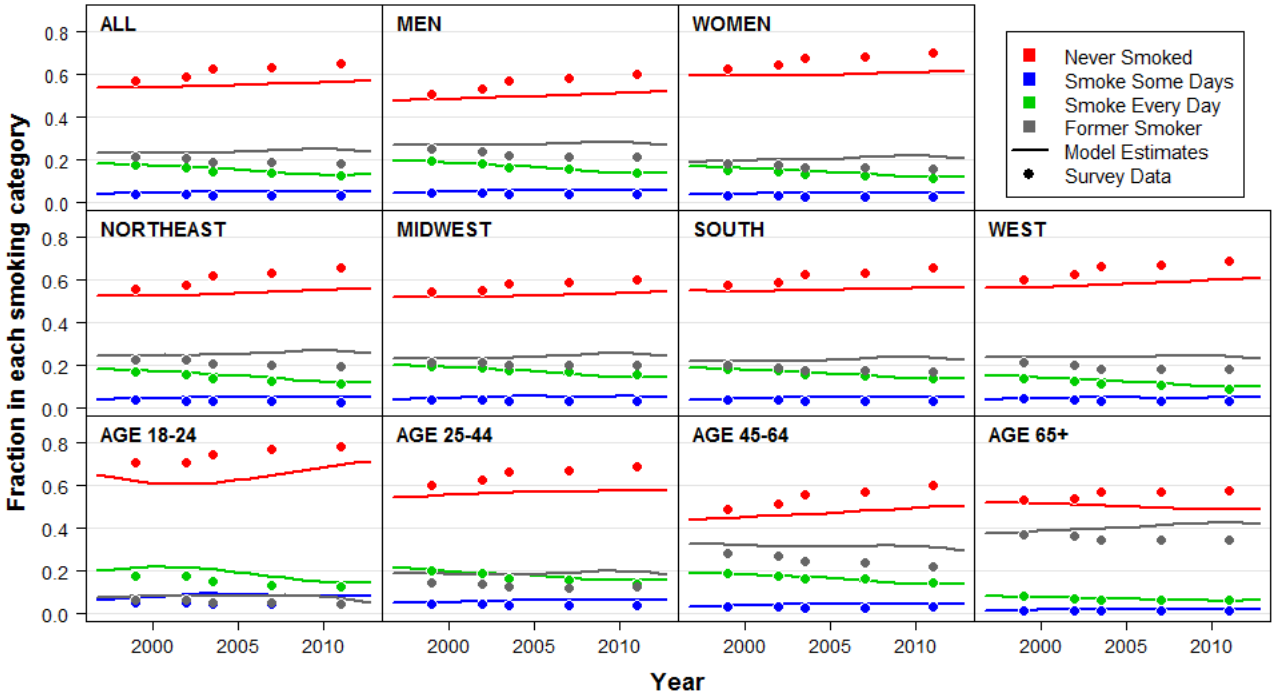

Figure 4.8. Comparison of modeled estimates to independent data on smoking prevalence from the Tobacco Use Supplement of the Current Population Survey*

* Unless stated otherwise, modeled estimates and TUS-CPS estimates relate to the population ≥15 years old (top and middle panels).

Figure 4.9 presents modeled estimates of all cause mortality in 2010 for discrete age groups, as compared to estimates for the same quantities published by the CDC's National Vital Statistics System. This comparison examines whether the approach used to create smoking-deleted life tables, then reintroducing smoking-attributable mortality risks, correctly recovers all-cause mortality rates. There is almost exact agreement with the published estimates for all age groups.

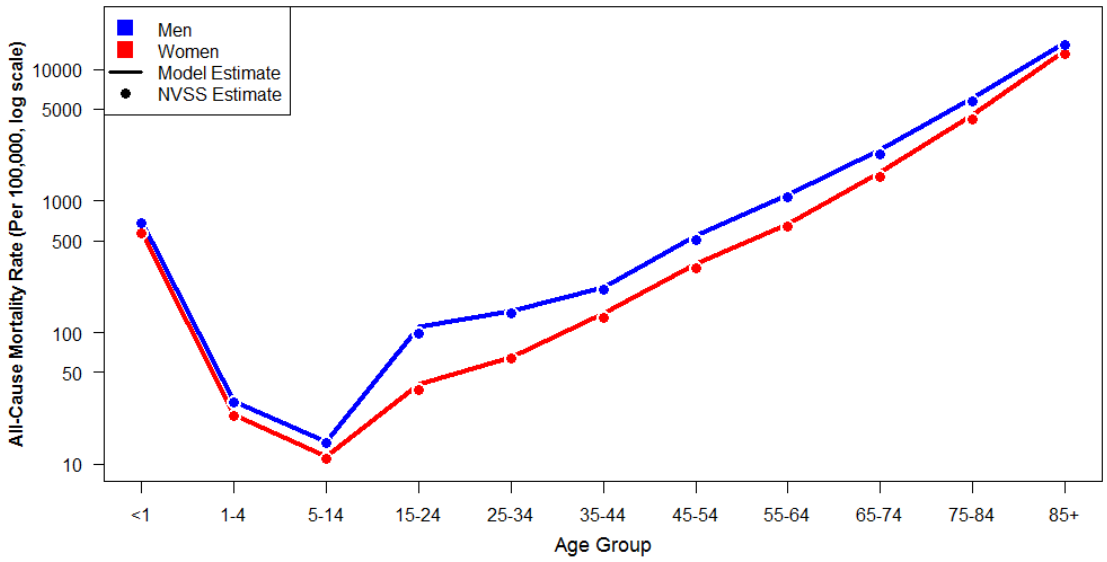

Figure 4.9. All-cause mortality rate for 2010 by age group and sex, comparing modeled estimates to published estimates from the CDC's National Vital Statistics System

Figure 4.10 compares modeled estimates of the size and distribution of the U.S. population with results from the 2010 census. For a number of age categories the modeled estimates appear to underestimate both female and male population size (top panel). This is particularly true between ages 15 and 40. This difference may be due to immigration, which is not captured in the model. The size of this difference, with modeled estimates of the total population on 2010 approximately 20 million smaller than census estimates, is consistent with Census Bureau estimates of immigration over this period (though at the high end). In addition, the age groups with the greatest discrepancy match the age groups with the highest observed levels of immigration [57]. A consequence of underestimating total population size is that absolute estimates of health outcomes reported in later sections of the results (e.g., life-years saved, or deaths averted) will represent a modest underestimate. The discrepancy between modeled population and census estimates is not evenly distributed by state, with Arizona, Florida and Nevada exhibiting the greatest relative difference.

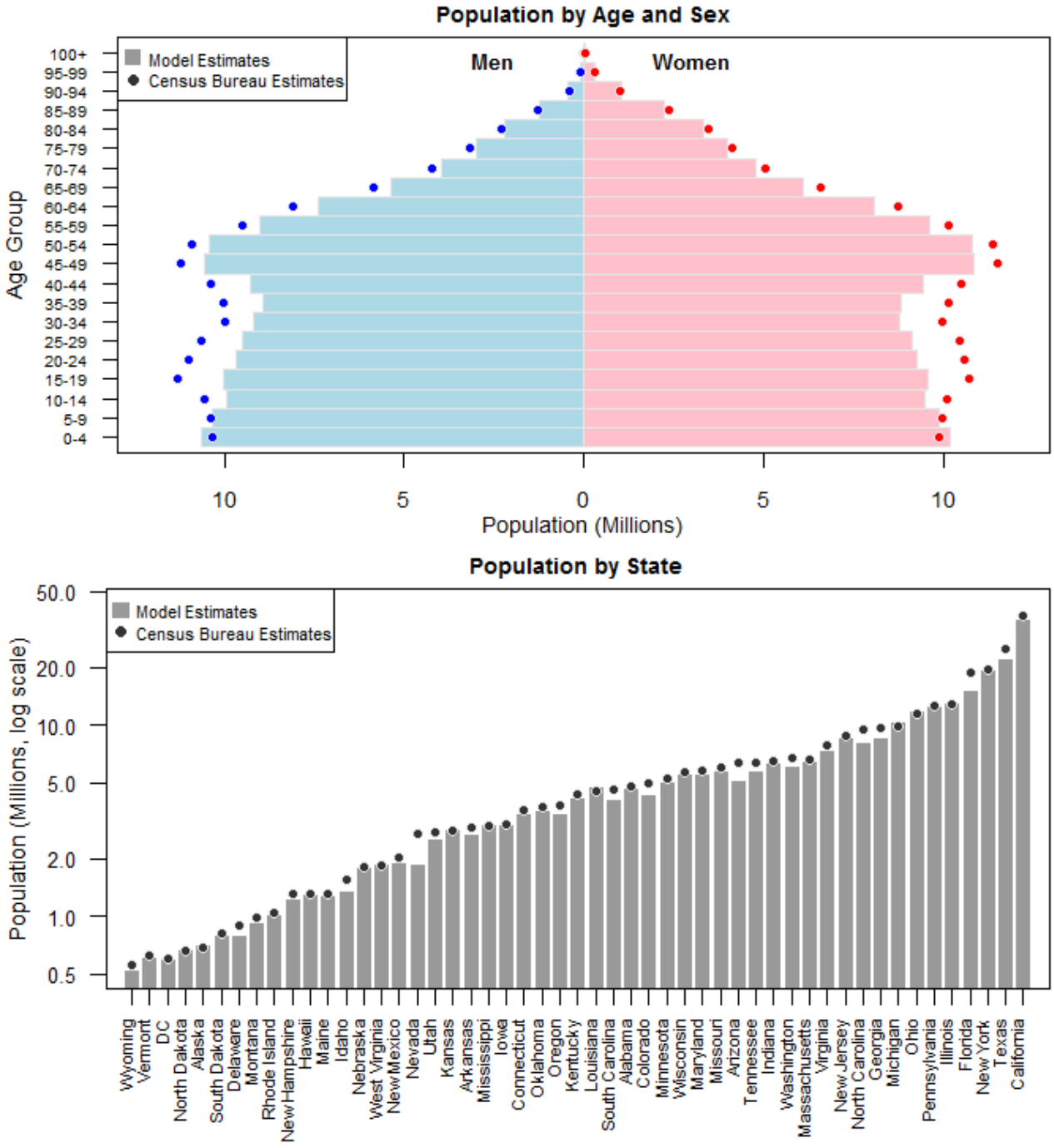

Figure 4.10. Population size and distribution in 2010, comparing modeled estimates to data from the 2010 U.S. Census

4.3.3. Parameter estimates for predictors of smoking behavior

Table 4.4 presents posterior mean and 95% posterior intervals for predictors of smoking behavior. Coefficients on the TX variable are generally negative, suggesting a reduction in smoking behavior associated with cigarette tax increases. However, the interpretation of these values for overall smoking prevalence and health outcomes is difficult, as smoking behavior will be determined by multiple parameters simultaneously. Whether changes in individual predictors are associated with meaningful and or statistically significant changes in smoking behavior and health outcomes is best understood by comparing results when the model is re-estimated under alternative taxation scenarios. These alternative scenarios are examined in Section 4.3.4.

Table 4.4. Posterior mean values for predictors of smoking behavior*

	Risk of smoking initiation (*nc*)		Probability of smoking every day, in current smokers (*P(E|C)*)		Probability of continued smoking, among current smokers (*P(C|F0C)*))	
	Men	Women	Men	Women	Men	Women
Unemployment rate (*UN*)	-0.010 (-0.028,0.003)	-0.061 (-0.069,-0.054)	-0.025 (-0.029,-0.020)	-0.020 (-0.024,-0.017)	0.025 (0.019,0.029)	0.028 (0.025,0.030)
Smoking restricted in workplaces (*WP*)	-0.015 (-0.057,0.057)	0.079 (0.036,0.116)	-0.017 (-0.046,0.056)	-0.013 (-0.028,-0.002)	0.038 (0.017,0.053)	0.050 (0.040,0.063)
Smoking restricted in restaurant (*RST*)	-0.241 (-0.271,-0.197)	-0.242 (-0.272,-0.210)	0.075 (0.056,0.095)	0.059 (0.046,0.071)	0.015 (0.005,0.028)	-0.012 (-0.020,-0.003)
Smoking restricted in bars (*BAR*)	0.076 (0.016,0.125)	-0.211 (-0.256,-0.168)	-0.022 (-0.081,0.017)	-0.034 (-0.050,-0.019)	-0.043 (-0.078,0.003)	-0.061 (-0.074,-0.047)
Anti-smoking sentiment (*ANTI*)	-0.538 (-0.649,-0.447)	-0.651 (-0.698,-0.608)	-0.759 (-0.804,-0.706)	-0.679 (-0.716,-0.635)	-0.240 (-0.285,-0.193)	-0.258 (-0.284,-0.236)
State cigarette tax increases (*TX*)	-0.056 (-0.088,-0.032)	0.007 (-0.015,0.028)	-0.020 (-0.037,-0.006)	-0.025 (-0.035,-0.014)	-0.055 (-0.065,-0.045)	-0.066 (-0.072,-0.060)

* Parameters for age and year splines not shown. Coefficients for continuous variables (unemployment rate, anti-smoking sentiment, cigarette tax) transformed to original scale. 95% posterior intervals shown in parentheses.

4.3.4. Causal effects of state cigarette taxes introduced over the period 1995-2013

4.3.4.1. Effect on smoking behavior

All results in this section compare the recent history of increasing state cigarette taxes with a counterfactual scenario in which these taxes were not introduced (i.e., all state cigarette taxes assumed to remain at their 1996 values). By comparing the incremental differences between these two scenarios we can understand the change in smoking behavior and other outcomes caused by the increase in state cigarette taxes since 1996.

Figure 4.11 shows the change in various measures of smoking behavior due to the recent tax increases, averaged at a national level. The cigarette taxes are seen to have caused improvements in most indicators of smoking behavior. By the end of 2012, male smoking prevalence in the United States is estimated to be 4.0% (3.3, 4.8)[15] lower that it would have been in the absence of the state cigarette taxes introduced since 1996, and female smoking prevalence is estimated to be 2.8% (1.8, 3.5) lower. Other indicators of smoking behavior—the fraction of the population who have ever smoked and the fraction of smokers who smoke every day—exhibit smaller changes. In the case of women, the fraction of the population who have ever smoked is estimated to rise, though the posterior 95% interval for this outcome includes zero. These various changes contribute to total cigarette consumption, which is estimated to be 4.4% (3.7, 5.3) lower among men and 3.6% (2.6, 4.2) lower among women (for a 4.0% (3.3, 4.6) overall reduction) by the end of 2012 compared to the counterfactual scenario that held taxes at their 1996 levels.

[15] Values in parentheses represent equal-tailed 95% posterior intervals.

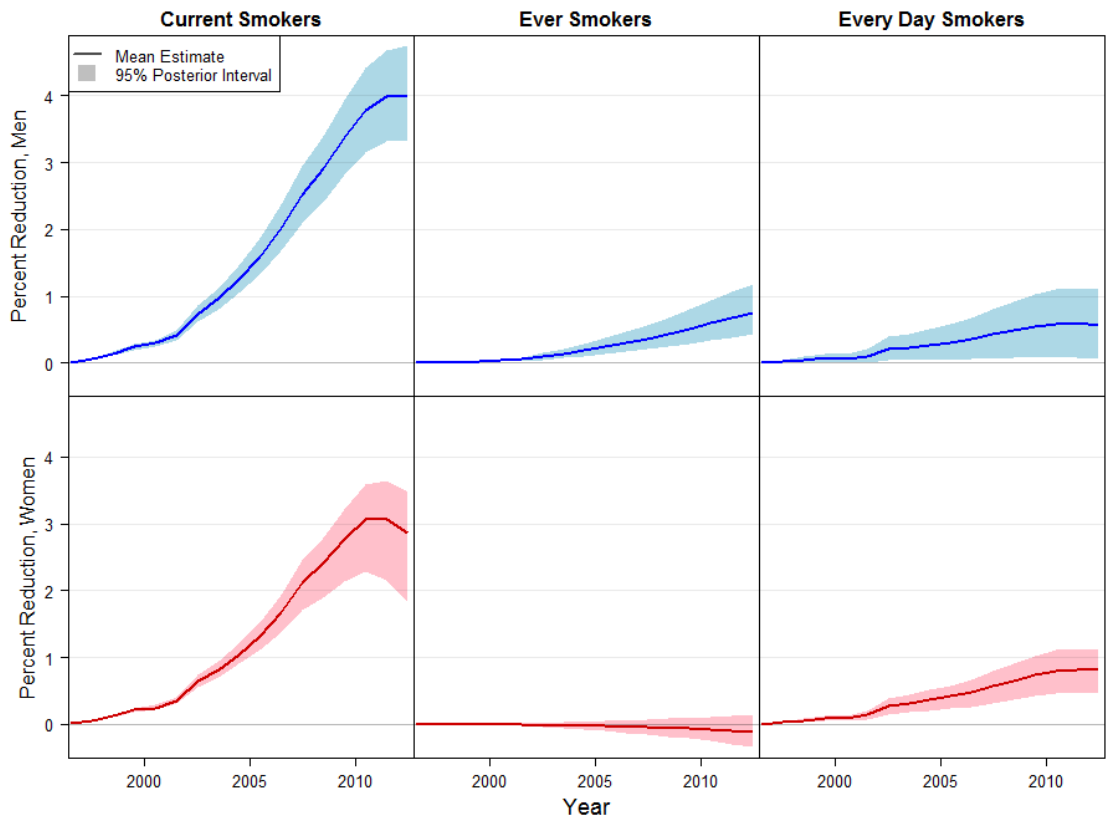

Figure 4.11. Change in various measures of smoking behavior (national-average) due to increases in state cigarette taxes over the period 1996-2013*

*All estimates are assessed in the total population, by sex. Reduction in every day smokers represents change in the fraction of current smokers who smoke every day.

Figure 4.12 presents results for the reduction in smoking prevalence due to recent cigarette taxes broken down by state. The cigarette tax for each state, in nominal dollars, is also plotted for comparison. As can be seen, reductions in smoking prevalence accrue in proportion to the magnitude of tax increases for a given state, with these reductions spread over the years following the tax increase. These changes in smoking prevalence are marginally larger for men than for women, consistent with the results presented in Figure 4.11.

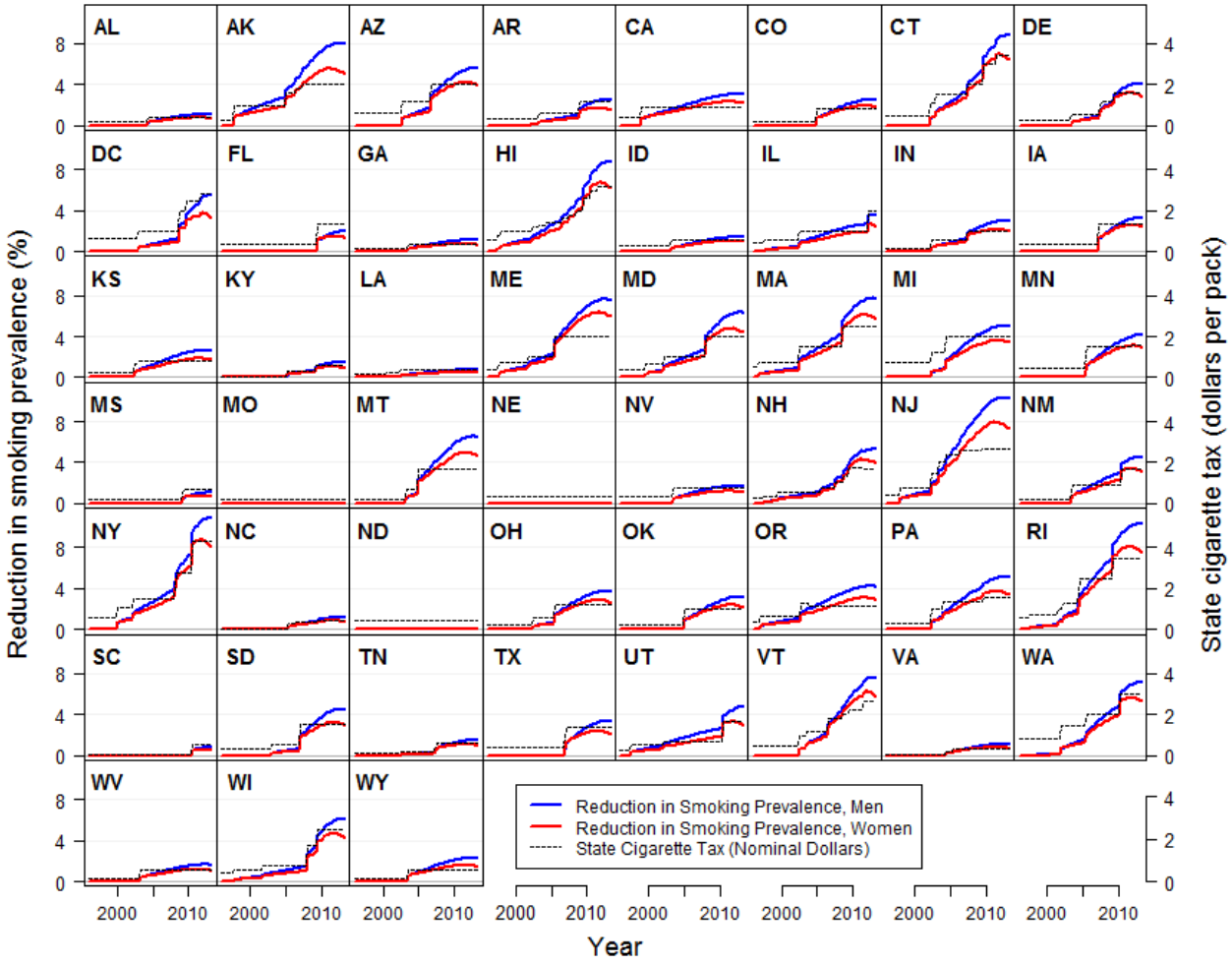

Figure 4.12. Reductions in state-level smoking prevalence due to increases in state cigarette taxes over the period 1996-2013*

*All estimates are reported for the total population of each state, by sex.

4.3.4.2. Effect on population health outcomes

Over the entire period 1996-2013, increases in state cigarette taxes are estimated to have reduced the total time spent smoking by 10.9 million (9.6, 12.4) person-years when summed nationally (6.3 million (5.2, 7.4) years among men and 4.6 million (3.9, 5.3) year among women). Smoking predisposes individuals to a large number of health conditions that could lead to premature mortality, and reductions in smoking behavior are estimated to have produced improvements in

health outcomes. Overall during the period 1996-2013, the increase in state cigarette taxes is estimated to have reduced the number of deaths by 14.4 thousand (9.9, 19.7) among men and 13.0 thousand (9.9, 16.8) among for women, for a total of 27.4 thousand (21.8, 34.1) deaths averted. These reductions in mortality were associated with an extra 61 thousand (39, 85) years of life lived by men and an extra 58 thousand (44, 78) years of life lived by women, for a total of 119 thousand (92, 151) life-years saved. Figure 4.13 disaggregates the total change in person-years smoking, deaths averted, and life-years saved by age group. Though the major reductions in years spent smoking are estimated to accrue during ages 20-59 the impact on mortality is felt in later years, with most deaths averted between ages 60-79. The same pattern can be observed for the additional life-years lived due to the tax increases.

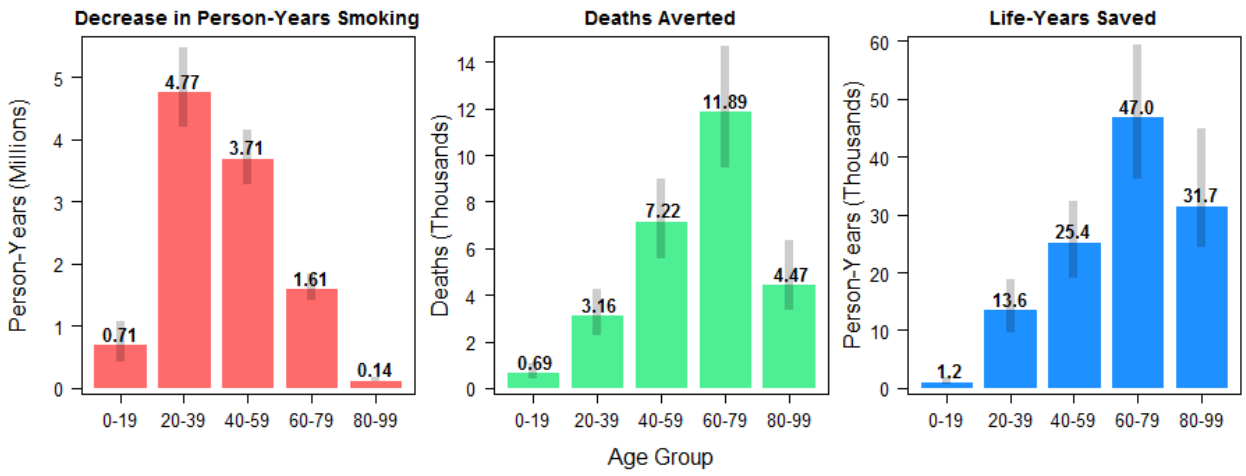

Figure 4.13. Changes in major behavioral and health outcomes over 1996-2013 due to increase in state cigarette taxes, disaggregated by age group*

* Figure compares a scenario in which state cigarette taxes follow their historical trajectory to a counterfactual scenario in which taxes are held constant at their 1996 values.

The results described above and in Figure 4.13 relate to the period 1996-2013. However, part of the benefits of the taxes introduced over this period will not be felt for many years, as tax-related changes in smoking initiation and cessation rates will take time to affect overall smoking prevalence, and subsequent changes in survival will be even further delayed. Figure 4.14 extends the analysis for an additional four decades into the future to understand how changes in smoking behavior and health outcomes might accumulate over a longer timeframe[16]. For each major outcome—reductions in years spent smoking, deaths averted, and life-years saved—the effect of the taxes increase in each successive decade. For estimates of the total years spent smoking, this increase slows over time, but the number of deaths averted increases approximately linearly until 2030-2039, after which point the reduction in mortality tapers as those who avoided smoking-related mortality begin to succumb to other ailments later in life. The number of life-years gained are estimated to increase with each successive decade, with over 6 million life-years saved over the next four decades compared to a scenario in which no new state cigarette taxes were introduce after 1996.

[16] This analysis compares a scenario in which state cigarette taxes are held at their 1996 values for the entire projection period, to one in which state cigarette taxes follow their historical trajectory and then remain constant at their current value for the remaining projection period. Projected trends in births and background mortality are based on published estimates, and all other variables (e.g., unemployment rates) are held at their 2013 values.

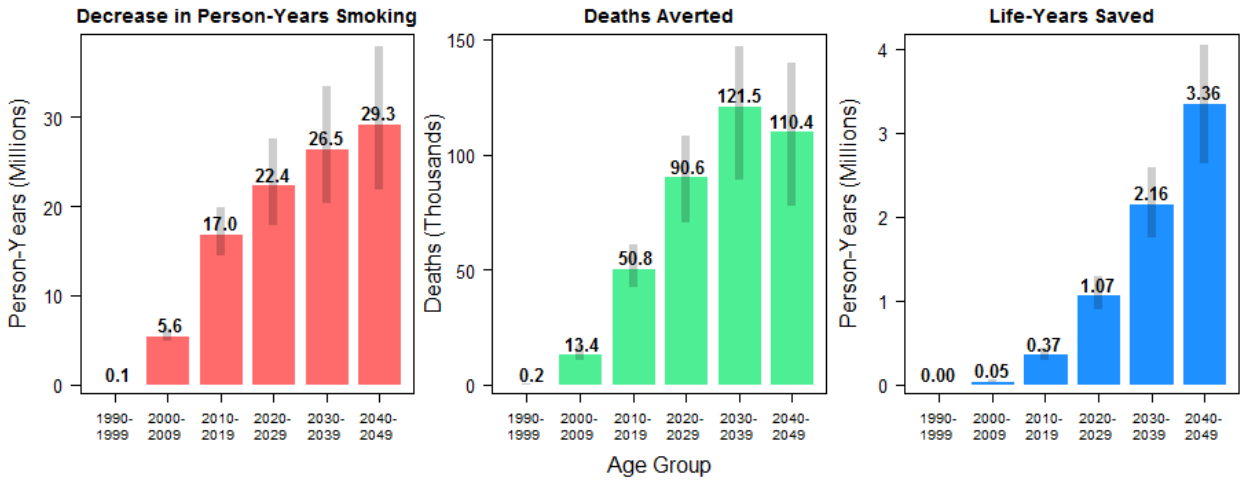

Figure 4.14. Projected changes in major behavioral and health outcomes over the next four decades due to increase in state cigarette taxes introduced between 1996 and 2013, by decade*

* Figure compares a scenario in which state cigarette taxes follow their historical trajectory and then hold constant at 2013 values to a counterfactual scenario in which taxes are held constant at their 1996 values.

The long term improvement in health outcomes can also be understood through changes in lifetime smoking patterns and life expectancy. We projected lifetime smoking patterns and life expectancy for the 2013 national birth cohort under the assumption that the cohort would be exposed to state cigarette taxes in force at the beginning of 2013. We compared these values to estimates calculated under the counterfactual scenario where individuals are exposed to 1996 cigarette tax levels. With taxes at their 1996 levels, the average number of years spent smoking over the lifetime is 13.6 (12.4, 15.0), and this value drops to 12.8 (11.8, 14.2) under the 2013 tax scenario. In combination with changes in smoking intensity, these reductions in years spent smoking are estimated to produce a 6.1% (4.5, 7.8) reduction in average lifetime cigarette consumption compared to the counterfactual scenario. The effect of these changes in smoking behavior is estimated to increased overall life expectancy from 78.7 (78.4, 79.0) years under the 1996 tax scenario to 78.9 (78.5, 79.1) years under the 2013 tax scenario, a gain in life expectancy equal to 2.0 (1.4, 2.7) months when

averaged over the entire 2013 birth cohort, representing a total of 2.7 million (1.9, 3.6) extra life-years lived. These life expectancy gains are predominantly due to greater survival at older ages, with 90% of the additional life-years lived being enjoyed by individuals over 60 years of age. These results are summarized in Table 4.5 for each sex, with men enjoying greater gains in life expectancy compared to women.

Table 4.5. Changes in lifetime smoking behavior and life expectancy for the 2013 national birth cohort exposed to 1996 tax levels as compared to 2013 tax levels*

		Outcomes calculated for 1996 state cigarette tax levels	Outcomes calculated for 2013 state cigarette tax levels	Incremental difference
Average no. years spent smoking	Men	12.9 (11.6, 14.2)	11.8 (10.7, 13.1)	-1.1 (-1.4,-0.8)
	Women	14.3 (12.4, 16.7)	13.9 (12.0, 16.5)	-0.4 (-0.7,-0.1)
	All	13.6 (12.4, 15.0)	12.8 (11.8, 14.2)	-0.8 (-1.0,-0.5)
Life expectancy	Men	77.0 (76.6, 77.3)	77.2 (76.9, 77.5)	0.25 (0.18, 0.34)
	Women	80.5 (79.9, 80.9)	80.6 (79.9, 81.0)	0.09 (0.01,0.14)
	All	78.7 (78.4, 79.0)	78.9 (78.5, 79.1)	0.17 (0.11, 0.22)

*Difference calculated as value from 2013 tax scenario minus value from 1996 tax scenario. 95% posterior intervals shown in parentheses.

4.3.5. Price elasticity of demand

Estimates of the price elasticity of demand were estimated using two approaches. In the first approach, elasticities were calculated based on the price changes and behavioral outcomes estimated for the period 1996-2013. With this approach, the elasticity was estimated to be -0.18 (-0.22, -0.15) for men and -0.14 (-0.16, -0.10) for women, producing an overall elasticity of -0.16 (-0.18, -0.13). The second approach attempted to estimate long-run elasticities, given the delayed effect of changes in smoking initiation rates and quitting rates on overall cigarette consumption. These long-run elasticity estimates were calculated in the context of the life-expectancy analysis,

comparing changes in price to predicted changes in lifetime cigarette consumption. Under this second approach, elasticity was estimated as -0.39 (-0.50, -0.30) for men, and -0.16 (-0.25, -0.06) for women, for an overall long-run elasticity of -0.27 (-0.35, -0.20).

4.3.6. Sensitivity analyses

We tested the robustness of the results to changes in how the state cigarette tax variable was operationalized. In the main analysis this variable described tax increases from 1996 levels for each state. In a sensitivity analysis we revised this variable to represent the absolute state cigarette tax (i.e., not set to zero in 1996 for each state). The results of this sensitivity analysis were similar to those of the original analysis, though with major health outcomes (total deaths averted and life-years saved) approximately 10-20% larger in the revised analysis. Table 4.6 compares main analysis and sensitivity analysis for a number of major outcomes.

Table 4.6. Comparison of parameter estimates and major outcomes from different approaches to operationalizing the effect of cigarette taxes on smoking behavior*

	Men			Women		
	Main analysis	Sensitivity analysis	Difference	Main analysis	Sensitivity analysis	Difference
Coefficient for tax effect on smoking initiation	-0.056	-0.080	-0.024	0.007	-0.022	-0.029
Coefficient for tax effect on smoking intensity	-0.020	-0.024	-0.004	-0.025	-0.028	-0.003
Coefficient for tax effect on smoking cessation	-0.055	-0.047	0.009	-0.066	-0.065	0.001
Reduction in smoking prevalence (%) by end 2012 due to taxes	4.00	4.12	0.12	2.86	3.43	0.57
Reduction in ever smokers (%) by end 2012 due to taxes	0.74	1.05	0.30	-0.10	0.23	0.34
Reduction in every day smokers (%) by end 2012 due to taxes	0.57	0.63	0.06	0.82	0.89	0.07
Reduction in years spent smoking 1996-2013 due to taxes (millions)	6.3	6.3	0.0	4.6	5.1	0.5
Reduction in total deaths 1996-2013 due to taxes (thousands)	14.4	16.8	2.4	13.0	14.2	1.2
Total life-years saved 1996-2013 due to taxes (thousands)	60.6	72.2	11.6	58.4	63.7	5.3

* For the main analysis, the state cigarette tax variable represented any increase in taxes from 1996 levels in each state, in 2013 constant dollars. For the sensitivity analysis, the state cigarette tax variable represented the absolute value of state cigarette taxes, in 2013 constant dollars. Difference represents value from sensitivity analysis minus value from main analysis.

We also assessed the robustness of results to alternative assumptions about future smoking patterns. In the analysis that projects results over the next four decades, assumptions must be made about secular trends in smoking behavior. In the main analysis it was assumed that all determinants of smoking behavior were fixed at their 2013 values. In sensitivity analyses we

allowed the changes in background smoking behaviors (as operationalized through the splines for time) estimated over the period 1996-2013 to be extrapolated linearly in to the future. This alternate set of assumptions produces lower estimates for future smoking prevalence, consistent with historical trends. The future benefits of the 1996-2013 tax increases is also lower with these alternate assumptions, with the absolute reduction in life-years spent smoking (as shown in Figure 4.14) reduced by 8% (6, 11), total deaths reduced by 14% (12, 17) and total life-years saved reduced by 9% (7, 10).

Finally, we assessed the sensitivity of elasticity estimates to a different assumption about the pass-through of taxes to prices. For the main analysis it was assumed that taxes would be passed through to prices one-to-one. In this sensitivity analysis we altered this assumption to assume a pass-through of 1.11 (i.e., that a $1.00 increase in the tax would produce a $1.11 increase in the price), based on analyses of interstate cigarette price variation over the period 1960-1990 by Keeler *et al*. [56]. Under these revised assumptions elasticity estimates are reduced. For changes in cigarette consumption by 2013, elasticity is estimated as -0.16 (-0.19,-0.13) for men, -0.12 (-0.14, -0.09) for women and -0.14 (-0.16, -0.11) overall. For long-run changes in cigarette consumption (calculated over the lifetime of a single cohort), elasticity is estimated as -0.34 (-0.44,-0.27) for men, -0.14 (-0.22, -0.05) for women and -0.24 (-0.30, -0.17) overall. For all of these individual results, the revised assumption produces a reduction in the magnitude of the elasticity estimate of 11-13% compared to the main analysis.

4.4. Discussion

This analysis used a novel approach to estimate the causal effect of recent increases in state cigarette taxes on smoking behaviors. These effects were estimated in the context of a behavioral

model that explicitly described the different processes contributing to overall smoking prevalence, allowing for separate effects of taxation on smoking initiation, smoking intensity, and smoking cessation. Based on data from 17 rounds of BRFSS survey data, the state cigarette taxes introduced over the period 1996-2013 were estimated to have produced a 4% drop in overall cigarette consumption, compared to a counterfactual scenario that assumed no changes in state taxes over this period, with these behavioral effects estimated to be slightly larger for men than for women.

While other analyses have assessed the impact of state cigarette taxes on smoking behavior, the specific states and time periods involved differ. For this reason the magnitude of the behavioral effects assessed by this and other studies can best be compared in terms of the elasticities implied by the results. In our study, the elasticity of demand for all adults was estimated to be -0.16 based on estimated differences in cigarette consumption in 2013, and -0.27 over the long-run. These estimates are considerably lower than the conventional understanding of the price elasticity for cigarettes [9], with a meta-analysis of published estimates finding a median value of -0.4 for short-run elasticity [10]. In contrast, the relative magnitude of the different elasticities we estimate conforms to expectations, with elasticity estimated to be of greater magnitude for men as compared to women[17], and over the long-run as compared to the short-run.

Our elasticity estimates can also be compared to the other recent studies that estimate tax effects from cross-state variation in taxes. Using 1991-2005 data from the Youth Risk Behavior Surveys,

---

[17] Our results conflict with those of Stehr [24], who finds that women are nearly twice as responsive to cigarette taxes as men, arguing that conventional estimates are biased due to a failure to control for differences in the distribution of male and female smoking participation across states. Our analysis explicitly allows for these inter-state differences, suggesting that the surprising findings reported by Stehr may have some other explanation.

Carpenter and Cook [15] estimate elasticities that range from -0.56 to -0.25 for youth smokers[18]. In contrast, using 1992-2002 data from the National Education Longitudinal Study DeCicca *et al*. estimate elasticities for youth smoking that are both small and statistically insignificant (ranging from -0.11 to 0.08) [12]. Similarly, using data from the 1997 cohort of the National Longitudinal Survey of Youth, Nonnemaker and Farrelly find effects of cigarette taxes on youth smoking to be smaller than conventional estimates and sensitive to changes in specification [16]. While much of the published literature on inter-state variation focusses on youth smoking, DeCicca and McLeod estimate outcomes for older adults, finding elasticities that range from -0.3 to -0.2 using data from BRFSS rounds 2000-2005 [11]. In sum, the elasticities estimated from inter-state variation in cigarette excise taxes are general smaller than other estimates, and our findings are consistent with this trend.

One feature of the relationship between state-level cigarette prices and purchasing behavior is the possibility for cross-border purchasing. It is possible that, in the face of differences in cigarette prices between abutting states, consumers respond to tax increases (and therefore price increases) in one state by moving cigarette purchasing to lower tax jurisdictions. If true, this effect would reduce the effect of cigarette taxes relative to a scenario in which consumers faced a common price, or a situation where taxes were raised across all jurisdictions (as would happen with changes in the federal tax). Recent work by DeCicca *et al*. investigated the magnitude of such cross-border purchases using data from the TUS-CPS, and concluded that cross-border purchases account for one quarter of the total reduction in purchases within a state following a price increase [21]. Stehr reaches a similar finding by comparing BRFSS data on smoking behaviors to state-level cigarette sales data [58]. As a consequence of cross-border purchasing, a naïve analysis of cigarette sales

[18] For whom elasticities are thought to be higher than the general population [10].

would over-estimate total changes in consumption for a state that raises its cigarette tax. This is not a problem for our analysis and ones like it, which use data on reported behaviors and so should not be affected by this bias. However, the existence of cross-border purchasing as a result of price differentials implies that tax changes in one jurisdiction should affect smoking behaviors in other jurisdictions. Such spillover effects would undermine the stable-unit treatment value assumption (SUTVA) that underlies the causal identification strategy for studies such as ours. If a tax hike in one state not only increases cigarette prices in that state but also increases effective prices for smokers living in abutting states, then the true benefits of state-level cigarette tax increases will be larger than what is estimated in our analysis, and this provides one potential explanation for lower elasticity estimates derived from studies of variation between U.S. states.

In addition to estimating tax-related changes in smoking behavior over the period 1996-2013, our analysis compared future trends in smoking behavior with taxes maintained at their 2013 levels to a counterfactual scenario that assumed no new taxes since 1996. The results of this analysis must be viewed as more speculative than the findings reported for the 1996-2013 period, as they depend on assumptions about future trends in smoking behavior. This analysis also assumes that the responsiveness to cigarette taxes observed in the study period will be maintained in the future. The major finding from this part of the analysis is that estimates of smoking prevalence in these two scenarios continue to diverge over time, such that the reduction in total years spent smoking for the 10 year period 2020-2029 is more than double the 11 million reduction in years spent smoking estimated for the 17 years 1996-2013. These long-term effects are consistent with our findings of long-run elasticities that are higher than those estimated for the short-run. Despite the greater uncertainty associated with the long-term projections, it seems clear that the behavioral outcomes of cigarette tax changes will continue to increase for many years after taxes are introduced.

The analytic model used for this study directly linked changes in current smoking behavior and smoking history to mortality risks. As a consequence of tax-related reductions in smoking behavior, our analysis estimated a mortality reduction of 27,000 deaths over the period 1996-2013, compared to a counterfactual scenario with no state tax increases since 1996. These survival gains were associated with 119,000 additional life-years lived over the same period, with these benefits mainly accruing to older adults. These mortality reductions are relatively modest, and when averaged over the 17 year period 1996-2013 represent less that 0.5% of the approximately 400,000 annual deaths attributed to smoking in the United States [35]. Even more than the changes in smoking prevalence, the reductions in mortality and extra years of life lived because of tax increases are estimated to be substantially delayed following tax introduction. In the analysis where outcomes were estimated for future decades, comparing 2013 tax levels to 1996 levels, reductions in mortality for the 10 year period 2020-2029 are more than triple the 27,400 estimate for total deaths averted for the 17 years 1996-2013, and the number of extra life-years lived is nine times the 119,000 extra life-years lived for the 1996-2013 period. While the health benefits estimated by this study are more substantial if future years are taken into account, these aggregate outcomes are still dwarfed by contemporary estimates of the total benefits of tobacco control measures in the U.S. Evaluating the effects of tobacco control since the surgeon general's report on smoking in 1964, Holford *et al*. estimate 157 million life-years saved by 2012 compared to a counterfactual with no tobacco control [59]. Our estimate for total life-years saved for the period 1996-2049 represents 4% of this total, despite covering a longer period (54 years vs. 49 years) and a larger population due to population growth. Our estimates of life expectancy gains are similarly small in comparison, representing 10% of the 2.3 year life expectancy gain Holford *et al.* estimate for men and 5% of the 1.6 year life expectancy gain estimated for women. These comparisons reinforce the relatively modest reductions in smoking behavior we estimate to have resulted from recent state cigarette tax increases.

This analysis has a number of limitations in addition to those mentioned already. A key assumption of the identification strategy is that controlling for state-level anti-smoking sentiment (and doing so using the index created by DeCicca *et al.* [12]) removes the relationship between this and other unmeasured factors that otherwise confound the observed relationship between the cigarette taxes that states impose and the smoking behavior of their residents. If this assumption does not hold, it is possible that our analysis will have over-estimated the effects of state cigarette taxes on smoking behavior, and that the effects estimated are not truly causal. Another assumption of our analysis is that the smoking behavior of a state's residents does not meaningfully influence the level of anti-smoking sentiment, and consequently the likelihood of further tobacco control legislation being introduced in the future. If there is a causal relationship between smoking behavior and anti-smoking sentiment it is likely negative, with a reduction in the number of individuals smoking weakening opposition to tobacco control[19]. What is more certain is that stronger anti-smoking sentiment will raise the probability of future cigarette tax hikes and other controls. If both of these relationships exist as described it is possible that our analysis, by ignoring the potential positive feedback between anti-smoking sentiment, smoking behaviors and tobacco control policies, has mischaracterized (and potentially underestimated) the causal effects of cigarette taxes. On a more concrete issue, the fact that the demographic model appears to underestimate population growth due to immigration means that the estimates of absolute impact (e.g., total life-years saved) will be modestly lower than they would be otherwise, particularly for future projections.

[19] A major argument for this relationship is self-interest, that people will be less willing to support price increases and other restrictions on an activity if they are directly affected by these controls. However, this is only speculation, and other arguments might predict a positive relationship.

Another limitation of this analysis is that it ignores important differences in smoking behaviors observed for individuals of different race, education, and income level. These differences have been well documented, with smoking prevalence substantially lower for those with some higher education, for those above the federal poverty line, and for those identifying as Asian or Hispanic [60]. Instead, the analysis calculates population-level averages for each subgroup of state, sex, age, and birth cohort. While the results will be valid for the subgroup as a whole, they may obscure important differences not only in general smoking behaviors but also the responsiveness to cigarette tax increases. The decision to average over some important individual-level predictors of smoking behavior was driven by concerns about model complexity, however it is possible that future research will allow investigation of tax effects among additional population groups and these stratifications are available in the BRFSS data. However, one group not included in the BRFSS is individuals under 18 years of age. This group was modeled for the analysis, in order to obtain correct estimates of overall population-level effects. The BRFSS data does provide indirect information on smoking initiation rates during this period, in that the aggregate effect of smoking initiation during the early and mid teens will need to match the smoking prevalence levels observed among older teens once they are eligible for the survey. Consequently, while aggregate smoking initiation behavior estimated for those below 18 will be correct, our results provide little insight into the specific timing of smoking initiation for those younger than 18.

Finally, it is possible that choices made in determining the structure of the model influence the outcomes that are reported. While we believe that the model equations represent a plausible formalization for how cigarette taxes might influence smoking behavior and subsequent mortality, we accept that other equally defensible model structures are possible. The use of a mechanistic model of smoking behavior and population demographics allows us to report detailed estimates of how outcomes are distributed across time, sex, age, and state. As far as we know, the use of a mechanistic model for identifying the causal effects of cigarette taxation is novel, and provides new

opportunities for understanding the relationship between taxes, behaviors and health outcomes. In particular, by allowing the estimation of many different quantities that can be compared to empirical data, we believe this approach allows natural opportunities for model refinement (for example, the comparison of modeled life tables to published life tables (Figure 4.10) reveals that more accurate long-term projections may be obtained by allowing for immigration), and allows the identification of misspecifications when simulated results don't match real world data.

4.5. Citations

1 U.S. Department of Health and Human Services. *Ending the tobacco epidemic: a tobacco control strategic action plan for the U.S*. Department of Health and Human Services. Washington, DC: Office of the Assistant Secretary for Health; 2010.

2 Institute of Medicine. *Ending the tobacco problem: a blueprint for the nation*. Washington DC: Institute of Medicine; 2007.

3 Orzechowski and Walker. *The tax burden on tobacco, historical compilation volume 46, 2011*. Arlington, VA: Orzechowski and Walker; 2011.

4 Jha P, Ramasundarahettige C, Landsman V, Rostron B, Thun M, Anderson RN, *et al*. 21st-century hazards of smoking and benefits of cessation in the United States. *New Engl J Med* 2013; 368:341–50.

5 Thun MJ, Carter BD, Feskanich D, Freedman ND, Prentice R, Lopez AD, *et al*. 50-year trends in smoking-related mortality in the United States. *New Engl J Med* 2013; 368:351–64.

6 Pirie K, Peto R, Reeves GK, Green J, Beral V. The 21st century hazards of smoking and benefits of stopping: a prospective study of one million women in the UK. *Lancet* 2013; 381:133–141.

7 U.S. Department of Health and Human Services. *The health consequences of smoking: a report of the Surgeon General*. Washington, DC: Government Printing Office; 2004.

8 Taylor DH, Hasselblad V, Henley SJ, Thun MJ, Sloan FA. Benefits of smoking cessation for longevity. *Am J Public Heal* 2002; 92:990–6.

9 Chaloupka FJ, Yurekli A, Fong GT. Tobacco taxes as a tobacco control strategy. *Tob Control* 2012; 21:172–80.

10 Gallet CA, List JA. Cigarette demand: a meta-analysis of elasticities. *Heal Econ* 2003; 12:821–35.

11 DeCicca P, McLeod L. Cigarette taxes and older adult smoking: evidence from recent large tax increases*. J Heal Econ* 2008; 27:918–29.

12 DeCicca P, Kenkel D, Mathios A, Shin Y-J, Lim J-Y. Youth smoking, cigarette prices, and anti-smoking sentiment. *Heal Econ* 2008; 17:733–49.

13 DeCicca P, Kenkel D, Mathios A. Cigarette taxes and the transition from youth to adult smoking: smoking initiation, cessation, and participation. *J Heal Econ* 2008; 27:904–17.

14 Levy DT, Hyland A, Higbee C, Remer L, Compton C. The role of public policies in reducing smoking prevalence in California: results from the California tobacco policy simulation model. *Health Policy* 2007; 82:167–85.

15 Carpenter C, Cook PJ. Cigarette taxes and youth smoking: new evidence from national, state, and local Youth Risk Behavior Surveys. *J Heal Econ* 2008; 27:287–99.

16 Nonnemaker JM, Farrelly MC. Smoking initiation among youth: the role of cigarette excise taxes and prices by race/ethnicity and gender. *J Heal Econ* 2011; 30:560–7.

17 Fichtenberg CM, Glantz SA. Association of the California Tobacco Control Program with declines in cigarette consumption and mortality from heart disease. *New Engl J Med* 2000; 343:1772–7.

18 Gilpin EA, Messer K, White MM, Pierce JP. What contributed to the major decline in per capita cigarette consumption during California's comprehensive tobacco control programme? *Tob Control* 2006; 15:308–16.

19 Barnoya J, Glantz S. Association of the California tobacco control program with declines in lung cancer incidence. *Cancer Cause Control* 2004; 15:689–95.

20 Al-Delaimy WK, Pierce JP, Messer K, White MM, Trinidad DR, Gilpin EA. The California Tobacco Control Program's effect on adult smokers: (2) Daily cigarette consumption levels. *Tob Control* 2007; 16:91–5.

21 DeCicca P, Kenkel D, Liu F. Excise tax avoidance: The case of state cigarette taxes. *J Heal Econ* 2013; 32:1130–1141.

22 Merriman D. The micro-geography of tax avoidance: evidence from littered cigarette packs in Chicago. *Econ Policy* 2010; 2:61–84.

23 Centers for Disease Control and Prevention (CDC). *Behavioral Risk Factor Surveillance System survey data*. Atlanta GA: U.S. Department of Health and Human Services; 1984.

24 Stehr M. The effect of cigarette taxes on smoking among men and women. *Heal Econ* 2007; 16:1333–43.

25 Sloan FA, Trogdon JG. The impact of the Master Settlement Agreement on cigarette consumption. *J Policy Anal Manag* 2004; 23:843–55.

26 Levy DT, Bauer JE, Lee H-R. Simulation modeling and tobacco control: creating more robust public health policies. *Am J Public Heal* 2006; 96:494–8.

27 Levy D, de Almeida LM, Szklo A. The Brazil SimSmoke policy simulation model: the effect of strong tobacco control policies on smoking prevalence and smoking-attributable deaths in a middle income nation. *PLoS Med* 2012; 9:e1001336.

28 Levy DT, Chaloupka F, Gitchell J, Mendez D, Warner KE. The use of simulation models for the surveillance, justification and understanding of tobacco control policies. Heal Care Manag Sci 2002; 5:113–20.

29 Eilers P, Marx B. Flexible smoothing with B-splines and penalties. *Stat Sci* 1996; 11:89–121.

30 Hogan DR, Salomon JA. Spline-based modelling of trends in the force of HIV infection, with application to the UNAIDS Estimation and Projection Package. *Sex Transm Infect* 2012; 88 Suppl 2:i52–7.

31 Kirshenbaum AP, Olsen DM, Bickel WK. A quantitative review of the ubiquitous relapse curve. *J Subst Abus Treat* 2009; 36:8–17.

32 Binder D. On the variances of asymptotically normal estimators from complex surveys. *Int Stat Rev* 1983; 51:279–92.

33 Pfeffermann D. The role of sampling weights when modeling survey data. *Int Stat Rev* 1993; 61:317–37.

34 Gelman A. Struggles with survey weighting and regression modeling. *Stat Sci* 2007; 22:153–164.

35 Adhikari B, Kahende J, Malarcher A, Pechacek T, Tong V. Smoking-attributable mortality, years of potential life lost, and productivity losses--United States, 2000-2004. *MMWR* 2008; 57:1226–8.

36 Rostron B. Smoking-attributable mortality by cause in the United States: revising the CDC's data and estimates. *Nicotine Tob Res* 2013; 15:238–46.

37 Arias E, Heron M, Tejada-Vera B. *United States life tables eliminating certain causes of death, 1999–2001*. Natl Vital Stat Reports 2013; 61:1–128.

38 Arias E. *United States life tables, 2008*. Natl Vital Stat Reports 2012; 61:1–63.

39 Anderson RN. *United States life tables, 1997*. Natl Vital Stat Reports 1999; 47:1–37.

40 Bell FC, Miller ML. *Life tables for the United States Social Security Area 1900-2100*. Actuarial Study No. 120. Washington DC: Office of the Chief Actuary, Social Security Administration; 2005.

41 U.S. Census Bureau Population Division. *Population estimates for the U.S. and states by single year of age and sex*. U.S. Census Bureau Population Division; 2000.

42 National Center for Health Statistics. *Natality public-use data on CDC WONDER Online Database, for years 1995-2002 published November 2005, for years 2003-2006 published March 2009, and for years 2007-2010 published December 2012*. Atlanta GA: National Center for Health Statistics, Division of Vital Statistics; 2012.

43 U.S. Census Bureau. *2012 national population projections*. Washington DC: U.S. Census Bureau; 2012.

44 U.S. Bureau of Labor Statistics. *Consumer price index: current series, all urban consumers*. Washington DC: U.S. Bureau of Labor Statistics; 2013.

45 U.S. Bureau of Labor Statistics. *Local area unemployment statistics*. U.S. Bureau of Labor Statistics; 2013.

46 American Nonsmoker's Rights Foundation. *U.S. Tobacco Control Laws Database*. Berkeley CA: American Nonsmoker's Rights Foundation; 2013.

47 Raftery AE, Bao L. Estimating and projecting trends in HIV/AIDS generalized epidemics using Incremental Mixture Importance Sampling. *Biometrics* 2010; 66:1162–73.

48 R Core Team. *R: A language and environment for statistical computing*. 2013. doi:ISBN 3-900051-07-0

49 Eddelbuettel D, Francois R. Rcpp: Seamless R and C++ Integration. *J Stat Softw* 2011; 40:1–18.

50 Lang S, Brezger A. Bayesian p-splines. *J Comput Graph Stat* 2004; 13:183–212.

51 Gelman A. Prior distributions for variance parameters in hierarchical models. *Bayesian Anal* 2006; 1:515–33.

52 U.S. Department of Commerce and Census Bureau. *Tobacco Use Supplement to the Current Population Survey (2010-11)*. Washington DC: U.S. Department of Commerce and Census Bureau; 2012.

53 U.S. Census Bureau. *2010 Census*. Washington DC: U.S. Census Bureau; 2010.

54 Hoyert DL, Xu J. Deaths: preliminary data for 2011. *Natl Vital Stat Reports* 2012; 61:6–51.

55 Boonn A. *State excise and sales taxes per pack of cigarettes: total Amounts and state rankings*. Washington DC: Campaign for Tobacco-Free Kids; 2013.

56 Keeler TE, Hu TW, Barnett PG, Manning WG, Sung HY. Do cigarette producers price-discriminate by state? An empirical analysis of local cigarette pricing and taxation. *J Health Econ* 1996; 15:499–512.

57 Bhaskar R, Cortes R, Scopilliti M, Jensen E, Dick C, Armstrong D, *et al*. *Estimating net international migration for 2010 demographic analysis: an overview of methods and results*. Washington DC: U.S. Census Bureau; 2013.

58 Stehr M. Cigarette tax avoidance and evasion. *J Health Econ* 2005; 24:277–97.

59 Holford TR, Meza R, Warner KE, Meernik C, Jeon J, Moolgavkar SH, *et al*. Tobacco control and the reduction in smoking-related premature deaths in the United States, 1964-2012. *JAMA* 2014; 311:164.

60 Rock V, Malarcher A, Kahende J, Asman K, Husten C, Caraballo R. Cigarette smoking among adults -- United States, 2006. *MMWR* 2007; 56:1157–61.

61 Hughes JR, Keely J, Naud S. Shape of the relapse curve and long-term abstinence among untreated smokers. *Addiction* 2004; 99:29–38.